



# VCU

Virginia Commonwealth University  
VCU Scholars Compass

---

Theses and Dissertations

Graduate School

---

2020

## THE IMPACT OF AGING AND MECHANICAL INJURY ON ALVEOLAR EPITHELIAL AND MACROPHAGE RESPONSES IN ACUTE LUNG INJURY AND INFLAMMATION

Michael S. Valentine  
*Virginia Commonwealth University*

Follow this and additional works at: <https://scholarscompass.vcu.edu/etd>

 Part of the [Biological Engineering Commons](#), [Biomechanics and Biotransport Commons](#), [Cell Biology Commons](#), [Disease Modeling Commons](#), [Immunotherapy Commons](#), [Laboratory and Basic Science Research Commons](#), [Lipids Commons](#), [Molecular Biology Commons](#), [Molecular, Cellular, and Tissue Engineering Commons](#), [Other Biomedical Engineering and Bioengineering Commons](#), [Pathological Conditions, Signs and Symptoms Commons](#), [Pharmaceutical Preparations Commons](#), and the [Respiratory Tract Diseases Commons](#)

© The Author

---

Downloaded from

<https://scholarscompass.vcu.edu/etd/6347>

This Dissertation is brought to you for free and open access by the Graduate School at VCU Scholars Compass. It has been accepted for inclusion in Theses and Dissertations by an authorized administrator of VCU Scholars Compass. For more information, please contact [libcompass@vcu.edu](mailto:libcompass@vcu.edu).

**THE IMPACT OF AGING AND MECHANICAL INJURY ON ALVEOLAR EPITHELIAL AND  
MACROPHAGE RESPONSES IN ACUTE LUNG INJURY AND INFLAMMATION**

A dissertation submitted in partial fulfillment of the requirements for the degree of  
Doctor of Philosophy at Virginia Commonwealth University

By

Michael Sean Valentine  
B.S. in Biology, University of Virginia, 2013

Director: Rebecca L. Heise, Ph.D.  
Associate Professor, Department of Biomedical Engineering

Virginia Commonwealth University  
Richmond, Virginia  
April 2020

## **ACKNOWLEDGEMENTS**

I would first like to thank my PI, Dr. Rebecca Heise, for all of her guidance and encouragement throughout my graduate career. Since my time as a laboratory technician in her lab, she has been a tremendous source of inspiration, direction, and support. Her mentorship and positive influence have been invaluable throughout my biomedical engineering endeavors. I would also like to extend my appreciation to Dr. Chris Lemmon, Dr. Angela Reynolds, Dr. Rene Olivares-Navarette, and Dr. John Ryan for their advice and support while serving as motivating members of my doctorate committee.

I would also like to give a special thanks to all of the past and current members of the Heise Laboratory: Dr. Robert Pouliot, Dr. Joseph Herbert, Dr. Bethany Young, Dr. Patrick Link, Franck Kamga Gninzeke, Matthew Schneck, Manav Parekh, Sahil Chindal, Keerthana Shankar, Krista Powell, Alex Ritchie, and Gabrielle Cotman for all of your help, support, and camaraderie. Likewise, I would like to especially acknowledge Dr. Spiegel and Cynthia Weigel for graciously providing their resources, assistance, and expertise with the lipid-related analyses.

Last, but certainly not least, I would like to give the utmost appreciations to my girlfriend, Ali Carey, my parents, Young and Larry, my sisters, Toi and Diana, and my friends for all of their caring support and motivation throughout this endeavor. They have been incredible foundations of inspiration, leisure, gratification, and optimism throughout this entire process and my life. I am incredibly fortunate to have such a compassionate and uplifting family that always inspires me to strive for more. Ali, I am so gracious for all of your love and care throughout all of this, you seem to make every day that much better.

This research was supported by the National Institutes of Health under Award Number R01AG041823 and the National Science Foundation (NSF) under Award Number CMMI-1351162. The content is solely the responsibility of the author and does not necessarily represent the official views of the National Institutes of Health or the NSF. Services and products in support of the research project were made by the VCU Massey Cancer Center Flow Cytometry Shared Resource, supported, in part, with funding from NIH-NCI Cancer Center Support Grant P30 CA016059 and by the VCU Massey Cancer Center Lipidomics Shared Resource, supported, in part, with funding from NIH-NCI Cancer Center Support Grant P30 CA016059.

## **TABLE OF CONTENTS**

COVER PAGE .....	1
ACKNOWLEDGEMENTS.....	2
TABLE OF CONTENTS.....	3
LIST OF FIGURES.....	5
LIST OF TABLES.....	7
GLOSSARY .....	8
ABSTRACT.....	9
CHAPTER 1: INTRODUCTION.....	12
1.1: Rationale.....	12
1.2: Objectives.....	19
CHAPTER 2: LITERATURE REVIEW.....	21
2.1: The Effects of Mechanical Injury and Aging on ATII and Macrophage Responses .....	21
2.2: Lung Structural and Functional Impairment Associated with Aging and Mechanical Injury .....	28
2.3: Endoplasmic Reticulum Stress and Therapeutic Potential in Aging and Acute Lung Injury.....	30
2.4: Sphingosine-1-Phosphate and S1P Lyase Suppression in Aging and Acute Lung Injury .....	39
CHAPTER 3: AGING INFLUENCES ATII AND MACROPHAGE RESPONSES TRIGGERED BY INJURIOUS CELL-STRETCH.....	49
3.1: Rationale.....	49
3.2: Materials and Methods.....	52
3.3: Results.....	55
3.4: Discussion.....	61
CHAPTER 4: PULMONARY RESPONSES IN AN AGING ALI/VILI Animal Model.....	66
4.1: Rationale.....	66
4.2: Materials and Methods.....	69
4.3: Results.....	72
4.4: Discussion.....	81

CHAPTER 5: IMPACT OF ER STRESS IN AGING AND ACUTE LUNG INJURY.....	85
5.1: Rationale.....	85
5.2: Materials and Methods.....	86
5.3: Results.....	93
5.4: Discussion.....	103
CHAPTER 6: PROTECTIVE ROLE OF S1P IN AGING AND ACUTE LUNG INJURY.....	106
6.1: Rationale.....	106
6.2: Materials and Methods.....	107
6.3: Results.....	110
6.4: Discussion.....	124
CHAPTER 7: CONCLUSIONS AND FUTURE DIRECTIONS.....	132
APPENDIX A.....	140
REFERENCES.....	144
CURRICULUM VITAE.....	159

## List of Figures

FIGURE 1: IMPLICATIONS OF AGING ON LUNG STRUCTURE, CELLULAR INTEGRITY, AND THE INNATE IMMUNE SYSTEM .....	14
FIGURE 2: GENERAL OVERVIEW SCHEMATIC OF THE AIMS AND APPROACH.....	18
FIGURE 3: PRIMARY ALVEOLAR TYPE II CELLS (ATII) EXPRESS SURFACTANT PROTEIN C.....	21
FIGURE 4: PROPOSED LUNG MACROPHAGE DEVELOPMENT AND CHANGES DURING LIFESPAN .....	25
FIGURE 5: TYPES OF LUNG MACROPHAGES IN THE ALVEOLAR BLOOD-GAS REGION .....	24
FIGURE 6: PARADIGM OF MACROPHAGE POLARIZATION.....	27
FIGURE 7: SCHEMATIC OVERVIEW OF ASSOCIATED ER STRESS-INDUCED UPR SIGNALING.. ..	31
FIGURE 8: SCHEMATIC DIAGRAM OF ER STRESS, THE UPR, AND SUBSEQUENT CELL RESPONSE OUTCOMES .....	32
FIGURE 9: PROPOSED TRIGGERS AND IMPLICATED DISEASES ASSOCIATED WITH ER STRESS AND THE UPR .....	33
FIGURE 10: THEORIZED ROLE OF ER STRESS AND THE UPR IN PATHOPHYSIOLOGY OF MECHANICAL-INDUCED ALI/VILI .....	35
FIGURE 11: PROPOSED MECHANISM FOR THE INDUCTION OF ER STRESS-INDUCED PULMONARY FIBROSIS .....	38
FIGURE 12: SCHEMATIC OVERVIEWS OF THE S1P SIGNALING AXIS AND THE CELLULAR ACTIONS OF S1P .....	40
FIGURE 13: PATHOPHYSIOLOGICAL CONDITIONS AND DISEASES THROUGHOUT THE BODY THAT ARE ASSOCIATED WITH S1P .....	41
FIGURE 14: TARGETING SPHINGOLIPID SIGNALING HAS THERAPEUTIC POTENTIAL IN FIBROSIS DISEASES, SUCH AS PULMONARY FIBROSIS, AS WELL AS MANY OTHER PATHOPHYSIOLOGIC CONDITIONS. ....	43
FIGURE 15: S1P SIGNALING AND MACROPHAGE RESPONSES.....	46
FIGURE 16: S1PR SIGNALING AND MACROPHAGE POLARIZATION IMPLICATED IN DISEASE.....	47
FIGURE 17: FLEXCELL FX-5000TM TENSION SYSTEM USED TO SIMULATE IN VIVO TISSUE STRAINS .....	49
FIGURE 18: SCHEMATIC OVERVIEW OF THE EXPERIMENTAL METHODS FOR AIM 1A THAT EXAMINES THE EFFECTS OF AGING IN AN INJURIOUS CELL-STRETCH MODEL USING ATII CELLS ISOLATED FROM YOUNG AND OLD MICE.....	52
FIGURE 19: AGING ALONE INFLUENCES THE EXPRESSION OF SEVERAL INFLAMMATORY MEDIATOR .....	56
FIGURE 20: CYCLIC STRETCH (15%) FOR 4 HOURS +/- AGE UPREGULATE INFLAMMATORY GENES.....	57
FIGURE 21: AGING OR CELL-STRETCH FOR 24HOURS HAD NO EFFECT ON IL-6 OR IL-10 GENE EXPRESSION .....	58
FIGURE 22: AGE AND MECHANICAL STRETCH CAUSE VARIATIONS IN MONOCYTE RECRUITMENT.....	59
FIGURE 23: MONOCYTE MIGRATION WITH (A) ATII GROWTH MEDIA (GM) AND (B) ATII CONDITIONED MEDIA .....	60
FIGURE 24: MONOCYTE MIGRATION WITH AGE-MATCHED AND MISMATCHED ATII CONDITIONED MEDIA.....	60
FIGURE 25: SCHEMATIC OVERVIEW OF AGE-RELATED ANIMAL MECHANICAL VENTILATION PROCEDURE AND COLLECTION .....	69
FIGURE 26: HIGH PCMV INDUCES INJURY IN YOUNG AND OLD C57BL/6 MICE .....	73
FIGURE 27: AGING AND HIGH PCMV CAUSE DEVIATIONS IN TISSUE MECHANICS AND PULMONARY FUNCTION .....	75
FIGURE 28: PRESSURE-VOLUME CURVES WERE GENERATED USING MATLAB .....	76
FIGURE 29: MACROPHAGES FROM AGED MICE AND MICE THAT UNDERWENT HIGH PCMV OVEREXPRESS ASSOCIATED POLARIZATION MARKERS CD80 AND CD206 .....	77
FIGURE 30: AGING AND HIGH PCMV INFLUENCE LUNG MACROPHAGE POLARIZATION IN C57BL/6 MICE.....	80
FIGURE 31: GENERAL OVERVIEW OF AIM 2A.....	87
FIGURE 32: GENERAL OVERVIEW OF AIM 2B .....	90
FIGURE 33: CYCLIC STRETCH (15%) FOR 24 H +/- AGE INFLUENCES DETECTION OF (A-H) CHOP AND (I-P) ATF4 IN ATII CELLS .....	93
FIGURE 34: QUANTIFICATION OF CHOP+ ATII CELLS AND ATF4+ ATII CELLS IN RESPONSE TO CYCLIC STRETCH (15%) FOR 24 H +/- AGE.....	95
FIGURE 35: (A) CHOP AND (B) ATF4 GENE EXPRESSION AFTER 24 H OF STRETCH OR STATIC CULTURE +/- 4PBA.....	96
FIGURE 36: EFFECT OF 4PBA ON (A) MCP-1 (CCL2) GENE EXPRESSION AND (B) CYTOKINE SECRETION AND (C) MIP-1b (CCL4) GENE EXPRESSION (D) AND CYTOKINE SECRETION IN ATII CELLS AFTER 24 H .....	97
FIGURE 37: 4PBA DIMINISHES YOUNG AND OLD BMDM RECRUITMENT.....	99
FIGURE 38: MONOCYTE MIGRATION WITH AGE-MATCHED AND MIS- MATCHED ATII CONDITIONED MEDIA .....	100
FIGURE 39: 4PBA PREVENTS NEUTRIPHIL ACCUMULATION IN YOUNG MICE FOLLOWING HIGH PCMV .....	101
FIGURE 40: 4PBA TREATMENT CAUSED FURTHER FLUCTUATIONS IN SEVERAL TISSUE MECHANICAL PROPERTIES IN YOUNG MICE .....	102
FIGURE 41: GENERAL OVERVIEW OF AIM 3 .....	107
FIGURE 42: EFFECTS OF AGING AND HIGH PCMV ON S1P LEVELS AND S1PL EXPRESSION IN LUNG TISSUE.....	112

<b>FIGURE 43: THI ATTENUATES LYMPHOCYTE AND NEUTROPHIL INFLUX FOLLOWING HIGH PCMV IN YOUNG MICE</b> .....	113
<b>FIGURE 44: THI MITIGATES LYMPHOCYTE, NEUTROPHIL, AND BASOPHIL INFLUX FOLLOWING HIGH PCMV IN OLD MICE</b> .....	114
<b>FIGURE 45: THI IMPROVES THE PROTEIN ACCUMULATION IN BALF SAMPLES OF YOUNG AND OLD MICE FOLLOWING HIGH PCMV</b> .....	115
<b>FIGURE 46: EFFECTS OF AGING AND HIGH PCMV ON YOUNG LUNG MACROPHAGE POLARIZATION IN C57BL/6 MICE</b> .....	116
<b>FIGURE 47: EFFECTS OF AGING AND HIGH PCMV ON OLD LUNG MACROPHAGE POLARIZATION IN C57BL/6 MICE</b> .....	116
<b>FIGURE 48: AGING AND HIGH PCMV INFLUENCE LUNG MACROPHAGE POLARIZATION IN C57BL/6 MICE</b> .....	118
<b>FIGURE 49: AGING AND HIGH PCMV INFLUENCE LUNG MACROPHAGE POLARIZATION IN C57BL/6 MICE</b> .....	120
<b>FIGURE 50: THI TREATMENT RESULTED IN THE ATTENUATION OF SEVERAL TISSUE MECHANICAL PROPERTIES IN YOUNG MICE</b> .....	122
<b>FIGURE 51: THI TREATMENT RESULTED IN THE ATTENUATION OF SEVERAL TISSUE MECHANICAL PROPERTIES IN OLD MICE</b> .....	123
<b>FIGURE 52: SUMMARY DIAGRAM OF THE DISSERTATION FINDINGS AND INFERENCES</b> .....	135
<b>FIGURE 53: THE SCHEMATIC OVERVIEW OF METHHODS TO FUTHER EXAMINE ER STRESS AND 4PBA IN THE AGING VILI MODEL</b> .....	136
<b>FIGURE 54: THE SCHEMATIC OVERVIEW OF METHHODS TO FUTHER EXAMINE S1P AND MACROPAHGE POLARIZATION IN VILI</b> .....	137
<b>FIGURE 55: THE SCHEMATIC OVERVIEW OF METHODS FOR FUTURE DIRECTIONS EXPERIMENTS</b> .....	139

## List of Tables

<b>TABLE 1: PHENOTYPES OF ALVEOLAR AND INTERSTITIAL MACROPHAGES IN THE HEALTHY MOUSE LUNG AND CORRESPONDING ANTIBODIES AND CONJUGATED FLUOROCHOMRES USED FOR FLOW CYTOMETRIC ANALYSIS.....</b>	<b>71</b>
<b>TABLE 2: LONG CHAIN (SPHINGOID) BASE CHANGES CAUSED BY AGING AND/OR HIGH PCMV .....</b>	<b>110</b>
<b>TABLE 3: CERAMIDE AND SPHINGOMYELIN BASE CHANGES CAUSED BY AGING AND/OR HIGH PCMV .....</b>	<b>111</b>

## GLOSARY

### **Keywords**

*Mechanotransduction*, Epithelial Barrier, Lung Injury and Repair, Macrophage Polarization

### **Abbreviations**

ARDS	Acute Respiratory Distress Syndrome
MV	Mechanical Ventilation
PCMV	Pressure-Controlled Mechanical Ventilation
VILI	Ventilator-Induced Lung Injury
ALI	Acute Lung Injury
ATIs	Alveolar Epithelial Type I Cells
ATIIs	Alveolar Epithelial Type II Cells
AMs	Alveolar Macrophages
IMs	Interstitial Macrophages
Mo/MΦs	Monocytes and Undifferentiated Macrophages
BMDMs	Bone Marrow Derived Macrophages
IHC	Immunohistochemical
ER	Endoplasmic Reticulum
4PBA	4-phenylbutyrate
THI	2-Acetyl-4-tetrahydroxybutyl Imidazole

## ABSTRACT

# THE IMPACT OF AGING ON ALVEOLAR EPITHELIAL AND MACROPHAGE RESPONSES IN ACUTE LUNG INJURY AND INFLAMMATION

By

Michael Sean Valentine

B.S. in Biology, University of Virginia, 2013

A dissertation submitted in partial fulfillment of the requirements for the degree of  
Doctor of Philosophy at Virginia Commonwealth University

Director: Rebecca L. Heise, Ph.D.

Associate Professor, Department of Biomedical Engineering

Patients with severe lung pathologies, such as Acute Respiratory Distress Syndrome (ARDS), often require mechanical ventilation as a clinical intervention; however, this procedure frequently exacerbates the original pulmonary issue and produces an exaggerated inflammatory response that potentially leads to sepsis, multisystem organ failure, and mortality. This acute lung injury (ALI) condition has been termed Ventilator-Induced Lung Injury (VILI). Alveolar overdistension, cyclic atelectasis, and biotrauma are the primary injury mechanisms in VILI that lead to the loss of alveolar barrier integrity and pulmonary inflammation. Stress and strains during mechanical ventilation are believed to initiate alveolar epithelial *mechanotransduction* signaling mechanisms that contribute to injury and repair responses and lead to the direct activation of resident lung and recruited macrophages. These types of cells, alveolar and interstitial macrophages, have various polarization states, such as M1 and M2, which are believed to play significant roles in tissue homeostasis and inflammatory regulation. Epidemiology studies have also suggested that **age** influences lung function and is a predictive factor in the severity of VILI; however,

the mechanisms of aging that influence the progression or increased susceptibility of VILI in the elderly are still unknown. Aging also critically impacts immune system function and may increase inflammation in healthy individuals, which is known as *inflammaging*.

Disruption to Endoplasmic Reticulum (ER) homeostasis results in a condition known as ER stress that leads to disruption of cellular homeostasis, apoptosis, and inflammation. ER stress is increased with aging and other pathological stimuli. We hypothesized that age and mechanical stretch increase alveolar epithelial cells' pro-inflammatory responses that are mediated by ER stress. Furthermore, we hypothesized that inhibition of this upstream mechanism with 4PBA, an ER stress reducer, alleviates subsequent inflammation and monocyte recruitment. Type II alveolar epithelial cells (ATII) were harvested from C57Bl6/J mice 2 months (young) and 20 months (old) of age. The cells were cyclically stretched at 15% change in surface area for up to 24 hours. Prior to stretch, groups were administered 4PBA or vehicle as a control. Mechanical stretch and age upregulated ER stress and proinflammatory signaling expression in ATIIs. Age increases susceptibility to stretch-induced ER stress and downstream inflammatory gene expression in a primary ATII epithelial cell model. Administration of 4PBA attenuated the increased ER stress and proinflammatory responses from stretch and/or age and significantly reduced monocyte migration to ATII conditioned media.

Recent studies also suggest a critical, protective role for the bioactive sphingolipid mediator sphingosine-1-phosphate (S1P) signaling in several lung pathologies and macrophage differentiation and function. It is unknown whether aging alters S1P signaling that appears involved in lung inflammation, injury, and apoptosis. We postulated that aging and injurious mechanical ventilation synergistically impair macrophage polarization in the lung that is associated with dysfunctional S1P signaling and produces amplified alveolar barrier damage and diminished pulmonary function. Young (2-3mo) and old (20-25mo) C57BL/6 mice were mechanically ventilated for 2 hours using pressure-controlled mechanical ventilation (PCMV). We assessed tissue mechanics, lung injury/repair responses, macrophage polarization, and S1P/S1PL lung activity. PCMV exacerbated lung injury in old mice. CD80 and CD206, classical and alternative macrophage markers, were both elevated in old alveolar and interstitial macrophages that

also further increased due to PCMV. S1P lung levels were elevated in the young ventilated mice compared to the control group, which was not observed with the old mice. S1P lyase expression increased in the young and old ventilated mice and the old nonventilated group. 2-Acetyl-4-tetrahydroxybutyl Imidazole (THI) administration reduced indications of ALI in both young and old mice and altered macrophage polarization.

The structural and cellular implications in injury responses of an aging lung more accurately represent clinical conditions and warrant further study at a cellular level. We found that aging significantly impacts alveolar epithelial and lung macrophage signaling and polarization; moreover, these aging disparities may result from elevated ER stress and/or a loss of protective S1P signaling in response to mechanical stretch that further contribute to the age-associated susceptibility and alveolar barrier dysfunction. Furthermore, administration of 4PBA, an ER stress inhibitor, and THI, an S1PL inhibitor, attenuated ER stress and S1PL activity, respectively, as well as several indications of ALI.

## CHAPTER 1: INTRODUCTION

### **1.1 Rationale:**

Several lung pathologies and conditions require mechanical ventilation (MV) as a clinical intervention; however, this medical procedure frequently exacerbates the original pulmonary insult and produces an exaggerated inflammatory response that potentially leads to sepsis, multisystem organ failure, and mortality<sup>1</sup>. This acute lung injury (ALI) condition is termed Ventilator-Induced Lung Injury (VILI). VILI is characterized by hypoxia, an influx of inflammatory cytokines, loss of alveolar barrier integrity, and decreased lung compliance, believed to be caused mainly by three mechanisms of injury: alveolar overdistention, cyclic atelectasis, and biotrauma<sup>1,5</sup>. The over-distension of aerated lung regions generates abnormally large strains on the epithelium that directly causes barrier disruption, cellular necrosis and apoptosis, and an immense secretion of pro-inflammatory cytokines<sup>1,9,10</sup>. The high transmural pressures produced can activate pro-inflammatory signaling pathways that further deteriorate alveolar barrier integrity<sup>1,11</sup>. These damaging mechanisms enhance the release of inflammatory mediators, classified as biotrauma, which can cause further lung and distal organ injury<sup>9,12</sup>. However, the factors that govern this progression need to be better understood to provide treatment targets.

Alveolar epithelial cells contribute to the initiation, amplification, and resolution of inflammatory processes in the lung<sup>13,14,16</sup>. Although macrophages are the predominating players in mediating inflammation and tissue remodeling<sup>15</sup>, there is a lack of understanding of the role of epithelial cells and the *mechanotransduction* signaling to macrophages in related pathophysiological states. Epithelial cells can produce inflammatory mediators assumed to be involved with injury and repair responses, such as the recruitment and regulation of macrophages<sup>13,14,16,28</sup>. While the alveolar epithelium is considerably involved with the *mechanotransduction* and inflammatory responses that are characteristic of VILI, the precise mechanisms of how mechanical strain leads to inflammation are still widely unknown.

Furthermore, the largest population negatively affected by mechanical ventilation is elderly with high in-hospital mortality rates (53%)<sup>10,18</sup>. Age is a predictive factor in the severity of VILI<sup>18,19</sup>; however, the exact relationship and mechanisms between age and the severity of VILI are still unknown. For example, experimental injurious mechanical ventilation caused worsened pulmonary permeability and lung tissue damage in older subjects compared with young counterparts<sup>19,20</sup>. The increased sensitivity and susceptibility in the elderly may be attributed to the changes in lung structure and function that occur with aging. Several lung and supportive extrapulmonary structural changes occur with aging that have significant impacts on pulmonary function and physiology<sup>21</sup>. These structural deviations lead to adverse respiratory mechanics, which impact expiratory flow, lung volumes, and overall gas exchange<sup>22</sup>. The following associations occur with aging and the respiratory system: the chest wall becomes less compliant, the lung parenchyma loses elasticity, the average alveolar diameter increases, and overall lung capacity diminishes<sup>19,21,22</sup>. Additionally, the lungs capacity to recover from injury weakens, and inflammatory responses are believed to increase over time. These physiological changes in the aging lung correlate to each of the proposed mechanisms of VILI. Accordingly, age is a predictive factor in the severity of VILI<sup>17-19</sup>; however, the exact relationship between age and the severity of VILI is currently unknown. The increase in the severity of VILI with patient age combined with the increased need for ventilation and mortality rate among the elderly stresses the need to investigate this relationship. The physiological changes in the aging lung correlate with the proposed mechanisms of VILI; however, the impact of age-related changes in pulmonary structure and function in VILI still lacks clarity. The increases in the severity and mortality rates of VILI with patient age combined with the greater need for mechanical ventilation among the elderly stresses the need to investigate the influence of aging in mechanical injury.

The aging lung also exhibits indications of cellular senescence and is linked to aging of the immune system, known as immunosenescence<sup>23</sup>, as shown in Figure 1. A condition of mild, systemic inflammation is associated with and predictive of many age-related diseases<sup>24</sup>. This state, termed *inflammaging*, occurs without overt infections or injury and is characterized by a state of chronic, low-intensity inflammation<sup>25</sup>. Comparative studies in healthy individuals suggest that the elderly have higher

signs of proinflammation compared with younger individuals, which may be associated with the increased susceptibility to ALI/VILI<sup>23–25</sup>. Aging of resident and systemic immune cells is believed to lead to an intensified proinflammatory environment and reduced capacity of fighting infectious diseases<sup>23,25</sup>.

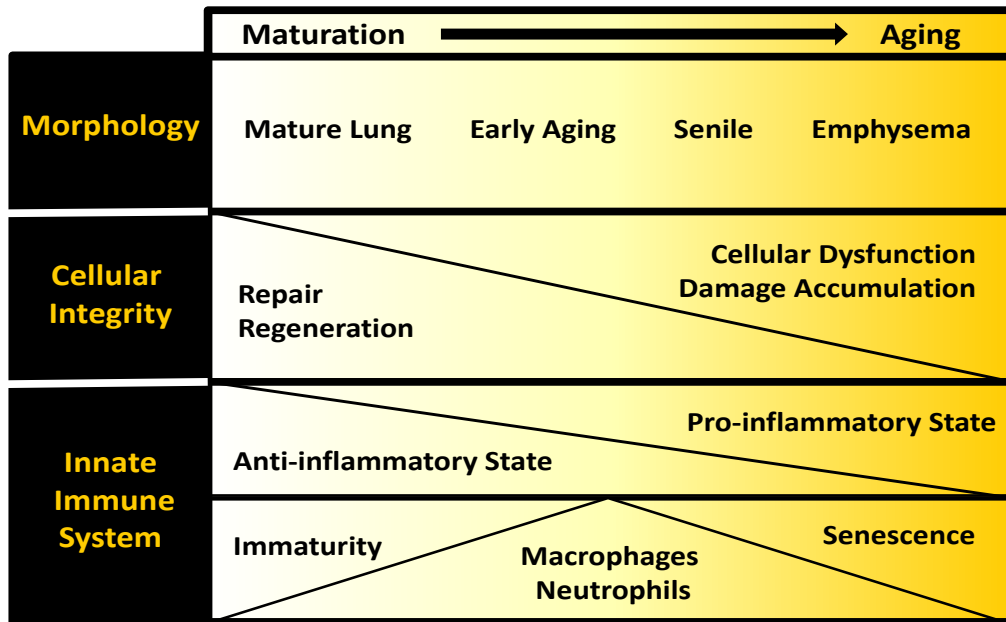


*Figure 1: Implications of Aging on Lung Structure, Cellular Integrity, and the Innate Immune System. Aging results in an emphysema like morphology, cellular dysfunction and an accumulation of damage, cellular senescence, and inflammation.*

Lung macrophages, comprising of alveolar and interstitial macrophages, act as the first immune defense system of the lung by clearing harmful pathogens and activating the innate immune system<sup>26</sup>. Lung macrophages also contribute to barrier integrity and local inflammation as mediators of inflammatory signaling between the epithelium and other immune cells<sup>13,27,28</sup>. In experimental VILI models, alveolar macrophages were shown to be vital to the increases in lung vascular and alveolar epithelial permeability and subsequent pro-inflammatory activation and amplification<sup>29</sup>. Studies on age-related effects of lung macrophages suggest that the cells' phagocytic capacity, TLR signaling, cytokine release, and reactive oxygen species (ROS) activity are critically impaired or elevated in older individuals<sup>23,30</sup>. However, the evidence for age-related changes in inflammatory signaling and cytokine expression and secretion by lung macrophages remains controversial. Several *in vitro* studies of monocyte or macrophage function have been contradictory, as few showed that the capacity of several

myeloid cells to produce certain inflammatory cytokines could be impaired in old age, while others have shown proinflammatory secretion only to be enhanced<sup>23,24</sup>. As most age-related diseases share an inflammatory pathogenesis, this phenomenon needs more clarification in the context of acute lung injury and is believed to be a significant risk factor for both morbidity and mortality in the elderly population.

Macrophages also show high plasticity and result in heterogenic subpopulations or polarized states that can be identified by specific cellular markers<sup>31</sup>. Macrophage phenotypes may be largely classified as either pro-inflammatory, also called M1 polarization, or they can reflect an M2 profile, which has been considered as anti-inflammatory<sup>24,32,33</sup>. M1 macrophages, or classical activation, promote the development of acute lung injury, whereas M2 macrophages, or alternative activation, may be involved in limiting or resolving lung inflammation<sup>31</sup>. Macrophage polarization is highly involved in physiological transitions from inflammation to tissue regeneration and is impaired with aging; however, the relevant studies have been contradictory and remain controversial.

One potential regulator of age-associated inflammation is the Endoplasmic Reticulum (ER). The ER is a multifunctional organelle responsible for lipid biosynthesis, calcium storage, and protein folding and processing<sup>34,52</sup>. Disruption to Endoplasmic Reticulum (ER) homeostasis results in activation of the unfolded protein response (UPR) and accumulation of misfolded proteins, known as ER stress, which may lead to the impairment of cellular functions, cellular apoptosis, and plays a key role in many chronic inflammatory disease states<sup>52,63</sup>. Specifically, ER stress regulates apoptosis and epithelial to mesenchymal transition in alveolar epithelial cells<sup>72</sup>. ER stress is increasingly dysregulated with age<sup>34,54</sup>. There is a general age-associated increase in the occurrence of protein misfolding and accumulation<sup>54</sup>. Unsurprisingly, ER stress is implicated as a promoter of many pathological disease states associated with aging<sup>34</sup>. For example, lung-related ER stress is implicated in the age-associated increase in pulmonary fibrosis<sup>61</sup>. To further validate that regulating the ER stress response may attenuate negative outcomes associated with ARDS and VILI, these aging inferences need to be investigated to understand the potential therapeutic targets.

While several studies have shown convincing evidence for a dominant role of ER stress in various diseases, there have only been a few studies investigating ER stress in the context of ALI/VILI. ER stress has been shown to be involved in numerous lung diseases, including lung cancer, pulmonary fibrosis, asthma, cystic fibrosis, hyperoxia-induced lung injury, cigarette smoke exposure, pulmonary infection, and ALI<sup>5,52</sup>. Several ER stress pathway proteins are key modulators of epithelial permeability and barrier dysfunction in young mice and rats<sup>59,60,71</sup>. Zeng et al showed that unresolved ER stress played a significant role in LPS-induced inflammation<sup>62</sup>. Extended epithelial stretch activates ER stress pathways, which resulted in increased alveolar permeability, cell death, and proinflammatory signaling<sup>63,133</sup>; however, these implications have yet to be investigated in an aging model. Dolinay et al., revealed that ER stress and the UPR are key modulators of epithelial permeability<sup>63</sup>. Furthermore, inhibition of an upstream regulator of the ER stress pathway managed to decrease injury signaling and improve overall barrier function after prolonged cyclic stretch and injurious mechanical ventilation<sup>63</sup>. Evidence also suggests that ER stress also regulates macrophage polarization that is involved in inflammation, host defense, and maintaining tissue homeostasis<sup>64,68</sup>. Together, these findings implicate the role of ER stress in numerous diseases, including lung conditions such as ALI/VILI. Furthermore, the studies provide evidence that therapeutic targeting ER stress and the UPR may attenuate ALI/VILI and needs further evaluation. There is also a lack of investigations on how aging influences these responses in ALI/VILI, illustrating the need to understand better how ER stress relates to the increased susceptibility of the elderly population.

The implication of ER stress in lung conditions and diseases suggest that targeting ER stress and the UPR may have vast therapeutic potential in mitigating ALI/VILI<sup>63</sup>. Dolinay et al., utilized a PERK inhibitor treatment for partial inhibition of the ER stress pathway following cyclic stretch and injurious mechanical ventilation, which caused reduced injury signaling and improved barrier function following injury induction<sup>63</sup>. More frequently, studies that examine ER stress intervention have utilized the chemical inhibitor, 4-phenylbutyrate (4PBA). 4PBA is a low molecular weight compound that acts as a general inhibitor of ER stress by stabilizing protein conformation, improving the folding capacity of the ER, and

chaperones mutant proteins to further suppress ER stress activity<sup>71,72</sup>. Zeng et al., demonstrated that 4PBA administration prevented the activation of the NF- $\kappa$ B pathway, decreased the secretion of pro-inflammatory mediators, such as IL-1 $\beta$ , TNF $\alpha$ , and IL-6, and significantly inhibited LPS-activated ER stress in a LPS-induced mouse model of ALI<sup>62</sup>. Furthermore, the authors showed that 4PBA also reduced autophagy activity, which may play a protective role through the classical AKT/mTOR signaling pathway<sup>62</sup>. We believe that 4PBA may attenuate the negative outcomes associated with mechanical injury and the increased susceptibility to injury from aging.

The cellular *mechanotransduction* that occurs at the alveolar barrier has a critical role in mediating ALI/VILI<sup>36</sup>. The *mechanotransduction* of the physical forces that stretch the pulmonary barrier leads to many biochemical and biophysical changes at the cellular and structural level that include extracellular matrix (ECM) remodeling, stress fiber reorientation, cell-cell and cell-ECM adhesions, activation of various nuclear transcription factors, and secretion of inflammatory cytokines and chemokines<sup>36</sup>. The mechanical forces from cell-stretch and injurious mechanical ventilation directly distend cell membranes and induce activation and phosphorylation of receptor<sup>73</sup>, cation channels<sup>74</sup>, phospholipases<sup>75</sup>, and relevant signaling pathways and transcription factors that regulate lung inflammation and injury<sup>76-78</sup>. Phospholipids and sphingolipids are membrane lipids that are present in all eukaryotic cells that act as structural components of cell membranes. Recently, evidence suggests these biomolecules and their metabolites also act as intracellular and extracellular signaling molecules in both normal and several pathological conditions<sup>79</sup>, including several lung conditions such as ALI/VILI<sup>37,80</sup>.

Sphingosine-1-Phosphate (S1P), a very bioactive sphingolipid, is involved in several cellular functions, such as cell growth and apoptosis, and signals both intracellular and extracellularly<sup>35</sup>. S1P Lyase (S1PL) irreversibly degrades S1P to hexadecenal and ethanolamine phosphate<sup>37</sup>. Recent studies suggest a critical role for S1P/S1PL signaling in several lung pathologies that includes sepsis, pulmonary artery hypertension, pulmonary fibrosis, asthma, and bronchopulmonary dysplasia<sup>36</sup>. Studies have shown that various ligands of G-protein coupled receptors, such as S1P, can greatly influence macrophage differentiation and function under physiological and disease conditions. To date, it is unknown whether

aging influences these signaling mechanisms that have been shown to help regulate lung inflammation, injury, and apoptosis<sup>36</sup>. Targeting the S1P metabolic pathway, including manipulating S1P levels or S1P Lyase expression with drugs, such as 2-Acetyl-4-tetrahydroxybutyl Imidazole (THI) that reduces S1PL expression, have shown tremendous promise in animal models of ALI and other lung diseases<sup>37</sup> and should be further investigated as a protective therapy from mechanical injury and the increased susceptibility from aging.

Implementing “protective ventilator strategies” has only marginally improved negative outcomes, and the overall mortality rates for ventilated patients are still unacceptably high<sup>1-6</sup>. Furthermore, few studies are performed on aged subjects, which is incongruent with the fact that elderly patients have a greater need for mechanical ventilation. These observations illustrate the major clinical need to develop treatments or therapies that prevent the cellular injury mechanisms and inflammation directly resulting from the pathological mechanical forces generated during mechanical ventilation.

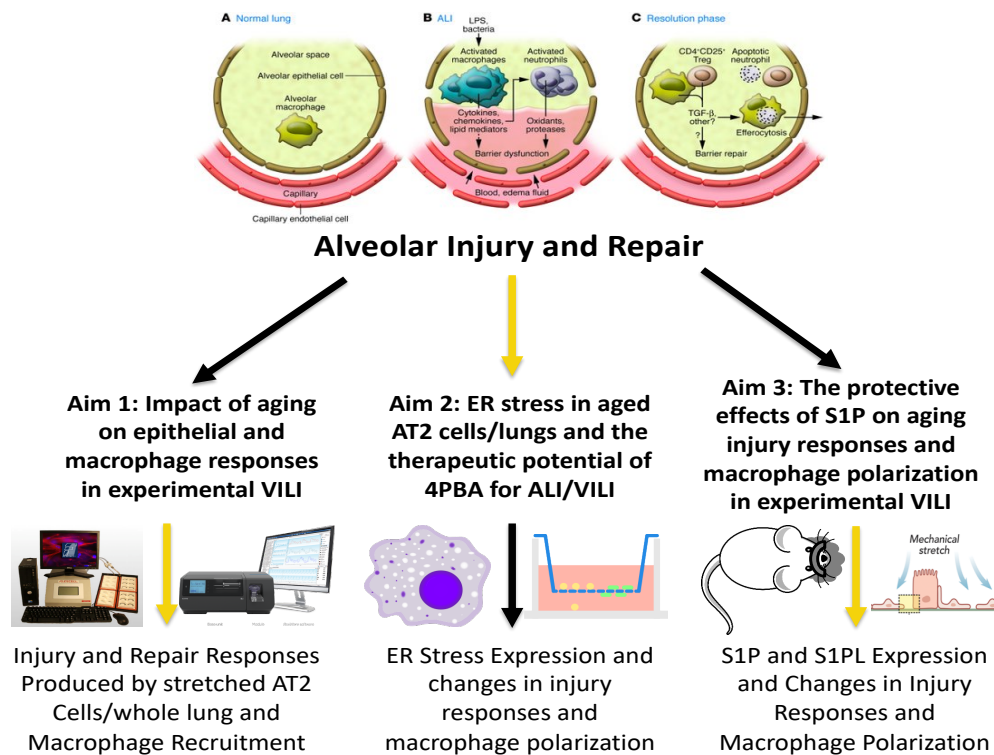


**Figure 2: General overview schematic of the aims and approach.** The objectives of this research investigation were broken down in three separate aims. Aim 1 evaluates injury responses in a cell-stretch and animal model of ALI/VILI. Aim 2 addresses the function of ER stress in the experimental ALI/VILI models. Aim 3 investigates the protective role of S1P in experimental ALI/VILI.

## **1.2 Objectives:**

The central focus of this research is to further understand the governing factors that contribute to the increased susceptibility of the elderly population to lung injury, specifically mechanical damage, and to determine the effectiveness of these identified, age-related therapeutic targets that may be manipulated to attenuate the lung injury and inflammation instigated by mechanical injury. We suspected that the cellular and structural changes in aged lungs cause the elderly to be more susceptible to the negative outcomes resulting from the mechanical stresses generated during mechanical ventilation. I hypothesized that the age-dependent impairment of ATEC injury responses and macrophage recruitment transpires from elevated endoplasmic reticulum stress, which may be mitigated with 4-phenylbutyrate (4PBA). Furthermore, I hypothesized that there is a loss of S1P signaling with aging that contributes to an enhanced, prolonged acute inflammatory response and further produces alveolar barrier damage, alters macrophage polarization, and diminishes pulmonary function in ventilator-induced lung injury. Additionally, the administration of THI, an S1P Lyase suppressor, will increase S1P levels in aged lung tissue and improve the age-related negative outcomes associated with mechanical injury. We will investigate these hypotheses through the following aims:

### **Aim 1A: Evaluate age-related disparities in alveolar epithelial type II cell injury and macrophage recruitment in an *in vitro* cell-stretch model.**

This aim was evaluated by exposing primary Alveolar Epithelial Type II cells from young (2mo) and old (20mo) C56BL6 mice to injurious mechanical stretch as a model of ALI/VILI and studying the acute injury and inflammatory responses. Injury and inflammatory signaling factors were quantified to better understand how aging impacts these mechanisms in an acute phase. Primary ATEC cells were stimulated with 0% or 15% cell-stretch for durations of 4 and 24 hours to evaluate the temporal behaviors of these responses. Macrophage recruitment was also evaluated by exposing bone-marrow derived macrophages (BMDMs) from young (2mo) and old (20mo) C57BL6 mice to conditioned media from young and old ATECs exposed to injurious mechanical stretch.

**Aim 1B: Assess pulmonary structure, function, and macrophage responses in an injurious age-related ALI/VILI/ rodent model.**

An injurious pressure-controlled mechanical ventilation protocol was modified and implemented on young (2mo) and old (20mo) mice to compare them to non-ventilated controls. Several indications of acute lung injury were assessed between the two age groups, such as histological airspace enlargement and neutrophil accumulation, as well as age-related deviations in pulmonary structure and function with and without injury induction. Aging disparities between alveolar and interstitial macrophage polarization was evaluated by implementing a modified, systematic flow cytometry approach recently developed to study macrophage subsets in a normal and bleomycin-induced fibrosis mouse model.

**Aim 2: Examine the role of ER stress and the administration of 4PBA, and ER stress reducer, as therapeutic intervention in experimental ALI/VILI models**

Age-related indications of Endoplasmic Reticulum (ER) stress were characterized in the experimental models of ALI/VILI. The administration of 4PBA, a known ER stress reducer, prior to mechanical stretch or ventilation was examined as a preventative therapy to attenuate the increases in alveolar barrier damage and dysregulated inflammatory responses observed in Aim 1. We also investigated the protective effects of 4PBA on macrophage recruitment by exposing young and old BMDMs to conditioned media of ATII cells that were administered 4PBA prior to mechanical stretch.

**Aim 3: Investigate the protective effects of S1P signaling and S1P lyase suppression as a therapeutic intervention in experimental ALIVILI models.**

Levels of Sphingosine-1-phosphate (S1P) and S1P lyase (S1PL) were quantified in the lung tissues of young and old ventilated mice and compared to non-ventilated controls to determine a protective role of S1P in response to mechanical injury. Following this characterization, the administration of 2-Acetyl-4-tetrahydroxybutyl Imidazole (THI), a drug that inhibits S1P lyase activity and elevates levels of S1P, was investigated as a protective therapy to mechanical injury.

## CHAPTER 2: BACKGROUND

### **2.1: The Effects of Mechanical Injury and Aging on ATII and Macrophage Responses:**

Mechanical ventilation frequently exacerbates underlying pulmonary conditions and produces an intensified inflammatory response that may lead to sepsis and multisystem organ failure<sup>1,7,8</sup>. This exacerbation or injury is classified as Ventilator-Induced Lung Injury (VILI). The pathophysiology of VILI is characterized by an exaggerated inflammatory cytokine release and influx of inflammatory cells, loss of alveolar barrier integrity and subsequent pulmonary edema formation, decreased lung compliance, and profound hypoxia<sup>1,5-8</sup>. These features reflect three integrated mechanisms of injury: alveolar over-distention, cyclic atelectasis, and inflammatory cell activation<sup>1,7,8</sup>. These physical injury mechanisms are frequently modeled *in vitro* with mechanical stretch using lung epithelial or endothelial cells<sup>14,74,78</sup>.

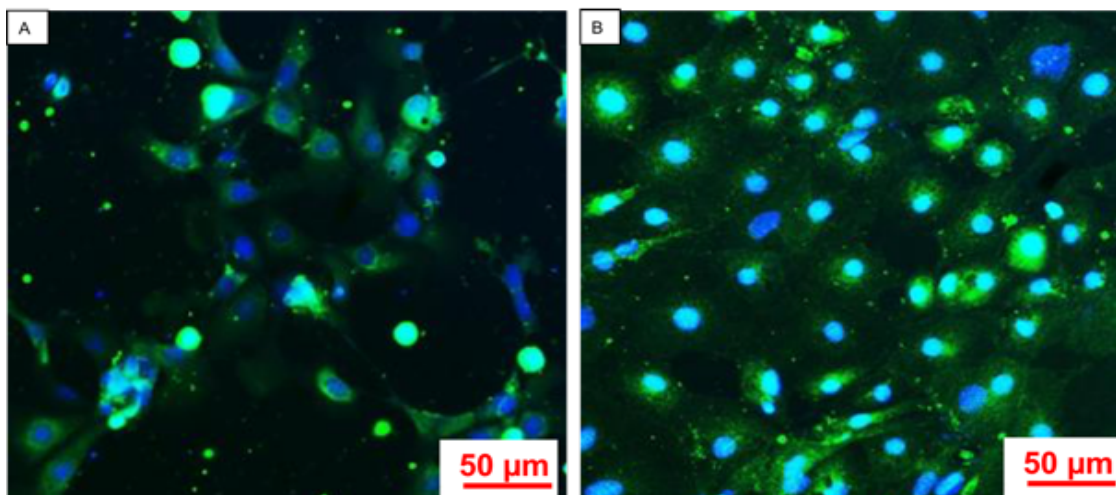


*Figure 3: Primary Alveolar Type II Cells (ATII) express Surfactant Protein C. Surfactant Protein C (Green) is used to validate cell purity and separate from other cell types during isolation. The nuclei were stained with DAPI(Blue). (A) Depicts ATII isolated from young mice and (B) portrays old ATII.*

The alveolar epithelium plays a major role in maintaining adequate gas exchange by greatly contributing to the barrier formation and maintenance<sup>28,127</sup>. The epithelium is mostly comprised of squamous type I alveolar cells (ATI) and cuboidal type II epithelial cells (ATII). Although ATI cells cover about 90% of the alveolar surface in adult lungs, ATII cells mediate surfactant homeostasis in order to

regulate surface tension in the lung and prevent total collapse leading to atelectasis injury<sup>28,127</sup>. AII cells are characterized by prosurfactant C staining<sup>28</sup>, as shown in Figure 3. They also serve as the main progenitor cells during repair of the alveoli by functioning as self-renewing cells that transition into type I alveolar cells<sup>28,127</sup>. These cells create multiple barriers that are important in maintaining adequate gas exchange via their secretory products, surface glycocalyxes and membranes, and intercellular junctional proteins<sup>28,127</sup>. Disruption to these complexes directly results in increased epithelial permeability and increases in local inflammation in both the conduction airways and the alveolar regions<sup>14,28,74,127</sup>. These responses are characteristic and contribute greatly to the pathogenesis of ARDS and VILI. Yet, the impact of aging on the alveolar epithelium's responses in injury and repair still needs to be examined.

Alveolar epithelial cells are exposed to a variety of physical forces during mechanical ventilation and mechanical stretch that lead to changes in structure, function, metabolism, and signaling<sup>28,127</sup>. These cells' ability to sense mechanical forces and relay that information to surrounding cells via signaling cascades has been evident in numerous studies<sup>28,74,127</sup>. However, the underlying mechanisms of alveolar epithelial *mechanosensation* and *mechanotransduction* are thus far insufficiently comprehended. A high level of mechanical stretch has been shown to induce increased epithelial cell necrosis and extracellular matrix remodeling<sup>14,28,74,127</sup>, which plays a major role in structural maintenance and tissue homeostasis<sup>28,127</sup>. Other more recent studies have also suggested that alveolar epithelial cells participate in lung inflammation, which is a major component of VILI<sup>13,14,28,127</sup>. Epithelial cells produce cytokines and inflammatory mediators that are assumed to be involved in the recruitment and regulation of macrophages<sup>13,14,28,127</sup>. Cyclic stretch of alveolar epithelial cells resulted in increased cell injury and death, apoptosis, acidification, bacterial growth, and general inflammatory response, which is often represented with amplified gene expression and release of IL-6 and IL-8, and other cytokines and chemokines<sup>14,28,74,127</sup>. Studies showed that alveolar epithelial cells significantly participated in the initiation, amplification, down-regulation, and tissue-repair stages associated with lung inflammation<sup>13</sup>. In an *in vitro* model, cyclic stretch of alveolar epithelial cells triggered inflammatory signaling mechanisms in a force- and frequency-dependent manner<sup>14,74,78,137</sup>. Specifically, there was an increase in interleukin-

8 (IL-8), which is a known marker of deformation-induced inflammatory signaling as it is a potent neutrophil chemoattractant that plays a major role in the pathogenesis of acute lung injury<sup>14,74</sup>. Mechanically stretched fetal rat lung cells induced significant cytokine production that may play a vital role in the induction and progression of VILI<sup>137</sup>. Mechanical stretch also generates a force- and frequency-dependent production in macrophage inflammatory protein 2 (MIP-2), which is a rodent homologue of human IL-8 and is a vital mediator in many inflammatory reactions<sup>127</sup>. Furthermore, stretch-induced release and activation of matrix metalloproteinases (MMPs) and the modification of proteoglycan and glycosaminoglycans, which are involved in tissue repair<sup>51,113</sup>. MMPs are known to play a significant role in regulating ECM remodeling, while proteoglycans and glycosaminoglycans impact inflammatory responses through the interaction with various chemokines and by acting as ligands for Toll-like receptors<sup>51</sup>. These downstream responses lead to the induction and progression of several lung pathologies, including VILI. These observations further suggest that certain mechanisms exist between alveolar epithelial and immune cell interactions to regulate the local inflammatory milieu and maintain tissue homeostasis. Although these interactions are recognized, the underlying signaling mechanisms are still not well elucidated.

Mechanical ventilation also leads to poorer outcomes in the elderly population. Mortality rates and hospital discharge to extended care facilities increased consistently for each decade of age over the age of 65 years in mechanically ventilated patients<sup>17-19</sup>. Epidemiological studies also suggest that age is a predictive factor in the severity of VILI<sup>17-19</sup>; however, the exact molecular mechanisms between age and VILI are still unknown<sup>17-19</sup>. In rodent models of VILI, we and others have shown that age increases susceptibility to ventilator-induced edema, injury, and mortality<sup>10,19</sup>.

The aging lung exhibits indications of cellular senescence and is closely linked to the aging of the immune system, known as *immunosenescence*<sup>23</sup>. A condition of mild, systemic inflammation is associated with and predictive of many age-related diseases<sup>24</sup>. This type of state, termed *inflammaging*, occurs without the presence of overt infections or injury and is characterized by a state of chronic, low-intensity inflammation<sup>25</sup>. Comparative studies in healthy individuals suggest that the elderly have higher

indications of proinflammation compared with younger individuals, which could be associated with the increased susceptibility to ALI/VILI<sup>23-25</sup>. Aging of resident and systemic immune cells leads to an intensified proinflammatory environment and reduced capacity of fighting infectious diseases<sup>23,25</sup>. As shown in Figure 4, *Inflammaging* is believed to be macrophage centered<sup>38</sup> and intensely associated with many aging and inflammatory pathologies.

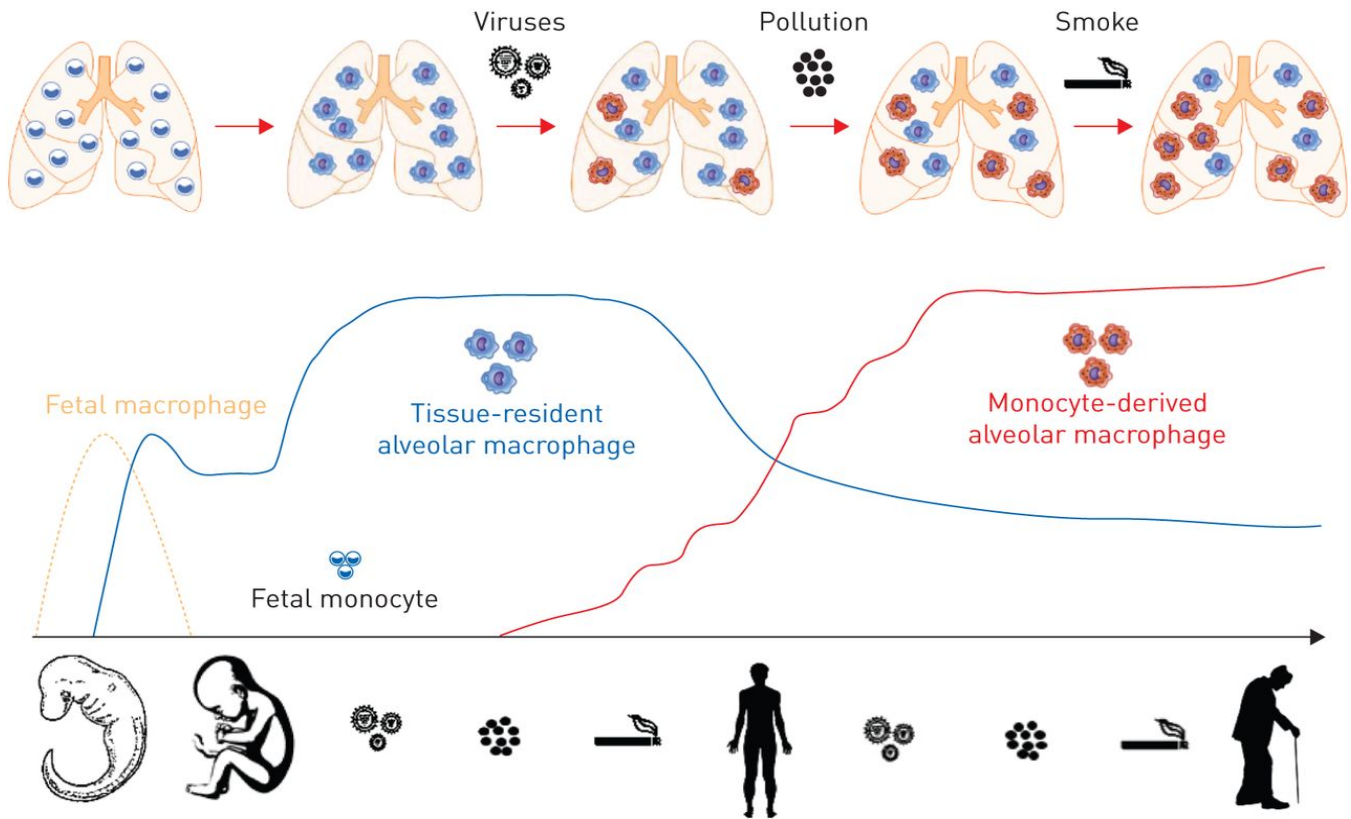


**Figure 4: Proposed Lung Macrophage development and changes during lifespan.** Exposure to environmental encounters over lifespan are believed to induce macrophage recruitment that differentiate into alveolar macrophages in response to local environment cues and stimuli. These monocyte-derived macrophages might remain in the lung and/or replace tissue-resident alveolar macrophages. Source: Morales-Nebreda et al., 2015<sup>157</sup>.

Macrophages are critical cells in many inflammatory responses and are highly involved with tissue healing and regenerative responses in various tissues<sup>15,24,26</sup>. These types of immune cells are a major signaling target of the epithelium in response to mechanical stretch or injury<sup>28,127</sup>. As shown in Figure 5, lung macrophages are comprised of alveolar and interstitial macrophages, which are believed to have different origins and life spans in the lungs<sup>23,27,31</sup>. These cells are suspected of being key regulators of pathological and reparative processes and greatly contribute to barrier integrity and local

inflammation<sup>15,24,26</sup>. It's been recently suggested that these two populations play opposing roles in lung injury<sup>31,101</sup>. Recent studies showed that alveolar macrophages appeared to limit neutrophil influx into the lung following acute injury induction or chronic exposure to dust, while interstitial macrophages were shown to promote neutrophil extravasation<sup>15,26,27,31</sup>. Frank et al., demonstrated that alveolar macrophages are vital to the increases in lung vascular and alveolar epithelial permeability that is characteristic of experimental VILI<sup>29</sup>. They showed that injurious mechanical ventilation directly activates alveolar macrophages and that these types of macrophages play a substantial role in the initial pathogenesis of VILI. Their study also suggests that alveolar epithelial cell-macrophage interaction was required for subsequent proinflammatory activation and amplification, indicating that mechanical stretch of epithelial cells or alveolar macrophages independently failed to result in significant, subsequent macrophage activation and inflammation. The specific roles of alveolar and interstitial macrophages in the context of acute lung injury and repair remain unclear and require further evaluation. As most age-related diseases share an inflammatory pathogenesis, this phenomenon needs more clarification in the context of ALI and is believed to be a highly significant risk factor for both morbidity and mortality in the elderly population.

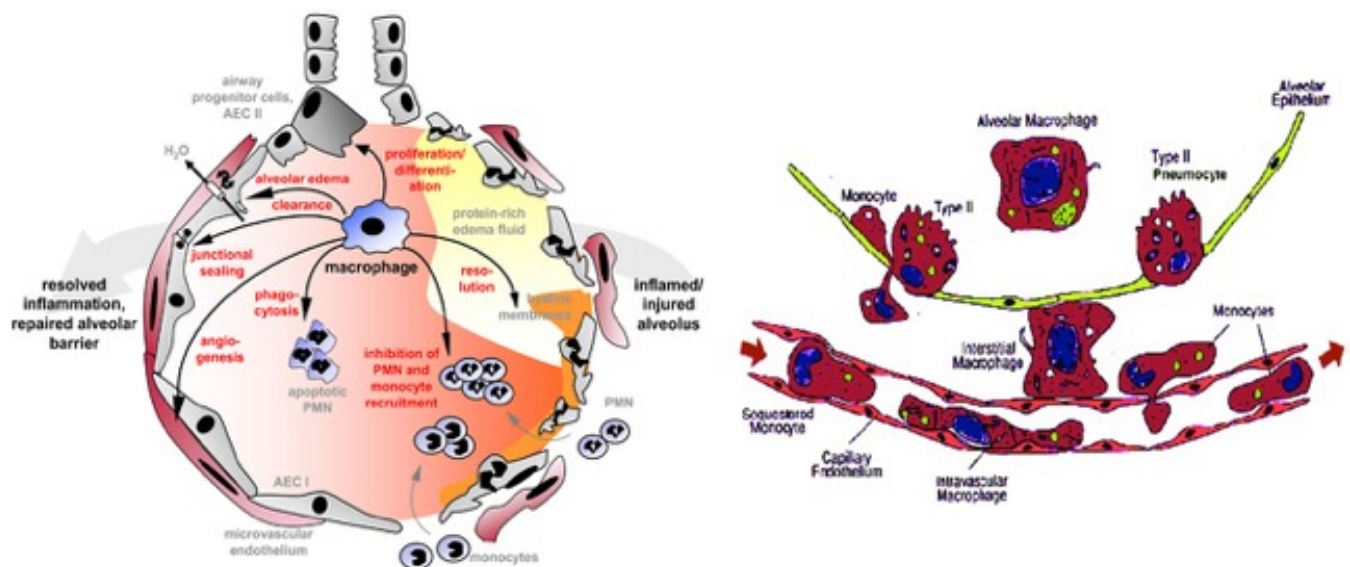


**Figure 5: Types of lung macrophages in the alveolar blood-gas region.** (A) Role of alveolar macrophages in injury and inflammatory responses in acute lung injury. Source: Herald et al., 2011<sup>158</sup>. (B) Lung macrophages consist of Alveolar and Interstitial Macrophages. This diagram depicts the location and types of immune cells around the alveolar blood-gas barrier. Source: Longworth 1997.

These roles are further complicated by the phenotypic plasticity of macrophages. As depicted in Figure 6, Macrophages show high plasticity, resulting in heterogenic subpopulations or polarized states that can be identified by specific cellular markers<sup>31</sup>. Macrophage phenotypes may be largely classified as either more proinflammatory or pro-injurious, also called classical macrophage polarization, or they can reflect an alternative activation profile, which has been considered as anti-inflammatory or pro-repair<sup>24,32,33</sup>. Classically-activated macrophages promote the development of acute lung injury, whereas alternatively-activated macrophages may be involved in limiting or resolving lung inflammation<sup>31</sup>. Classical macrophage activation can be induced by various environmental cues, such as interferon-gamma (IFN- $\gamma$ ), Toll-like receptor (TLR) signaling, and many others<sup>24,32,33,39</sup>. This polarization state is associated with activation of transcription factors STAT1 and NF- $\kappa$ B<sup>24</sup>. IL-4 and IL-13 may induce alternative macrophage polarization, and STAT6 is the main transcription factor involved<sup>24</sup>. Classical polarization is characterized by an upregulation of iNOS, CD80, CD86, and HLA-DR and elevated cytokine release of TNF- $\alpha$ , IL-6, IL-1, IL-12, IL-23, and type 1 interferon<sup>24,31</sup> in murine macrophages. Alternative activated murine macrophages are characterized by a cytokine release profile of IL-4, IL-10, IL-13, and IL-1 $\alpha$  and have increased expression of CD206, Ym1, CD163, CCL1, CCL18, FIZZ1, arginase 1 (Arg1), CD71, RELM $\alpha$ , and chitotriosidase<sup>24,31</sup>. Macrophage polarization is highly involved in physiological transitions from inflammation to tissue regeneration and it's believed to be impaired with aging; however, the relevant studies have been contradictory and remain controversial. Mahbub et al., found that M1 polarized splenocytes from aged mice resulted in decreased IL-1 $\beta$  and TNF- $\alpha$  protein levels compared to young counterparts<sup>40</sup>. Barrett et al., demonstrated that aged M1 polarized macrophages from rats had elevated responses to inflammatory stimuli compared to young counterparts, such as significantly higher levels of TNF- $\alpha$  expression<sup>41</sup>. Gibon et al. showed that aged macrophages overexpress both M1 and M2 surface markers, aged M1s upregulated TNF- $\alpha$ , aged M2 cells had reduced expression of Arg1 and CD206, and that aged M1 macrophages increase TNF- $\alpha$  secretion with no negative feedback<sup>42</sup>. These observations further indicate that the impact of aging on macrophage

polarization and function, especially in the context of acute lung injury, has been insufficiently investigated. The role of lung macrophage plasticity in response to VILI, and how aging impairs these mechanisms still lack clarity; however, the numerous subsets of activated macrophages appear to play a significant role in the progression and resolution of inflammatory responses, especially in the lung.

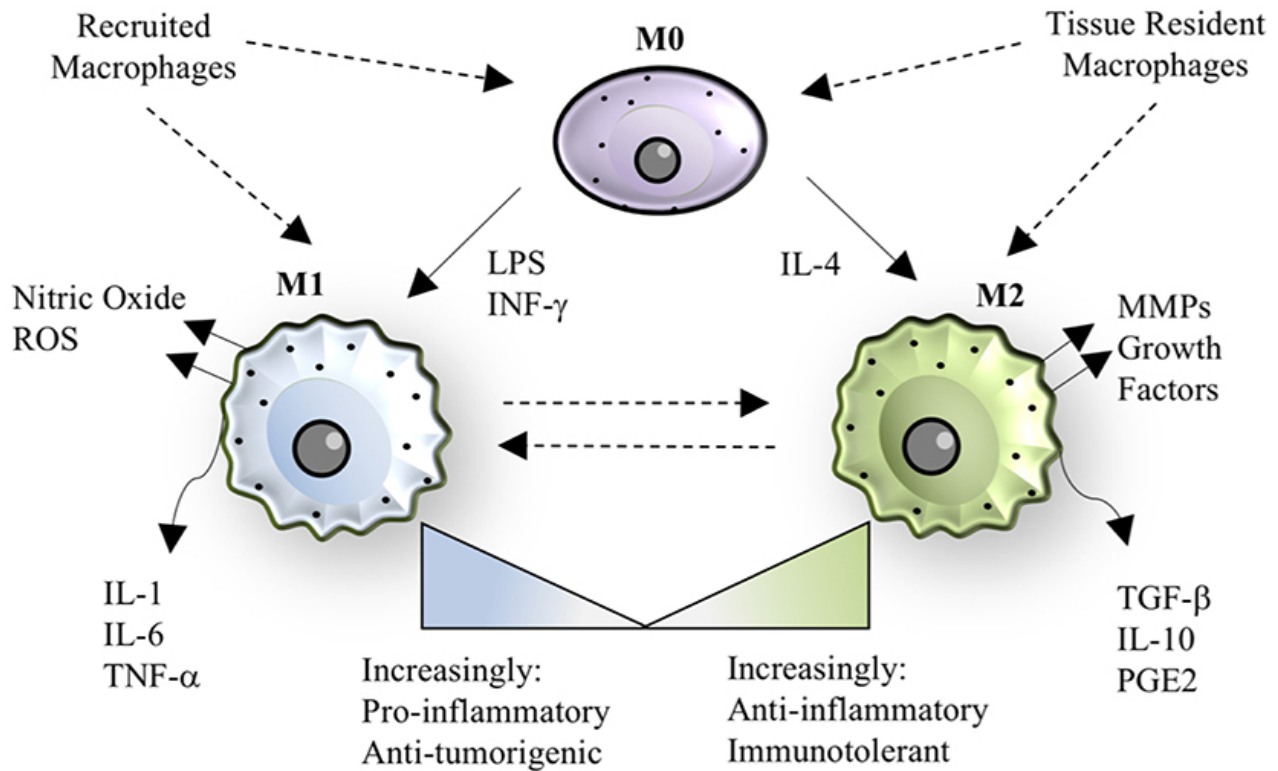


**Figure 4: Paradigm of Macrophage Polarization.** Diagram illustrates sources, stimuli, activation status, and signaling responses of associated M1 and M2 polarized macrophages. The graphic also depicts their proposed roles in tissue inflammation and cancer. Source: Stahl et al., 2018<sup>159</sup>.

Age-specific cell signaling mechanisms by ATII cells or macrophages could be viable therapeutic targets for patients requiring mechanical ventilation by preventing or regulating the exaggerated inflammatory response that often leads to sepsis and mortality. More recently, novel therapies attempt to target macrophage polarization, which could be an effective, innovative method to regulate the downstream inflammation and prevent subsequent alveolar barrier destruction. As the majority of patients that are diagnosed with VILI are the elderly, better understanding the age-dependent factors associated with the mechanotransduction between the alveolar epithelium and innate immune system is detrimental to developing treatments for these types of lung diseases.

## **2.2: Lung Structural and Functional Impairment Associated with Aging and Mechanical Injury:**

As the majority of patients that receive mechanical ventilation as a medical intervention are the elderly and evidence suggest that the elderly population has increased proneness to lung injury and infection, it is critical to investigate the factors that may contribute to this sensitivity. Experimental injurious mechanical ventilation caused worsened pulmonary permeability and lung tissue damage in older subjects compared with young counterparts<sup>19,20</sup>. The increased sensitivity and susceptibility in the elderly may be attributed to or enhanced by the changes in lung structure and function that occur with aging. It is believed that these deviations in the mechanical properties of the lung and full respiratory system may significantly contribute to the predisposition of the elderly to ALI.

The four major injury mechanisms associated with ALI/VILI are volutrauma, barotrauma, atelectrauma, and biotrauma<sup>1,7-9</sup>. The volutrauma caused by higher tidal volumes, the barotrauma caused by elevated airway pressures, and the atelectrauma caused by the cyclic collapse and reopening are the three primary injury mechanisms associated with mechanical ventilation that contributes to VILI<sup>1,7-9</sup>. The over-distension of aerated lung regions generates abnormally large stretching forces on the epithelium that directly causes barrier disruption, cellular necrosis and apoptosis, and an immense secretion of pro-inflammatory cytokines<sup>1,7-9</sup>. The atelectasis caused by the cyclic closure and reopening of fluid-filled airways generates dynamic air-liquid interfacial stresses that also contribute to significant barrier disruption and plasma membrane rupture<sup>1,7-9</sup>. The high transmural pressures produced can activate pro-inflammatory signaling pathways that further deteriorate alveolar barrier integrity<sup>1,7-9</sup>. These damaging mechanisms often lead to an enhanced release of local and systemic pulmonary inflammatory mediators that can cause further lung and distal organ injury that is classified as biotrauma<sup>9</sup>. However, the factors and mechanisms that govern this progression still need to be better characterized and understood.

Several pulmonary and supportive extra pulmonary structural changes occur with aging that have significant impacts on pulmonary function and physiology<sup>22,23,43,44</sup>. These structural deviations lead to adverse respiratory mechanics, which impact expiratory flow, lung volumes, and overall gas exchange<sup>22</sup>. Alveolar duct dilation and enlargement of alveolar air spaces that occur with aging lead to a reduction in

alveolar surface tension, increased lung compliance, and declines in tissue elasticity and dampening<sup>44</sup>. Changes in supportive extra pulmonary structures with aging include decreases in chest wall compliance and reductions in respiratory muscle strength which lead to increases in residual volumes and decreases in total lung capacities<sup>22,43,44</sup>. Age-related changes in gas exchange include V/Q inequality, which is the amount of air that reaches alveoli regions divided by the amount of blood flow in the alveoli capillaries, and decreased diffusion capacity of the lung for carbon monoxide, which cause an increased alveolar-arterial oxygen gradient and decreased PaO<sub>2</sub><sup>44</sup>. These physiological changes in the aging lung correlate with the proposed mechanisms of VILI; however, the impact of age-related changes in pulmonary structure and function in VILI still lacks great clarity. The increases in the severity and mortality rates of VILI with patient age combined with the greater need for mechanical ventilation among the elderly stresses the need to investigate possible associations between the structural and cellular changes that occur with aging and the increased susceptibility to lung injury of this population.

Damaged lungs are especially susceptible to the dynamic stresses and strains and injury mechanisms associated with VILI, such as volutrauma, barotrauma, and atelectrauma<sup>45</sup>. This is partially caused by the reduction in number of recruitable lung units and alveoli participating in gas exchange<sup>6,28,45</sup>. Collectively, the injury mechanics are believed to result in vast lung structural and functional changes, such as the degradation of lung mechanical properties<sup>46</sup>. Atelectrauma, caused by the increasing alveolar instability with cyclic alveolar recruitment and derecruitment and edema formation has been directly connected to reduction in lung mechanical properties<sup>46</sup>. Volutrauma and barotrauma result from the overdistention of interalveolar septa at high volumes or pressures, which have been shown to cause stress failure from interactions between cells and cell-matrix<sup>47</sup>. These injury mechanisms physically damage the alveolar barrier, lead to inflammation, and may produce secondary lung conditions such as pneumothorax or emphysema. The overdistention causes cell detachment from basement membranes, barrier cell junction ruptures, alveolar and interstitial edema, and cell death<sup>48</sup>. The secondary inflammatory response associated with VILI, known as biotrauma, leads to local tissue injury and cell death, edema formation, immune cell recruitment, and possible systemic and distal organ dysfunction.

Together, these responses cause vast alterations in lung structure and function. VILI is characterized by increased pulmonary pressure, diminished respiratory compliance, and increased physiological dead space in the lungs<sup>36</sup>. Surfactant dysfunction, alveolar collapse, edema formation, lung inflammation, fibrotic remodeling, and other characteristics of VILI impose harmful stresses and strains on surrounding tissue during ventilation that ultimately result in deviations in lung volume and structure, lung supportive structures, and cell/tissue composition<sup>48</sup>. These structural fluctuations result in vast variations in lung mechanical properties and lung function; such as the reduction in lung compliance and increased lung and chest wall elastance associated with VILI<sup>48–50</sup>. There is also a significant level of matrix remodeling that occurs following VILI. The increased cell proliferation, reduced collagen levels, and elevated MMP activity<sup>51</sup>. These indications of matrix remodeling lead to changes in lung structure and function<sup>51</sup>.

### **2.3 Endoplasmic Reticulum Stress and Therapeutic Potential in Aging and Acute Lung Injury:**

As indications of biotrauma and lung inflammation are elevated in acute lung injury and aging appears to exaggerate these responses, it is critical to understand better the cellular mechanisms that regulate this age-related intensification. One potential component that may contribute to the age-associated injury and inflammation is the endoplasmic reticulum (ER).

The ER is a multifunctional organelle responsible for lipid biosynthesis, calcium storage, and protein folding and processing<sup>34,52</sup>. The ER contains high concentrations of molecular chaperones and enzymes that assist the folding of specific proteins<sup>34,52,54,60</sup>. Protein aggregation in the ER occurs if the rate at which new proteins enter the ER exceeds its folding and secretion potential, which is known as ER stress<sup>34,52,54,60</sup>. Due to the innate inefficiency of protein folding, there can be as many as 30% of proteins that never acquire their fully folded, programmed conformation<sup>34,52,54,60</sup>. The unfolded protein response (UPR) is the collective cellular processes that defend against ER stress by reducing the activity of ribosomes with mechanisms to increase the protein-folding capacity of the ER. Additionally, misfolded proteins are identified and transported to the cytoplasm for degradation by the ubiquitin proteasome system<sup>34,52,54,60</sup>. This type of ER-associated protein degradation appears to be enhanced by the UPR and

maintains the removal of misfolded secretory proteins from the cell. When these protective systems fail and sustained ER stress remains unresolved, cellular death pathways become activated and the cell undergoes apoptosis<sup>34,52,54,60</sup>. For example, ER stress has been shown to regulate apoptosis in alveolar epithelial cells<sup>72</sup>. The misfolding of proteins in the ER affects the pathogenesis of copious disorders and diseases that includes many lung diseases, such as pulmonary fibrosis and cancers<sup>34,52,54,60</sup>. Under normal physiological conditions, protein aggregates do not accumulate in the cells and protective cellular mechanisms are detected and activated<sup>53</sup>. The ER prevents protein aggregation by accurately initiating and regulating transcription and translation, chaperoning nascent or unfolded proteins, and transporting improperly folded polypeptides to degradation, preventing their accumulation<sup>34,52,54,60</sup>.

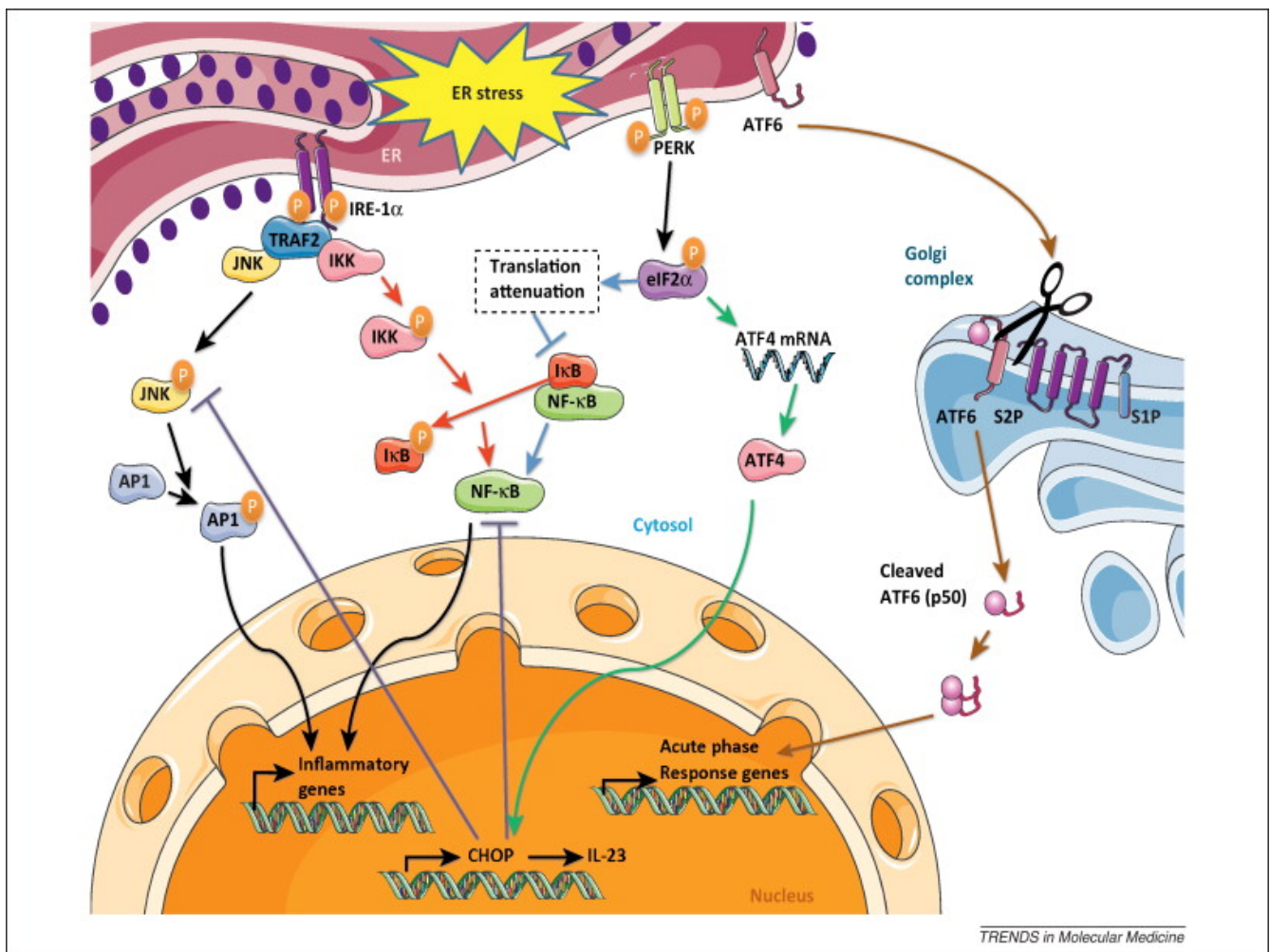


**Figure 5: Schematic Overview of associated ER stress-induced UPR signaling.** Diagram depicts the several signaling branches associated with ER stress between the ER, cytosol, Golgi complex, and nucleus within a cell. These mechanisms are activated in order to reduce causes of ER stress and reestablish homeostasis. Source: Garg et al., 2012<sup>160</sup>.

At the cellular level, the UPR activates three types of protective cellular responses: (1) increase ER chaperone activity, such as BiP/GRP78, to aid in the refolding of proteins; (2) protein translation attenuation by mediating PERK activity, which phosphorylates eIF2 $\alpha$  and reduces protein translation; and degradation of misfolded proteins by the proteasome via the ER-associated degradation (ERAD) pathway<sup>34,52,54,60</sup>. Ultimately, the three UPR responses are protective cell mechanisms to limit protein load and resolve ER stress<sup>34,52,54,60</sup>. If the UPR fails to restore folding capacity and prolonged ER stress occurs, inflammatory signaling and intrinsic and extrinsic apoptotic pathways are activated<sup>34,52,54,60</sup>. ER stress-related apoptosis is mainly mediated by C/EBP homologous protein (CHOP), which is downstream of the PERK and ATF6 pathways. CHOP induces the expression of numerous pro-apoptotic factors such as Tribbles 3, GADD34, and DR5<sup>34,52,54,60</sup>. Additionally, Bcl-2 family molecules, caspase-12, and JNK kinases are also involved in ER stress-mediated apoptosis<sup>54</sup>.

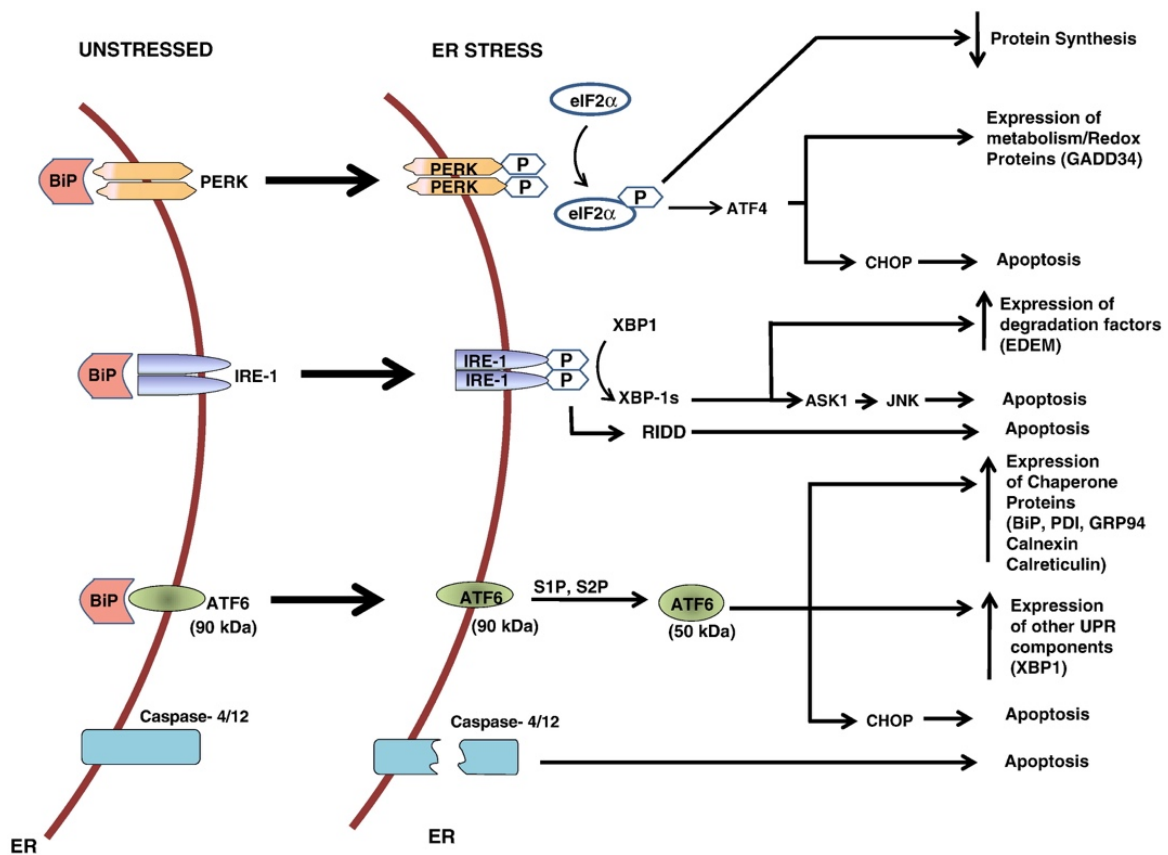


**Figure 6: Schematic diagram of ER stress, the UPR, and subsequent cell response outcomes.** Many of the UPR branches attempt to reduce the causes of ER stress; however, prolonged, unresolved ER stress results in inflammation and apoptosis. Source: Tanjore et al., 2013<sup>161</sup>.

Recent studies suggest a role for unfolded/misfolded proteins in normal aging and age-related cognitive dysfunction<sup>54</sup>. ER stress has been implicated in numerous age-related diseases and disorders such as Type 2 diabetes and other metabolic disorders, sleep deprivation, neurodegenerative diseases, atherosclerosis and Hyperhomocysteinemia, cancer, and more<sup>34,52,54</sup>. Age-related reductions in cellular factors leads to increased protein misfolding, accumulation, and aggregation<sup>34,52,54,60</sup>. Studies suggest this is partially due to a gradual loss or impairment of chaperoning systems and important ER enzymes, such as BiP, PDI, calnexin, and GRP94, that assist with the reduction of misfolding proteins in the ER<sup>55</sup>. Chaperones are continuously oxidized with aging, and this incessant process may contribute to their functional dwindling. Generally, proteins or protein fragments change from native soluble forms into insoluble fibrils or aggregated plaques that cluster in organs in many age-associated diseases. Evidence suggests that there is a transition that occurs during aging, where the protective adaptive response of the UPR becomes significantly reduced and the pro-apoptotic signaling becomes more robust<sup>53,56,57</sup>.

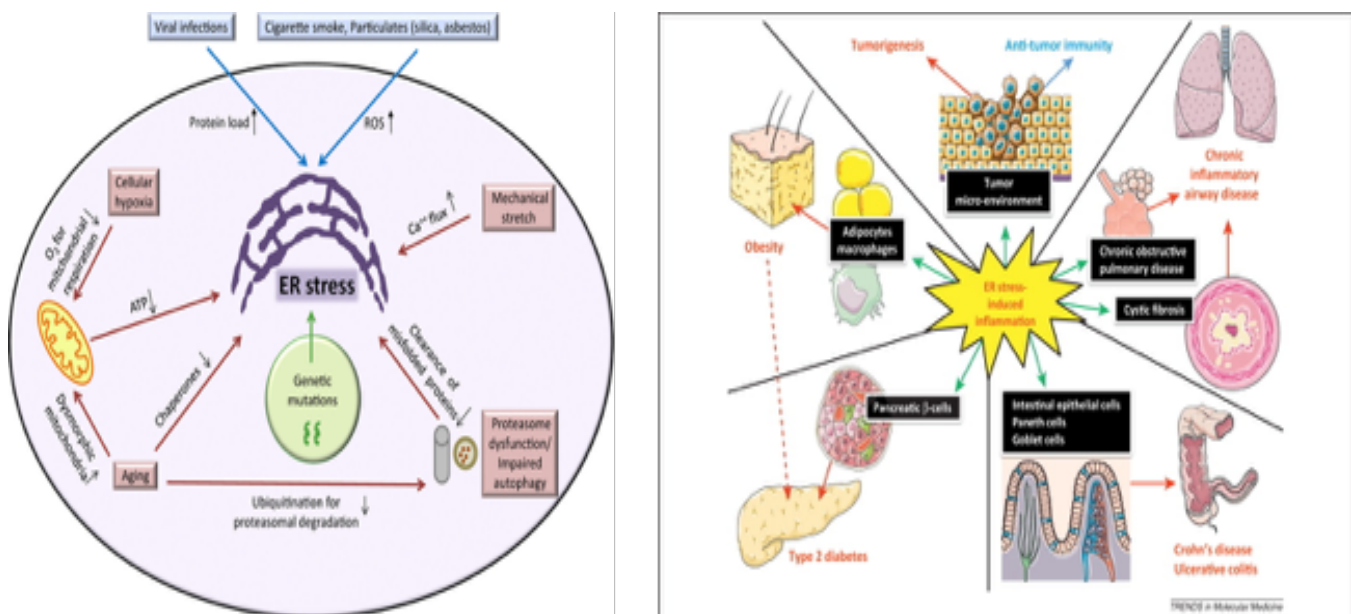


**Figure 7: Proposed triggers and implicated diseases associated with ER stress and the UPR.** (A) Potential causes that lead to cellular ER stress. Source: Burman et al., 2018<sup>61</sup>. (B) Related inflammatory diseases associated with ER stress. Interaction between inflammation and ER stress signaling is believed to compound or impede the pathogenesis and/or progression of certain diseases. Source: Garg et al., 2012<sup>160</sup>.

Naidoo et al., showed that BiP protein levels were decreased 30% in the cerebral cortex of aged (22-24-month old) C57/B6 mice compared to young (3-month old) mice<sup>53</sup>. Additionally, BiP mRNA and protein expression levels were decreased in the hippocampus of aged (23-26-month-old) Wistar rats compared to young (4-6-month-old)<sup>56</sup>. Evidence also suggests that BiP protein expression in peripheral tissue, such as the lung, is higher in young animals compared to aged<sup>57</sup>. Aging also impacts other components of the UPR than just the chaperones and enzymes. PERK mRNA was diminished in the hippocampus of aged rats compared to young<sup>56</sup>. Studies also showed that eIF2a kinase was less efficient when isolated from aged rat brain tissue compared to young rats. Additionally, GADD34 increased expression was observed in the cortical tissue of aged mice<sup>57</sup>. GADD34 suppresses the translation block and allows for the synthesis of pro-apoptotic proteins like CHOP. Furthermore, increased basal and inducible CHOP expression levels are associated with aging. CHOP and Caspase-12 expression, which are both related to apoptotic activation, were induced in stressed aged rats, but not in the stressed young rats. JNK kinases, which contribute to the induction of apoptosis, are also upregulated with aging<sup>63</sup>. Collectively, these age-related changes suggest that aged animals are more vulnerable to ER stress and apoptosis. The UPR triggers autophagy in order to eliminate aggregates of misfolded proteins that are unable to be degraded by the ERAD pathway. Autophagy provides protection by augmenting clearance of the protein accumulations; however, autophagy also declines with age as the rate of autophagosome formation and maturation and the efficiency of autophagosome/lysosome fusion are greatly reduced<sup>58</sup>.

While several studies have shown convincing evidence for a dominant role of ER stress in various diseases, there have only been a few studies investigating ER stress in the context of ALI/VILI. ER stress is involved in numerous lung diseases, including lung cancer, pulmonary fibrosis, asthma, cystic fibrosis, hyperoxia-induced lung injury, cigarette smoke exposure, pulmonary infection, and ALI<sup>59,60</sup>. ER stress responses in ATII, fibroblasts, and macrophages has been linked to pulmonary fibrosis<sup>61</sup>. In septic shock models and LPS-induced ALI models, ER stress occurs in the injured lung and seems to be a prominent pathological feature in the process<sup>59</sup>. Local inflammatory cytokines and neutrophil accumulation/activation appear to be associated with the development of ER stress and activation of the

UPR<sup>59</sup>. Several ER stress pathway proteins are key modulators of epithelial permeability and barrier dysfunction in young mice and rats<sup>59,60</sup>. Zeng et al., showed that unresolved ER stress played a significant role in LPS-induced inflammation<sup>62</sup>. Extended epithelial stretch activates ER stress pathways, which resulted in increased alveolar permeability, cell death, and proinflammatory signaling<sup>63</sup>; however, these implications have yet to be investigated in an aging model. Dolinay et al., revealed that ER stress and the UPR are key modulators of epithelial permeability<sup>63</sup>. Prolonged stretch of rat primary type I-like alveolar epithelial cells and injurious mechanical ventilation cause ER stress and activate the UPR, which lead to increased alveolar permeability, apoptosis, and proinflammation<sup>63</sup>. Furthermore, chemical inhibition of an upstream regulator of the ER stress pathway managed to reduce injury signaling and recover overall barrier function following prolonged cyclic stretch and damaging mechanical ventilation<sup>63</sup>. Together, these findings implicate the role of ER stress in numerous diseases, including lung conditions such as ALI/VILI. Furthermore, the studies provide reinforced evidence that therapeutic targeting ER stress and the UPR may attenuate ALI/VILI and needs further evaluation. There is also a lack of investigations on how aging influences these responses in ALI/VILI, illustrating the need to better understand how ER stress relates to the increased susceptibility of the elderly population.

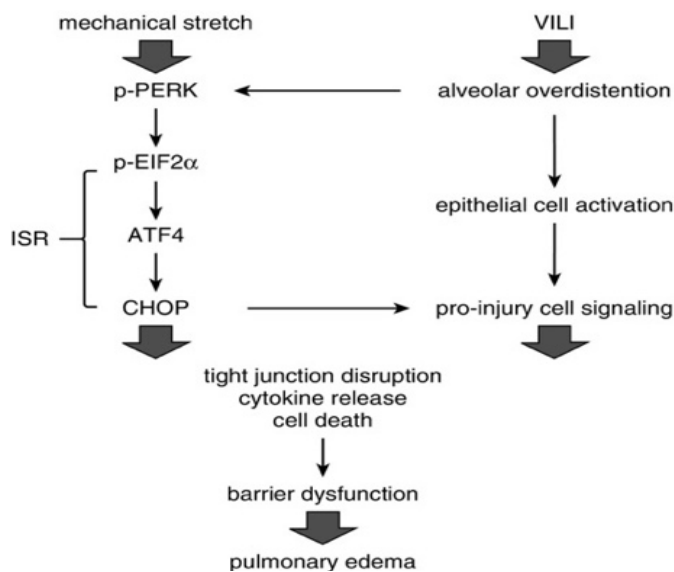


**Figure 8: Theorized role of ER stress and the UPR in pathophysiology of mechanical-induced ALI/VILI. Reprinted with permission of the American Thoracic Society. Copyright © 2020 American Thoracic Society. All rights reserved. Dolinay et al., 2017<sup>63</sup>. The American Journal of Respiratory Cell and Molecular Biology is an official journal of the American Thoracic Society.**

As mentioned before, macrophages play critical roles in tissue inflammation, host defense, and maintenance of tissue homeostasis. Their activation is generally described as pro-inflammatory (M1) that assist in tissue destruction and host defense, or anti-inflammatory (M2) that are believed to participate in tissue regeneration and repair<sup>64</sup>. ER stress is activated in macrophages, and this stimulation resulted in an M1 polarization state following the activation of the IRE1 $\alpha$  component of the ER stress and UPR signaling in a fatty liver disease model<sup>64</sup>. This ER stress-dependent activation resulted in increased ischemia-reperfusion injury<sup>64</sup>. Additionally, another study found that the TRAF2 component, another component of the IRE1 $\alpha$  signaling branch, is also activated in macrophages stimulated with palmitic acid<sup>65</sup>. Furthermore, preliminary studies indicated that ATF6 and IRE1 $\alpha$ , two of the major ER membrane resident proteins, may be involved with macrophage polarization<sup>66</sup>. Evidence also suggests that ER stress is activated during NAFLD progression in macrophages and prolonged ER stress induces proinflammatory polarization. A recent study showed that this ER stress related macrophage polarization was regulated via pancreatic eIF-2 $\alpha$  kinase (PERK), which plays a major role in ER stress<sup>64</sup>.

There is also evidence for ER stress regulating macrophage polarization in several lung conditions and diseases<sup>61</sup>. Kennedy et al., demonstrated that macrophage cytokine production and UPR responses to ER stress are dependent on the M1 or M2 polarization state in COPD (Kennedy 2013). The authors showed that ER stress upregulated 33 proinflammatory genes in M1 macrophages compared to M2, which included IL-8, TNF, IL-6, and CCL8. ER stress also induced the activation of the inflammasome of M1 macrophages; however, this did not occur in M2 macrophages. Furthermore, the expression of the UPR components and specific pathways were distinct between M1 and M2 macrophages, where the M2 macrophages did not express UPR components that induced apoptosis in response to ER stress<sup>67</sup>. In addition to COPD, studies suggest that ER stress is implicated in other lung diseases, such as pulmonary fibrosis<sup>61</sup>. ER stress has been reported in lung macrophages obtained by bronchoalveolar lavage from asbestosis patients and in alveolar macrophages in a murine asbestos-induced lung fibrosis model<sup>61</sup>. Yao et al., showed that M2 macrophages had increased expression of CHOP in IPF patients<sup>68</sup>. Burman et al., suggests that ER stress-activated in ATII cells, fibroblasts, and macrophages greatly contribute to

the initiation and progression of pulmonary fibrosis<sup>61</sup>. ER stress activated in ATIs leads to apoptosis and epithelial-to-mesenchymal transition, which produces loss of lung structure, impaired reepithelization, and increased presence of mesenchymal cells. They also suggest that ER stress induces an M2 polarization state in macrophages, which leads to increased production of profibrotic mediators, such as TGF $\beta$  and PDGFB. Together, these ER stress-induced cell responses result in pro-fibrotic conditions and fibrosis development<sup>61</sup>. While several studies have shown that ER stress may influence macrophage polarization, most reports are inconsistent and remain controversial. In murine obesity models, increased M2 macrophages resulted from genetic deficiencies surrounding IRE1 $\alpha$  or CHOP, resulting in a loss of ER stress activation (Shan 2017, Grant 2014). Conversely, other studies indicate that ER stress induces macrophages towards M2 polarization, possibly via ER stress-induced JNK activation<sup>69</sup>. CHOP induces M2 polarization in lung macrophages in bleomycin models of pulmonary fibrosis and a murine model of allergic airway inflammation<sup>68,70</sup>. Furthermore, chemical inhibition of ER stress in bone marrow-derived macrophages prevented palmitate-induced M2 polarization. While these studies indicate a direct effect of ER stress activation and macrophage polarization. ER stress may also have indirect effects on macrophage responses. Evidence suggests that ER stress can induce apoptosis in macrophages, which would abrogate the effects of M2 polarization<sup>61</sup>. This relationship between macrophage polarization and ER stress needs better understanding in the context of aging and mechanical injury in order to develop therapies that target these types of molecular mechanisms.

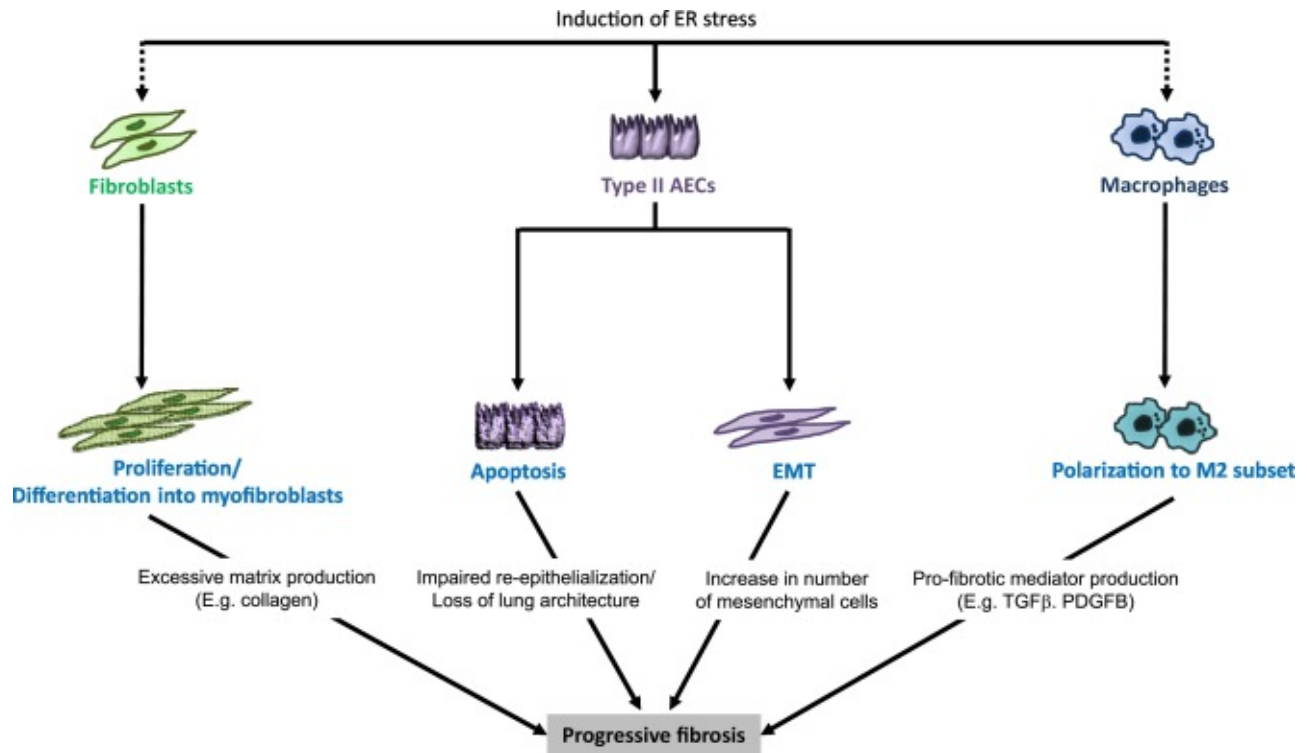


Figure 9: Proposed mechanism for the induction of ER stress-induced Pulmonary Fibrosis. ER stress is believed to influence ATEC, macrophage, and fibroblast differentiation and signaling. Source: Burman et al., 2018<sup>61</sup>.

The implication of ER stress in lung conditions and diseases suggest that targeting ER stress and the UPR may have vast therapeutic potential in mitigating ALI/VILI<sup>63</sup>. Dolinay et al., utilized a PERK inhibitor treatment for the chemical inhibition of ER stress and UPR following cyclic stretch and injurious mechanical ventilation, which inhibits the PERK branch of the ER stress mechanism and resulted in decreased injury signaling and improved barrier function following injury induction<sup>63</sup>. More frequently, studies that examine ER stress intervention have utilized the chemical inhibitor, 4-phenylbutyrate (4PBA). 4PBA is a low molecular weight compound that acts as a general inhibitor of ER stress by stabilizing protein conformation, improving the folding capacity of the ER, and chaperones mutant proteins to further suppress ER stress activity<sup>71,72</sup>. Zeng et al., showed that 4PBA dosing prevented the activation of the NF-κB pathway, decreased the secretion of pro-inflammatory mediators, such as IL-1b, TNFα, and IL-6, and significantly inhibited LPS-activated ER stress in a LPS-induced mouse model of ALI<sup>62</sup>. Furthermore, the authors showed that 4PBA also reduced autophagy activity, which may play a protective role through the classical AKT/mTOR signaling pathway.

Our objective was to understand better how lung cells, such as ATIIs and macrophages, contribute and respond to ER stress and how aging and mechanical injury affect these behaviors. To further validate that therapeutic targeting of the ER stress response may attenuate VILI, we investigated the therapeutic potential of 4PBA in our age-related experimental VILI models.

#### **2.4 Sphingosine-1-Phosphate and S1P Lyase Suppression in Aging and Acute Lung Injury:**

The cellular *mechanotransduction* that occurs at the alveolar barrier has a critical role in mediating ALI/VILI<sup>36</sup>. The *mechanotransduction* of the physical forces that stretch the pulmonary barrier leads to many biochemical and biophysical changes at the cellular and structural level that include extracellular matrix (ECM) remodeling, stress fiber reorientation, cell-cell and cell-ECM adhesions, activation of various nuclear transcription factors, and secretion of inflammatory cytokines and chemokines<sup>28</sup>. The mechanical forces from cell-stretch and injurious mechanical ventilation directly distend cell membranes and induce activation and phosphorylation of receptor<sup>73</sup>, cation channels<sup>74</sup>, phospholipases<sup>75</sup>, and relevant signaling pathways and transcription factors that regulate lung inflammation and injury<sup>76-78</sup>. Phospholipids and sphingolipids are membrane lipids that are present in all eukaryotic cells that act as structural components of cell membranes. Recently, evidence suggests these biomolecules and their metabolites also act as intracellular and extracellular signaling molecules in both normal and several pathological conditions<sup>79</sup>, including several lung conditions such as ALI/VILI<sup>37,80</sup>.

Sphingolipids are specialized constituents present in all eukaryotic cells that provide structural integrity to cell membranes and are essential to development and maintenance<sup>80</sup>. They are comprised of a distinct group of lipids that encompass sphingosine, sphinganine (dihydrosphingosine), or phytosphingosine as a sphingoid base backbone that is attached to long-chain fatty acids<sup>37</sup>. Recent studies suggest that Sphingosine-1-Phosphate (S1P), a bioactive sphingolipid metabolite, acts as an effective bioactive lipid signaling molecule with the potential to regulate numerous cell processes and behaviors that include cell proliferation, survival/apoptosis, barrier function, inflammation, immune regulation<sup>81,82</sup>, motility and cytoskeletal reorganization<sup>83</sup>, adherens junctions<sup>84</sup>, tight junction assembly<sup>85</sup>,

autophagy<sup>86,87</sup>, and many more<sup>80</sup>. Evidence suggests that S1P produces both intracellular and extracellular signaling pathways that may play crucial roles in development and disease related pathologies, including respiratory disorders<sup>37</sup>. It is suggested that the S1P-related metabolic pathway that's associated with various respiratory diseases may be an effective target for numerous lung diseases and that influencing S1P levels could be a viable therapy in attenuating lung conditions such as ALI/VILI.

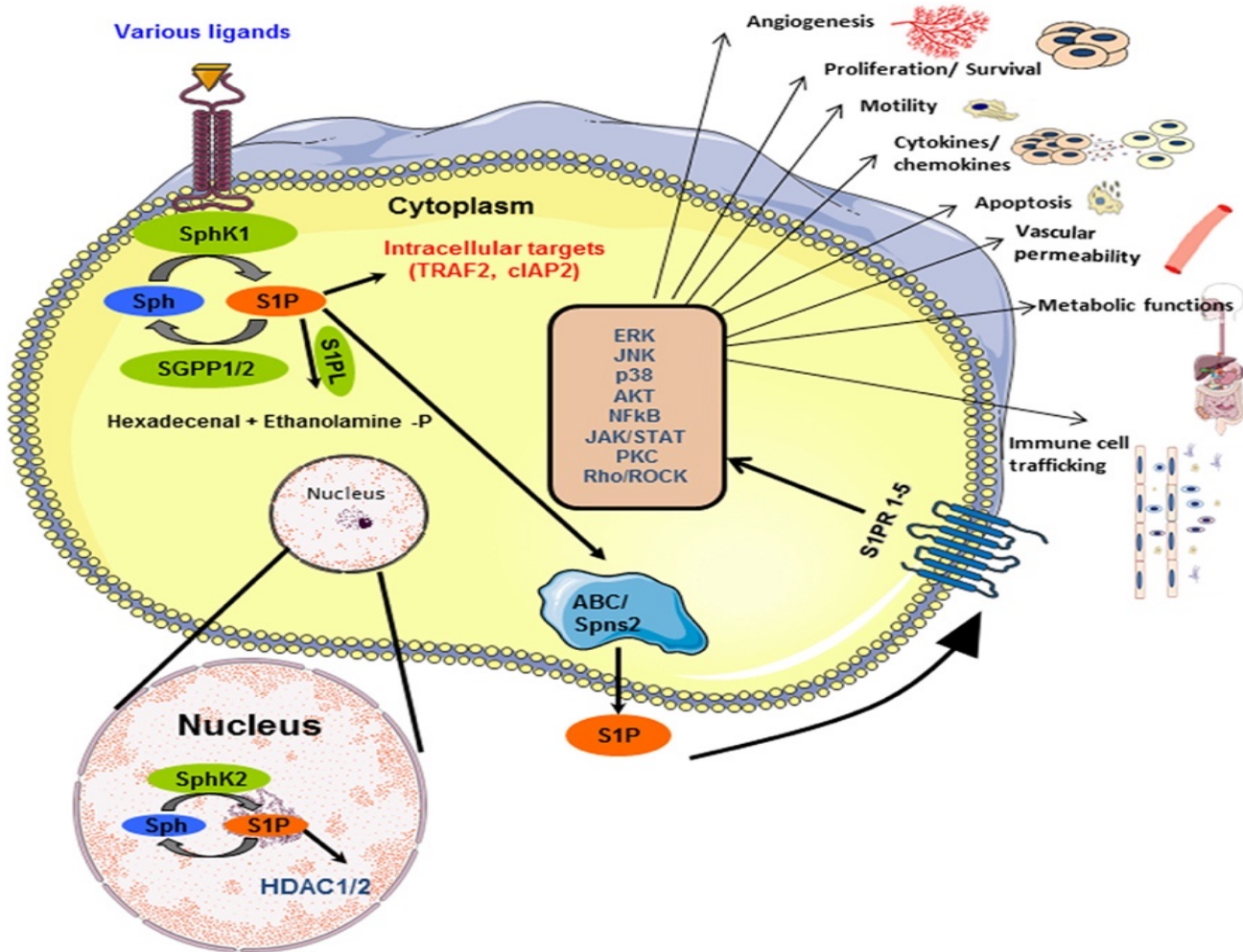


**Figure 10: Schematic overviews of the S1P signaling axis and the cellular actions of S1P.** S1P synthesis and related S1P/SphKs/S1PL signaling axis. Figure also depicts Intracellular and extracellular S1P signaling actions Source: Muhammed et al., 2017<sup>80</sup>.

S1P is synthesized through the phosphorylation of sphingosine by the activation of specific kinases, SphK1 and SphK2, which rigorously controls the cellular S1P concentrations. Sphingosine is generally produced from the conversion of ceramide via ceramidases<sup>88</sup>. S1P degradation can either be

through reversible phosphorylation, such as S1P phosphatases (SPPs) or lipid phosphate phosphatases (LPPs), or through irreversible phosphorylation, which occurs by S1P Lyase (S1PL). S1PL irrevocably converts S1P into hexadecenal and ethanolamine phosphate<sup>89</sup>. S1P signaling is mediated in a G-protein coupled receptor-dependent manner through S1P receptors 1-5 located on cell membranes, or through a receptor independent manner, such as the intracellular targets HDACs and TRAF2. Intracellularly, S1P acts as a second messenger and helps regulate calcium homeostasis; although, there is a lack of information regarding intracellular targets of S1P<sup>37</sup>.

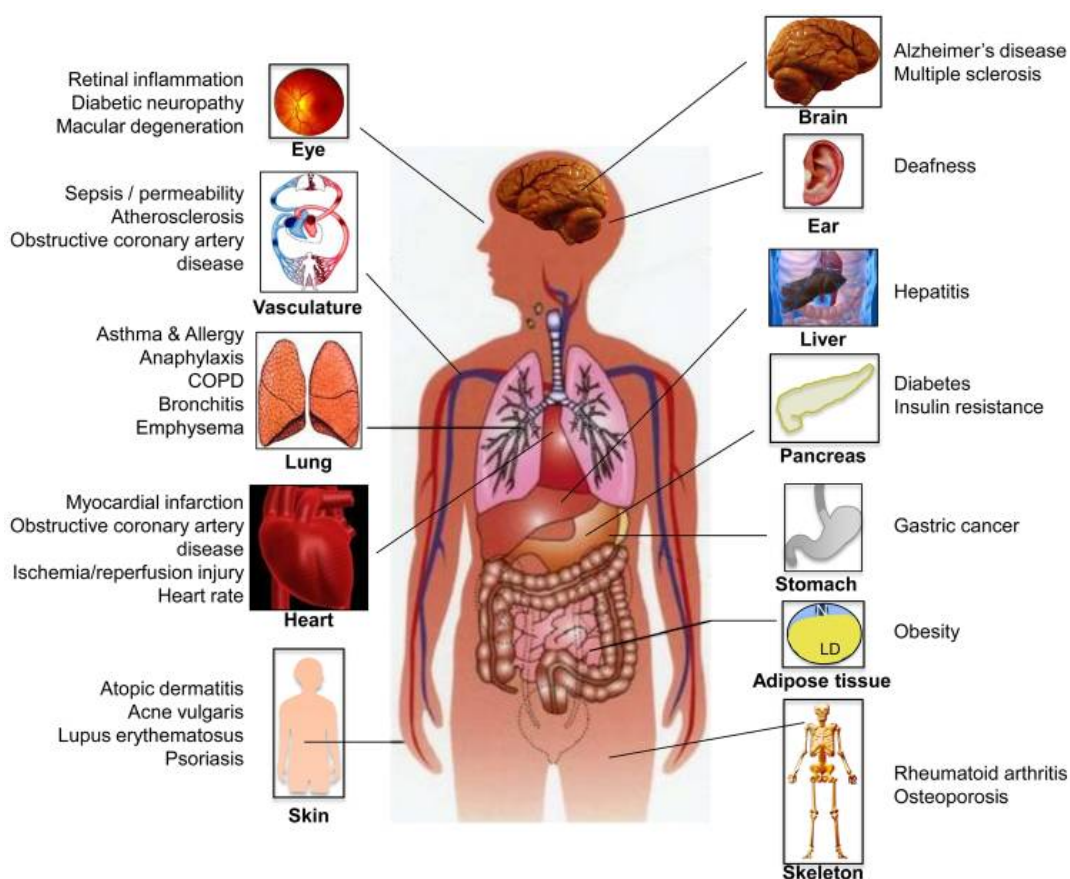


**Figure 11: Pathophysiological conditions and diseases throughout the body that are associated with S1P.** Evidence suggests that S1P is implicated in several diseases and conditions that affect almost every organ in the body, including almost every type of cancer. Source: Maceyka et al., 2012<sup>79</sup>.

Studies have shown that the SphK/S1P/S1PL metabolic pathway is associated in several diseases, such as cardiovascular disease, cancer, inflammatory diseases, obesity, as well as many others, and is often considered for therapeutic targeting<sup>79</sup>. Furthermore, the expression levels of S1P and

SphK1 appear to correlate with certain disease grades, severity, and patient mortality<sup>80</sup>. As for lung disorders, various studies suggest that S1P and sphingolipid signaling is implemented in asthma, lung cancer, pulmonary hypertension, cystic fibrosis, pulmonary fibrosis, chronic obstructive pulmonary disease, influenza, and acute lung injury (ALI)<sup>80</sup>. Several studies suggest that the S1P/SphK1/S1PL signaling axis may have a significant impact in the pathophysiology of ALI<sup>35,90,91</sup>. For example, the administration of S1P diminished lung edema formation and promoted survival in an acute lung injury model produced by loss of Forkhead protein in endothelial cells<sup>80</sup>. The S1P role in endothelial barrier function is attributed to its S1P<sub>1</sub> and S1P<sub>3</sub> signaling that activates downstream Rho GTPases and cytoskeletal rearrangement<sup>83</sup>. Additionally, the knockdown of Forkhead protein leads to increased expression of S1P<sub>1</sub>, which was suggested to help maintain barrier integrity<sup>80</sup>. Sphk1 has also been shown to provide protection against radiation-induced lung injury, SphK1<sup>-/-</sup> mice were highly susceptible to the radiation damage; furthermore, S1P receptor agonists were administered and attenuated the radiation damage<sup>80</sup>. Currently, glucocorticoids are in clinical trials for patients with ALI. Glucocorticoid treatments enhance the synthesis of Sphk1 and S1P formation and blocking Sphk1 expression inhibited the effects of glucocorticoids in ALI. Additionally, SphK1<sup>-/-</sup> mice had greater vascular leakage and reduced recovery from LPS-induced ALI, and these negative outcomes were assuaged by the administration of exogenous S1P<sup>80</sup>. In other LPS-induced murine ALI models, intravenous S1P administration also reduced lung vascular permeability and inflammation<sup>92</sup>. There has also been a genetic link between S1P and ALI, although indirectly. Genetic screening of ALI patients identified a robust connection between a single nucleotide polymorphism in cortactin gene and ALI. Interestingly, this cortactin-related polymorphism, which is involved in maintaining barrier integrity was responsible for making endothelial cells more susceptible to ALI by reducing the barrier protective effects of S1P<sup>80</sup>. Collectively, studies generally suggest that the barrier enhancing effects of S1P occurs via ligation to S1P<sub>1</sub>. This activates downstream signaling cascades that includes Rac activation, cortactin translocation, myosin light chain phosphorylation, and focal adhesion and adherens junction protein rearrangement<sup>101</sup>. Conversely, several *in vitro* and *in vivo* studies demonstrated that elevated concentrations of S1P (>5-10uM) may

produce barrier disruption. Furthermore, intravenous infusion of S1P at 0.5 mg/kg body weight produced pulmonary edema in mice<sup>93</sup>. Alternatively, to S1P<sub>1</sub> ligation, ligation of S1P to S1P<sub>3</sub> leads to cell migration and vascular barrier dysfunction<sup>101</sup>. Likewise, genetic knockdown of Sphk1 in mice caused increased susceptibility and elevated negative outcomes in an LPS-induced ALI model<sup>94</sup>. S1PL expression also appears to be elevated in LPS-induced lung injury models, which reduces the S1P levels in the lung and increases inflammation and injury<sup>95</sup>. Collectively, these observations demonstrate the role and association of S1P signaling in various lung disorders and insinuate that the S1P metabolic pathway has vast therapeutic potential against ALI.

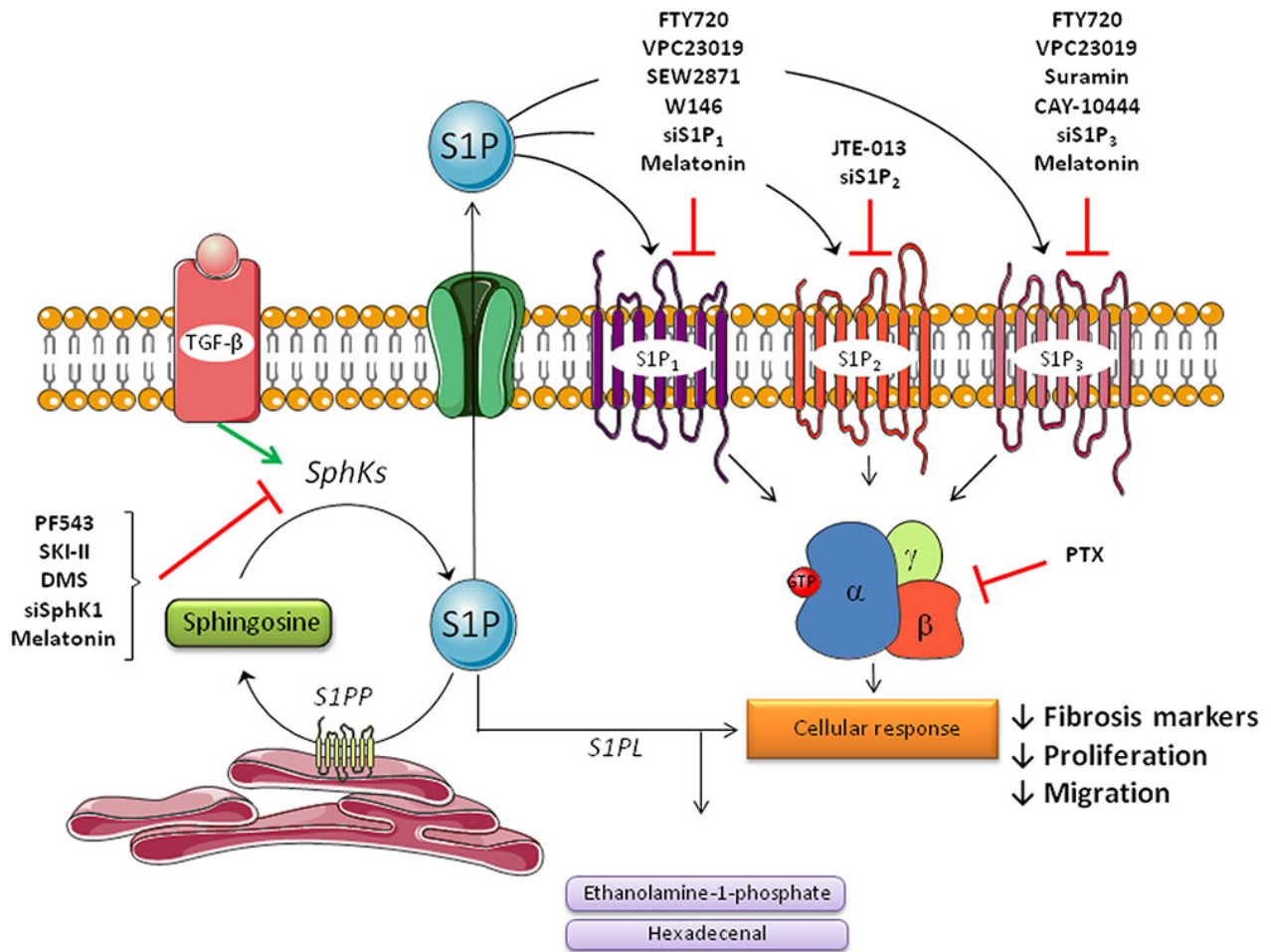


**Figure 12: Targeting sphingolipid signaling has therapeutic potential in fibrosis diseases, such as pulmonary fibrosis, as well as many other pathophysiologic conditions.** This diagram depicts many of the inhibitors of S1P signaling that target enzymes involved in the sphingolipid pathway. This includes Sphingosine Kinase Inhibitors, Agonizing/antagonizing S1P Receptors, and others. Source: Gonzales-Fernandez et al., 2017<sup>162</sup>.

While there have been a few studies that have examined the role of S1P signaling in acute lung injury models, only a small fraction is focused on mechanically induced ALI. Suryadevara et al., indicated that volume-controlled mechanical ventilation (30 mL/kg,4hr) in mice resulted in elevated S1PL expression, reduced S1P levels in lung tissue, and increased inflammation, injury, and apoptosis. They demonstrated that deletion of SphK1 mitigated VILI in mice. Moreover, the authors revealed that alveolar epithelial MLE-12 cells exposed to 18% cyclic stretch caused increased S1PL expression and changes to levels of sphingoid bases compared to physiological stretch conditions<sup>36</sup>. Administration of 4-deoxypridozine, a S1PL inhibitor, prior to pathophysiological stretch also attenuated barrier dysfunction, cell apoptosis, and cytokine secretion. Collectively, these findings further suggest that S1PL inhibition may have therapeutic potential and protection against VILI. While there are only a few investigating the protective roles of S1P and S1PL inhibition in VILI, there are currently no studies examining the consequences of aging on these protective roles in VILI that would offer greater pathological insight.

Interestingly, studies have shown that sphingolipids play critical roles in regulating lifespan in certain organisms, such as yeast, worms, and flies<sup>96</sup>. There has also been evidence of sphingolipids regulating cellular senescence in mammalian cells<sup>96</sup>. Furthermore, mechanisms upstream and downstream of sphingolipid metabolism have been shown to be associated in regulating senescence<sup>96</sup>. Several studies have suggested that membrane lipids, specifically sphingolipids, are biomarkers of human aging<sup>97</sup>. Profiling serum samples of long-lived humans indicated an increase in specific sphingolipids with aging. Furthermore, certain plasma sphingolipids and their metabolites were increased in long-lived naked mole rats. While these studies suggest an increase of sphingolipids in circulation with aging, other investigations suggest that ceramide levels increase and S1P levels decrease in aged tissue. The balance between the S1P and ceramides modulates the aging process<sup>97</sup>. In healthy aged brain tissue, ceramide levels were increased and S1P levels were reduced with aging<sup>98</sup>. While very few studies have examined the role of S1P signaling with healthy aging, numerous findings reveal reduced S1P levels in age-related diseases, such as neurodegenerative diseases and diabetes, suggesting that the S1P and S1P metabolites are greatly implicated in those diseases<sup>98</sup>.

S1P signaling has an essential role in controlling complex immune regulatory networks that contribute to homeostasis and disease, including pulmonary conditions and diseases<sup>79</sup>. Sphingolipids act as important mediators involved in cell survival, stress responses, and inflammation<sup>99</sup>. Sphingosine-1-phosphate and the S1P receptors are extensively involved in inflammatory diseases<sup>100</sup> (Yang 2018). Studies have shown that S1P, along with the S1P signaling axis, can greatly influence macrophage differentiation and function under physiological and disease conditions<sup>101</sup>. Evidence suggests that S1P binding to certain S1P receptors on macrophages produced specific functional responses. These macrophage responses have been implicated in particular diseases and conditions<sup>101</sup>. Yang et al., showed that bone marrow derived-macrophages expressed S1P<sub>1-3</sub>, but not S1P<sub>4/5</sub>. Furthermore, the authors found that S1PR<sub>2/3</sub> mediated S1P-induced M1 macrophage polarization. Interestingly, S1P<sub>1</sub> had no effect on macrophage polarization. Additionally, the use of inhibitors prevented the upregulation of M1 gene expression mediated by S1P/S1PR<sub>2/3</sub><sup>100</sup>. Conversely, Muller et al., found that all 5 S1P receptors were expressed in bone marrow-derived macrophages<sup>102</sup>. They provided evidence that suggests that M1 and M2 polarized macrophages resulted in significant downregulation of S1P<sub>1</sub> and influenced the expression of S1P<sub>4</sub>. This study also indicated that S1P induced chemotaxis in M1 macrophages and altered cytokine secretion in M2 macrophages. Interestingly, S1P increased expression of iNOS only under M2-polarizing conditions, but it had no effect on phagocytosis of either M1 or M2 macrophages<sup>102</sup>. Another study found that exogenous S1P administration increased iNOS expression in mouse bone marrow-derived macrophages stimulated with LPS/IFN-gamma<sup>102</sup>. Evidence suggests that S1P<sub>3</sub> is implicated in LPS-induced ALI models and might be the most important S1P receptor on macrophages regulating inflammation<sup>101</sup>. Early studies in human alveolar macrophages indicated that S1P induced (NOX)2-dependent production of ROS to promote IL-1 $\beta$  and TNF- $\alpha$  production by murine peritoneal macrophages. Previously, Intracellular S1P produced by Sphk1 was also suggested as a cofactor involved in macrophage activation. IL-1 signaling, an activator in NF $\kappa$ B inflammation, also requires Sphk1-dependent S1P as an intracellular cofactor<sup>103</sup>. Sphk1 is also activated downstream of other inflammatory stimuli, such as LPS<sup>104–106</sup>. Stimulation of human THP-1 macrophages with LPS required

Sphk1 activity to generate IL-6, IL-1 $\beta$ , TNF- $\alpha$ , and/or NO<sup>104</sup>. In RAW264.7 macrophages, S1P<sub>1</sub> and S1P<sub>2</sub> were involved in IL-6 production in a LPS-induced ALI model<sup>107</sup>. Furthermore, S1P<sub>1</sub> binding increased ARG1 activity and suppressed NO production, suggesting a shift from M1 to M2 polarization states in murine macrophages<sup>108</sup>. S1P<sub>5</sub> on macrophages is associated with impaired phagocytosis; however, it remains unclear if this S1P receptor impacts macrophage polarization<sup>101</sup>. Collectively, these observations suggest that S1P modulates macrophage activation and responses according to the local environment, the intracellular and extracellular concentrations of S1P, and the S1P receptors activated on specific<sup>101</sup>.

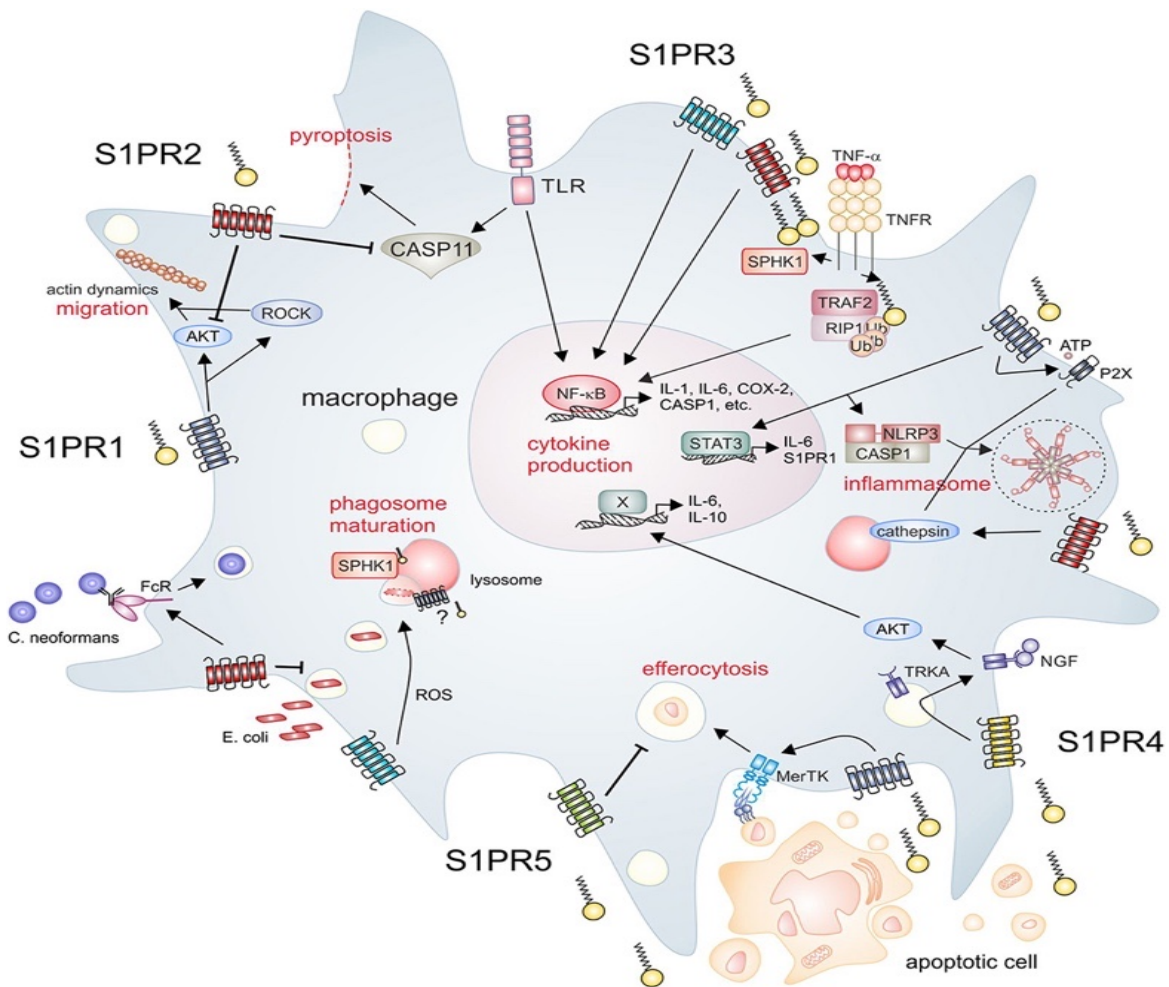


**Figure 13: S1P signaling and macrophage responses.** Evidence suggests that the S1P/Sphks/S1PR signaling axis may regulate critical macrophage functions and polarization states. Source: Weigert et al., 2019<sup>101</sup>.

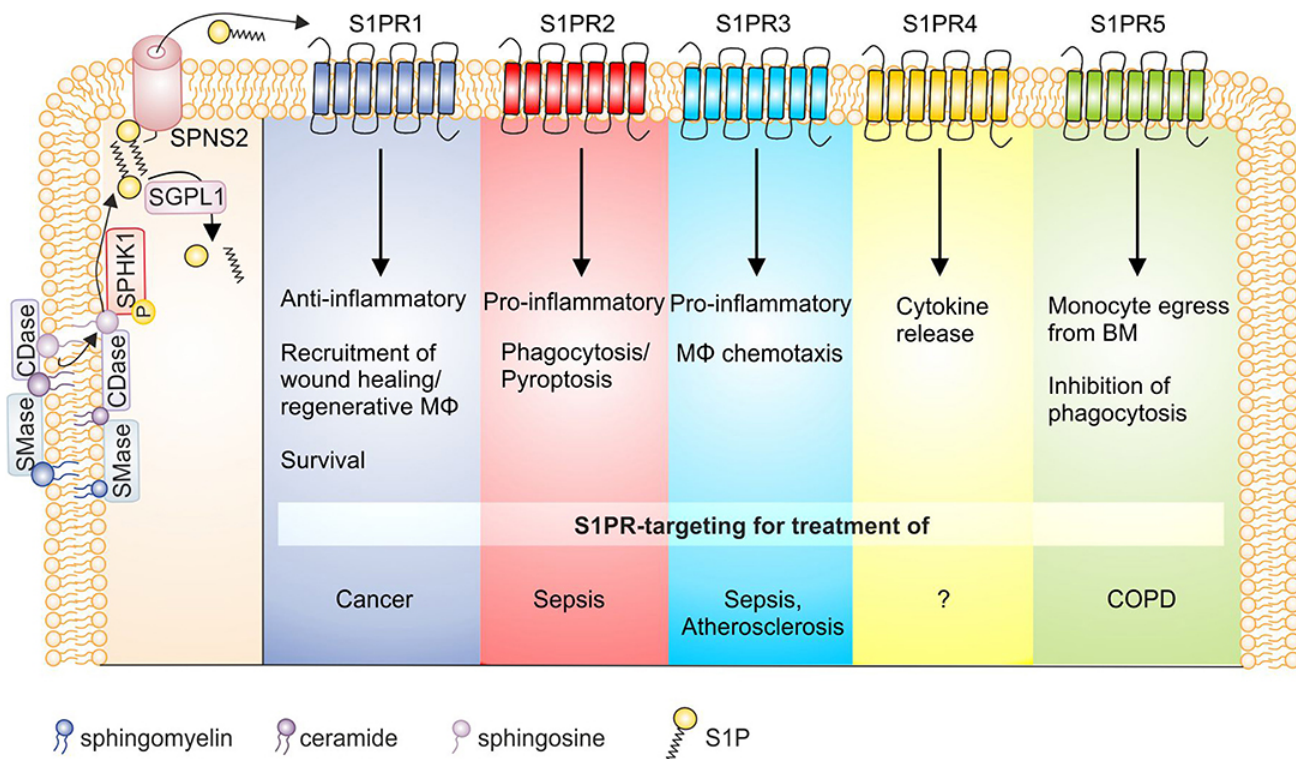


**Figure 14: S1PR signaling and macrophage polarization implicated in disease.** S1P binds to S1P receptors on macrophages that activate certain functional responses. These S1P receptor-specific responses represent potential therapeutic targets for various diseases or conditions. Source: Weigert et al., 2018<sup>101</sup>.

There are numerous studies that focus on targeting various components of S1P signaling for several diseases, including some lung disorders. The intracellular and extracellular signaling mechanisms of S1P that allow for various autocrine and paracrine effects and its implementation in disease progression provides vast therapeutic potential for numerous diseases; including respiratory disorders<sup>37</sup>. Targeting S1P levels in certain conditions by increasing or decreasing S1P levels in circulation or tissue is significantly effective<sup>35,109,110</sup>. For example, the administration of anti-S1P monoclonal antibodies to deactivate extracellular S1P and hinder its receptor signaling is being investigated in pre-clinical and phase I and II trials for tumor growth suppression and age-related macular degeneration<sup>111</sup>. As studies have shown that S1PL expression is elevated in several ALI models, such as LPS-induced, that causes reduced S1P levels and increased inflammation, targeting S1PL has shown promise in attenuating many of the negative outcomes associated with ALI<sup>95</sup>. Targeting S1PL *in vitro*

using siRNA in human lung microvascular endothelial cells that received LPS lead to reduced barrier disruption, IL-6 secretion, and LPS-induced p38 MAPK phosphorylation<sup>95</sup>. Zhao et al., further showed that inhibiting S1PL expression *in vivo* resulted in increased intracellular S1P levels and decreased LPS-induced inflammation. Mice that were treated with 2-Acetyl-4-tetrahydroxybutyl Imidazole (THI) (0.05 mg/mL water), which inhibits S1PL expression, for 2 days retained raised S1P levels in the lung tissues and BALF fluids following intratracheal LPS instillation. Furthermore, THI treatment resulted in reduced neutrophil infiltration in the alveolar space and reduced IL-6 secretion as protection against LPS-induced lung injury<sup>95</sup>, further suggesting the therapeutic potential of targeting S1PL, specifically via THI intervention.

We hypothesized that influencing S1P signaling may be a viable therapeutic approach to attenuating age-related negative outcomes associated with mechanical injury and acute lung injury. Further investigation is critical to understand the protective effects of S1P signaling and S1PL inhibition in the context of aging and mechanical injury. The loss of S1P levels or elevated S1PL expression in the lungs of aged individuals may represent age-specific mechanisms leading to the elderly's increased susceptibility to lung injury. The possible molecular regulation of these signaling components represents promising, potential therapeutic targets for age-related ALI.

## CHAPTER 3: AGING INFLUENCES ATII AND MACROPHAGE RESPONSES

### TRIGGERED BY INJURIOUS CELL-STRETCH

Some of the content in this chapter was previously published in 2018 with the following citation: Valentine et al., Inflammation and Monocyte Recruitment due to Aging and Mechanical Stretch in Alveolar Epithelium are Inhibited by the Molecular Chaperone 4-phenylbutyrate, *Cell and Mol. Bioengineering*, 2018

#### 3.1 Rationale:

Mechanical ventilation frequently exacerbates underlying pulmonary conditions and produces an exaggerated inflammatory response that potentially leads to sepsis and multisystem organ failure<sup>1,73,112</sup>. This exacerbation or injury is classified as Ventilator-Induced Lung Injury (VILI). The pathophysiology of VILI is characterized by an exaggerated proinflammatory cytokine release and influx of inflammatory cells, loss of alveolar barrier integrity and subsequent pulmonary edema formation, decreased lung compliance, and profound hypoxia. These features reflect three integrated mechanisms of injury: alveolar over-distention, cyclic atelectasis, and inflammatory cell activation<sup>1,5,73</sup>. These physical injury mechanisms are frequently modeled in vitro with mechanical cyclic stretch using lung epithelial or endothelial cells.

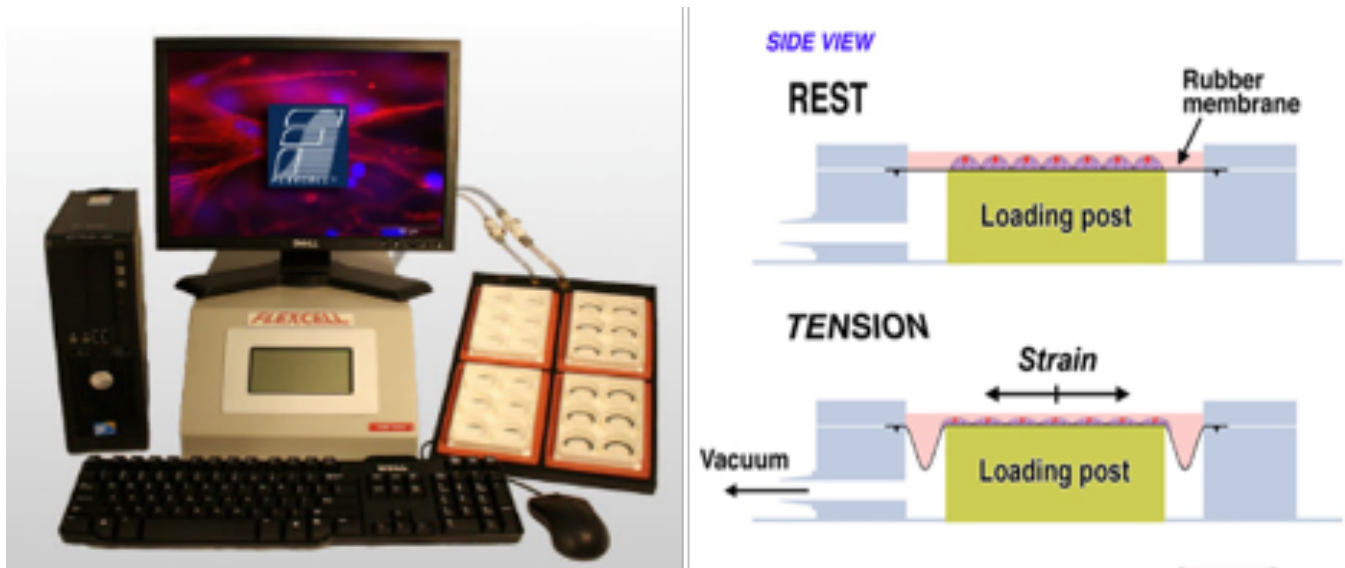


*Figure 15: Flexcell FX-5000TM Tension System used to simulate in vivo tissue strains. The cell-stretch system produces a defined, controlled, static or cyclic deformation to a monolayer of cells. Mimics in vivo conditions for cells in the lung and other organ systems. Source: Flex Cell International Corporation*

Lung tissues are continuously exposed to cyclic stretch during spontaneous breathing or mechanical ventilation<sup>28,127</sup>. The alveolar epithelium maintains adequate gas exchange during these activities by greatly contributing to the barrier formation and maintenance; however, there are prominent changes in mechanical stresses and strains and the microenvironments in pathological lung conditions, such as ALI/VILI, that influence the barrier's integrity<sup>113</sup>. Once the alveolar barrier integrity is compromised, pulmonary edema and increased susceptibility to infection occur and repair of the barrier is a critical determinant of outcome. The overdistension of aerated lung regions generates abnormally large strains on the epithelium that directly causes barrier disruption, cellular necrosis and apoptosis, and an immense secretion of pro-inflammatory cytokines<sup>1</sup>. The repetitive collapse and reopening of the alveoli produces atelectrauma, which also injures alveoli<sup>1,5</sup>. The high transmural pressures produced can activate proinflammatory signaling pathways that may further deteriorate alveolar barrier integrity<sup>5,114</sup>. These damaging mechanisms often lead to biotrauma, an enhanced release of local and systemic pulmonary inflammatory mediators that can cause further lung and distal organ injury<sup>45</sup>.

Although volutrauma, atelectrauma, and biotrauma injury mechanisms have been proposed to occur *in vivo*, there is little direct understanding of the changes in mechanical forces and the resulting deformation responses in age-related experimental ALI/VILI models. Furthermore, while overdistention of alveolar epithelial cells is thought to play a significant role in the initiation of ALI/VILI, there is limited evidence of these cells' *mechanotransduction* responses and mechanisms that lead to epithelial dysfunction and limited repair. These cells' ability to sense mechanical forces and relay that information to surrounding cells via signaling cascades has been evident in numerous studies; although, the underlying mechanisms of alveolar epithelial mechanosensation and mechanotransduction are thus far insufficiently comprehended. A high level of mechanical stretch has been shown to induce increased epithelial cell necrosis and extracellular matrix (ECM) remodeling, which plays a major role in structural maintenance and tissue homeostasis<sup>28,127</sup>. Studies showed that alveolar epithelial cells significantly contribute to the initiation, amplification, down-regulation, and tissue-repair stages associated with lung inflammation<sup>13,28,127</sup>. Epithelial cells produce cytokines and inflammatory mediators that are assumed to

be involved in the recruitment and regulation of macrophages<sup>13,28,127</sup>. Furthermore, cyclic stretch of epithelial cells grown on deformable membranes causes injury and induces cytokine release by alveolar epithelial cells<sup>74,78</sup>. Cyclic stretch of alveolar epithelial cells resulted in increased cell injury and death, apoptosis, acidification, bacterial growth, and general inflammatory response, which is often represented with amplified gene expression and release of IL-6 and IL-8<sup>13,28,63,127</sup>. Cyclic stretch of alveolar epithelial cells also triggered inflammatory signaling mechanisms in a force- and frequency-dependent manner<sup>14,74,78,137</sup>. These mechanotransduction responses are believed to have a significant impact with the induction and progression of several lung pathologies, including ALI/VILI.

Mechanical ventilation also leads to poorer outcomes in the elderly population. Mortality rates and hospital discharge to extended care facilities increased consistently for each decade of age over the age of 65 years in mechanically ventilated patients<sup>17-19</sup>. Epidemiological studies also suggest that age is a predictive factor in the severity of VILI; however, the exact molecular mechanisms between age and VILI are still unknown<sup>17-19</sup>. In rodent models of VILI, we and others have shown that age increases susceptibility to ventilator-induced edema, injury, and mortality<sup>10,19</sup>. In general, advanced age is also known to promote an increasingly dysregulated innate immune/inflammatory response to injury with an overall shift towards a proinflammatory state that is known as *inflammaging*<sup>25,38</sup>. Aging promotes chronic inflammation in the murine lung<sup>25,38</sup> and also inhibits repair of the lung epithelium following influenza insult<sup>25,38</sup>. Better understanding these age-associated influences are critical to developing therapeutic approaches that aim to target the possible age-associated mechanisms of injury.

As VILI is characterized by inflammation, recent evidence has suggested that lung-recruited monocytes may also play a significant role in the pathogenesis of ALI<sup>124,126</sup>. Recent studies show that immature monocytes enter the circulation from the bone marrow and migrate to local sites of inflammation and injury<sup>126</sup>. Using mouse models, monocytes have been shown to be rapidly recruited to the lung during inflammation and contribute to the development of ALI by promoting the activation of pulmonary endothelial and epithelial cells<sup>126</sup>. Additionally, monocyte recruitment has been shown to be heavily involved in the development of pulmonary edema under harmful mechanical ventilation<sup>1,7-9</sup>. Furthermore,

advanced age has also been shown to impact the function and responsiveness of monocytes and macrophages, although why this occurs and how it impacts the age-associated susceptibility to lung injury and inflammaging conditions are not clear<sup>24,25,38</sup>.

We hypothesized that the alveolar type II (ATII) cells respond age-dependently to mechanical stretch with increased inflammation and monocyte recruitment. To investigate this relationship, we isolated and cultured primary alveolar epithelial ATII cells from young and old murine subjects. These cells were exposed to cyclic mechanical stretch to model alveolar over-distension. We measured age-associated differences in cell injury/inflammation and apoptosis. Additionally, we quantified the migration of bone marrow-derived monocytes to ATII conditioned media. Our data suggest that age and mechanical stretch influence inflammatory responses and monocyte recruitment in alveolar type II epithelial cells.

### 3.2 Materials and Methods:

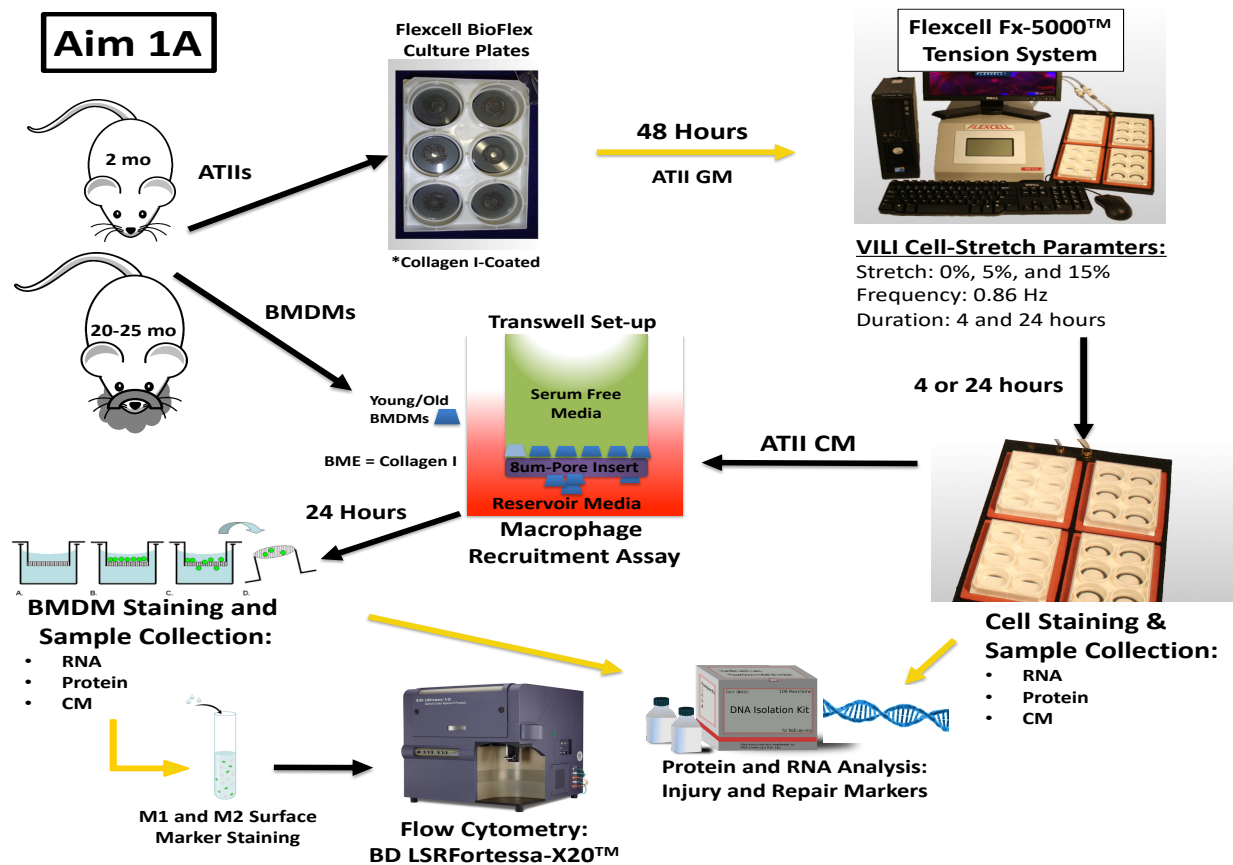


Figure 16: Schematic overview of the experimental methods for Aim 1A that examines the effects of aging in an injurious cell-stretch model using ATII cells isolated from young and old mice.

**C57BL/6J Mice:** All C57BL/6J mice were housed in accordance with guidelines from the American Association for Laboratory Animal Care and Research protocols and approved by the Institutional Animal Care Use Committee at Virginia Commonwealth University (Protocol No. AD1000009).

**ATII cell isolation and culture:** We harvested, isolated, and cultured ATII primary alveolar epithelial cells from young (2 months) and old (20 months) C57BL/6J wild-type mice using previously cited methods<sup>115</sup>. We selected to use an aged-mouse model as it has previously been suggested that mice are an ideal mammalian model for studying the effects of aging and due to the lack of availability of aged-human cell lines or clinical specimens<sup>116</sup>. ATII were then cultured in Bronchial Epithelial Cell Growth Media (BEGM, Lonza), with the included supplements except for hydrocortisone, supplemented with 10 ng/ml keratinocyte growth factor (KGF, PeproTech). For stretch experiments, cells were plated onto Collagen I-coated, 6-well silicone bottomed plates (Flexcell International Corp., BF-3001A BioFlex) and cultured for 48 hours prior to stimulation. ATII were found to be greater than 93% pure in both young and old cultures by staining for positive pro-surfactant C and the inclusion of lamellar bodies. Cell viability was also validated with MTT assays (Roche) according to manufacturer's instructions.

**Mechanical Cell-Stretch:** Using the Flexcell Tension Plus System (Flexcell Inc), we applied radial, cyclic (0.86Hz) stretch corresponding to a 15% change in surface area. Statically cultured ATII cells were used as controls. Cells underwent stretch or static conditions, and after 4 hours or 24 hours, RLT buffer (Qiagen) or 4% paraformaldehyde were added to wells for further processing. Cell supernatants were collected for cytokine analysis and conditioned media experiments.

**Immunofluorescence Staining:** Fixed wells were probed for CHOP (L63F7) mouse mAB (1:3200) and ATF-4 (D4B8) rabbit mAB (1:200) using secondary antibodies anti-mouse Alexa Fluor® 594 conjugate (1:250) and anti-rabbit Alexa Fluor® 488 conjugate respectively. All primary and secondary antibodies were obtained from Cell Signaling Technology (Danvers, MA, USA). The counterstaining was done using

Prolong® Gold antifade mounting with DAPI (ThermoFisher, Waltham, MA, USA). Finally, samples were imaged with an Olympus IX71 under appropriate emission/excitation wavelengths.

**Quantitative real-time Polymerase Chain Reaction:** Total RNA was isolated and purified from each treatment group using RLT buffer (Qiagen) and the RNeasy mini kit (Qiagen, Valencia, CA). We then synthesized the complementary DNA using the iScript RT kit (Biorad). For cDNA from the ATII primary alveolar epithelial cell, we used custom QPCR plates (Biorad) to perform an analysis of IL-6st, MCP-1 (CCL2), and MIP-1 $\beta$  (CCL4). QPCR was performed using Sybr Green (Applied Biosystems) and the CFX96 Touch™ Real-Time PCR Detection System (Biorad). Data were analyzed using the  $2^{-\Delta\Delta CT}$  method, and target genes were normalized to two housekeeping genes using ribosomal 18s and GAPDH.

**Inflammatory Mediator Analysis:** We measured the concentrations of MCP-1/CCL2 and MIP-1 $\beta$ /CCL4 inflammatory cytokines in the collected cell media of each experimental group using MCP-1 (DY479) and MIP-1 $\beta$  (DY451) Mouse DuoSet ELISA kits (R&D Systems) according to the manufacturer's instructions.

**Monocyte Invasion Assay:** Bone marrow-derived monocytes (BMDMs) were isolated from young (2 months) and old (20 months) C57BL/6J mice, as described by Trouplin et al.,<sup>117</sup>. Monocyte migration was then evaluated using an invasion assay, performed as described by Murray et al.,<sup>118</sup>, with minor modifications. BMDMs were seeded at a density of  $1 \times 10^5$  cells/100ul BMDM growth media without FBS, on Collagen I-coated (Sigma-Aldrich) Transwell inserts with 8.0 um pore sizes (Corning, USA). 0.6 ml of BEGM or conditioned media from the ATII 24-hour groups were placed in the reservoir.

**A Live/Dead Viability Assay** (ThermoFisher) was used to quantify cell invasion through the Transwell membrane. Live/Dead images were taken immediately after the staining procedure an Olympus IX71 Microscope (Olympus). Total cell counts were performed using ImageJ's particle analysis function with the following inclusion parameters: Size (in Pixels): 10-120. Circularity: 0.10-0.99.

**Statistics:** A total of 114 mice were used for this study. All experiments were performed with a minimum of n=3 primary cell isolations in triplicate wells. Larger n values were utilized where possible. Limitations exist in the number of 20-month-old mice available from the National Institute on Aging. Therefore, minimum numbers to achieve statistical significance via a power analysis were used. Results are presented as mean +/- SD. GraphPad Prism was used for all statistical analyses. For multiple-group comparisons, we used a two-way analysis of variance (ANOVA) with age and stretch as factors, followed by a post-hoc Tukey test to determine significance. P<0.05 was considered statistically significant.

### **3.3 Results:**

We first examined the impact of age and mechanical stretch on the inflammatory response of alveolar epithelial type II cells (ATII), which is one of the indications of ALI/VILI. The mechanically stimulated ATII cells were cyclically stretched up to a 15% change in surface area for durations of 4 or 24 hours, after which RNA was isolated and analyzed. We evaluated changes in gene expression of several inflammatory signaling molecules caused by aging alone (Figure 19) and aging and mechanical injury for 4 hours (Figure 20). This includes Monocyte Chemoattractant Protein 1 (MCP-1/CCL2), CCL3, Macrophage Inflammatory Protein 1 beta (MIP-1 $\beta$ /CCL4), CCL7, CCL9, CCL12, CCL20, IL-1a, IL-6, and IL-10. These proinflammatory chemokines are heavily involved in leukocyte recruitment and lung injury and inflammatory signaling (48, 64, 82). Binding of IL-6 to IL-6R induces IL-6st expression (37), and IL-6 is a proinflammatory cytokine that has previously been shown to increase after mechanical stimulation of ATII with cyclic stretch (10, 61). Fold changes of gene expression in ATII cells stretched or static for 4 hours are normalized to the Young Static ATII group (Figures 19-20). When comparing Old Static ATII with Young Static ATII, advanced age alone resulted in significantly increased gene expression of MCP-1/CCL2, CCL7, CCL9, CCL12, IL-1a, and IL-6. Aging alone did not cause any considerable gene expression changes that were detectable for CCL3, CCL4, CCL20, and IL10.

## Young vs Old Static Inflammatory Gene Expression

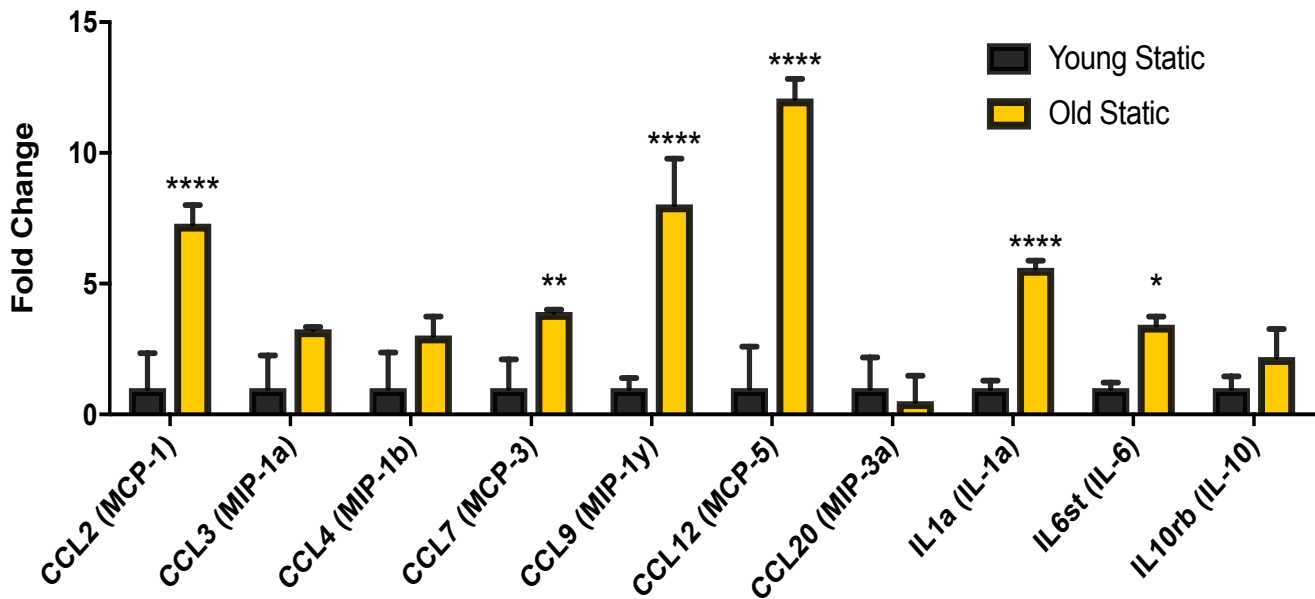


*Figure 17: Aging alone influences the expression of several inflammatory mediator. These genes are associated with proinflammatory signaling and immune cell recruitment/activation and samples were collected following 4 hours of static conditions. Columns are normalized fold change differences in gene expression obtained through qPCR compared with Young Static. Data are presented as mean  $\pm$  SD,  $n = 3$  per group. \* $p < 0.05$ , \*\* $p < 0.01$ , \*\*\* $p < 0.001$ , \*\*\*\* $p < 0.0001$ , compared to young static of same gene.*

As shown in Figure 20, we also observed increased gene expression following 4 hours of cell-stretch for CCL2, CCL3, CCL4, CCL7, CCL12, and CCL20 when we compared Young ATIIs that were stretched to Young ATIIs that were static in culture. Interestingly, there was no difference in IL-6 or IL-10 gene expression when comparing Young ATIIs that were stretched to young ATIIs that remained static in culture. When we compared Old ATIIs that were stretched to Old ATIIs that were static in culture, we found that the gene expression of CCL2, CCL3, CCL4, CCL12, CCL20, and IL-10 were considerably different. Interestingly, CCL2 and IL-10 gene expression were substantially reduced, while CCL3, CCL4, CCL12, and CCL20 chemokines were notably upregulated from cell-stretch. We then examined the differences in inflammatory gene expression caused by age and mechanical injury. Unexpectedly, we observed diminished gene expression of MCP-1/CCL2, CCL3, MIP-1 $\beta$ /CCL4, CCL7, CCL12, and CCL20 when comparing Old Stretched ATIIs to Young Stretched ATIIs. Additionally, there was no change in gene expression of IL-6 or IL-10 when comparing Old Stretched ATIIs to Young Stretched ATII cells.

Surprisingly, none of the inflammatory genes examined were upregulated in the Old ATIIIs subjected to cell-stretch compared to the young ATIIIs undergoing mechanical injury. These results show that aging and/or mechanical injury induce specific deviations in the expression of several inflammatory genes.

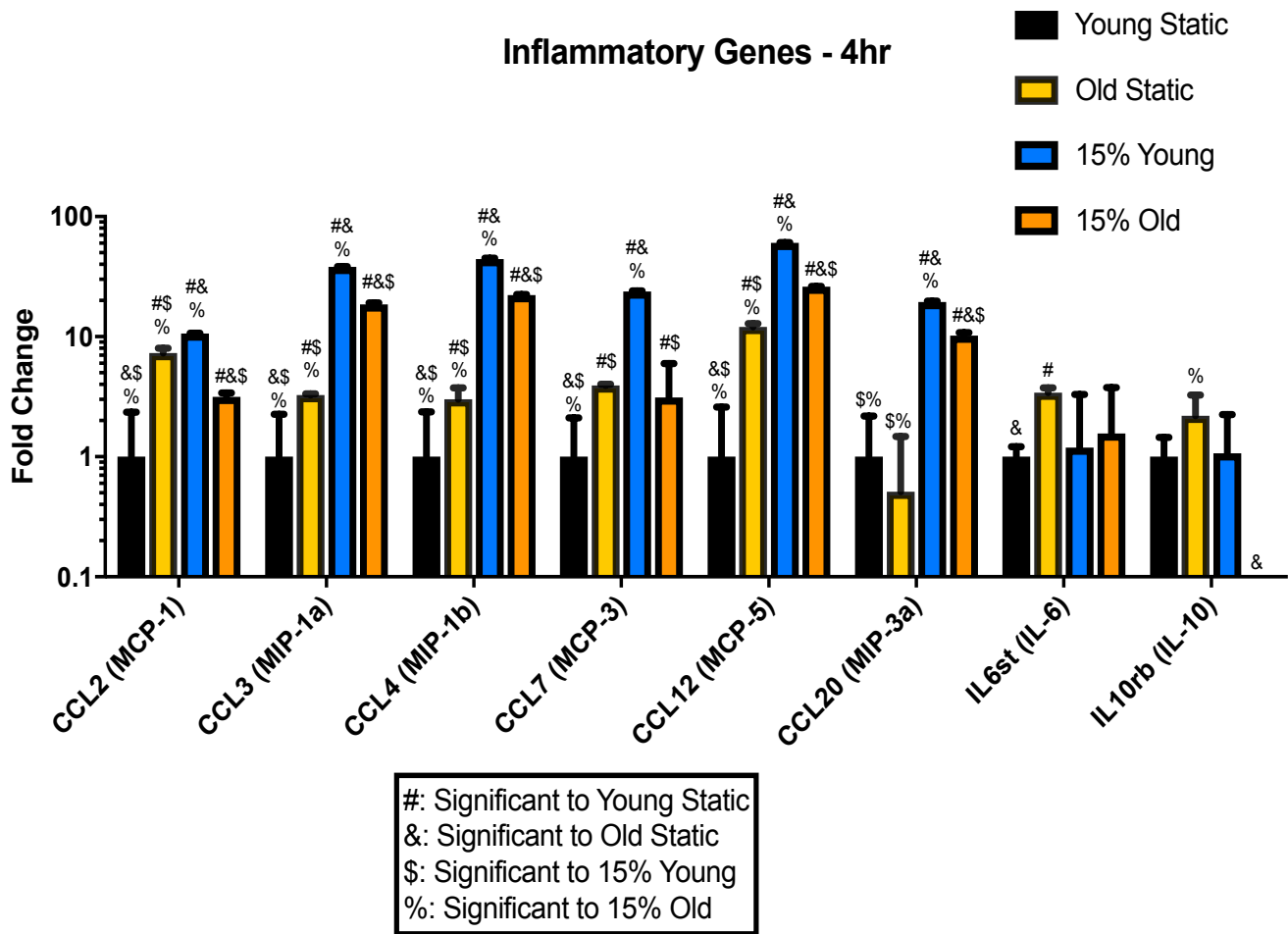


*Figure 18: Cyclic Stretch (15%) for 4 hours +/- age upregulate inflammatory genes. These genes are associated with proinflammatory signaling and immune cell recruitment/activation. Columns are normalized fold change differences in gene expression compared with Young Static placed on a log10 scale to observe large changes in expression. Data are presented as mean +/- SD, n = 3 per group. Statistically significance is shown on figure.*

Gene expression for MCP-1/CCL2 remained significantly elevated after 24 hours when comparing Old Stretched ATII cells to Old Static ATIIIs. Furthermore, MCP-1/CCL2 gene expression was significantly increased in Old Stretched ATIIIs compared to Young Stretched ATII cells; however, there was no

significant difference in gene expression between Old Static and Young Static groups or between Young Stretched and Young Static ATII cells (Figure shown in Chapter 5). After evaluating changes in MCP-1/CCl2 gene expression, we assessed the differences in corresponding protein secretion. These concentrations were normalized by the average number of ATII cells per experimental condition as determined by its corresponding MTT data (Figure shown in Chapter 5). We observed significantly greater MCP-1/CCL2 secretion by Old Static ATII cells compared to Young Static ATII cells as well as from Old Stretched ATII cells compared to Young Stretched ATII cells. Interestingly, we did not observe any differences in the secretion of this cytokine when comparing age-matched stretched to static conditions. Cyclic stretch significantly increased MIP-1 $\beta$ /CCL4 gene expression after 24 hours in Young ATII cells (Figure shown in Chapter 5). Age significantly increased MIP-1 $\beta$ /CCL4 gene expression, regardless of stimulation with mechanical stretch. Concurrent with the gene expression data for 4 (Figure 20) and 24 hours (Figure shown in Chapter 5), MIP-1 $\beta$ /CCL4 cytokine concentration in the media was elevated after 24 hours in Old Stretched and Static ATII cells compared to Young Stretched and Static groups. As seen before with the MCP-1/CCl2 protein secretion, there was no difference in MIP-1 $\beta$ /CCL4 production when comparing the age-matched stretched to static conditions. Interestingly, we observed no differences in IL-6 or IL-10 gene expression triggered by aging and/or cell-stretch for 24 hours, as shown in Figure 22.

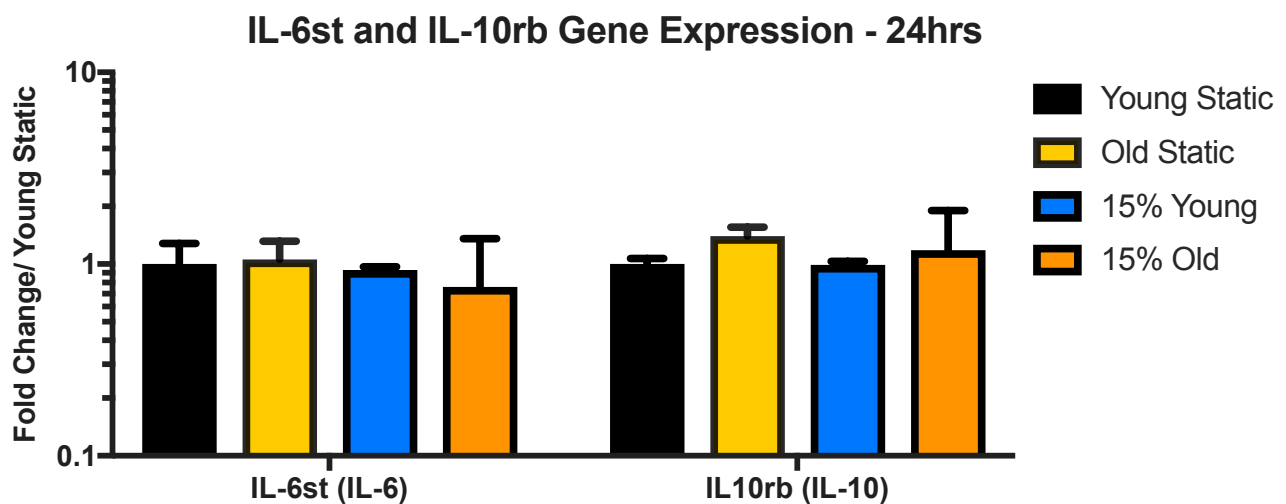


*Figure 19: Aging or Cell-stretch for 24hours had no effect on IL-6 or IL-10 gene expression. These inflammatory cytokines are often associated with ALI models and cell recruitment; however, no changes in gene expression were detected due to age or mechanical stretch. Data are presented as mean +/- SD, n = 3 per group*

In order to determine the ability of age and stretch to influence ATII recruitment of monocytes, we performed conditioned media experiments by exposing primary BMDMs to ATII conditioned media (CM) from all groups. As shown in Figure 22, we performed a live-dead stain on the cells following the 24 migration period to discriminate and quantify viable BMDMs that were recruited to the bottom reservoir. Representative images taken at 4x magnification show viable cells (green) and dead cells (red) that attached to the bottom of the transwell. We first quantified Young and Old BMDM migration using the ATII growth media (Figure 23A) and age-matched CM from the ATII stretch experiments (Figure 23B). As before, we normalized the recruited monocyte cell counts by the average number of ATII cells per condition as determined by the MTT data. We observed significantly decreased ( $p < 0.05$ ) BMDM migration with Old BMDMs/Old Static ATII CM in comparison to Young BMDMs/Young ATII Static CM. We also observed this same significant decrease ( $p < 0.05$ ) in migration with Old BMDMs/Old ATII Stretch CM in comparison to Young BMDMs/Young ATII Stretch CM.

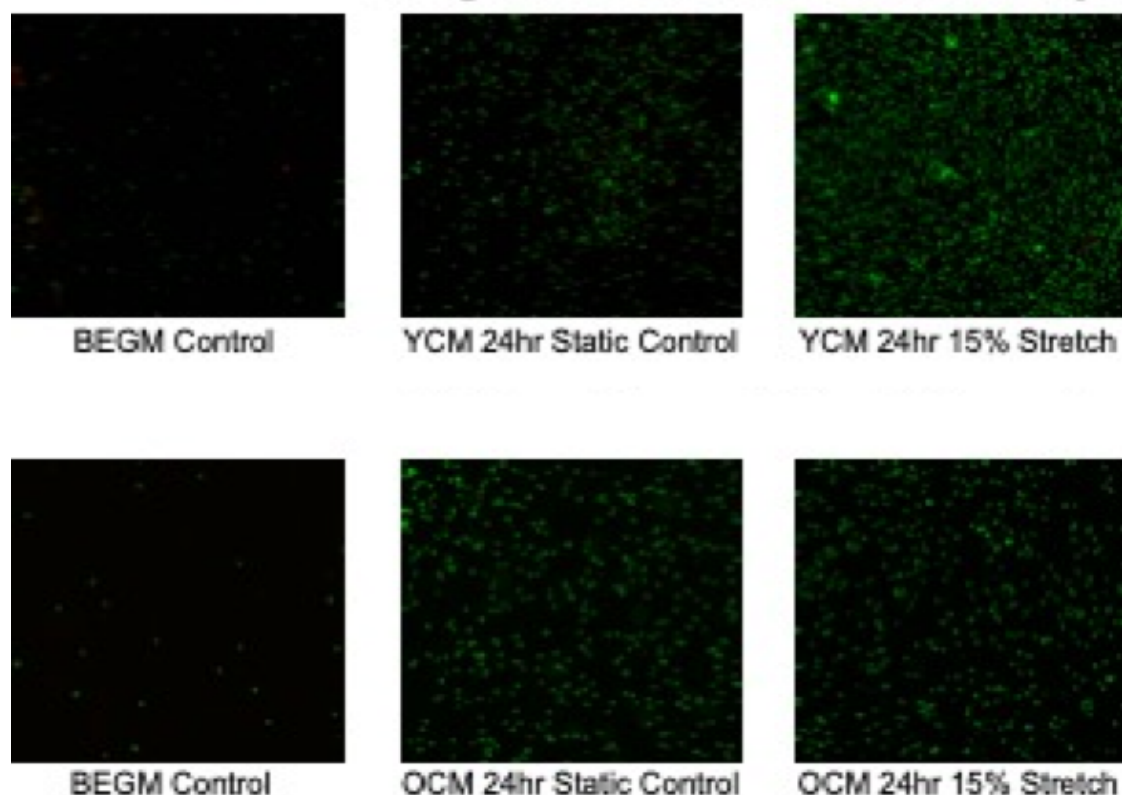


**Figure 20: Age and Mechanical Stretch Cause Variations in Monocyte Recruitment.** Young and Old BMDMs were placed in wells of an invasion assay with the various condition medias in the reservoirs. The cells were allowed to migrate for 24 hours and were then stained using Live/Dead Stain Kit to quantify the recruitment. Live cells are shown in green and dead cells are shown in red. Magnification = 4x.

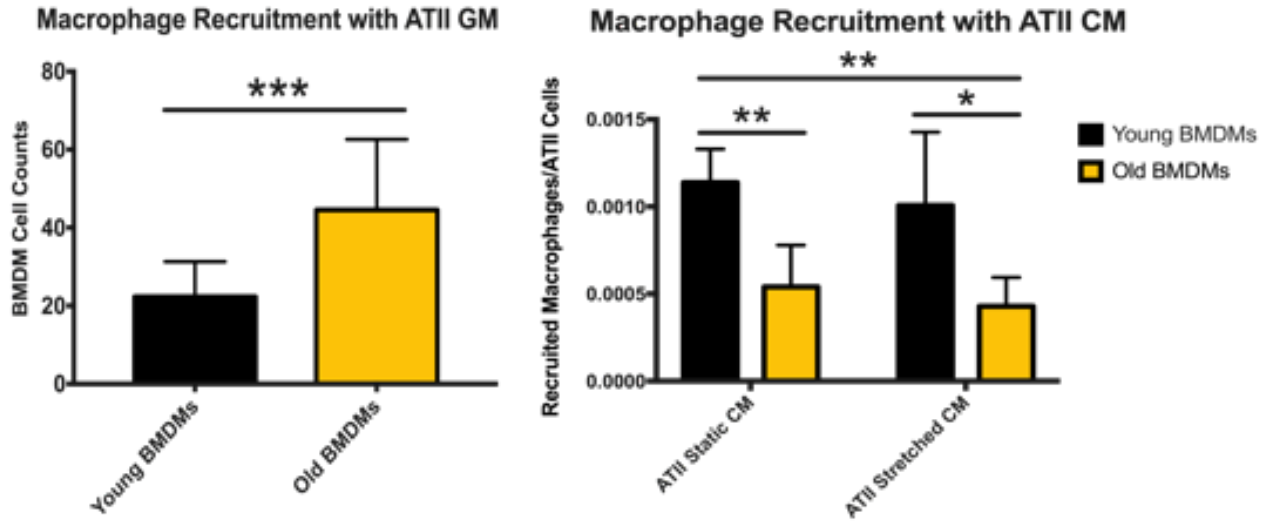


Figure 21: Monocyte Migration with (A) ATII Growth Media (GM) and (B) ATII Conditioned Media. Old BMDMs resulted in increased recruitment when stimulated with ATII GM. Young BMDMs had increased recruitment compared to Old BMDMs when stimulated with Young ATII Static or Stretch CM. Data are presented as mean +/- SD, n = 3 per group, \*p < 0.05, \*\*p < 0.01, \*\*\*p < 0.001.

In order to determine if it was the age of the ATII cells producing the CM or the age of the BMDMs that more greatly influenced migration, we quantified migration of Young BMDMs with CM from the Old Stretched and Static groups and Old BMDMs with conditioned media from the Young Stretched and Static groups to represent Mismatched CM monocyte recruitment (Figure 24). Young BMDMs/Young ATII Static CM significantly increased migration,  $p < 0.05$ , compared to Old BMDMs/Young ATII Static CM and Old BMDMs/Old ATII Stretch CM.

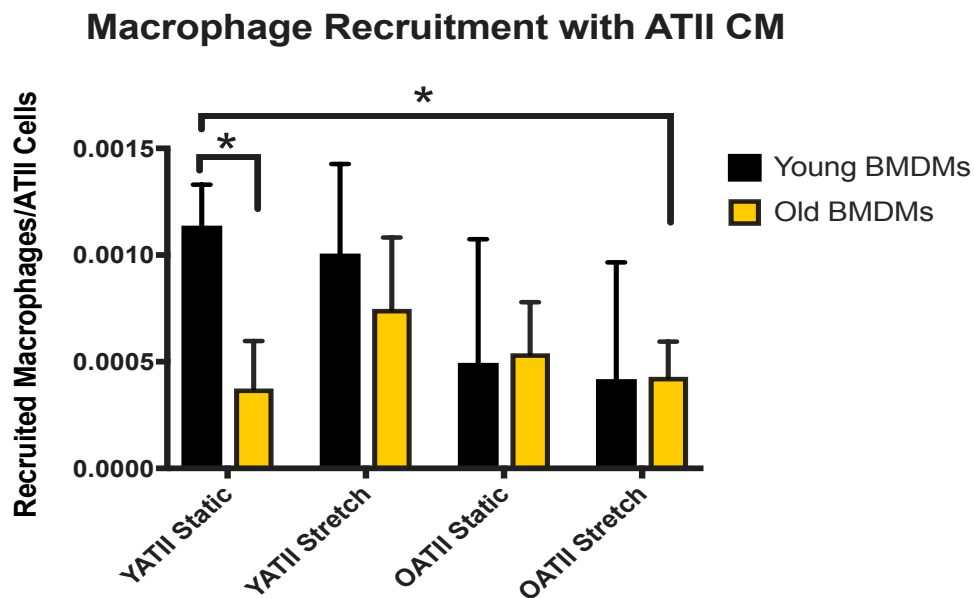


Figure 22: Monocyte Migration with Age-Matched and Mismatched ATII Conditioned Media. Data are presented as mean +/- SD, n = 3 per group, \*p < 0.05.

### **3.4 Discussion:**

VILI is characterized by an influx of inflammatory cytokines, loss of alveolar barrier integrity with pulmonary edema formation, and altered tissue mechanics. Mechanical ventilation causes alveolar overdistension and other types of lung injury in inflamed regions of the lung<sup>1,7-9</sup>. The over-distension of aerated lung regions generates abnormally large mechanical stretching forces on the epithelium that causes an immense secretion of proinflammatory cytokines and increased permeability<sup>1,7-9</sup>. Implementing “protective ventilator strategies” has only marginally improved negative outcomes, and the overall mortality rates for ventilated patients are still unacceptably high<sup>1-9</sup>. Furthermore, few studies are performed on aged subjects, which is incongruent with the fact that elderly patients have a greater need for mechanical ventilation<sup>17-19</sup>. These observations illustrate the major clinical need to develop treatments or therapies that prevent the cellular injury mechanisms and inflammation directly resulting from the pathological mechanical forces generated during mechanical ventilation.

We observed significant increases in the expression of MCP-1/CCL2 and MIP-1 $\beta$ /CCL4 in response to advanced age and/or mechanical stretch after 4 hours (Figure 20). These genes are associated with increased levels of inflammation in the lung and leukocyte recruitment which are characteristic of VILI<sup>9,14,74,134</sup>. MCP-1/CCL2 showed increased gene expression with age alone, mechanical stretch alone in the Young ATII cells, and with the combination of age and stretch when compared to Young Static ATII cells. Interestingly, mechanical stretch resulted in decreased MCP-1/CCL2 in Old ATII cells compared to the Old Static ATII cells. More interestingly, there was also less expression of MCP-1/CCL2 when comparing Old Stretched ATII cells to Young Stretched groups. These results suggest that MCP-1/CCL2 expression or activation is sensitive due to age under static conditions, and mechanical stretch differentially alters this activation based on the age of the ATII cells. MCP-1/CCL2 is a well-studied chemokine that is believed to assist in the recruitment of monocytes, memory T cells, and dendritic cells to sites of inflammation in response to tissue injury or infection<sup>14,74,134</sup>. It has also been shown to increase in aged mice in response to injury or infection<sup>135</sup>. Other studies have shown increased MCP-1/CCL2 expression and protein production in experimental VILI models<sup>14,74,134</sup>. Furthermore, we observed

increased MIP-1 $\beta$ /CCL4 (macrophage inflammatory protein-1 $\beta$ ) expression in response to advanced age or mechanical stretch (Figure 20). However, as seen with the changes in MCP-1/CCL2 expression, the Young Stretched ATII cells resulted in increased MIP-1 $\beta$ /CCL4 gene expression compared to the Old Stretched ATII cells. MIP-1 $\beta$ /CCL4 is believed to be a chemoattractant for monocytes, natural killer cells, and other immune cell participants<sup>14,74,134</sup>. Taken together, these results validate that advanced age and mechanical stretch impact ATII inflammatory signaling. It appears that the Old ATII cells have increased proinflammatory signaling during non-injurious or baseline conditions, and then they fail to respond as intensely as the Young ATII cells in response to injury. It is possible that the initial increased proinflammatory state of the unstimulated Old ATII cells reduces their sensitivity and ability to properly respond properly when an injury occurs. This behavior was previously observed and suggested with advanced age and several immune cell responses, such as with macrophages<sup>24</sup>. We selected MCP-1/CCL2 and MIP-1 $\beta$ /CCL4 as the targets for further study in age-associated ER stress and inflammatory experiments due to the significant changes in gene expression observed from mechanical injury and advanced age. In addition to its role in monocyte/macrophage recruitment<sup>14</sup>, numerous studies indicate that MCP-1/CCL2 is significantly increased in experimental models of mechanically ventilated mice<sup>14,134</sup> and in lipopolysaccharide (LPS)-induced acute lung injury models using lung epithelial cells<sup>62,95,134,135</sup>. While MIP-1 $\beta$ /CCL4 also plays a role in monocyte/macrophage recruitment, studies demonstrate that it is also increased in experimental acute lung injury models<sup>14,74,134</sup>.

Intriguingly, we did not observe significant changes in IL-6st, Interleukin 6 Signal Transducer, gene expression due to advanced age or in response to cyclic stretch for 4 or 24 hours. As mentioned before, the binding of IL-6 to IL-6R induces IL-6st activation<sup>9</sup>. The proinflammatory gene IL-6 is a known biological marker of ventilator-induced lung injury and has previously been shown to be upregulated in *in vitro* and *in vivo* models of VILI<sup>1,9,14,74,134</sup>. It is possible that this may be the result of implementing a 15% change in surface area for our cyclic stretch conditions, which may not be large enough for modeling pathophysiological alveolar over-distension. Additionally, much of the evidence for IL-6 increases in experimental VILI models are derived from *in vivo* models or *in vitro* models using MLE-12 or A549 cells.

It's possible that cyclic stretch on only primary murine ATII cells does not show the same upregulated proinflammatory profile. Furthermore, this gene may not be influenced by advanced age, which may explain why we did not observe changes in gene expression when comparing Young Static ATII cells to Old Static ATII cells.

Downstream from alveolar epithelial cells' contribution to injury and inflammatory signaling, monocytes/macrophages are thought to be one of the major targets of the mechanically stretch-induced signaling mechanisms of the alveolar epithelium<sup>28,127</sup>. Macrophages in the alveolar space greatly contribute to barrier integrity and local inflammation as they are a major participant in inflammatory signaling between the epithelium and innate immune response<sup>15</sup>. Furthermore, more recent studies have shown that macrophage polarization and function are impaired with aging<sup>24,25,38</sup>. This concept has been classified as "inflammaging" in which a chronic progressive increase in the proinflammatory status with a decrease in adaptive and innate immune response occurs with aging<sup>25,38</sup>. Due to incongruent findings between recent studies, the effects of aging on macrophage function and polarization are still insufficiently investigated and remain controversial<sup>24</sup>. Consequently, we investigated the impact of age and/or stretch on monocyte recruitment using Bone Marrow-Derived Monocytes (BMDMs) to understand the interaction between macrophages/monocytes and epithelial cell signaling that occurs in ALI and VILI. We chose to use this primary cell type in order to examine age-related differences because large quantities are more easily obtained with BMDMs compared with alveolar macrophages, and they are more suitable for microscopy applications<sup>117</sup>.

Collectively, the age-matched and age mismatched experiments (Figure 24) suggest that advanced age greatly influences the cellular behavior and responses of the alveolar epithelial cells and/or monocytes regardless of injury conditions. We are the first to demonstrate age-dependent differential response of epithelial and monocyte/macrophage interaction and signaling. Overall, our results indicate that aged ATII cells produce greater concentrations of proinflammatory cytokines/chemokines under resting and stretched conditions, the age-related increased MCP-1/CCL2 and MIP-1 $\beta$ /CCL4 chemokines interestingly failed to correlate with age-related increased monocyte recruitment, and aged BMDMs

responded differently and were recruited to a lesser extent than younger BMDMs. These findings further validate and elucidate the concept of *inflammaging* and its impact on lung injury and inflammation. Our observations also correlate the recent study by Gibon et al., which suggested that aged bone marrow macrophages respond differentially to polarizing stimuli compared to younger cells. They showed that aged bone marrow macrophages exist in a preactivated resting state with increased baseline cytokine secretion compared to younger resting macrophages. Furthermore, the authors suggest that the aged macrophages may have less feedback control over inflammatory signaling in the context of resolution and healing. Overall, they found that aged bone marrow macrophages had increased resting levels of oxidative stress, skewed ratios of proinflammatory to anti-inflammatory markers, and delayed healing response mechanisms compared to younger macrophages<sup>24</sup>, which correlate with our findings.

It was somewhat unexpected that we observed less monocyte recruitment induced by the Old ATII CM compared to BMDM's stimulated with the Young ATII CM after the aged ATII cells expressed and secreted greater amounts of the proinflammatory cytokines/chemokines MCP-1/CCL2 and MIP-1 $\beta$ /CCL4 (Figures 23 & 24). This incongruity is perplexing; however, it may be influenced by several factors. While the chemokines are believed to be important chemoattractants for monocytes and other immune cells<sup>134</sup>, our data suggest that an increase in these proteins by ATII cells either had little to no significant impact on monocyte migration. There may be other inflammatory proteins secreted in the conditioned media due to advanced age and/or mechanical stretch that may be more influential in injury signaling and leukocyte migration. We plan to investigate and characterize additional inflammatory proteins in our CM groups in future work. Additionally, Franck et al. demonstrated that a direct interaction between alveolar epithelial cell and macrophages were required for subsequent macrophage activation and signaling to occur in their study<sup>29</sup>, which may also explain why our conditioned media led to unexpected recruitment. Another possible cause may be derived from age-related differences in the secreted chemokines or chemokine receptors on the BMDMs. Further molecular analysis of the structure and bioactivity of the chemokines produced by the Young and Old ATII cells and surface characterization of the BMDMs are required to examine these possibilities.

There are some minor limitations in this the study. Multiple studies have suggested that 15% stretch is insufficient to injure young alveolar epithelial cells<sup>137,138</sup>. This possibility might explain why we did not see the same inflammatory changes that we observed in the Old ATII cells. However, our results suggest that advanced age impacts inflammatory activation in ATII cells in response to physiologically relevant mechanical stimuli. We have shown previously that while cell membrane integrity is retained, cyclic stretch of Young ATII cells at 15% change in surface area is sufficient to affect gene expression and phenotype<sup>139</sup>. Our results indicate that Old ATII cells respond differently to mechanical stretch compared with young ATII cells, potentially indicating that even under low tidal volume mechanical ventilation, older subjects may have an intensified or altered inflammatory response.

As the compounding effects of aging and mechanical injury reveal significant changes in ATII and macrophage responses, we need to better understand the mechanisms and implications of these age-dependent factors associated with the increased susceptibility of the elderly to ALI/VILI.

## **CHAPTER 4: AGING IMPACTS PULMONARY RESPONSES IN A HIGH PRESSURE-CONTROLLED MECHANICAL VENTILATION ALI/VILI MODEL**

### **4.1 Rationale:**

Although patients with Acute Lung Injury (ALI) or other severe lung conditions often require mechanical ventilation to provide adequate gas exchange for survival, this intervention often produces several pathological mechanical forces. These mechanical forces produce or exacerbate a pre-existing lung injury causing ventilator-induced lung injury (VILI) that results in alveolar barrier damage, pulmonary edema, hypoxia and hypoxemia, and chronic inflammation. These conditions often prolong the necessity of mechanical ventilation, which may result in further lung injury, multi-system organ failure, and mortality<sup>1</sup>. The over-distension of aerated lung regions generates abnormally large strains on the epithelium that directly causes barrier disruption, cellular necrosis and apoptosis, and an immense secretion of pro-inflammatory cytokines<sup>1,9,10</sup>. The high transmural pressures produced can activate pro-inflammatory signaling pathways that further deteriorate alveolar barrier integrity<sup>1,11</sup>. These damaging mechanisms enhance the release of inflammatory mediators, classified as biotrauma, which can cause further lung and distal organ injury<sup>9,12</sup>. However, the factors and mechanisms that govern this progression need to be better understood to provide treatment targets.

The largest population of patients requiring mechanical ventilation is the elderly, and age is a known predictor for the severity of VILI. Experimental injurious mechanical ventilation caused worsened pulmonary permeability and lung tissue damage in older subjects compared with young counterparts<sup>19,20</sup>. The increased sensitivity and susceptibility in the elderly may be attributed to or enhanced by the changes in lung structure and function that occur with aging. Several pulmonary and supportive extra pulmonary structural changes occur with aging that have significant impacts on pulmonary function and physiology<sup>22,23,43,44</sup>. These structural deviations lead to adverse respiratory mechanics, which impact expiratory flow, lung volumes, and overall gas exchange<sup>22</sup>. Alveolar duct dilation and enlargement of alveolar air spaces that occur with aging lead to a reduction in alveolar surface tension, increased lung

compliance, and declines in tissue elasticity and dampening<sup>44</sup>. Changes in supportive extra pulmonary structures with aging include decreases in chest wall compliance and reductions in respiratory muscle strength, which lead to increases in residual volumes and decreases in total lung capacities<sup>22,43,44</sup>. Age-related changes in gas exchange include V/Q inequality and decreased diffusion capacity of the lung for carbon monoxide, which cause an increased alveolar-arterial oxygen gradient and decreased PaO<sub>2</sub><sup>44</sup>. These changes in the aging lung correlate with the proposed mechanisms of VILI; however, the impact of age-related changes in lung structure and function in VILI still lacks great clarity. The increases in the severity and mortality rates of VILI with patient age combined with the greater need for mechanical ventilation among the elderly stresses the need to investigate associations between the structural and cellular changes that occur with aging and the increased susceptibility to lung injury of this population.

The aging lung also exhibits indications of cellular senescence and is closely linked to aging of the immune system, known as *immunosenescence*<sup>23</sup>. A condition of mild, systemic inflammation is associated with and predictive of many age-related diseases<sup>24</sup>. This type of state, termed *inflammaging*, occurs without the presence of overt infections or injury and is characterized by a state of chronic, low-intensity inflammation<sup>25</sup>. Comparative studies in healthy individuals suggest that the elderly have higher indications of proinflammation compared with younger individuals, which could be associated with the increased susceptibility to ALI/VILI<sup>23-25</sup>. Aging of resident and systemic immune cells leads to an intensified proinflammatory environment and reduced capacity of fighting infectious diseases<sup>23,25</sup>. *Inflammaging* is believed to be macrophage centered<sup>38</sup> and intensely associated with many aging and inflammatory pathologies.

Lung macrophages, comprising of alveolar and interstitial macrophages, act as the first immune defense system of the lung by clearing harmful pathogens and activating the innate immune system<sup>26</sup>. Lung macrophages also contribute to barrier integrity and local inflammation as mediators of inflammatory signaling between the epithelium and other immune cells<sup>13,27,28</sup>. In experimental VILI models, alveolar macrophages were shown to be vital to the increases in lung vascular and alveolar epithelial permeability and subsequent proinflammatory activation and amplification<sup>29</sup>. Studies on age-

related effects of lung macrophages suggest that the cells' phagocytic capacity, TLR signaling, cytokine release, and reactive oxygen species (ROS) activity are critically impaired or elevated in older individuals<sup>23,30</sup>. However, the evidence for age-related changes in inflammatory signaling and cytokine expression and secretion by lung macrophages remains controversial. Several *in vitro* studies of monocyte or macrophage function have been contradictory, as few showed that the capacity of several myeloid cells to produce certain inflammatory cytokines can be impaired in old age, while others have shown proinflammatory secretion only to be enhanced<sup>23,24</sup>. As most age-related diseases share an inflammatory pathogenesis, this phenomenon needs more clarification in the context of ALI/VILI and is believed to be a highly significant risk factor for both morbidity and mortality in the elderly population.

Macrophages also show high plasticity and result in heterogenic subpopulations or polarized states that can be identified by specific cellular markers<sup>31</sup>. Macrophage phenotypes may be largely classified as either more proinflammatory or pro-injurious, also called classical macrophage polarization, or they can reflect an alternative activation profile, which has been considered as anti-inflammatory or pro-repair<sup>24,32,33</sup>. Classically-activated macrophages promote the development of acute lung injury, whereas alternatively-activated macrophages may be involved in limiting or resolving lung inflammation<sup>31</sup>. Classical macrophage activation can be induced by various environmental cues, such as interferon-gamma (IFN- $\gamma$ ), Toll-like receptor (TLR) signaling, and many others<sup>24,32,33,39</sup>. This polarization state is associated with activation of transcription factors STAT1 and NF- $\kappa$ B<sup>24</sup>. Alternative macrophage polarization may be induced by IL-4 and IL-13, and STAT6 is the main transcription factor involved<sup>24</sup>. Classical polarization is characterized by an upregulation of iNOS, CD80, CD86, and HLA-DR and elevated cytokine release of TNF- $\alpha$ , IL-6, IL-1, IL-12, IL-23, and type 1 interferon<sup>24,31</sup> in murine macrophages. Alternative activated murine macrophages are characterized by a cytokine release profile of IL-4, IL-10, IL-13, and IL-1 $\alpha$  and have increased expression of CD206, Ym1, CD163, CCL1, CCL18, FIZZ1, arginase 1 (Arg1), RELM $\alpha$ , and chitotriosidase<sup>24,31</sup>. Macrophage polarization has been

shown to be highly involved in physiological transitions from inflammation to tissue regeneration and it's believed to be impaired with aging; however, the relevant studies have been contradictory.

This work is based on the scientific premise that the structural and cellular changes in aged lungs precondition the elderly to be more susceptible to injury and other negative outcomes resulting from the damaging stresses generated during mechanical ventilation. We hypothesize that aging and injurious mechanical ventilation synergistically impair macrophage polarization in the lung. This impairment produces amplified alveolar barrier damage and diminished pulmonary function. We tested this hypothesis utilizing young and old mice exposed to high-pressure mechanical ventilation and characterized their response.

#### **4.2 Materials and Methods:**

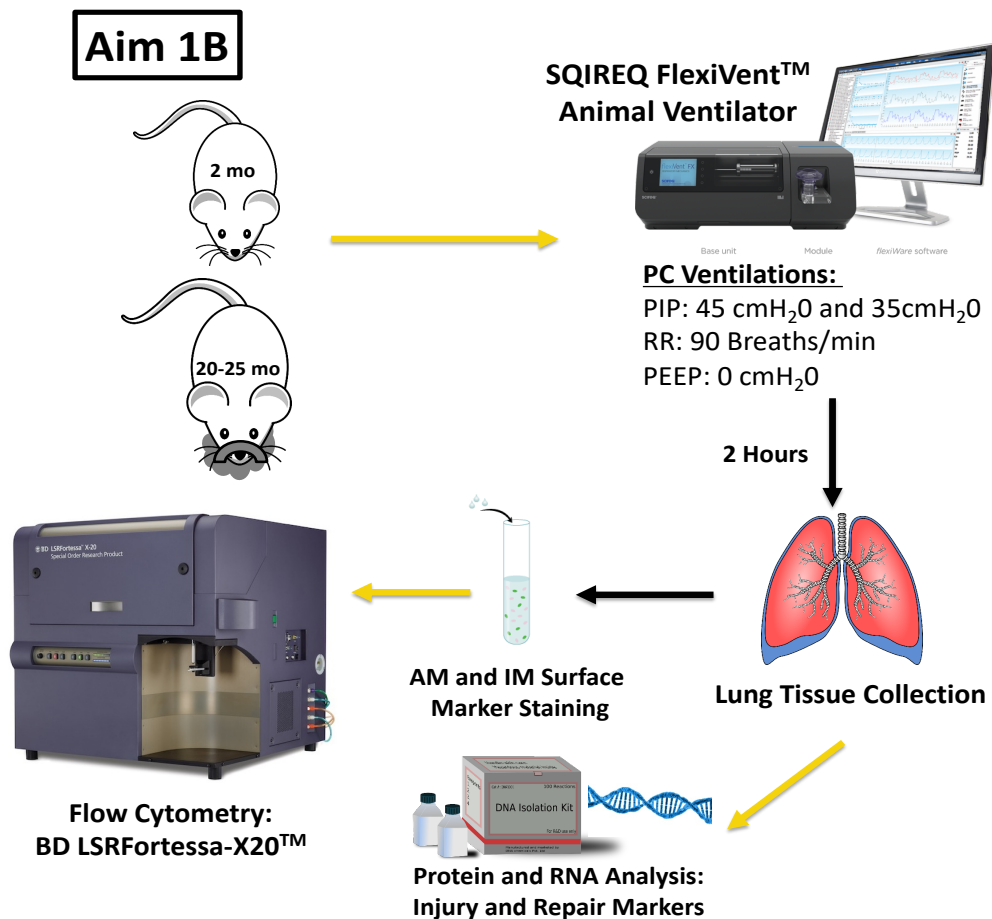


*Figure 23: Schematic overview of age-related animal mechanical ventilation procedure and collection. Figure depicts the SQIREQ FlexiVent Animal Ventilator that delivers the high PCMV.*

**Animals:** Male C57BL/6 mice 8 weeks of age were purchased from Jackson Laboratory (Bar Harbor, ME). Male C57BL/6 mice 20 months of age were provided by the National Institute on Aging (Bethesda, MD). All animals were housed in accordance with guidelines from the American Association for Laboratory Animal Care and Research protocols and approved by the Institutional Animal Care Use Committee at Virginia Commonwealth University (Protocol No. AD10000465).

**Pressure-Controlled Ventilator-Induced Lung Injury Model:** We mechanically ventilated young (2-3 mo.) and old (20-25 mo.) C57BL/6J wild-type mice using a Scireq FlexiVent computer-driven small-animal ventilator (Montreal, Canada) and previously cited methods<sup>10</sup> with slight modifications. Mice were anesthetized, tracheotomized, and then ventilated for 5 minutes using a low pressure-controlled strategy (peak inspiratory pressure (PIP): 15 cmH<sub>2</sub>O, respiratory rate (RR): 125 breaths/min, positive end-expiratory pressure (PEEP): 3 cmH<sub>2</sub>O). Mice were then ventilated for 2 hours using a high pressure-controlled mechanical ventilation (PCMV) protocol (PIP: 35-45 cmH<sub>2</sub>O, RR: 90 breaths/min, and PEEP: 0 cmH<sub>2</sub>O). Pulmonary function and tissue mechanics were measured and collected at baseline and every hour during the 2-hour high PCMV duration using the SCIREQ FlexiVent system and FlexiWare 7 Software. A separate group of mice was anesthetized, tracheotomized, and maintained on spontaneous ventilation for 2 hours.

**Tissue Processing:** Immediately following mechanical ventilation, the right lobes of the lung were snap-frozen with liquid nitrogen, then stored at -80°C for further analysis. The left lobes of the lung were then inflated with digestion solution containing 1.5 mg/mL of Collagenase A (Roche) and 0.4 mg/mL DNaseI (Roche) in HBSS with 5% fetal bovine serum and 10mM HEPES and processed as previously described<sup>119</sup>. The resulting cells were counted, and dead cells were excluded using trypan blue. Subsets of the experimental groups were also used to collect bronchoalveolar lavage fluid (BALF) fluid, differential cell counts, and left lobes for histological analysis.

**Flow Cytometric Analysis:** Following live cell counts,  $4 \times 10^6$  cells per sample were incubated in blocking solution containing 5% fetal bovine serum and 2% FcBlock (BD Biosciences) in PBS. The cells were then stained using a previously validated immunophenotyping panel of fluorochrome-conjugated antibodies<sup>31</sup> with slight modifications, as shown in Table 1. Following the staining procedure, cells were washed and fixed with 1% paraformaldehyde in PBS. Data were acquired and analyzed with a BD LSRFortessa-X20 flow cytometer using BD FACSDiva software (BD Bioscience). Histogram plots were generated using FCS Express 5 software (De Novo). Compensation was performed on the BD LSRFortessa-X20 flow cytometer at the beginning of each experiment. “Fluorescence minus one” controls were used when necessary. Cell populations were identified using a sequential gating strategy that was previously developed<sup>31</sup>. The expression of activation markers is presented as median fluorescence intensity (MFI).

Marker	Alveolar Macrophages	Interstitial Macrophages	Clone	Isotype	Fluorochrome Conjugate	Dilution Factor
CD45	+	+	30-F11	Rat IgG2b, $\kappa$	BB515	1:100
CD11b	-	+	M1/70	Rat IgG2b, $\kappa$	BUV395	1:100
CD11c	+	+	HL3	Armenian Hamster IgG1, $\lambda$ 2	BV786	1:50
CD24	-	-	M1/69	Rat IgG2b, $\kappa$	AF700	1:300
CD64	+	+	X54-5/7.1	Mouse IgG1, $\kappa$	PE	1:200
MHCII	+/-	+	M5/114.1 5.2	Rat IgG2b, $\kappa$	PerCP-Cy5.5	1:300
CD80 (M1)	+/-	+/-	16-10A1	Armenian Hamster IgG1, $\lambda$ 2	BV421	1:200
CD206 (M2)	+/-	+/-	MR5D3	Rat IgG2a	AF647	1:200

*Table 1: Phenotypes of Alveolar and Interstitial Macrophages in the Healthy Mouse Lung and Corresponding Antibodies and Conjugated Fluorochromes Used for Flow Cytometric Analysis.*

**Bronchoalveolar Lavage Fluid (BALF) Cytometry and Protein Concentrations:** The BALF was collected and centrifuged to collect a cell pellet and supernatant, as previously described<sup>10</sup>. Cell pellets were resuspended in saline and mounted onto glass slides using a cytospin device (Thermo Shandon). Cells were stained (3 Diff-Quick solutions staining kit) and immune cell populations were quantified. The quantification of total BALF protein in the supernatants was measured by using the Pierce BCA Protein Assay Kit (Thermo Scientific).

**Histology:** Lung tissue samples were embedded and stained with hematoxylin and eosin (H&E). The mean linear intercept ( $L_m$ ), an index of airspace enlargement, quantify relative differences in alveolar airspace area within lung histology sections and were measured and analyzed as previously described<sup>10</sup>.

**Statistics:** A total of 44 young and old mice were used for this study. All experiments were performed with a minimum of  $n=3$ . Larger  $n$  values were utilized where possible. Limitations exist in the number of 20-25-month-old mice available from the National Institute on Aging. Therefore, we used minimum numbers to achieve a power of 0.8. Results are presented as mean  $\pm$  SEM. GraphPad Prism was used for all statistical analyses. For multiple-group comparisons, we used a two-way analysis of variance (ANOVA) with age and mechanical ventilation as factors, followed by a posthoc Tukey test to determine significance.  $P<0.05$  was considered statistically significant.

### **4.3 Results:**

#### **High PCMV-induced VILI is Elevated in Aged Mice Compared to Young**

The induction of ALI was assessed by evaluating the histological evidence of tissue injury, alteration of the alveolar-capillary barrier, and the existence of an inflammatory response following mechanical ventilation. As shown in Figure 26, these studies showed a highly reproducible degree of ALI in both age groups following the 2-hour duration of high PCMV.

Increased BAL fluid protein concentrations in the young and old mice that received high PCMV groups compared to their non-ventilated counterparts suggest there was sufficient indication of acute tissue injury (Figure 26A). Increases in BALF protein indicate pulmonary edema and alveolar-capillary barrier leakage, which were significantly elevated in young and old high PCMV mice compared to controls. Differential cell counts also showed that neutrophil accumulation in the BAL fluid were substantially elevated in both young and old high PCMV mice compared to their non-ventilated counterparts as well (Figure 26B). This result indicates the presence of an age-related inflammatory

response<sup>120</sup>. High PCMV enlarged the airspace in both young and old mice. Representative images are shown in Figure 26C. The mean linear intercept ( $L_m$ ), which is an index of airspace enlargement, was quantified to further assess the extent of injury (Figure 26C). There was significantly increased airspace enlargement in the old PCMV group compared to the young and old non-ventilated controls. These findings suggest that there was a substantial generation of acute lung injury in both the young and old age groups; however, the severity appears intensified with the old mice.

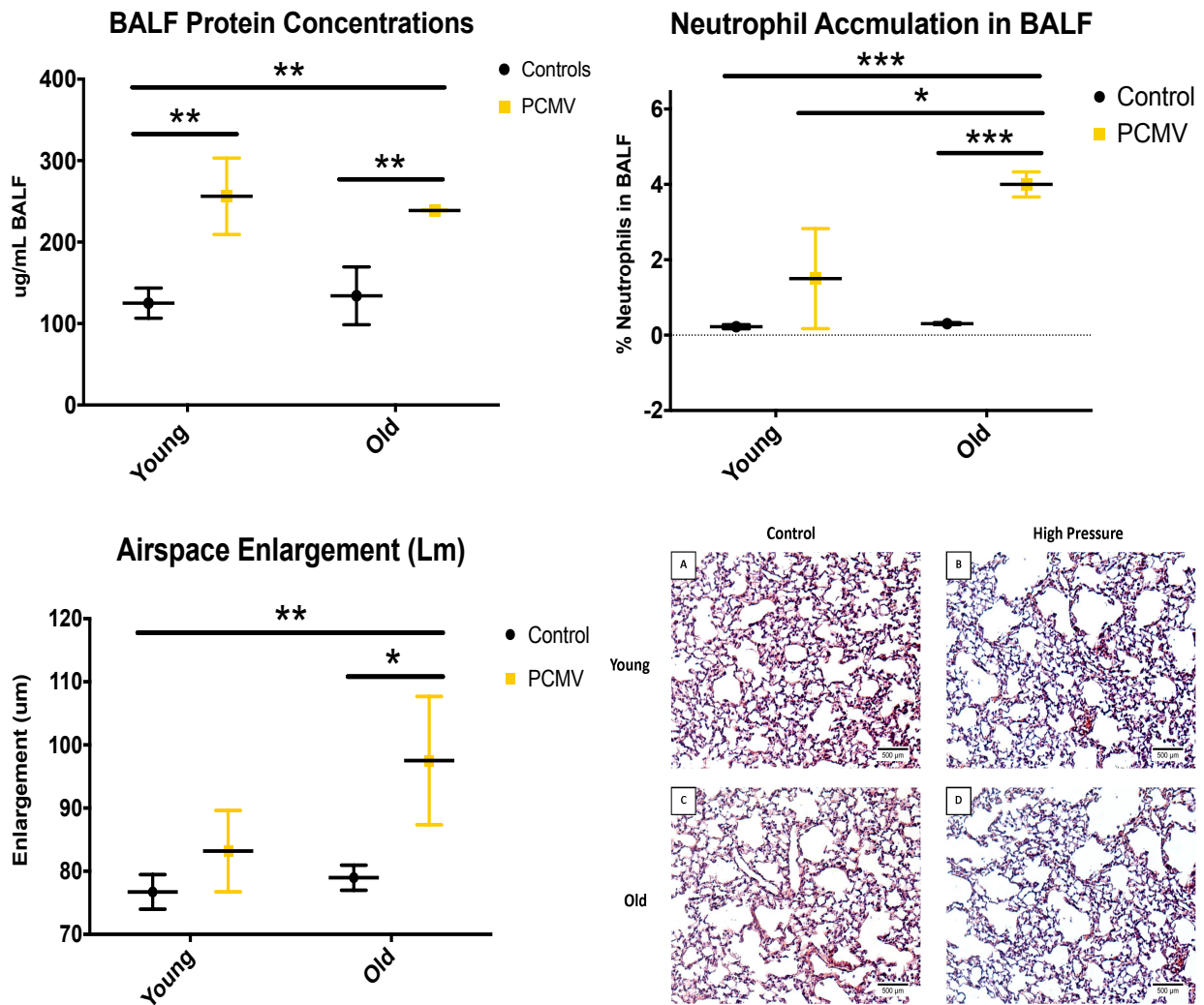


**Figure 24: High PCMV Induces Injury in Young and Old C57BL/6 Mice.** (A) Bronchoalveolar Lavage (BAL) fluids from control and high PCMV mice were analyzed for total protein (A) and neutrophil accumulation (B). Lung tissue sections from control and high PCMV mice were processed for staining with hematoxylin and eosin for histological analysis. Shown is a representative staining of the lung tissue from at least three independent experiments (C). Quantification of airspace enlargement of the stained histological sections using the mean linear intercept ( $L_m$ ) as described previously (D). Data are presented as mean  $\pm$  SEM,  $n \geq 3$  per group. \*  $p < 0.05$ , \*\*  $p < 0.01$ , \*\*\*  $p < 0.001$ , \*\*\*\*  $p < 0.0001$  as indicated.

## **Aged Mice Exhibit More Severe Changes in Pulmonary Function and Tissue Mechanics Following High PCMV**

Assessing the respiratory system mechanics and lung function in this investigation revealed significant differences between the young and old mice at baseline and following the high PCMV, as shown in Figure 27. The baseline inspiratory capacity (Figure 27A) and respiratory system compliance (C) (Figure 27C) were all significantly higher in aged mice compared to young. These properties were also higher following 1 hour and 2 hours of high PCMV in the old mice compared to young. There was also a significant reduction in the respiratory system compliance of old mice seen after 1 hour of high PCMV and substantial declines in the inspiratory capacity and respiratory system compliance of old mice after 2 hours of high PCMV.

The Newtonian resistance ( $R_n$ ), which is indicative of airway resistance (Figure 27B), the lung tissue damping (G) (Figure 27E), and the lung tissue elasticity (H) (Figure 27F) properties were all significantly lower in old mice compared to young at baseline. The tissue damping and tissue elasticity properties were also lower following 1 and 2 hours of high PCMV in the aged mice compared to the young. There was also a substantial increase in tissue elasticity following 2 hours of high PCMV in both the young and old mice; however, there was only a significant increase in lung tissue damping in the aged mice when comparing the measurements collected following the 2-hour PCMV to baseline indications.

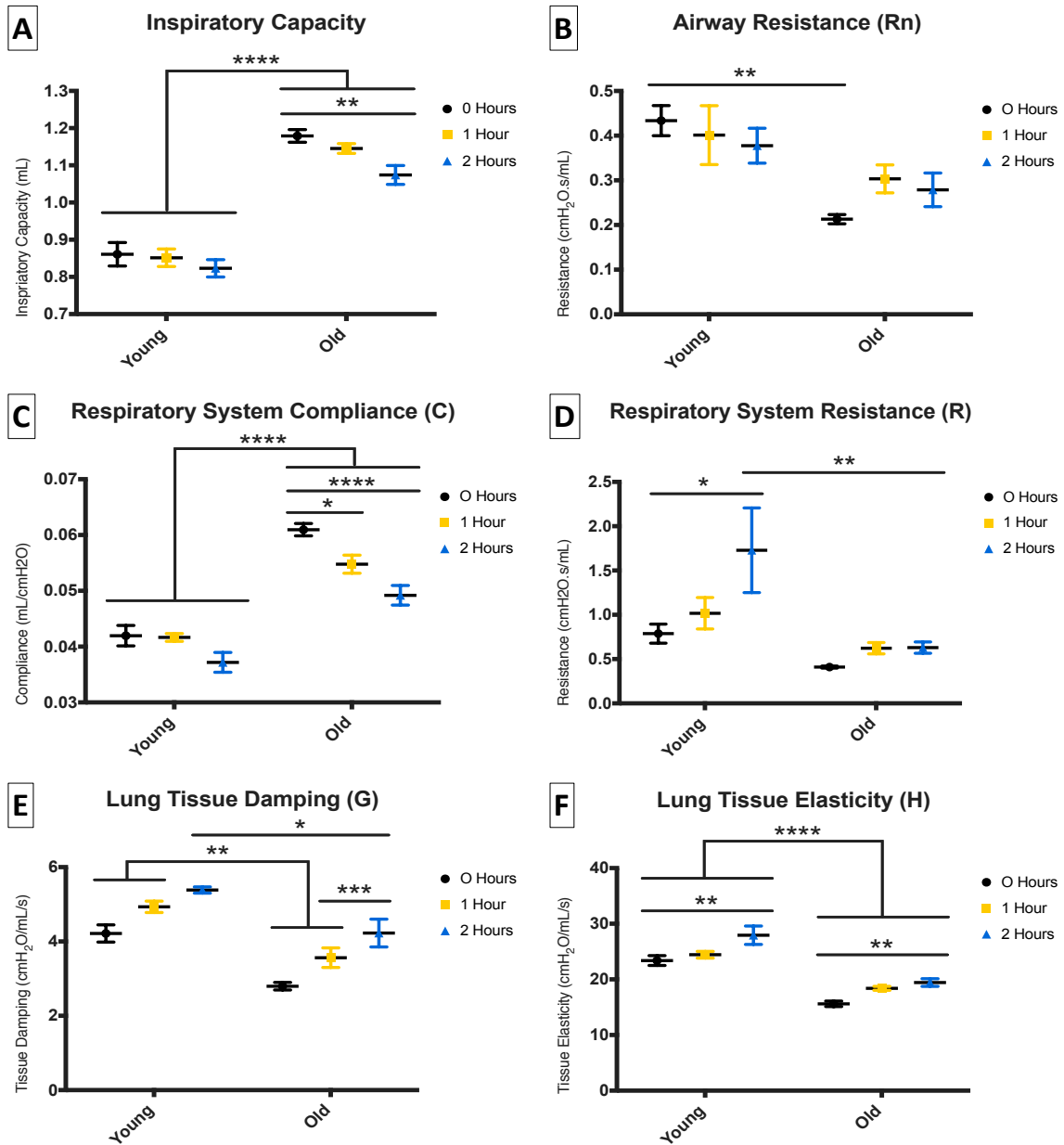


**Figure 25: Aging and high PCMV cause Deviations in Tissue Mechanics and Pulmonary Function.** Tissue mechanics and lung function was determined with a SCIREQ FlexiVent rodent ventilator for mice. Changes were determined in inspiratory capacity (A), airway resistance (B), respiratory system compliance (C), respiratory system resistance (D), lung tissue damping (E), and lung tissue elasticity (F). Data are presented as mean +/- SEM,  $n \geq 6$  per experimental group. \*  $p < 0.05$ , \*\*  $p < 0.01$ , \*\*\*  $p < 0.001$ , \*\*\*\*  $p < 0.0001$  as indicated.

While there was no difference in the total respiratory resistance (R) (Figure 27B) between young and old mice at baseline, there was a substantial increase in this property in the young mice that received high PCMV compared to the young controls; which was not observed in the old mice. R was also substantially lower in old mice compared to young following high PCMV for 2 hours.

Together, these considerable alterations in tissue mechanics and lung function from aging and high PCMV further validate the induction of acute lung injury in both the young and old mice using the high PCMV; moreover, most of the mechanics deviated more severely in the old mice that underwent high PCMV compared to the young. There were noteworthy differences in several of these properties between the young and old at baseline. These observations indicate that the structural changes that occur with aging and injury, independently, are intensified and compounded in the older population during mechanical ventilation.

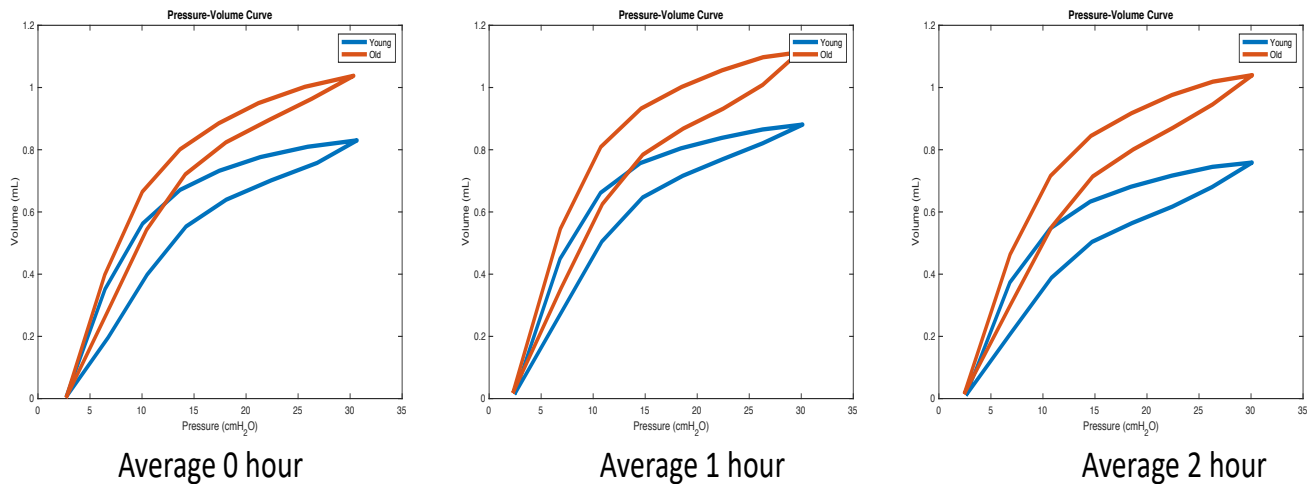


*Figure 26: Pressure-Volume Curves were generated using MATLAB. The diagram depicts the average changes in PV curves over the 2-hour time course of mechanical ventilation for young (blue) and old (red) mice.*

We also examined the pressure-volume curve data obtained during the mechanical ventilation procedures from the FlexiVent's PV-V and PV-P perturbations. The collected data points from the same experimental groups were then averaged for each time point of the PCMV procedure and used to generate PV curves using MATLAB. As shown in Figure 28, the PV curves represent the average values of young (blue) and old (red) mice at time 0h (A), 1h(B), and 2h(C). The slopes of the PV curves depict the respiratory system's compliance of young and old mice. As depicted in the figure, the slopes of young and old mice are decreasing over the 2 hour time course of high PCMV.

## Changes in CD80 and CD206 Expression Reveal Classical and Alternative Polarization Shifts of Lung Macrophages Caused by Aging and High PCMV

As shown in the representative histograms in Figure 29, analyzing the alveolar and interstitial macrophages using the standardized flow cytometric analysis revealed significant age-related changes to CD80 and CD206 expression of these cells, as well as deviations produced by 2 hours of high PCMV. The expression of CD80 is a surface marker associated with classically activated state of macrophages. CD206 (mannose receptor) is a surface marker that is associated with alternatively activated polarization state of macrophages.

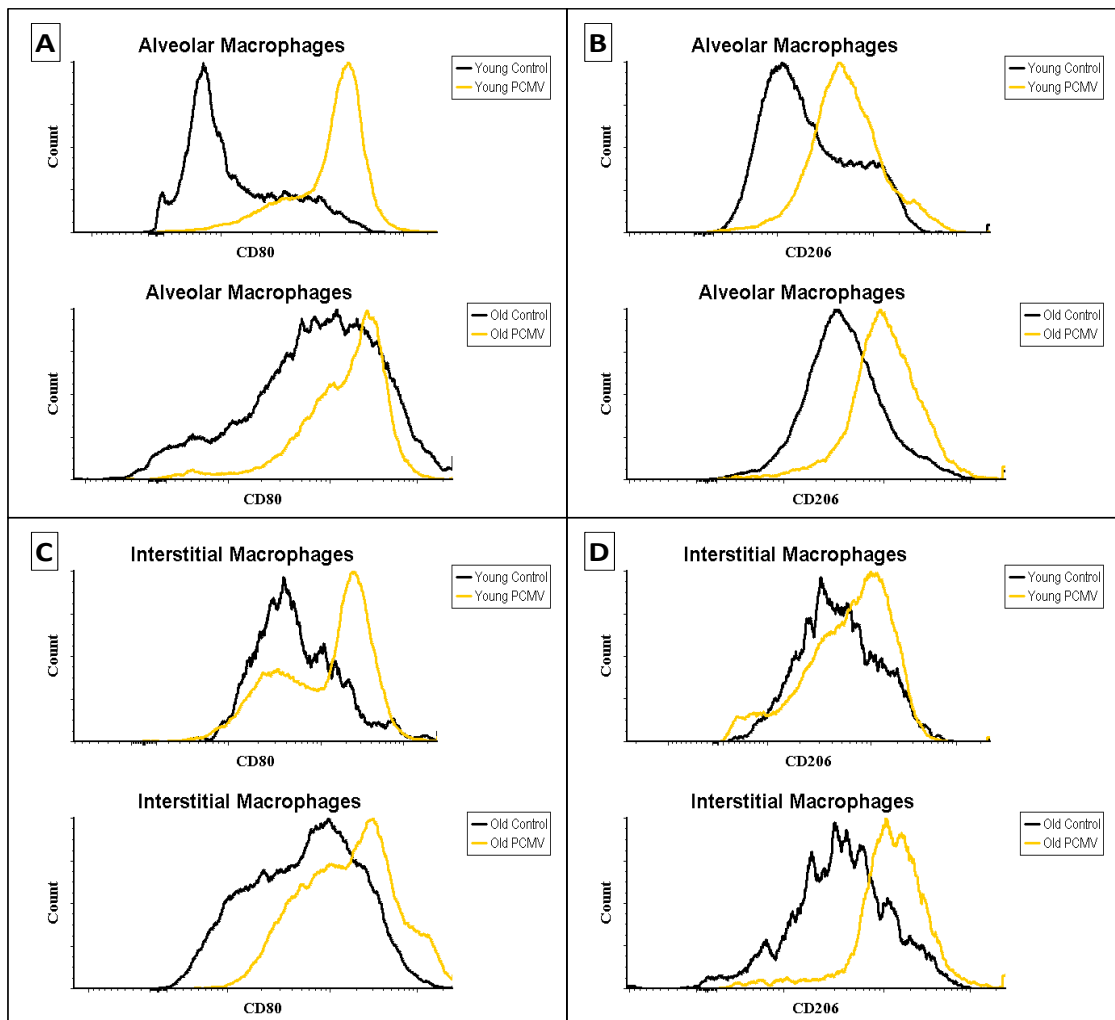


**Figure 27: Macrophages from Aged Mice and Mice that Underwent High PCMV Overexpress Associated Polarization Markers CD80 and CD206.** Histograms displaying the expression levels of markers associated with classical (CD80) and alternative (CD206) activated alveolar (A&B) and interstitial macrophages (C&D) from young and old mice with and without high PCMV. Black curves represent nonventilated control groups and the yellow curves depict PCMV groups. Histogram plots are representative of at least 4 independent experiments.

There is an overall increase in both CD80 and CD206 expression on both alveolar and interstitial macrophages isolated from the unventilated aged mice compared to the isolated young control mice (Figure 29). There were increases in both CD80 and CD206 expression in the alveolar macrophage populations (Figure 29) from both the young and old mice; however, the histogram peak shifts were more considerable in the young mice than the old compared to their respective controls. Furthermore, the histogram peaks of CD80 and CD206 were also shifted in the old nonventilated and the old PCMV alveolar macrophages compared to their young counterparts, suggesting increased expression of both classical and alternative macrophage activation markers due to aging and high PCMV. There was also a greater change in CD80 expression than CD206 expression in the young PCMV alveolar macrophages compared their respective controls. This was not observed with the old alveolar macrophages. The interstitial macrophage populations (Figure 29) revealed similar relationships; however, they were less pronounced compared to the alveolar macrophage populations. While comparable changes in CD80 and CD206 expression were observed with these cell populations due to aging and PCMV, the histogram peak shifts were less prominent. These findings suggest that both aging and high PCMV for 2 hours causes both main types of lung macrophages to overexpress both classical and alternative activation surface markers or shifts in their polarization states.

We supplemented a final gating strategy in order to identify and enumerate alveolar and interstitial macrophage subset populations, such as CD80<sup>-</sup>/CD206<sup>-</sup> cells (Figure 30A&B), CD80<sup>+</sup> cells (Figure 30C&D), CD206<sup>+</sup> cells (Figure 30E&F), and CD80<sup>+</sup>/CD206<sup>+</sup> double-positive cells (Figure 30G&H). By doing so, we observed interesting age-related differences that exist at baseline and changes to these populations caused by high PCMV. When comparing the old controls to the young controls, we found that the percentages of CD80<sup>-</sup>/CD206<sup>-</sup> alveolar macrophages (Figure 30A) and CD206<sup>+</sup> interstitial macrophages (Figure 30F) substantially decreases due to age alone. In the same comparison, the percentages of CD80<sup>-</sup>/CD206<sup>-</sup> interstitial macrophages (Figure 30B) and CD80<sup>+</sup>/CD206<sup>+</sup> double-positive alveolar macrophages (Figure 30G) significantly increased. When assessing the factor of high PCMV alone, there was a considerable rise in the percentage of CD80<sup>+</sup> alveolar macrophages (Figure 30C) and

CD80<sup>+</sup>/CD206<sup>+</sup> double-positive alveolar macrophages (Figure 30G) when comparing young mice that received high PCMV to young controls. The percentage of CD206<sup>+</sup> alveolar macrophages (Figure 30E) decreased in old mice that underwent high PCMV for 2 hours compared to the old control mice. When evaluating the influence of both aging and high PCMV, we discovered that the percentage of CD80<sup>-</sup>/CD206<sup>-</sup> (Figure 30A) and CD206<sup>+</sup> alveolar macrophages (Figure 30E) was reduced, while CD80<sup>+</sup>/CD206<sup>+</sup> alveolar macrophages increased (Figure 30G), when comparing old mice that received high PCMV to young controls. When comparing young and old mice that underwent PCMV, there were less CD80<sup>-</sup>/CD206<sup>-</sup> alveolar macrophages (Figure 30A) and more CD80<sup>+</sup>/CD206<sup>+</sup> alveolar macrophage populations (Figure 30G) when further looking at age-related differences between the groups.

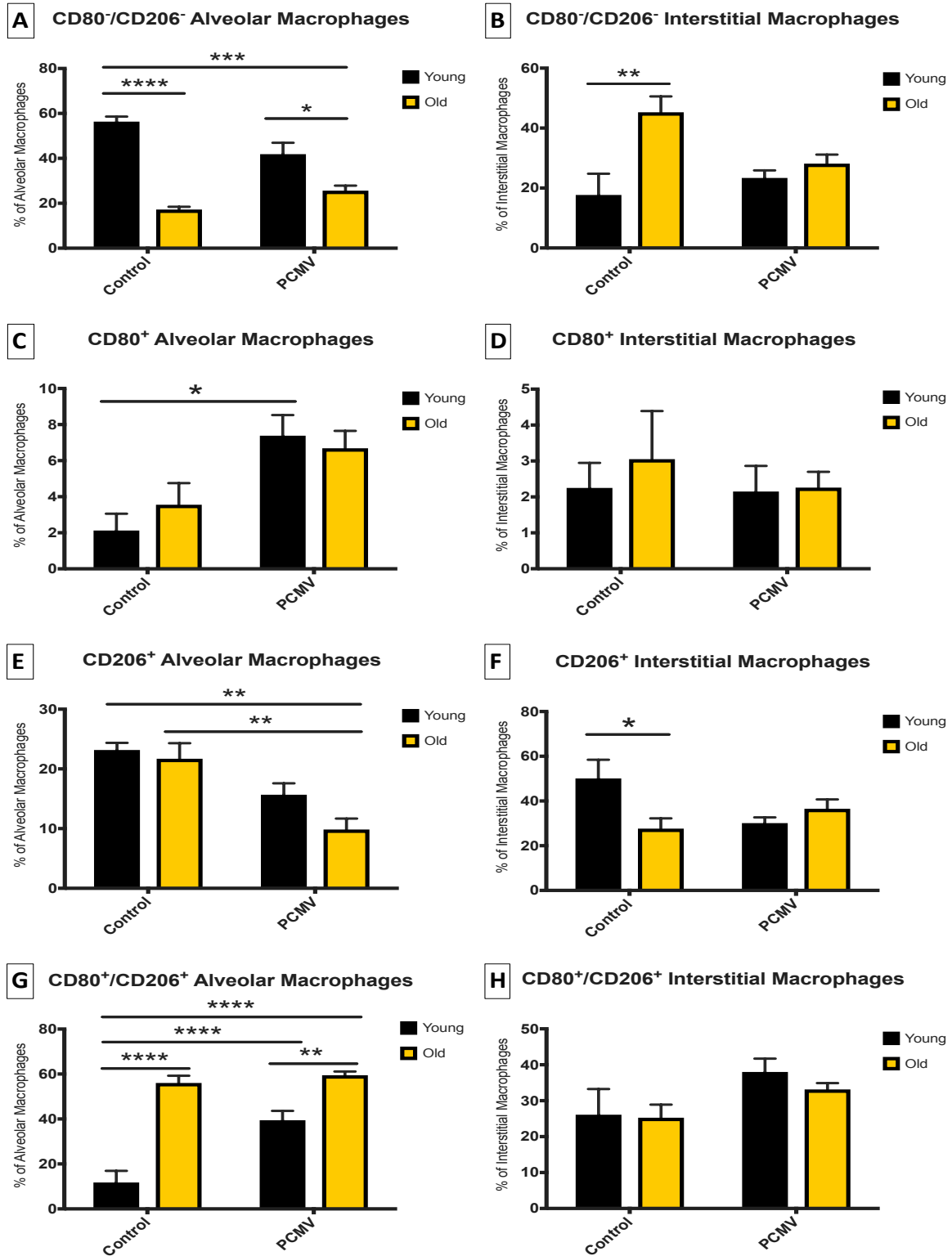


**Figure 28: Aging and High PCMV Influence Lung Macrophage Polarization in C57BL/6 Mice.** Quantifiable changes of macrophage subsets were identified using the set of surface markers and gating strategy described in the methods. The populations of CD80<sup>-</sup>/CD206<sup>-</sup> (A&B), CD80<sup>+</sup> (C&D), CD206<sup>+</sup> (E&F), and CD80<sup>+</sup>/CD206<sup>+</sup> (G&H) macrophages are depicted as percentages of total alveolar (A, C, E, G) and interstitial macrophage (B, D, F, H) populations. Data are presented as mean +/- SEM, n ≥ 4 per experimental group. \* p<0.05, \*\* p<0.01, \*\*\* p<0.001, \*\*\*\* p<0.0001 as indicated.

#### **4.4 Discussion:**

Despite recent advances in our knowledge of the pathophysiology of ALI and VILI, successful treatments do not exist for this lung condition and the mortality rates remain high, especially for the elderly population<sup>19,95</sup>. The aim of the current study was to better understand how aging primes the lung to be more susceptible to ALI (VILI) and to determine how aging and injurious PCMV influence the polarization states of lung macrophages. The outcomes of this investigation provide further evidence that aging exacerbates outcomes of acute lung injury, which resulted in a greater deterioration in lung function, elevated inflammation, and impairment to macrophage polarization.

As elderly patients comprise a substantial proportion of patients requiring mechanical ventilation in the clinic, we need a better understanding of the age-related factors that increase these patients' susceptibility to lung injury. Furthermore, epidemiological data suggest that advanced age strongly correlates with a significant increase in ventilator mortality<sup>19,121</sup>. Additionally, experimental studies showed that injurious mechanical ventilation caused elevated pulmonary permeability and lung tissue damage in aged, senescent rats compared with young<sup>20</sup>. Senescence-associated changes in pulmonary structure and function in the elderly population may prime the lungs to be more susceptible to injury or insults, including the stresses and strains induced by mechanical ventilators. While our data, as shown in Figure 26, and others support the notion that an association between aging and enhanced vulnerability to VILI exists, the underlying age-related mechanisms that cause increased susceptibility remain unclear.

In addition to structural and functional lung changes that occur with advanced age, recent studies have revealed that the acute innate immune response is highly impaired with advanced age that results in the upregulation of low-grade inflammation in various tissues<sup>24,25,122</sup>. As macrophages amplify and orchestrate inflammatory responses and help regulate tissue healing and regenerative responses in various tissues<sup>24</sup>, we investigated how aging and injurious PCMV impact alveolar and interstitial macrophage polarization. Macrophage polarization is broadly defined as proinflammatory/pro-injurious, or classical activation, and anti-inflammatory/pro-repair, or alternative activation. As mentioned before, macrophage polarization influences physiological transitions from inflammation to tissue regeneration

which may be highly impaired with aging; however, these findings have been conflicting and remain highly controversial<sup>33,41</sup>. While other studies found either increases or decreases in the proinflammatory responses of aged classically activated macrophages, Gibon et al. revealed that aged macrophages overexpress both classical and alternative activation surface markers, aged alternative activated macrophages had reduced expression of Arg1 and CD206, and that aged classical activation macrophages increase TNF- $\alpha$  secretion with no negative feedback<sup>24</sup>. These observations further indicate that the impact of aging on macrophage polarization and function, especially in the context of acute lung injury, needs further investigation.

The subsets of activated macrophages appear to play a significant role in the progression and resolution of inflammatory responses, especially in the lung. Alveolar and interstitial lung macrophages possess different origins and life spans in the lung and may play opposing roles in lung injury<sup>31</sup>. Studies have shown that alveolar macrophages are tissue-resident cells that inhabit lung tissue during early development. These cells remain viable for longer periods and have minimal replenishment from bone marrow-derived monocytes<sup>123</sup>. Contrarily, interstitial macrophages originate from bone marrow-derived monocytes and have shorter lifespans<sup>124</sup>. Evidence suggests that alveolar macrophages regulate lung homeostasis by removing pathogens and particulate without the recruitment of monocytes and neutrophils, while interstitial macrophages are recruited monocyte-derived cells from the circulation following acute lung injury and are major contributors to inflammatory responses. For example, studies have shown that alveolar macrophages limit neutrophil influx into the lung during acute lung injury<sup>125</sup> while interstitial macrophages promote neutrophil extravasation<sup>126</sup>. The complex architecture of the lung causes the external stresses to be transmitted throughout a discrete three-dimensional (3D) meshwork that focuses the stress into the parenchyma where alveolar and interstitial macrophages are located<sup>127</sup>. Modeling the micromechanics of the parenchyma showed that the basal lamina and ECM are the principal support structures that resist stress and become stress-bearing at larger lung volumes<sup>128</sup>. These are the structures that form the scaffold to which alveolar cells, interstitial cells, and endothelial cells are fixed via focal adhesions and other cell-matrix interactions<sup>46</sup>. Stress and strains acting on the ECM are transmitted

to the stress-bearing elements of these cell types via cell-matrix and cell-cell contacts that may result in cellular deformation, differentiation, and signaling<sup>28,46</sup>; however, it remains unclear how the magnitudes and types of stresses and strains vary between alveolar and interstitial lung macrophages during both physiological and pathological states.

We observed age-related differences that exist at baseline and changes to the macrophage subpopulations caused by high PCMV, as indicated in Figure 29 and Figure 30. We detected enhanced CD80 and CD206 expression on both alveolar and interstitial macrophages isolated from the unventilated aged cells, young PCMV cells, and old PCMV cells compared to the young control cells (Figure 29); however, the greatest change occurred in the old PCMV group. The shifts of CD80 and CD206 were more intense in the young PCMV cells compared to the old PCMV cells when normalized to their respective control groups. Furthermore, we observed elevated expression of the polarization markers of aged cells at baseline compared to young. When assessing age only, we found that there was a substantial reduction in CD80<sup>-</sup>/CD206<sup>-</sup> alveolar macrophages (Figure 30) and CD206<sup>+</sup> interstitial macrophages (Figure 30). We also observed significant increases in CD80<sup>-</sup>/CD206<sup>-</sup> interstitial macrophages (Figure 30) and CD80<sup>+</sup>/CD206<sup>+</sup> double-positive alveolar macrophage populations (Figure 30). These age-related impairments to macrophage polarization may contribute to the elevated baseline inflammation in aged mice and desensitized responses of aged cells observed in several *inflammaging* studies as there are less inactivated cells present to respond to stimuli and polarization states and less alternative activated interstitial macrophages that are associated with inflammatory resolution, tissue repair, tissue regeneration, ECM remodeling, and fibrosis responses<sup>24,25,30,129</sup>. The impact of high PCMV alone produced rises in CD80<sup>+</sup> alveolar macrophages (Figure 30) in young mice only and increases in CD80<sup>+</sup>/CD206<sup>+</sup> double-positive alveolar macrophages (Figure 30) in both young and old mice compared to their respective controls. As alveolar macrophages act as the first line of cellular defense against respiratory pathogens and are involved with inflammatory responses<sup>26</sup>, the loss of this classical activation potential in the aged mice may reflect their reduced ability to respond to injurious stimuli leading to a dysfunctional or impaired inflammatory response. CD80<sup>-</sup>/CD206<sup>-</sup> alveolar macrophages (Figure 30) were

reduced in both young and old mice; however, there was a more significant decrease in the young cells compared to the old. This observation further reflects the loss of potential or efficiency in aged cells to respond to injury following stimulation. High PCMV also caused a loss in CD206<sup>+</sup> alveolar macrophages (Figure 30) in old mice compared to the control group. The reduction of alternative activation macrophages following injurious stimulation may also contribute to inflammaging, dysfunctional age-related inflammatory responses, and the increased susceptibility of injury in aged populations. Evidence suggests that this macrophage population is highly involved in inflammatory resolution and tissue repair responses<sup>26,32</sup>. Our findings indicate that aging, injurious PCMV, and the combination of the two factors differentially impact macrophage polarization that resulted with an overall age-related loss in activation efficiency of the aged cells in response to mechanical stimuli. The impairments to macrophage polarization appear to have similar changes as the age-related indications of injury and lung function deviations. These observations suggest that the macrophage polarization deviations caused by aging and PCMV may act as a cellular mechanism for the age-related increased susceptibility to injury in the aged populations.

## **CHAPTER 5: PULMONARY ENDOPLASMIC REITICULUM STRESS RESPONSE ASSOCIATED WITH AGING AND MECHANICAL INJURY AND THE THERAPEUTIC EFFECTS OF 4PBA**

Some of the content in this chapter was previously published in 2018 with the following citation: Valentine et al., Inflammation and Monocyte Recruitment due to Aging and Mechanical Stretch in Alveolar Epithelium are Inhibited by the Molecular Chaperone 4-phenylbutyrate, *Cell and Mol. Bioengineering*, 2018

### **5.1 Rationale:**

Mechanical ventilation frequently exacerbates underlying pulmonary conditions and produces an exaggerated inflammatory response that potentially leads to sepsis and multisystem organ failure<sup>1,7-9</sup>. This exacerbation or injury is classified as Ventilator-Induced Lung Injury (VILI). The pathophysiology of VILI is characterized by an exaggerated proinflammatory cytokine release and influx of inflammatory cells, loss of alveolar barrier integrity and subsequent pulmonary edema formation, decreased lung compliance, and profound hypoxia. These features reflect three integrated mechanisms of injury: alveolar over-distention, cyclic atelectasis, and inflammatory cell activation<sup>1,7-9</sup>.

One potential regulator of age-associated inflammation is the Endoplasmic Reticulum (ER). The ER is a multifunctional organelle responsible for lipid biosynthesis, calcium storage, and protein folding and processing<sup>34,52,60</sup>. Disruption to Endoplasmic Reticulum (ER) homeostasis results in activation of the unfolded protein response (UPR) and accumulation of misfolded proteins that is known as ER stress, which may lead to the impairment of cellular functions, cellular apoptosis, and has been shown to play a key role in many chronic inflammatory disease states<sup>34,52</sup>. Specifically, ER stress has been shown to regulate apoptosis and epithelial to mesenchymal transition in alveolar epithelial cells<sup>72</sup>.

As VILI and ER stress are characterized by inflammation, recent evidence has suggested that lung-recruited monocytes may also play a significant role in the pathogenesis of ALI<sup>15,126</sup>. Recent studies show that immature monocytes enter the circulation from the bone marrow and migrate to local sites of inflammation and injury<sup>15,126</sup>. Using mouse models, monocytes are rapidly recruited to the lung during

inflammation and contribute to the development of ALI by promoting the activation of pulmonary endothelial and epithelial cells<sup>15,126</sup>. Additionally, monocyte recruitment is heavily involved in the development of pulmonary edema under harmful mechanical ventilation<sup>126</sup>. Furthermore, advanced age has also been shown to impact the function and responsiveness of monocytes and macrophages, although why this occurs and how it impacts the age-associated susceptibility to lung injury and inflammaging conditions are not clear<sup>25,38</sup>.

ER stress has also been shown to be increasingly dysregulated with age<sup>34,53</sup>. There is a general age-associated increase in the occurrence of protein misfolding and accumulation. Unsurprisingly, ER stress is implicated as a promoter of many pathological disease states associated with aging<sup>34,53</sup>. Additionally, lung-related ER stress is involved in the age-associated increase in pulmonary fibrosis<sup>61</sup>.

While various studies have shown convincing evidence for the dominant role of ER stress in various inflammatory disease states, there have only been a few studies investigating ER stress in the context of acute lung injury and/or ventilator-induced lung injury in young adults. Several ER stress pathway proteins are key modulators of epithelial permeability and barrier dysfunction in young mice and rats<sup>59,63</sup>. Extended epithelial stretch activates ER stress pathways, which resulted in increased alveolar permeability, cell death, and proinflammatory signaling<sup>63</sup>; however, these implications have yet to be investigated in an aging model. To further validate that therapeutic targeting of the ER stress response may attenuate VILI, these inferences need to be investigated in the context of aging to understand the potential therapeutic targets.

We postulated that the alveolar type II (ATII) cells respond age-dependently to mechanical stretch with increased inflammation and monocyte recruitment, dependent upon ER stress. To investigate this relationship, we isolated and cultured primary alveolar epithelial ATII cells from young and old murine subjects. These cells were exposed to cyclic mechanical stretch to model alveolar over-distension. We measured age-associated differences in ER stress mediators, cell injury/inflammation, and apoptosis. We then used the chaperone 4-phenylbutyrate (4PBA), an ER stress reducer (42). Additionally, we quantified the migration of bone marrow-derived monocytes to ATII conditioned media.

## 5.2 Materials and Methods:

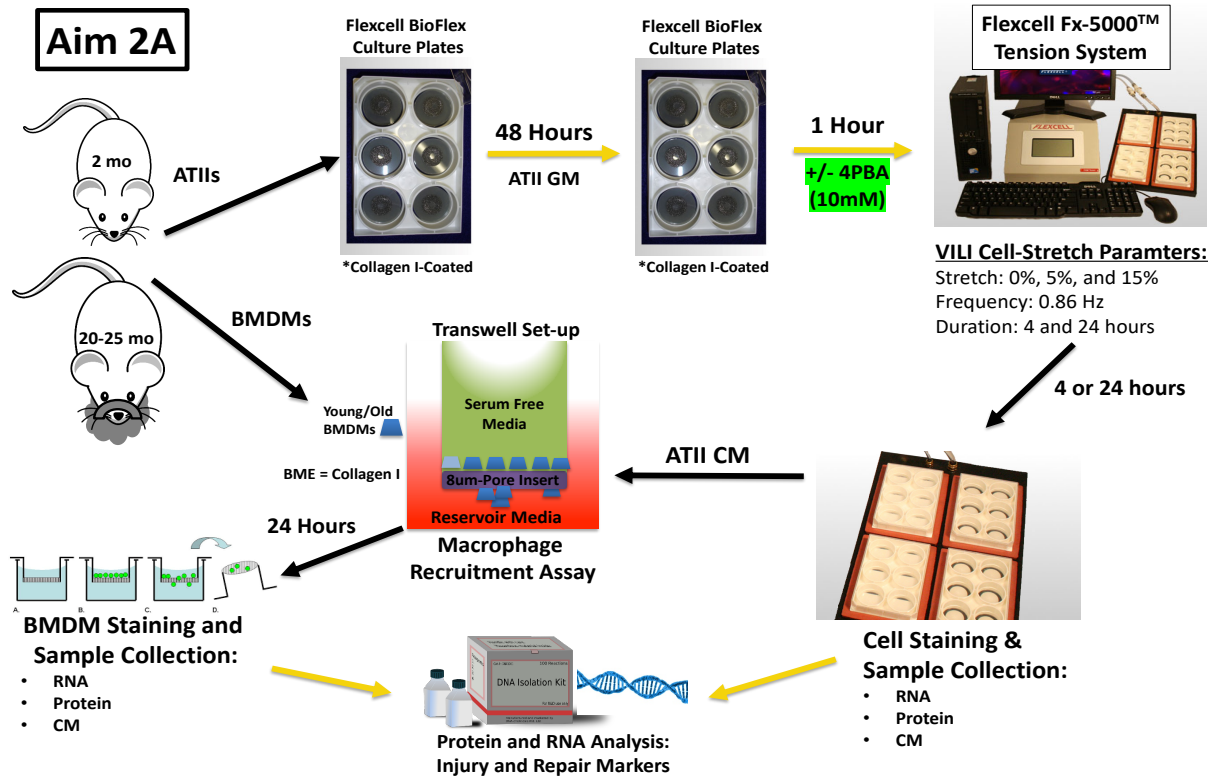


Figure 29: General overview of Aim 2A. This aim investigates the role of Aging, ER stress, and the therapeutic intervention of 4PBA in injurious mechanical stretch.

**Mice:** All C57BL/6J mice were housed in accordance with guidelines from the American Association for Laboratory Animal Care and Research protocols and approved by the Institutional Animal Care Use Committee at Virginia Commonwealth University (Protocol No. AD1000009).

**ATII cell isolation and culture:** We harvested, isolated, and cultured ATII primary alveolar epithelial cells from young (2 months) and old (20 months) C57BL/6J wild-type mice using previously cited methods<sup>115</sup>. We selected to use an aged-mouse model as it has previously been suggested that mice are an ideal mammalian model for studying the effects of aging and due to the lack of availability of aged-human cell lines or clinical specimens<sup>116</sup>. ATII were then cultured in Bronchial Epithelial Cell Growth Media (BEGM, Lonza), with the included supplements except for hydrocortisone, supplemented with 10 ng/ml keratinocyte growth factor (KGF, PeproTech). For stretch experiments, cells were plated onto Collagen

I-coated, 6-well silicone bottomed plates (Flexcell International Corp., BF-3001A BioFlex) and cultured for 48 hours prior to stimulation. ATIIs were found to be greater than 93% pure in both young and old cultures by staining for positive pro-surfactant C and the inclusion of lamellar bodies. Cell viability was also validated with MTT assays (Roche) according to manufacturer's instructions.

**Mechanical Cell-Stretch:** Using the Flexcell Tension Plus System (Flexcell Inc), we applied radial, cyclic (0.86Hz) stretch corresponding to a 15% change in surface area. Statically cultured ATII cells were used as controls. Cells underwent stretch or static conditions, and after 4 hours or 24 hours, RLT buffer (Qiagen) or 4% paraformaldehyde were added to wells for further processing. Cell supernatants were collected for cytokine analysis and conditioned media experiments.

**ER Stress Intervention in Cell-Stretch:** One hour before mechanical stretch, each well received either 20ul vehicle (ultrapure water) or 10 mM sodium 4-phenylbutyrate (4PBA) (Calbiochem, San Diego, CA) in ultrapure water. 4PBA is approved by the FDA and is already in use clinically as a successful treatment for chronic inflammatory diseases and some age-related diseases, such as type II diabetes and obesity-caused chronic inflammation<sup>130,131</sup>. 4PBA acts as an ER stress reducer<sup>130</sup> by inhibiting misfolded protein accumulation, and 4PBA showed no effect on ATII cell viability in the MTT assays.

**Immunofluorescence Staining for CHOP, ATF4:** Fixed wells were probed for CHOP (L63F7) mouse mAB (1:3200) and ATF4 (D4B8) rabbit mAB (1:200) using secondary antibodies anti-mouse Alexa Fluor® 594 conjugate (1:250) and anti-rabbit Alexa Fluor® 488 conjugate respectively. All primary and secondary antibodies were obtained from Cell Signaling Technology (Danvers, MA, USA). The counterstaining was done using Prolong® Gold antifade mounting with DAPI (ThermoFisher, Waltham, MA, USA). Samples were imaged with an Olympus IX71 under appropriate emission/excitation wavelengths.

**Quantitative real-time Polymerase Chain Reaction:** Total RNA was isolated and purified from each treatment group using RLT buffer (Qiagen) and the RNeasy mini kit (Qiagen, Valencia, CA). We then synthesized the complementary DNA using the iScript RT kit (Biorad). For cDNA from the ATII primary alveolar epithelial cell, we used custom QPCR plates (Biorad) to perform an analysis of IL-6st, MCP-1 (CCL2), and MIP-1 $\beta$  (CCL4). Additional primers for ER stress-related genes, CHOP and ATF4, were purchased from Integrated DNA Technologies. QPCR was performed using Sybr Green (Applied Biosystems) and the CFX96 Touch™ Real-Time PCR Detection System (Biorad). Data were analyzed using the  $2^{-\Delta\Delta CT}$  method, and target genes were normalized to two housekeeping genes using ribosomal 18s and GAPDH.

**Inflammatory Mediator Analysis:** We measured the concentrations of MCP-1/CCL2 and MIP-1 $\beta$  /CCL4 inflammatory cytokines in the collected cell media of each experimental group using MCP-1 (DY479) and MIP-1 $\beta$  (DY451) Mouse DuoSet ELISA kits (R&D Systems) according to the manufacturer's instructions.

**Monocyte Invasion Assay:** Bone marrow-derived monocytes (BMDMs) were isolated from young (2 months) and old (20 months) C57BL/6J mice, as described by Trouplin et al.<sup>117</sup>. Monocyte migration was then evaluated using an invasion assay, performed as described by Murray et al.<sup>118</sup>, with minor modifications. BMDMs were seeded at a density of  $1 \times 10^5$  cells/100ul BMDM growth media without FBS, on Collagen I-coated (Sigma-Aldrich) Transwell inserts with 8.0 um pore sizes (Corning, USA). 0.6 ml of BEGM or conditioned media from the ATII 24-hour groups were placed in the reservoir.

**A Live/Dead Viability Assay** (ThermoFisher) was used to quantify cell invasion through the Transwell membrane. Live/Dead images were taken immediately after the staining procedure an Olympus IX71 Microscope (Olympus). Total cell counts were performed using ImageJ's particle analysis function with the following inclusion parameters: Size (in Pixels): 10-120. Circularity: 0.10-0.99.

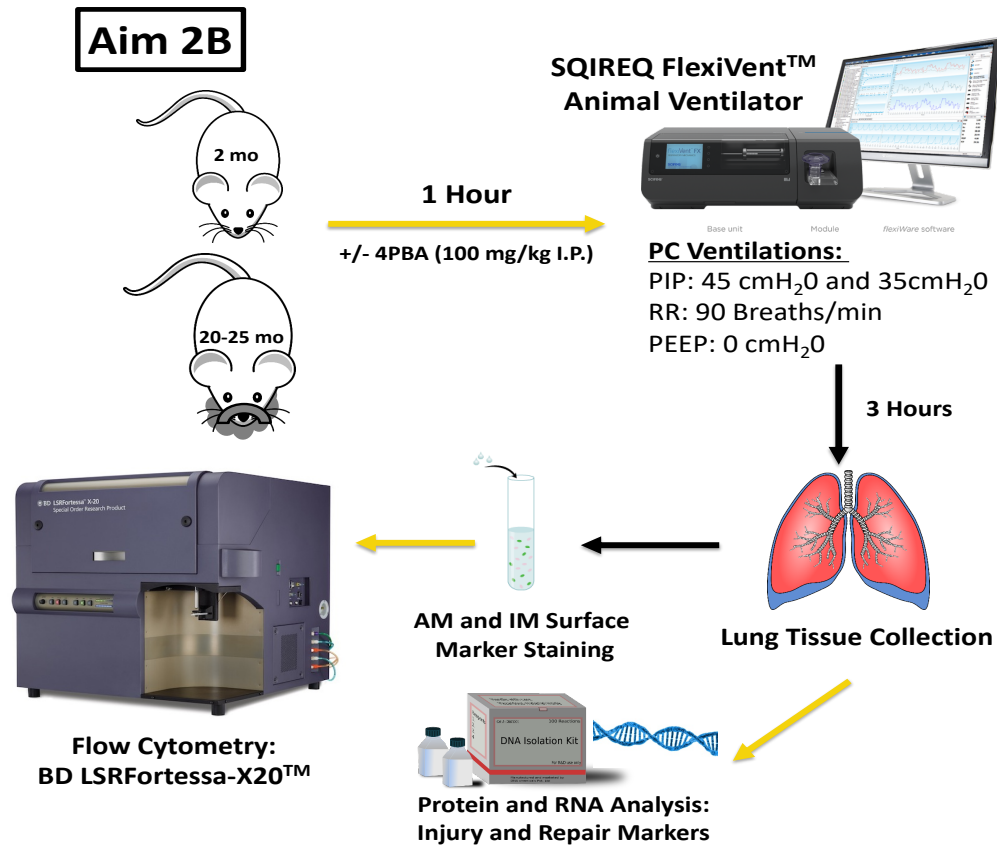


*Figure 30: General overview of Aim 2B. This aim investigates the role of Aging, ER stress, and the therapeutic intervention of 4PBA in an experimental VILI model.*

**Animals:** Male C57BL/6 mice 8 weeks of age were purchased from Jackson Laboratory (Bar Harbor, ME). All animals were housed in accordance with guidelines from the American Association for Laboratory Animal Care and Research protocols and approved by the Institutional Animal Care Use Committee at Virginia Commonwealth University (Protocol No. AD10000465).

**Pressure-Controlled Ventilator-Induced Lung Injury Model:** We mechanically ventilated young (2-3 mo.) and old (20-25 mo.) C57BL/6J wild-type mice using a Scireq FlexiVent computer-driven small-animal ventilator (Montreal, Canada) and previously cited methods<sup>10</sup> with slight modifications. Mice were anesthetized, tracheotomized, and then ventilated for 5 minutes using a low pressure-controlled strategy (peak inspiratory pressure (PIP): 15 cmH<sub>2</sub>O, respiratory rate (RR): 125 breaths/min, positive end-

expiratory pressure (PEEP): 3 cmH<sub>2</sub>O). Mice were then ventilated for 3 hours using a high pressure-controlled mechanical ventilation (PCMV) protocol (PIP: 35-45 cmH<sub>2</sub>O, RR: 90 breaths/min, and PEEP: 0 cmH<sub>2</sub>O). Pulmonary function and tissue mechanics were measured and collected at baseline and every hour during the 2-hour high PCMV duration using the SCIREQ FlexiVent system and FlexiWare 7 Software. A separate group of mice was anesthetized, tracheotomized, and maintained on spontaneous ventilation for 3 hours.

**ER Stress Intervention in Cell-Stretch:** One hour before mechanical ventilation, each mouse received either 100 mg/kg vehicle (ultrapure water) or 4-phenylbutyrate (4PBA) (Calbiochem, San Diego, CA) in ultrapure water, I.P injection.

**Tissue Processing:** Immediately following mechanical ventilation, the right lobes of the lung were snap frozen with liquid nitrogen, then stored at -80°C for further analysis. The left lobes of the lung were then inflated with digestion solution containing 1.5 mg/mL of Collagenase A (Roche) and 0.4 mg/mL DNaseI (Roche) in HBSS with 5% fetal bovine serum and 10mM HEPES and processed as previously described<sup>119</sup>. The resulting cells were counted, and dead cells were excluded using trypan blue. Subsets of the experimental groups were also used to collect bronchoalveolar lavage fluid (BALF) fluid, differential cell counts, and left lobes for histological analysis.

**Flow Cytometric Analysis:** Following live cell counts, 4x10<sup>6</sup> cells per sample were incubated in blocking solution containing 5% fetal bovine serum and 2% FcBlock (BD Biosciences) in PBS. The cells were then stained using a previously validated immunophenotyping panel of fluorochrome-conjugated antibodies<sup>31</sup> with slight modifications (See S1 Table for a list of antibodies, clones, manufacturers, and concentrations). Following the staining procedure, cells were washed and fixed with 1% paraformaldehyde in PBS. Data were acquired and analyzed with a BD LSRFortessa-X20 flow cytometer using BD FACSDiva software (BD Bioscience). Histogram plots were generated using FCS Express 5

software (De Novo). Compensation was performed on the BD LSRFortessa-X20 flow cytometer at the beginning of each experiment. “Fluorescence minus one” controls were used when necessary. Cell populations were identified using a sequential gating strategy that was previously developed<sup>31</sup>. The expression of activation markers is presented as median fluorescence intensity (MFI).

**Bronchoalveolar Lavage Fluid (BALF) Cytometry and Protein Concentrations:** The BALF was collected and centrifuged to collect a cell pellet and supernatant, as previously described<sup>10</sup>. Cell pellets were resuspended in saline and mounted onto glass slides using a cytospin device (Thermo Shandon). Cells were stained (3 Diff-Quick solutions staining kit) and immune cell populations were quantified. The quantification of total BALF protein in the supernatants was measured by using the Pierce BCA Protein Assay Kit (Thermo Scientific).

**Histology:** Lung tissue samples were embedded and stained with hematoxylin and eosin (H&E). The mean linear intercept ( $L_m$ ), an index of airspace enlargement, quantify relative differences in alveolar airspace area within lung histology sections and were measured and analyzed as previously described<sup>10</sup>.

**Statistics:** A total of 114 young mice were used for this study. All experiments were performed with a minimum of  $n=3$  primary cell isolations in triplicate wells. Larger  $n$  values were utilized where possible. Limitations exist in the number of 20-month-old mice available from the National Institute on Aging. Therefore, minimum numbers to achieve statistical significance via a power analysis were utilized. Results are presented as mean  $\pm$  SD. GraphPad Prism was used for all statistical analyses. For multiple-group comparisons, we used a two-way analysis of variance (ANOVA) with age and stretch as factors, followed by a post-hoc Tukey test to determine significance.  $P<0.05$  was considered statistically significant.

### 5.3 Results:

#### 4PBA Treatment Diminishes Associated ER Stress Markers CHOP and ATF4 Induced by Mechanical Stretch and/or Aging:

After observing the upregulation of the inflammatory and injury related chemokines by age and/or mechanical stretch, we assessed the role of ER stress as a potential upstream regulator, which has been shown to increase inflammation and apoptosis. In order to evaluate alveolar epithelial ER stress responses of young and old cells exposed to mechanical stretch, we investigated the immunofluorescent staining and gene expression of two key indicators and downstream markers of ER stress and the Unfolded Protein Response (UPR): C/EBP homologous protein expression (CHOP) and Activating Transcription Factor 4 (ATF4). These results are shown in Figures 33.

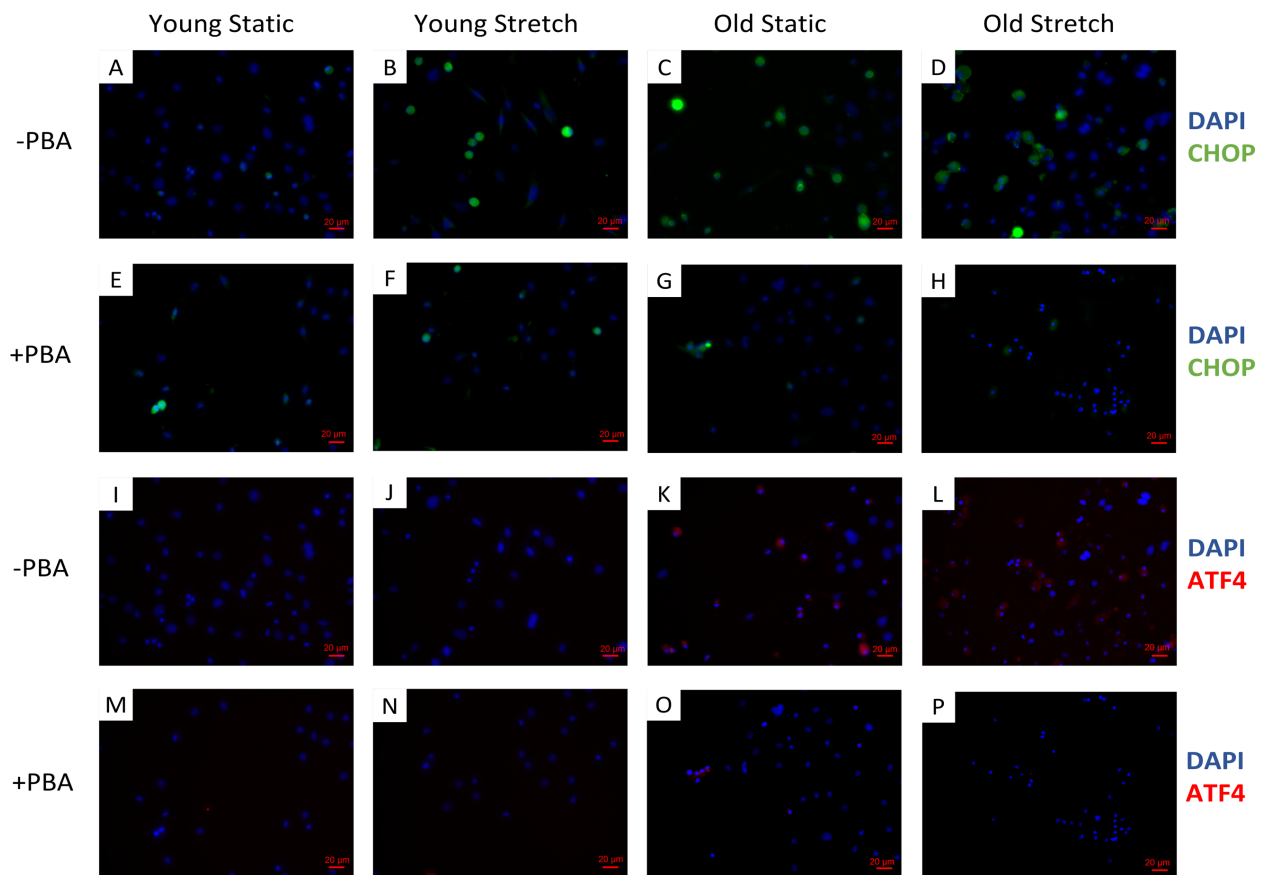


**Figure 31: Cyclic Stretch (15%) for 24 h +/- Age influences detection of (a-h) CHOP and (i-p) ATF4 in AII Cells.** Representative images were randomly chosen from individual wells in replicated ( $n = 3$ ) experiments for each condition: (a and i) Young Static, (b and j) Young Stretch, (c and k) Old Static, (d and l) Old Stretch, (e and m) Young Static + 4PBA, (f and n) Young Stretch + 4PBA, (g and o) Old Static + 4PBA, and (h and p) Old Stretch + 4PBA. (a-h) DAPI (blue) and CHOP (green). (i-p) DAPI (blue) and ATF4 (red). Scale bars represent 20 μm

We first assessed and quantified the CHOP+ ATII cells and ATF4+ ATII cells through the immunofluorescent staining (Fig. 33). Qualitatively, the Old Static ATII cells (Fig. 33E) were more positively stained for CHOP when compared to the Young Static ATII cells (Fig. 33A). Also, the presence of CHOP is more accentuated with stretch in the Young ATII cells (Fig. 33A and 33B). Additionally, 4PBA attenuated CHOP (Fig. 33E, 33F, 33G, and 33H) compared to the PBS vehicle controls (Fig. 33A, 33B, 33C, and 33D). Similarly, Old ATII cells (Fig. 33K) were more positively stained for ATF4 under static conditions when compared to Young ATII cells (Fig. 33I), though the difference is less pronounced compared to the CHOP stained images. Similarly, the presence of ATF4 is more accentuated with stretch in the Old ATII cells (Fig. 33K and 33L). 4PBA also attenuated the positive staining of ATF4 (Fig. 33M, 33N, 33O, and 33P) compared to vehicle controls (Fig. 33I, 33J, 33K, and 33L).

#### **Aging and/or Prolonged Mechanical Injury Trigger Activation of CHOP and ATF4 in ATII Cells; 4PBA Treatment Attenuates ER Stress Indications Caused by Aging and/or Cell-stretch.**

After qualitatively assessing the immunofluorescent staining in the ATII cells, we also quantified the mean fraction of CHOP+ ATII cells and ATF4+ ATII cells from the total number of cells per field of view. These findings are shown as in Figure 34. We found that there was a significant increase in the fraction of CHOP+ ATII cells in the Old Static and Young Stretch groups compared to the Young Static ATII cells. We also observed a reduction in the fraction of CHOP+ ATII cells in the Old Static + 4PBA experimental group compared to the Old Static ATII cells (Fig. 34A). Interestingly, we did not see any difference in the fraction of ATF4+ ATII cells between any of the experimental groups (Fig. 34B).

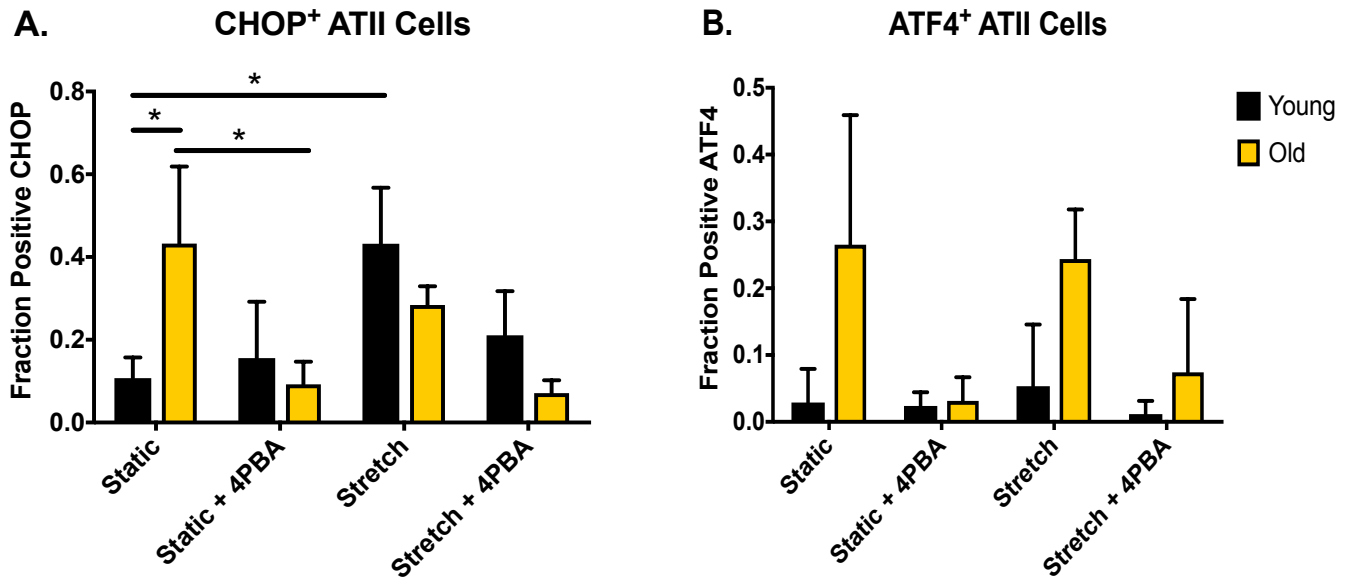
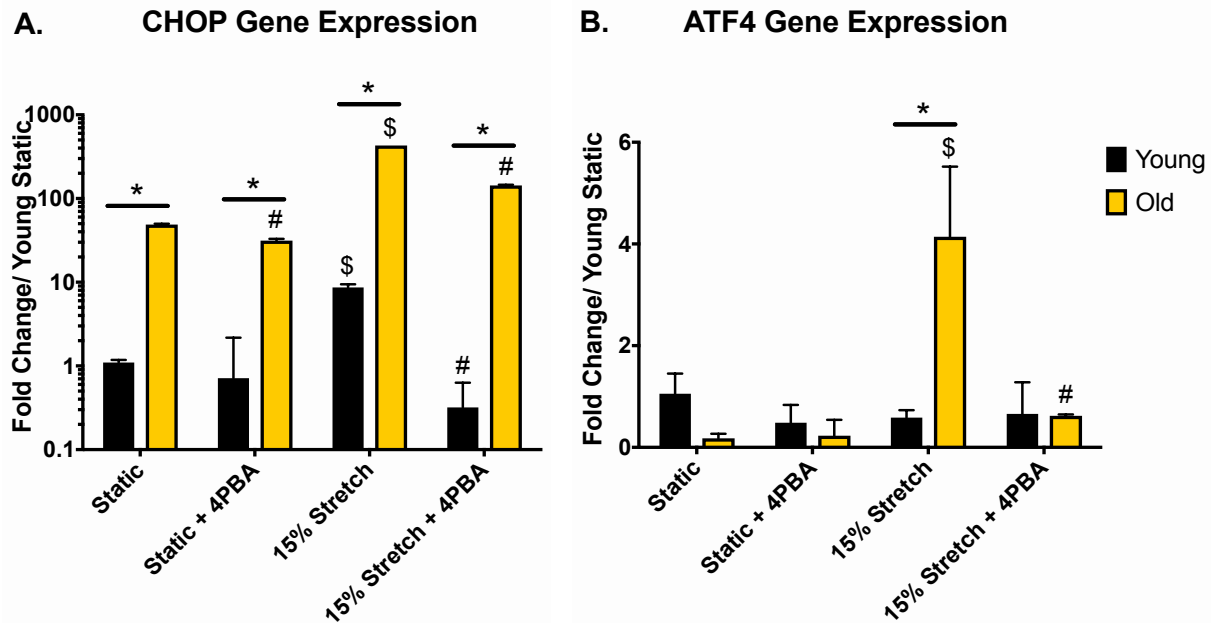


Figure 32: Quantification of CHOP<sup>+</sup> ATII Cells and ATF4<sup>+</sup> ATII Cells in response to Cyclic Stretch (15%) for 24 h +/- Age. Columns are fraction of positive-stained cells for (A) CHOP and (B) ATF4. Data are presented as mean  $\pm$  6 SD, n = 3 per group. \*p < 0.05 as indicated.

In order to further verify the differences in ER stress between the experimental conditions, we evaluated the gene expression of these markers in response to both age and mechanical stretch. We observed significantly increased CHOP expression in response to advanced age alone, mechanical stretch alone, and in combination (Fig. 35A). CHOP is a transcription factor activated by ER stress, which is believed to help mediate cellular apoptosis and inflammation<sup>68</sup>. As before with the findings in Figure 33, we did not see the same age- and stretch-induced upregulation with ATF4 (Fig. 35B), which regulates several UPR target genes, such as those involved in ER stress-mediated apoptosis<sup>52</sup>. However, we observed significantly increased ATF4 gene expression in the Old ATII cells in response to mechanical stretch. After administering 4PBA, an ER stress reducer, we observed significant decreases in the ER stress marker CHOP in Young and Old ATII cells that received mechanical stretch and in statically cultured Old ATII cells; however, CHOP expression did not change in statically cultured Young ATII cells (Fig. 35). 4PBA administration also attenuated increased ATF4 expression in the Old Stretched ATII cells; however, there was no change in Young Stretched ATII cells, or in the statically cultured cells.



**Figure 33: (A) CHOP and (B) ATF4 gene expression after 24 h of stretch or static culture +/- 4PBA.** Columns are normalized fold change differences in gene expression relative to Young Static. Data are presented as mean +/- SD, n = 3 per group. (A) A log<sub>10</sub> scale was used to observe large changes in expression. (A) & (B) \*p < 0.05, when comparing Old experimental groups to their \$# Young counterpart. p < 0.05, when comparing same-age stretch groups to their static counterparts. p < 0.05, when comparing same age and stretch groups with PBA to those without PBA.

### 4PBA Treatment Mitigates Inflammatory Responses Induced by Aging and/or Prolonged, Cell-stretch of ATII Cells:

We next examined the effect of 4PBA administration on MCP-1/CCL2 and MIP-1 $\beta$ /CCL4 inflammatory signaling after 24 hours, which we previously showed were upregulated due to age and/or cyclic stretch for 4 hours (Fig. 36). Gene expression for MCP-1/CCL2 remained elevated after 24 hours when comparing Old Stretched ATII cells to Old Static ATII cells. Furthermore, MCP-1/CCL2 gene expression was considerably increased in Old Stretched ATII cells compared to Young Stretched ATII cells; however, there was no significant difference in gene expression between Old Static and Young Static groups or between Young Stretched and Young Static ATII cells (Fig. 36A). 4PBA notably decreased MCP-1/CCL2 gene expression in Old Stretched ATII cells, but 4PBA did not decrease MCP-1/CCL2 gene expression in the Young Stretched ATII cells or the Young and Old Static groups (Fig. 36A). After evaluating changes in MCP-1/CCL2 gene expression, we assessed the differences in corresponding protein secretion. These concentrations were normalized by the average number of ATII cells per experimental condition as

determined by its corresponding MTT data (Fig. 36B). We observed significantly greater MCP-1/CCL2 secretion by Old Static ATII cells compared to Young Static ATII cells as well as from Old Stretched ATII cells compared to Young Stretched ATII cells. Interestingly, we did not observe any differences in the secretion of this cytokine when comparing age-matched stretched to static conditions. Furthermore, 4PBA significantly reduced MCP-1/CCL2 secretion in both static and stretched conditions with Young and Old ATII cells (Fig. 36B), while there was still a significant difference in MCP-1/CCL2 secretion in the Old Stretched and Static groups with 4PBA compared to the Young Stretched and Static ATII cells with 4PBA.

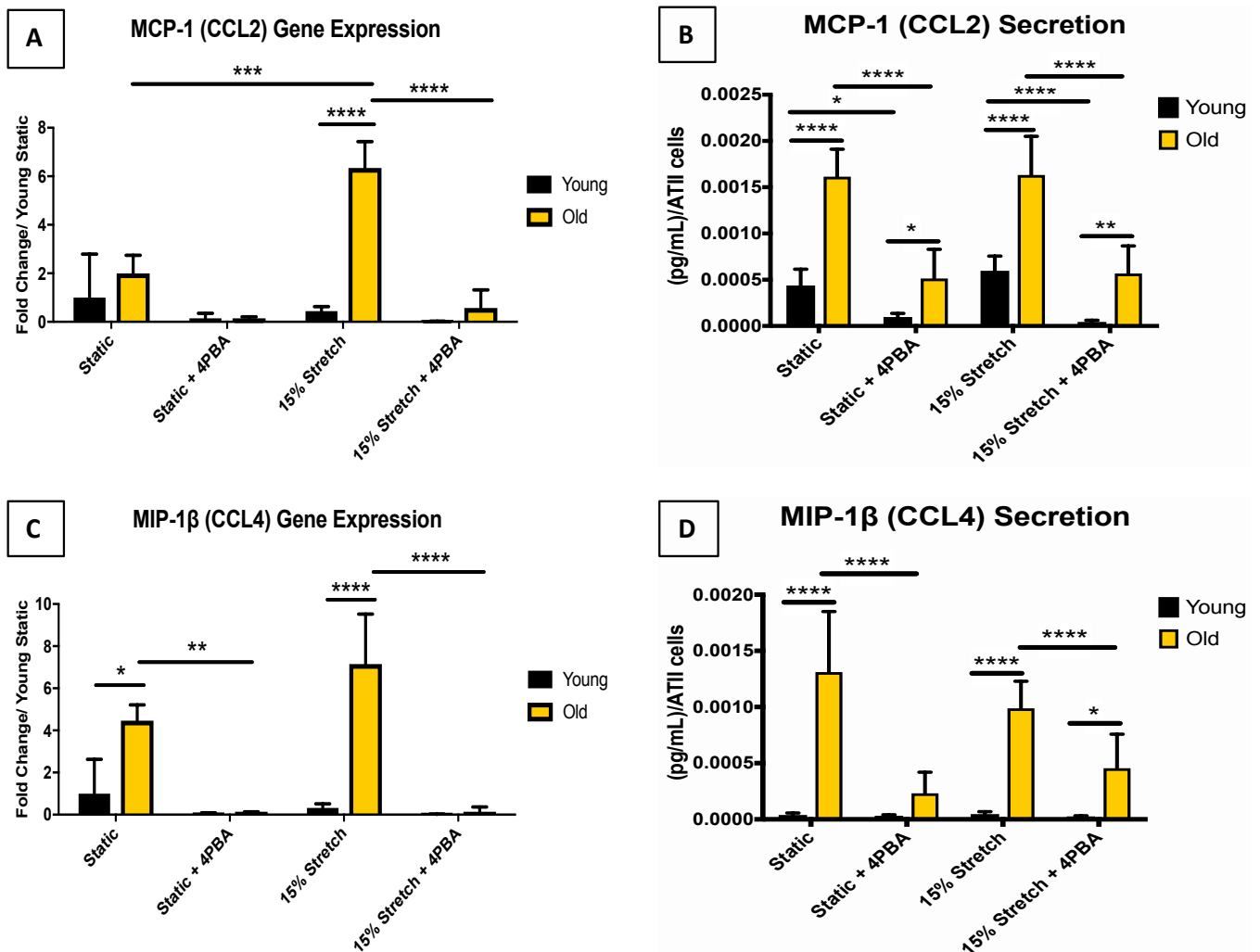


Figure 34: Effect of 4PBA on (a) MCP-1 (CCL2) gene expression and (b) cytokine secretion and (c) MIP-1b (CCL4) gene expression (d) and cytokine secretion in ATII cells after 24 h. Gene expression data are fold change compared with static Young. Data are presented as mean  $\pm$  SD,  $n = 3$  per group, in triplicate. \* $p < 0.05$ , \*\* $p < 0.01$ , \*\*\* $p < 0.001$ , \*\*\*\* $p < 0.0001$  as indicated.

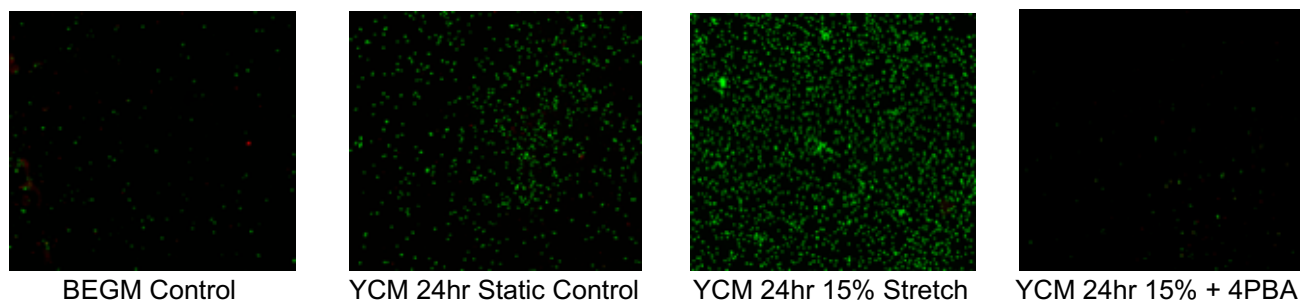
Cyclic stretch significantly increased MIP-1 $\beta$ /CCL4 gene expression after 24 hours in Young ATII cells (Fig. 36C). Age significantly increased MIP-1 $\beta$ /CCL4 gene expression, regardless of stimulation with mechanical stretch (Fig. 36C). The administration of 4PBA attenuated the increased MIP-1 $\beta$ /CCL4 expression in Old Stretched or Static ATII; however, there were no significant differences seen in Young Stretched or Static groups. Concurrent with the gene expression data for 24 hours (Fig. 36C), MIP-1 $\beta$ /CCL4 cytokine concentration in the media was elevated after 24 hours in Old Stretched and Static ATII cells compared to Young Stretched and Static groups (Fig. 36D). As seen before with the MCP-1/CCl2 protein secretion, there was no difference in MIP-1 $\beta$ /CCL4 production when comparing the age-matched stretched to static conditions. Additionally, the administration of 4PBA decreased MIP-1 $\beta$ /CCL4 concentrations in the Old Stretched and Static conditions; however, this effect was not seen in the Young ATII groups (Fig. 36D).

#### **4PBA Administration Reduces Monocyte Recruitment Caused by Aging and/or Mechanical Injury:**

In order to determine the ability of age and stretch to influence ATII recruitment of monocytes, we performed conditioned media experiments by exposing primary BMDMs to ATII conditioned media (CM) from all groups. As shown in Figure 37, the representative images depict the young and old monocyte recruitment stimulated with the growth media of ATII and various ATII conditioned media from the cell-stretch experiments. We first quantified Young and Old BMDM migration using age-matched CM from the ATII stretch experiments (Fig. 38). As before, we normalized the recruited monocyte cell counts by the average number of ATII cells per condition as determined by the MTT data. We observed significantly decreased ( $p < 0.05$ ) BMDM migration with Old BMDMs/Old Static ATII CM in comparison to Young BMDMs/Young ATII Static CM. We also observed this same significant decrease ( $p < 0.05$ ) in migration with Old BMDMs/Old ATII Stretch CM in comparison to Young BMDMs/Young ATII Stretch CM. There was also a significant reduction in migration with Young BMDMs/Young ATII Static CM + 4PBA in comparison to Young BMDMs/Young ATII Static CM. This same reduction in migration with 4PBA was also observed in Young BMDMs/Young ATII Stretch CM + 4PBA in comparison to Young BMDMs/Young

ATII Stretch CM. Although not statistically significant, 4PBA appeared to decrease both Young and Old BMDM migration in response to Old ATII Stretch or Static CM + 4PBA (Fig. 38) when compared to Old ATII Stretch and Static CM, respectively. In order to determine if it was the age of the ATII cells producing the CM or the age of the BMDMs that more greatly influenced migration, we quantified migration of Young BMDMs with CM from the Old Stretched and Static groups and Old BMDMs with conditioned media from the Young Stretched and Static groups to represent Mismatched CM monocyte recruitment (Fig. 38, gray bars in Young ATII and black bars in Old ATII). Young BMDMs/Young ATII Static CM significantly increased migration,  $p < 0.05$ , compared to Young BMDMs/Old ATII Static CM and Old BMDMs/Old ATII static CM. Furthermore, Young BMDMs/Young ATII Stretch CM resulted in increased migration,  $p < 0.05$ , in comparison to Young BMDMs/Old ATII Stretch CM and Old BMDMs/Old ATII Stretch CM. In summary, Old ATII CM with Young and Old BMDM caused a significant decrease in migration compared with Young ATII CM with Young BMDMs in both stretched and static groups (as indicated by “sy”, Fig. 38).

### Young Bone Marrow Derived Monocytes



### Old Bone Marrow Derived Monocytes

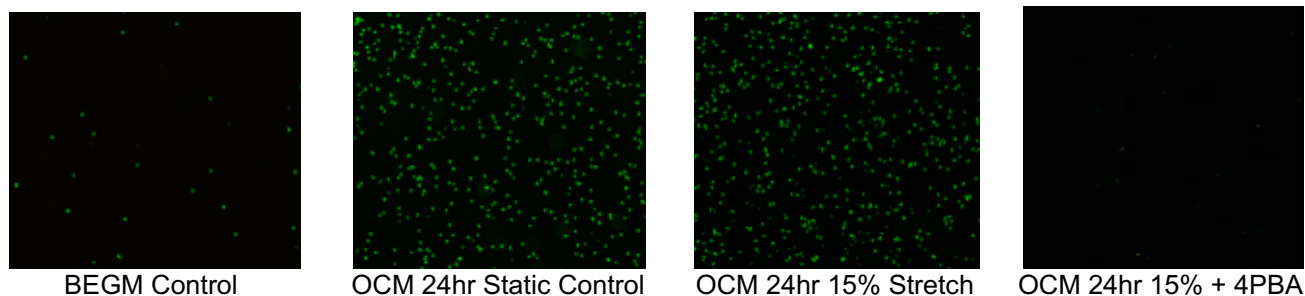


**Figure 35: 4PBA diminishes Young and Old BMDM recruitment.** Young and Old BMDMs were placed in wells of an invasion assay with the various condition medias in the reservoirs. The cells were allowed to migrate for 24 hours and were then stained using Live/Dead Stain Kit to quantify the recruitment. Live cells are shown in green and dead cells are shown in red. Magnification = 4x.

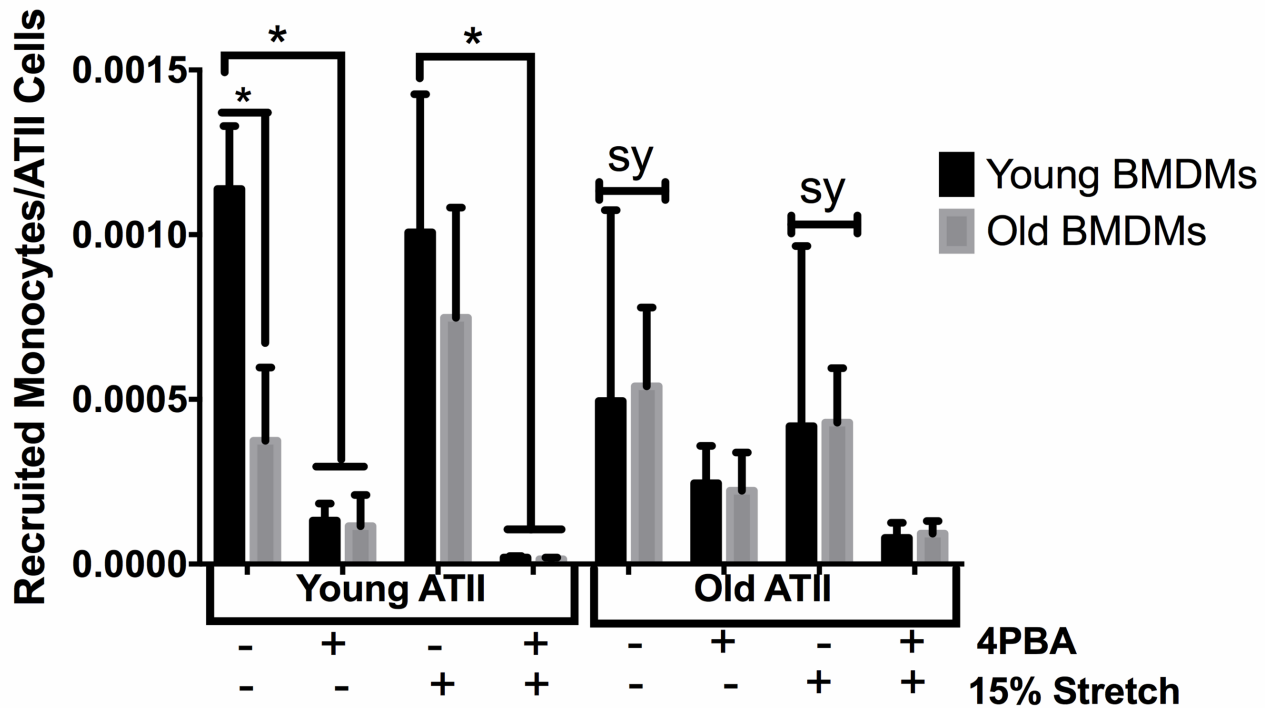
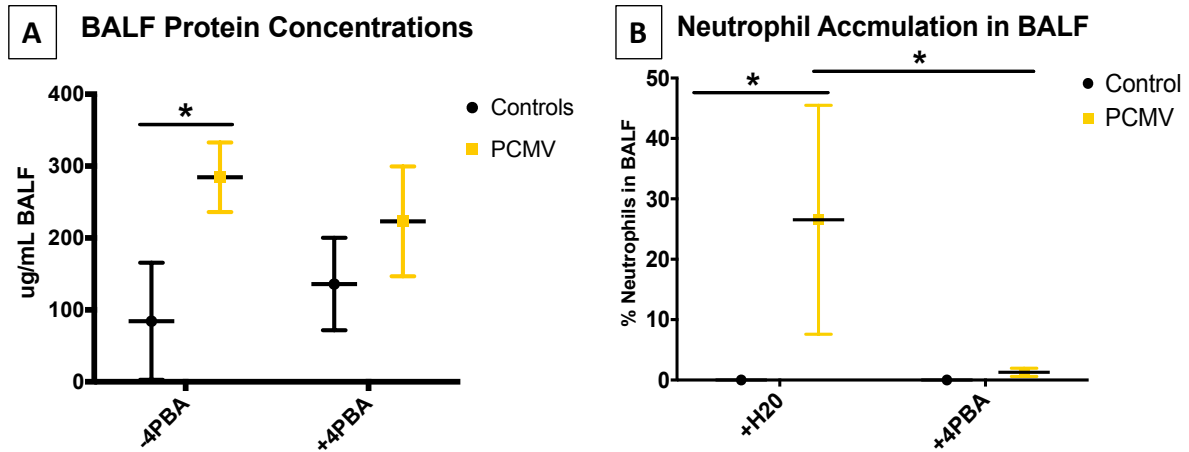


Figure 36: Monocyte Migration with Age-Matched and Mismatched ATII Conditioned Media. Data are presented as mean  $\pm$  SD,  $n = 3$  per group, \* $p < 0.01$ , sy statistically significant with  $p < 0.05$  compared with Young ATII/Young BMDMs counterpart. Additional statistically significant differences are described in the Results section.

### The Effects of 4PBA Administration Prior to High PCMV-induced ALI/VILI in Young Mice:

After examining the implications of aging and ER stress in our cell-stretch model with ATII and providing evidence for the beneficial effects of administering the preventative treatment, 4PBA, prior to mechanical injury, it was critical to determine the effectiveness of the 4PBA therapy and ER stress reduction in our animal model using high PCMV to induce ALI/VILI. While the Old ATII cells that received mechanical injury produced more severe indications of ER stress and ALI, we also detected signs of ER stress and ALI in the young ATII cells that were stimulated with injurious, cyclic cell-stretch. Additionally, 4PBA treatment effectively reduced several inflammatory responses and monocyte recruitment produced by both the Young and Old ATII cells following mechanical injury. Therefore, we chose to initially assess the therapeutic effects of 4PBA in young, healthy individuals that develop ALI/VILI.



*Figure 37: 4PBA prevents neutrophil accumulation in Young mice following high PCMV. Bronchoalveolar Lavage Fluid (BALF) samples were analyzed for total protein (A) and neutrophil accumulation (B). Data are presented as mean +/- SEM, n ≥ 3 per group. \* p<0.05, as indicated.*

We found that 4PBA treatment dispensed at a concentration of 100 mg/kg in a single dose IP given one hour before mechanical injury effectively attenuated neutrophil accumulation that is associated with ALI development and progression. Neutrophil influx was substantially reduced in young mice that received 4PBA prior to high PCMV. Additionally, high PCMV for a duration of 3 hours resulted in elevated neutrophil accumulation when compared to high PCMV for 2 hours (comparison not shown on figure, please see Fig. 26). However, 4PBA treatment failed to improve protein accumulation in the BALF samples of young mice that were mechanically injured, which is another indication of ALI/VILI.

We also assessed the preventative effects of 4PBA on the mechanical property changes that occur with ALI/VILI development and progression in young mice. We initially examined the effects of 4PBA on the baseline mechanics of young mice, prior to mechanical injury stimulation. Interestingly, 4PBA caused significant changes to lung elasticity and the respiratory system elastance (E) at baseline prior to high PCMV. Nevertheless, 4PBA treatment had no effect on any of the other lung or respiratory system mechanical properties at baseline in Young mice. Unfortunately, 4PBA treatment appears to exacerbate the changes in tissue mechanical properties of young mice leading to greater deteriorations and fluctuations following 3 hours of high PCMV, as shown in Figure 40. While 3 hours of high PCMV caused protein accumulation, immune cell influx, and other indications of ALI/VILI in young mice, the lung and respiratory mechanical properties did not significantly change following the 3 hours of mechanical injury.

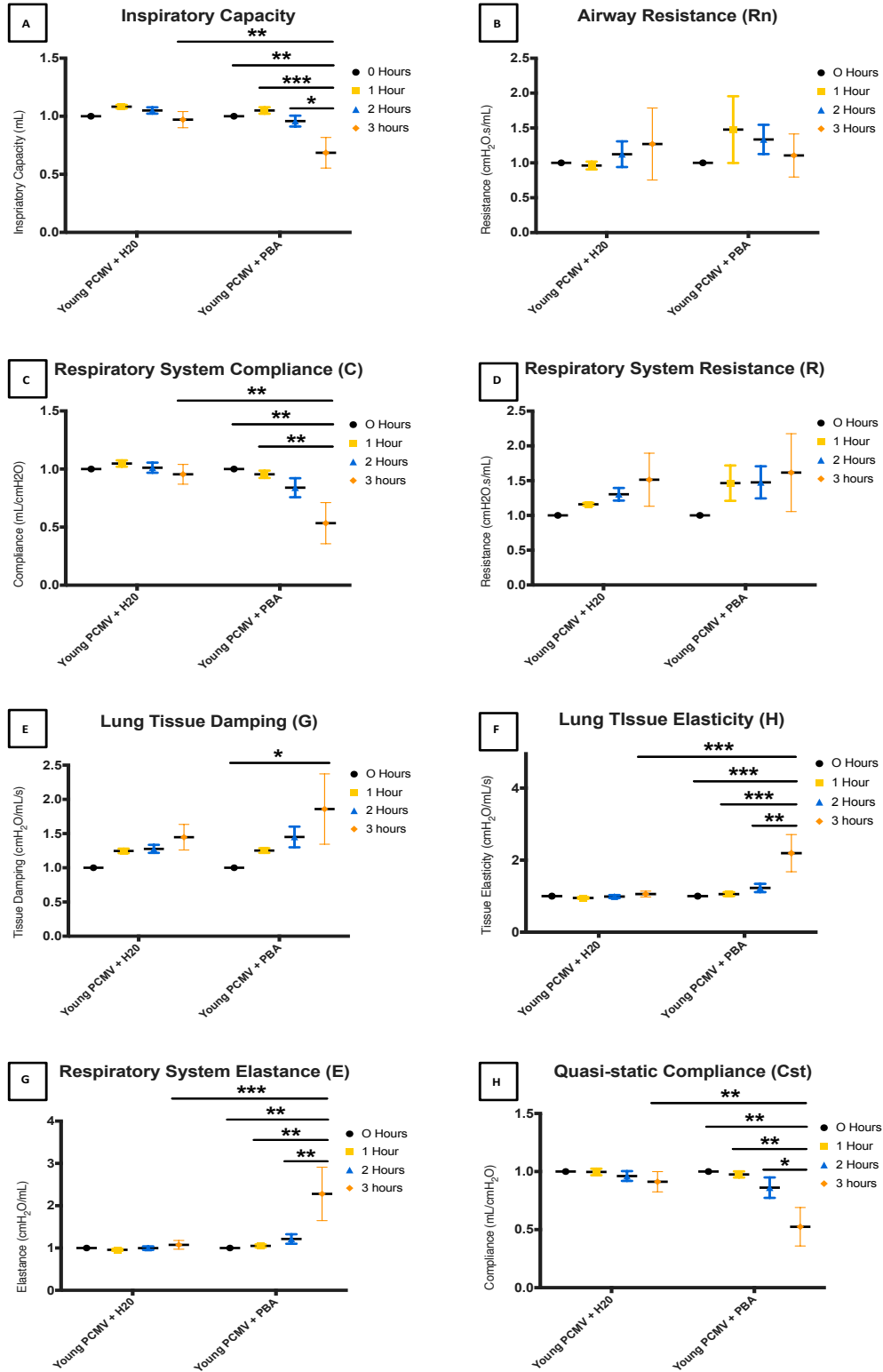


**Figure 38: 4PBA treatment caused further fluctuations in several tissue mechanical properties in young mice. Tissue mechanics and lung function was determined with a SCIREQ FlexiVent rodent ventilator for mice. Figure depicts Changes were determined in inspiratory capacity (A), airway resistance (B), respiratory system compliance (C), respiratory system resistance (D), lung tissue damping (E), lung tissue elasticity (F), and quasi-static compliance (G). Data are presented as mean +/- SEM, n ≥ 3 per experimental group. \* p<0.05, \*\* p<0.01, \*\*\* p<0.001, as indicated.**

#### **5.4 Discussion:**

We investigated ER stress as a mediator of the stretch and age-induced inflammation because ER stress plays a significant contributory role in age-related diseases and chronic inflammation<sup>52,58,60</sup>. Conditions such as hypoxia, calcium ion depletion, oxidative injury, infections, and inflammatory cytokines have the ability to disrupt the ER and prevent the normal protein folding<sup>35,52,60,63</sup>. The accumulation of folded and misfolded proteins in the ER leads to ER stress and the Unfolded Protein Response (UPR). Failure of the cell to mitigate protein accumulation leads to inflammation<sup>35,52,60,63</sup>. Age and/or mechanical stretch likely further disrupt the epithelial cells' ability to alleviate the unfolded and misfolded protein accumulation in the ER, which leads to intensified inflammation and apoptosis that contribute to barrier dysfunction and increased permeability<sup>24,52</sup>. While it has been recently shown that ER stress regulates alveolar epithelial homeostasis in response to mechanical stimuli<sup>63</sup>, our current study provides the first evidence that aging significantly impacts the ER stress-related gene expression and inflammatory signaling in alveolar epithelial cells with and without the addition of mechanical stretch.

In order to attenuate the age-associated increases in mechanical stretch-induced ER stress and inflammation, we administered 4PBA or PBS vehicle to the A11 cultures. 4PBA is believed to be an ER stress reducer and acts as a molecular chaperone to aid in the prevention of misfolded protein accumulation<sup>62,132,133</sup>. 4PBA is commercially available, approved by the FDA, clinically used to cure cyclic urea disorders<sup>130</sup>. Additionally, several studies have already demonstrated that 4PBA can be effective in alleviating chronic inflammation and age-related disease outcomes, such as lipopolysaccharide (LPS)-induced lung inflammation in a murine model, through mitigation of ER stress<sup>62,71</sup>. Based upon these prior results, we tested 4PBA in our *in vitro* cell-stretch model.

4PBA successfully induced a reduction in concentrations of inflammatory cytokines secreted into the cell media (Figure 36). The reduction in these concentrations may also be linked to the significantly reduced monocyte recruitment, as they are believed to help regulate monocyte and other immune cell recruitment and activation<sup>134-136</sup>. While we did not see significant differences in the secretion of MCP-1/CCl2 and MIP-1 $\beta$ /CCL4 due to mechanical stretch alone, we did observe substantial disparities due to

advanced age. This suggests that age alone may be a dominant factor contributing to the altered injury and inflammatory response signaling of ATII cells. Similar to the recent findings published by Gibon et al., we also showed that aged cells express and produce increased proinflammatory cytokines/chemokines at baseline conditions compared to younger cells<sup>42</sup>. While that study shows how aging impacts primary bone marrow macrophages, we are the first to validate that aged epithelial cells also express and secrete greater amounts of proinflammatory cytokines/chemokines under static, baseline conditions and after stimulation with mechanical stretch. Notably, the administration of 4PBA (Figure 38) also significantly reduced BMDM recruitment with Young BMDMs/Young Static CM, Young BMDMs/Young Stretch CM, and with Old BMDMs/Young Stretch CM. Our findings suggest that 4PBA inhibits or reduces the alveolar epithelial ER stress and subsequent inflammatory responses, which consequently lessens the monocyte recruitment. These results further indicate that 4PBA may quell inflammation and macrophage recruitment in response to mechanical stretch-induced lung injury.

There are some minor limitations in this the study. Some studies have suggested that 15% stretch is insufficient to injure young alveolar epithelial cells<sup>137,138</sup>. This possibility might explain why we did not see the same inflammatory or ER stress response changes that we observed in the Old ATII cells. However, our results suggest that aging impacts inflammatory and ER stress activation in ATII cells in response to physiologically relevant mechanical stimuli. We have shown previously that while cell membrane integrity is retained, cyclic stretch of Young ATII cells at 15% change in surface area is sufficient to affect gene expression and phenotype<sup>139</sup>. Our results indicate that Old ATII cells respond differently to cell-stretch compared with young ATII cells, potentially indicating that even under low tidal volume mechanical ventilation, older subjects may have an intensified or altered inflammatory response.

After observing the preventative effects of 4BPA treatment on the inflammatory signaling and monocyte recruitment generated by injurious cell-stretch, we examined the therapeutic effects of 4PBA *in vivo*. We assessed 4PBA administration prior to mechanical ventilation in the development and progression of ALI/VILI development in Young mice. Regrettably, 4PBA treatment failed to improve several of the indicaitons of ALI/VILI in young mice that received mechanical ventilation. 4PBA treatment

attenuated the neutrophil accumulation in BALF samples of young mice; however, it did not improve protein accumulation, lung and respiratory mechanics, deteriorations in lung structure, or other immune cell recruitment. It is important to note that the injury induction of ALI/VILI using the high PCMV protocol was less severe in young mice compared to old; therefore, it is possible that insufficient injury was produced from high PCMV in the young mice to observe significant effects of treatment. Other possible causes for the limited effectiveness of 4PBA in the prevention of ALI/VILI that we observed in the young mice include the drug delivery method and delivered dosage. We selected to administer 4PBA in a single dose at a concentration of 100 mg/kg via Intraperitoneal (IP) delivery 1 hour before injury induction because previous studies have shown its effectiveness using that delivery method in other types of ALI models, such as LPS-induced, and we believed that this drug delivery method would yield the highest efficacy of the 4PBA treatment in our ALI/VILI model. Intraperitoneal drug delivery is an alternate route to the more conventional drug delivery routes, such as I.V. or oral drug delivery. Previous studies that examined 4PBA treatment in various disease applications suggested that the route of administration possibly influences its efficacy<sup>140</sup>. The concentration of 4PBA, number of doses, and time of dosing utilized may also limit the effectiveness of 4PBA and explain our lack of improvement in preventing ALI/VILI<sup>141,142</sup>. Furthermore, as the old mice presented more severe indications of ER stress and inflammation compared to young mice and that mechanical injury further intensified these indications in old subjects, 4PBA therapy should be investigated in aged mice stimulated with mechanical injury that better represents clinical patients.

As the compounding effects of aging on lung injury and inflammation are becoming increasingly recognized, these age-dependent factors that may be associated with the injury and inflammation responses between the alveolar epithelium and innate immune system still need more clarity. While the administration of 4PBA shows promise in treating the ER stress and inflammation responses following mechanical stretch, the age- and stretch-dependent mechanisms and the use of 4PBA to mitigate inflammation and ER stress require further in vivo study to prove their practicality for future lung injury-related clinical potential.

## **CHAPTER 6: PROTECTIVE ROLE OF SPHINGOSINE-1-PHOSPHATE IN ALI/VILI AND THE APPLICATION OF TETRAHYDROXYBUTYLIMIDAZOLE (THI) THERAPY FOR AGE-RELATED ALI**

### **6.1 Rationale:**

While cytokines and chemokines highly regulate macrophage differentiation and function, other molecules, such as lysophospholipids, can also considerably influence macrophage differentiation and function<sup>102,143</sup>. Sphingosine-1-phosphate (S1P) is a highly active lysophospholipid that has been recently shown to be significantly involved in the regulation of immune responses under both physiological and pathological conditions<sup>35,80,144</sup>. It exerts its biological action as an extracellular messenger via G-protein coupled receptors on cell membranes, but it can also signal intracellularly through intracellular generation and catabolism of S1P involving sphingomyelin, ceramide, sphingosine kinases, and S1P lyases<sup>35,80,95</sup>. Five different S1P binding receptors (S1P<sub>1-5</sub>) have been identified, and S1P signaling affects many biological responses of various macrophage populations in both healthy and diseased states<sup>102,143</sup>. The substantial effects of S1P on barrier integrity, cell growth and migration, apoptosis, cytokine release, inflammation, and neutrophil accumulation in alveoli are evident in several *in vitro* and *in vivo* studies<sup>36,80,95,145</sup>. These observations suggest that S1P acts as a protective mechanism for barrier maintenance and integrity, under both healthy and injured states. Furthermore, recent studies indicate significant involvement of S1P signaling in various disease conditions, including many lung diseases<sup>35,80,145</sup>. While the involvement of S1P signaling in ALI and other lung diseases is evident, the influence of aging and macrophage polarization linking S1P signaling remains unclear and may reveal therapeutic targets for clinical intervention.

This work is based on the scientific premise that the structural and cellular changes in aged lungs precondition the elderly to be more susceptible to injury and other negative outcomes resulting from the damaging stresses generated during mechanical ventilation. We hypothesized that aging and injurious mechanical ventilation elevate S1PL activity that diminishes S1P lung levels and causes further alveolar

barrier damage and impaired pulmonary function. Furthermore, the administration of THI, a S1PL inhibitor, prior to injury elevates S1P lung levels and restores S1P-associated protection against ALI.

**6.2 Materials and Methods:**

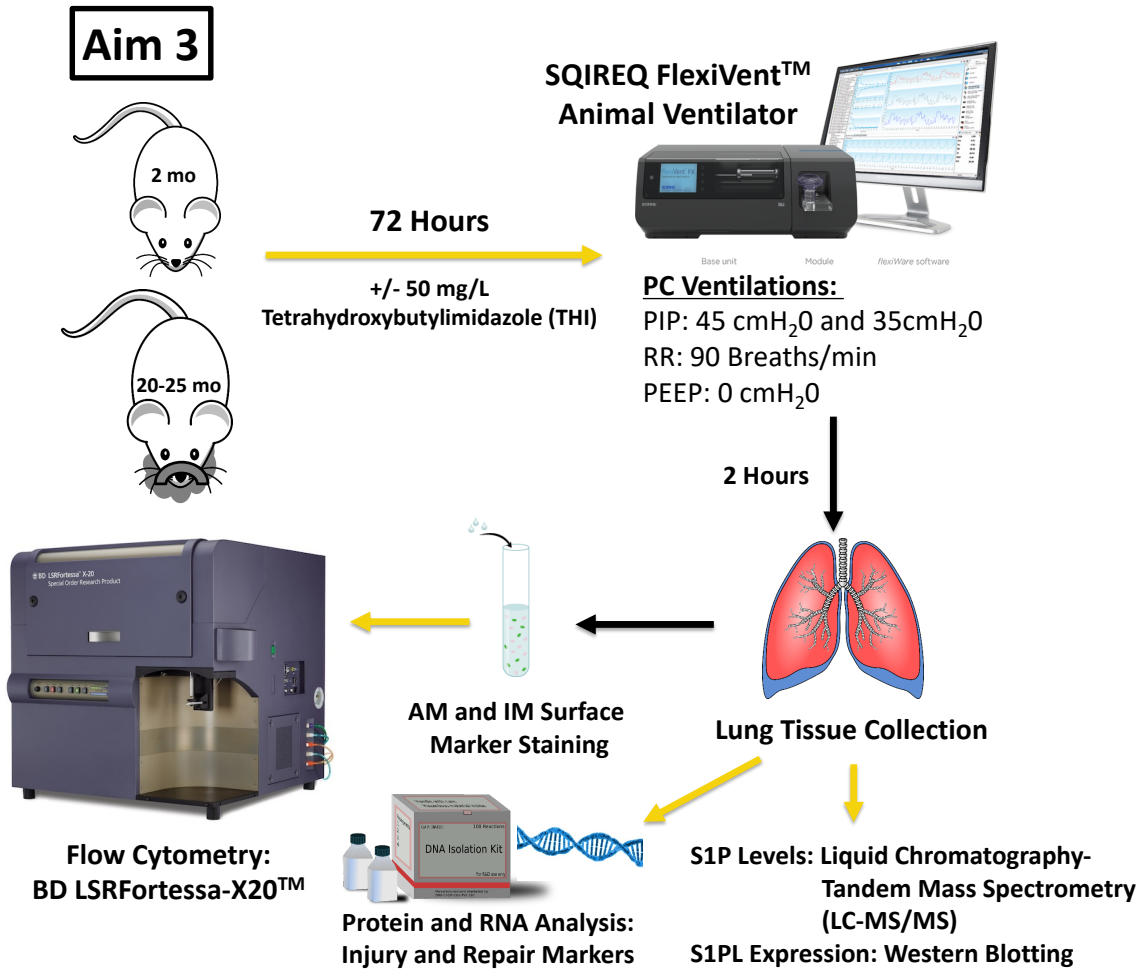


*Figure 39: General overview of Aim 3. Aim 3 investigates the protective role of S1PL Inhibition using THI.*

**Animals:** Male C57BL/6 mice 8 weeks of age were purchased from Jackson Laboratory (Bar Harbor, ME). Male C57BL/6 mice 20 months of age were provided by the National Institute on Aging (Bethesda, MD). All animals were housed in accordance with guidelines from the American Association for Laboratory Animal Care and Research protocols and approved by the Institutional Animal Care Use Committee at Virginia Commonwealth University (Protocol No. AD10000465).

**Pressure-Controlled Ventilator-Induced Lung Injury Model:** We mechanically ventilated young (2-3 mo.) and old (20-25 mo.) C57BL/6J wild-type mice using a Scireq FlexiVent computer-driven small-animal ventilator (Montreal, Canada) and previously cited methods<sup>10</sup> with slight modifications. Mice were anesthetized, tracheotomized, and then ventilated for 5 minutes using a low pressure-controlled strategy (peak inspiratory pressure (PIP): 15 cmH<sub>2</sub>O, respiratory rate (RR): 125 breaths/min, positive end-expiratory pressure (PEEP): 3 cmH<sub>2</sub>O). Mice were then ventilated for 2 hours using a high pressure-controlled mechanical ventilation (PCMV) protocol (PIP: 35-45 cmH<sub>2</sub>O, RR: 90 breaths/min, and PEEP: 0 cmH<sub>2</sub>O). Pulmonary function and tissue mechanics were measured and collected at baseline and every hour during the 2-hour high PCMV duration using the SCIREQ FlexiVent system and FlexiWare 7 Software. A separate group of mice was anesthetized, tracheotomized, and maintained on spontaneous ventilation for 2 hours.

**THI Administration:** C57BL/6 mice received vehicle or 50 mg/L Tetrahydroxybutylimidazole (THI) administered ad libitum in water 72 hours before mechanical ventilation. Water intake was not different between vehicle- and THI-treated groups.

**Tissue Processing:** Immediately following mechanical ventilation, the right lobes of the lung were snap frozen with liquid nitrogen, then stored at -80°C for further analysis. The left lobes of the lung were then inflated with digestion solution containing 1.5 mg/mL of Collagenase A (Roche) and 0.4 mg/mL DNaseI (Roche) in HBSS with 5% fetal bovine serum and 10mM HEPES and processed as previously described<sup>119</sup>. The resulting cells were counted, and dead cells were excluded using trypan blue. Subsets of the experimental groups were also used to collect bronchoalveolar lavage fluid (BALF) fluid, differential cell counts, and left lobes for histological analysis.

**Flow Cytometric Analysis:** Following live cell counts,  $4 \times 10^6$  cells per sample were incubated in blocking solution containing 5% fetal bovine serum and 2% FcBlock (BD Biosciences) in PBS. The cells were then stained using a previously validated immunophenotyping panel of fluorochrome-conjugated antibodies<sup>31</sup>

with slight modifications. Following the staining procedure, cells were washed and fixed with 1% paraformaldehyde in PBS. Data were acquired and analyzed with a BD LSRFortessa-X20 flow cytometer using BD FACSDiva software (BD Bioscience). Histogram plots were generated using FCS Express 5 software (De Novo). Compensation was performed on the BD LSRFortessa-X20 flow cytometer at the beginning of each experiment. “Fluorescence minus one” controls were used when necessary. Cell populations were identified using a sequential gating strategy that was previously developed<sup>31</sup>. The expression of activation markers is presented as median fluorescence intensity (MFI).

**Bronchoalveolar Lavage Fluid (BALF) Cytometry and Protein Concentrations:** The BALF was collected and centrifuged to collect a cell pellet and supernatant, as previously described<sup>10</sup>. Cell pellets were resuspended in saline and mounted onto glass slides using a cytospin device (Thermo Shandon). Cells were stained (3 Diff-Quick solutions staining kit) and immune cell populations were quantified. The quantification of total BALF protein in the supernatants was measured by using the Pierce BCA Protein Assay Kit (Thermo Scientific).

**Analysis of Sphingoid Base-1-Phosphates and S1P Lyase:** S1P levels were evaluated in the lung tissue and bronchoalveolar lavage (BAL) fluids by reverse-phase high-performance liquid chromatography separation, negative-ion electrospray ionization, and tandem mass spectrometry analysis, as previously described<sup>36</sup>. S1P lyase (S1PL) expression was determined in the lung tissue lysates by western blotting; S1P-Lyase (H-300); rabbit; 1:1,000; sc-67368 (Santa Cruz Biotechnology).

**Histology:** Lung tissue samples were embedded and stained with hematoxylin and eosin (H&E). The mean linear intercept ( $L_m$ ), an index of airspace enlargement, quantify relative differences in alveolar airspace area within lung histology sections and were measured and analyzed as previously described<sup>10</sup>.

**Statistics:** A total of 44 young and old mice were used for this study. All experiments were performed with a minimum of  $n=3$ . Larger  $n$  values were utilized where possible. Limitations exist in the number of

20-25-month-old mice available from the National Institute on Aging. Therefore, we used minimum numbers to achieve a power of 0.8. Results are presented as mean +/- SEM. GraphPad Prism was used for all statistical analyses. For multiple-group comparisons, we used a two-way analysis of variance (ANOVA) with age and mechanical ventilation as factors, followed by a posthoc Tukey test to determine significance. P<0.05 was considered statistically significant.

### **6.3 Results:**

#### **Aging and/or High PCMV Alters Levels of Sphingoid Bases and Expression of S1P Lyase in C57/Bl6 Mouse Lungs:**

Aging and High PCMV resulted in several changes to various sphingoid bases, as shown in Table 2. Interestingly, we did not detect any significant variations to sphingosine, dihydrosphingosine, S1P, or dihydrosphingosine-1-phosphate concentrations in aged lung tissue compared to young mice. Conversely, aged mice contained significant alterations in concentrations of various ceramide and sphingomyelin forms in their lung tissue compared to young mice (Table 3). High PCMV alone caused substantial deviations to sphingosine, dihydrosphingosine, and S1P (Table 2); however, High PCMV did not lead to significant changes in ceramide or sphingomyelin bases (Table 3). The aged mice that received high PCMV resulted in noteworthy fluctuations in dihydrosphingosine, S1P, and specific ceramide and sphingomyelin bases, as depicted in Table 2&3.

<b>Table 1: Lipidomic Changes due to Age and/or High PCMV</b>			
	Changes with Age at Baseline	Changes with High PCMV	Young Control Compared to Old PCMV
Sphingosine	n.s.	* (w/ Y)	n.s.
DHSo	n.s.	* (w/ Y and O)	*
S1P	n.s.	** (w/ Y)	**
DHS1P	n.s.	n.s.	n.s.

*Table 2: Long Chain (Sphingoid) Base Changes caused by Aging and/or High PCMV. Data are presented as mean +/- SEM, n ≥ 3 per experimental group. \*p<0.05, \*\* p<0.01, as indicated*

Table 1: Lipidomic (Ceramides) Changes due to Age and/or High PCMV				Table 1: Lipidomic (Sphingomyelin) Changes due to Age and/or High PCMV			
	Changes with Age at Baseline	Changes with High PCMV	Young PCMV Compared to Old PCMV		Changes with Age at Baseline	Changes with High PCMV	Young PCMV Compared to Old PCMV
C14:0	**	n.s.	n.s.	C14:0	**	n.s.	n.s.
C16:0	*	n.s.	n.s.	C16:0	*	n.s.	n.s.
C18:1	**	n.s.	n.s.	C18:1	**	n.s.	n.s.
C18:0	*	n.s.	**	C18:0	*	n.s.	**
C20:0	**	n.s.	*	C20:0	**	n.s.	*
C22:0	**	n.s.	*	C22:0	**	n.s.	*
C24:0	*	n.s.	*	C24:0	*	n.s.	*
C26:0	*	n.s.	n.s.	C26:0	*	n.s.	n.s.

*Table 3: Ceramide and Sphingomyelin Base Changes Caused by Aging and/or High PCMV. Data are presented as mean +/- SEM, n ≥ 3 per experimental group. \*p<0.05, \*\* p<0.01, as indicated.*

High PCMV for a duration of 2 hours significantly increased S1P levels (~2-fold) in the young mouse lung tissue compared to mice with spontaneous breathing (Figure 42A). The slight increase in S1P levels in the old mouse lung tissue that underwent high PCMV was not statistically different compared to the non-ventilated control groups. Following high PCMV for 2 hours, the aged mice failed to produce a significant increase in S1P compared to the young counterparts. The effects of aging and high PCMV on the expression of S1PL, which is highly involved in the catabolism and metabolism of S1P, was also assessed. The old non-ventilated controls and both the young and old high PCMV groups resulted in increased expression of S1PL compared to the young non-ventilated control group (Figure 42B), which was assessed by immunoblotting. This finding indicates that aging and high PCMV enhance S1PL expression.

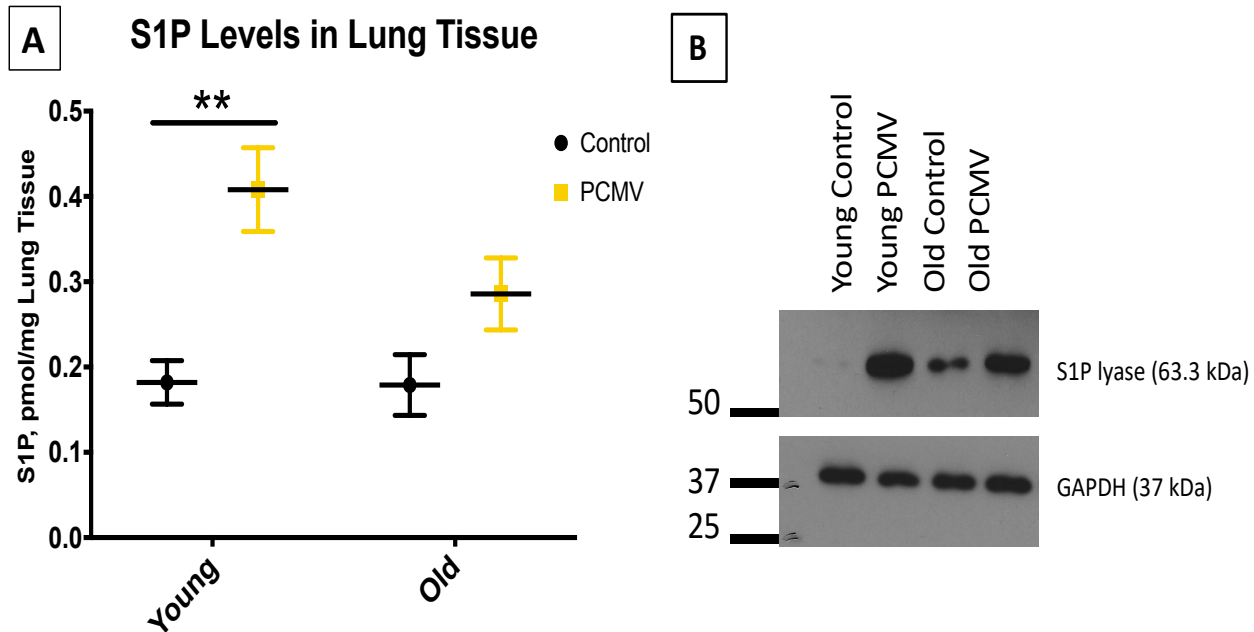


**Figure 40: Effects of Aging and High PCMV on S1P levels and S1PL expression in lung tissue.** S1P levels in lung tissue (A) were quantified by liquid chromatography-tandem mass spectrometry (LC-MS/MS). Data are presented as mean  $\pm$  SEM,  $n \geq 4$  per experimental group. \*\*  $p < 0.01$ , as indicated. Total lung tissue lysates from control and high PCMV mice were also analyzed for S1PL protein expression by Western Blotting (B). Shown are representative blots of S1PL expression from three independent experiments.

These findings indicate that aging and high PCMV differently altered sphingoid bases levels in the lung, including ceramide and sphingomyelin base forms. Aging and mechanical injury also enhanced S1PL protein expression in the aged mice, with and without PCMV, and in young mice instigated with mechanical injury. The enhanced S1PL expression reflects similar macrophage polarization deviations and increased injury outcomes from mechanical injury (shown in Chapter 3), such as the M1 alveolar macrophage populations and the CD80+/CD206+ alveolar macrophages.

### **THI Attenuates Lymphocyte and Neutrophil Accumulation Following High PCMV in Young Mice:**

High PCMV caused elevated lymphocyte (Figure 43A), neutrophil (Figure 43B), and basophil accumulation (Figure 43C) that were detected in the BALF samples of young mice. Neutrophil influx is a hallmark of ALI/VILI<sup>45</sup>. The cells in the BALF were subjected to a Cytospin protocol, mounted to microscope slides, and stained using a differential-stain kit to separate and count the different types of immune cells in the BALF. Young mice that received THI in drinking water for three days prior to

mechanical ventilation resulted in reduced lymphocyte (Figure 43A) and neutrophil (Figure 43B) influx compared to young mice that underwent PCMV without THI administration. Important to note, THI administration had no effect on these cell populations without PCMV. Interestingly, the basophil influx did not change with THI dosing prior to PCMV compared to young mice without THI.

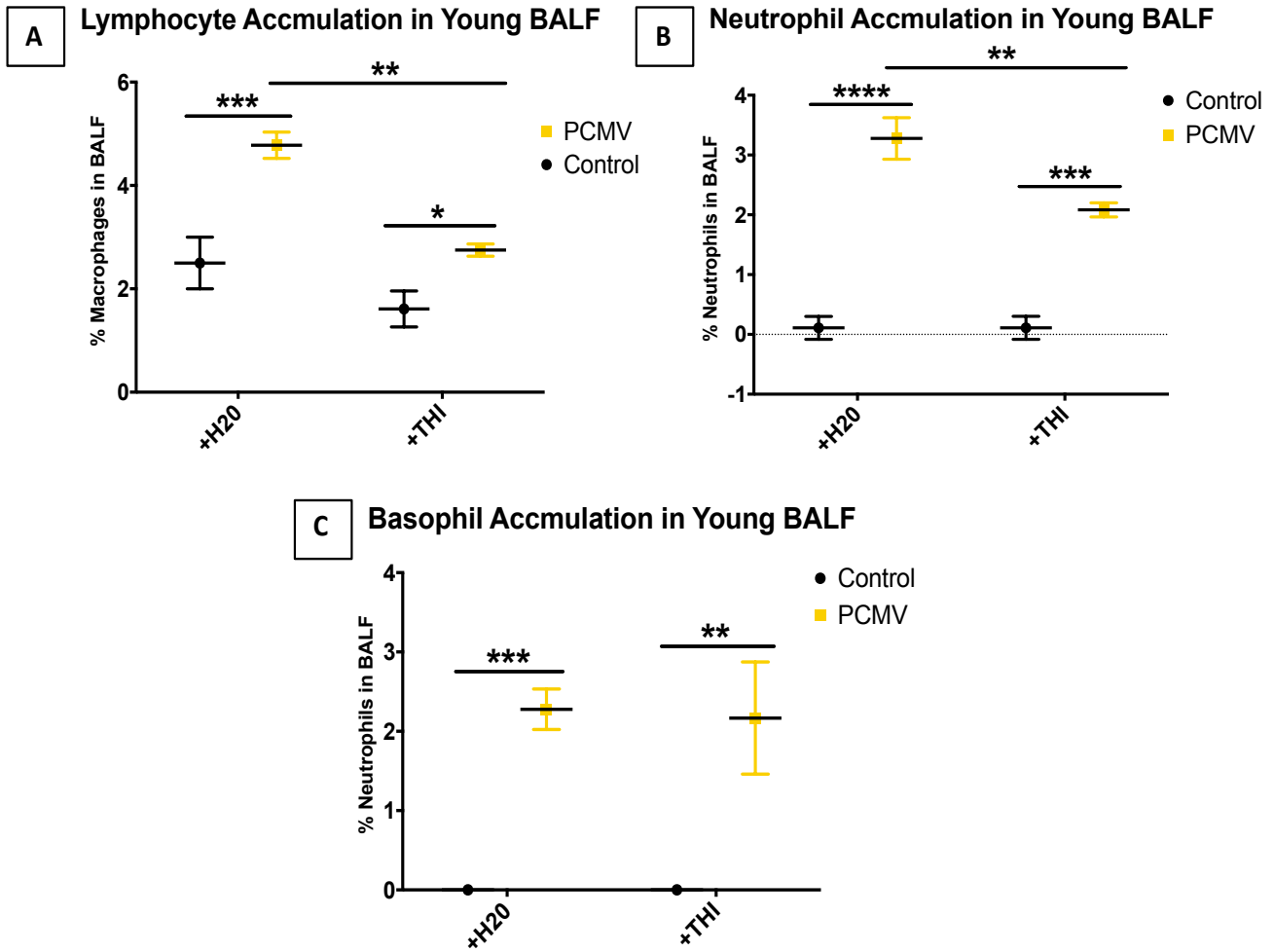


**Figure 41: THI attenuates lymphocyte and neutrophil influx following high PCMV in young mice.** Differential cell counts were performed on cytospin samples prepared from the BALF of young mice that received THI or vehicle control following high PCMV or spontaneous breathing. Data are presented as mean  $\pm$  SEM,  $n \geq 3$  per experimental group. \*  $p < 0.05$ , \*\*  $p < 0.01$ , \*\*\*  $p < 0.001$ , \*\*\*\*  $p < 0.0001$  as indicated.

## THI Treatment Diminishes Lymphocyte, Neutrophil, and Basophil Accumulation Following High PCMV in Old Mice Lungs:

The aged mice that were stimulated with high PCMV resulted in increased lymphocyte (Figure 44A), neutrophil (Figure 44B), and basophil accumulation (Figure 44C) in BALF samples compared to aged, nonventilated control mice. Important to note, although not depicted in the figures, the percentages of immune cell accumulation were overall higher that were collected in the old mice BALF samples compared to the young mice data that is shown in Figure 43. Old mice that were treated with THI prior to high PCMV developed reductions in lymphocyte (Figure 44A), neutrophil (Figure 44B), and basophil influx compared to aged mice that underwent PCMV without THI administration. As with the young mice, there was no significant effect of the THI treatment alone to any of these immune cell populations.

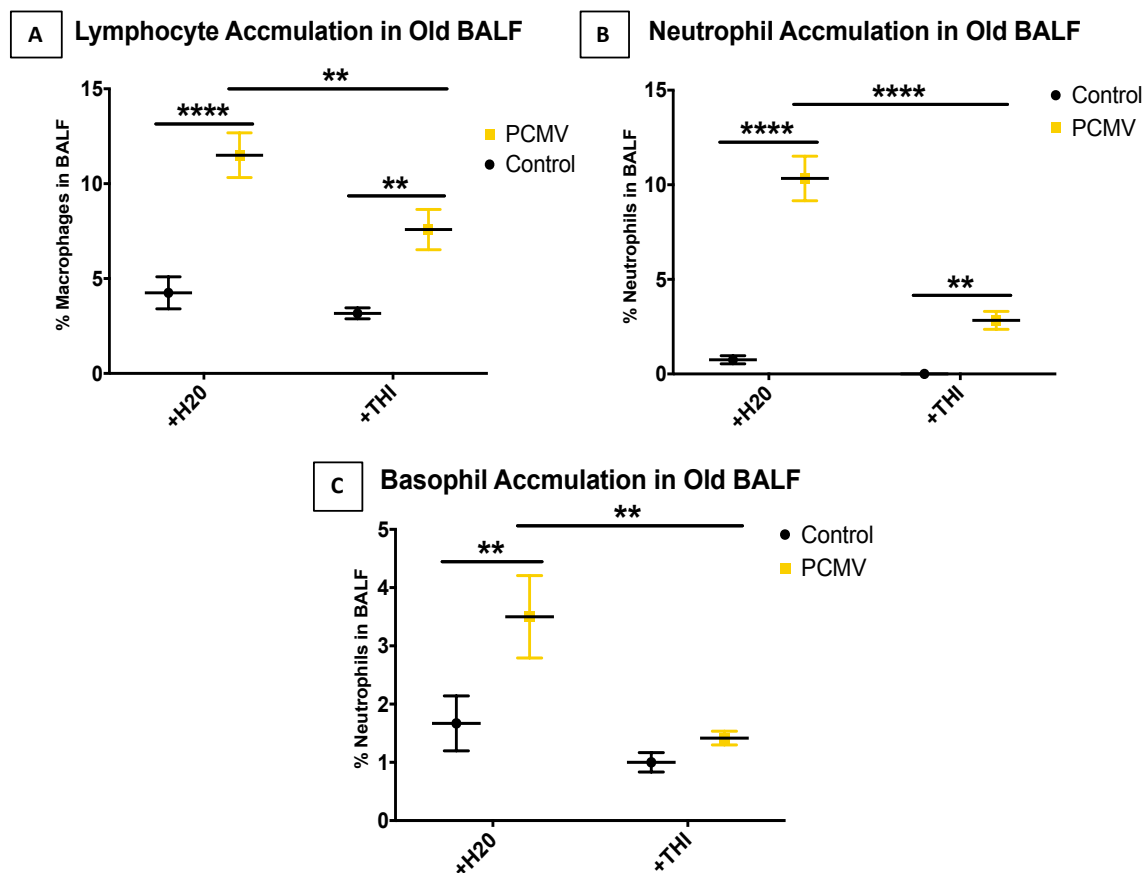


**Figure 42: THI mitigates lymphocyte, neutrophil, and basophil influx following high PCMV in old mice.** Differential cell counts were performed on cytopsin samples prepared from the BALF of old mice that received THI or vehicle control following high PCMV or spontaneous breathing. Data are presented as mean +/- SEM, n ≥ 2 per experimental group. \* p<0.05, \*\* p<0.01, \*\*\* p<0.001, \*\*\*\* p<0.0001 as indicated.

## The Impact of THI Administration on Lung Protein Accumulation Following High PCMV in Young and Old Mice:

High PCMV produced increased protein concentrations in the BALF samples of both young and old mice that underwent high PCMV compared to their age-matched control groups (Figure 45); however, there were no differences in BALF protein concentrations detected between young and old controls. Notably, there was no substantial change in BALF protein levels in young or old mice that received THI treatments prior to high PCMV compared to their age-matched control groups that were also administered THI. Interestingly, there was no change in BALF protein accumulation in the young control mice that received THI compared to young control mice that did not. However, there was a significant decrease in BALF protein concentrations of old control mice with THI compared to old control mice without THI.

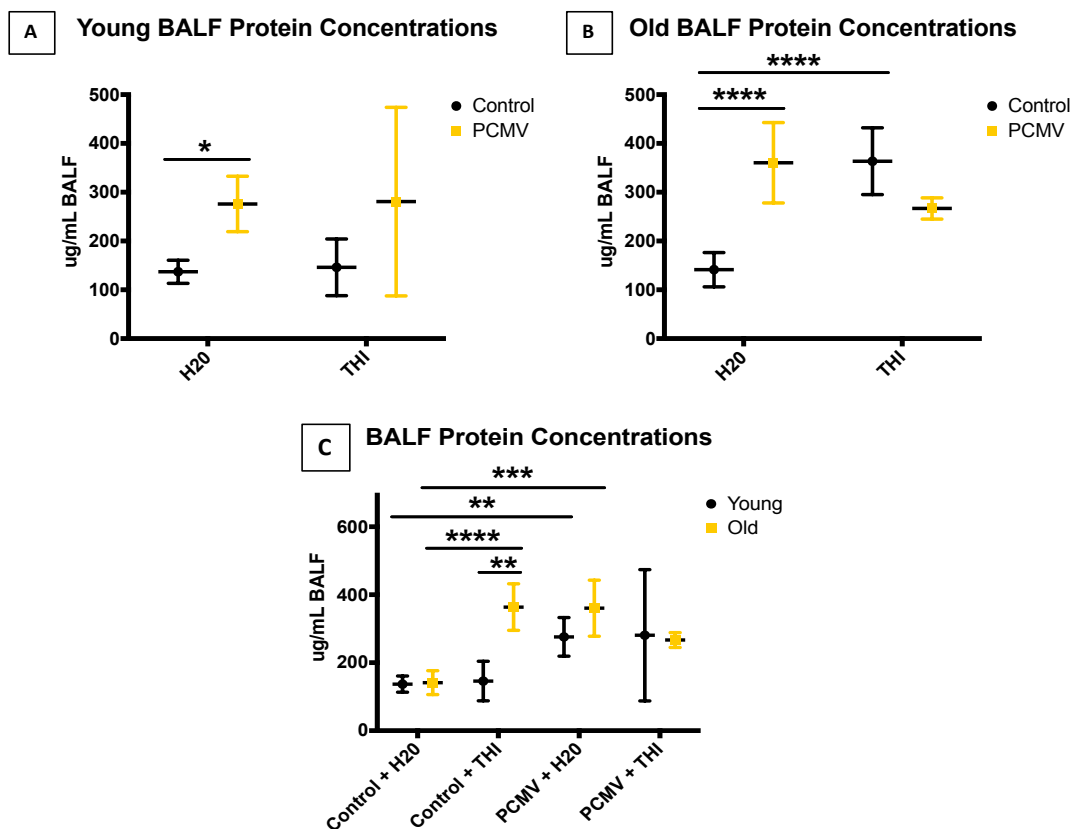


**Figure 43: THI improves the protein accumulation in BALF samples of young and old mice following high PCMV.** Bronchoalveolar Lavage (BAL) fluids from (A) young and (B) old mice that received THI or vehicle control following high PCMV or spontaneous breathing were assessed for protein concentrations. (C) Shows the comparison of both age groups. Data are presented as mean +/- SEM, n ≥ 3 per group. \* p<0.05, \*\*\* p<0.001, \*\*\*\* p<0.0001 as indicated.

## The Effect of TH1 Treatment on Alveolar and Interstitial Macrophage Populations in Young and Old Mice Following High PCMV:

TH1 treatment produced several changes in macrophage populations of young mice. Young mice that received high PCMV resulted in a loss in total alveolar macrophage populations; however, young mice that were administered TH1 prior to high PCMV led to no significant loss in total alveolar macrophages. There were no detectable changes in overall interstitial macrophage populations from high PCMV or the TH1 treatment.

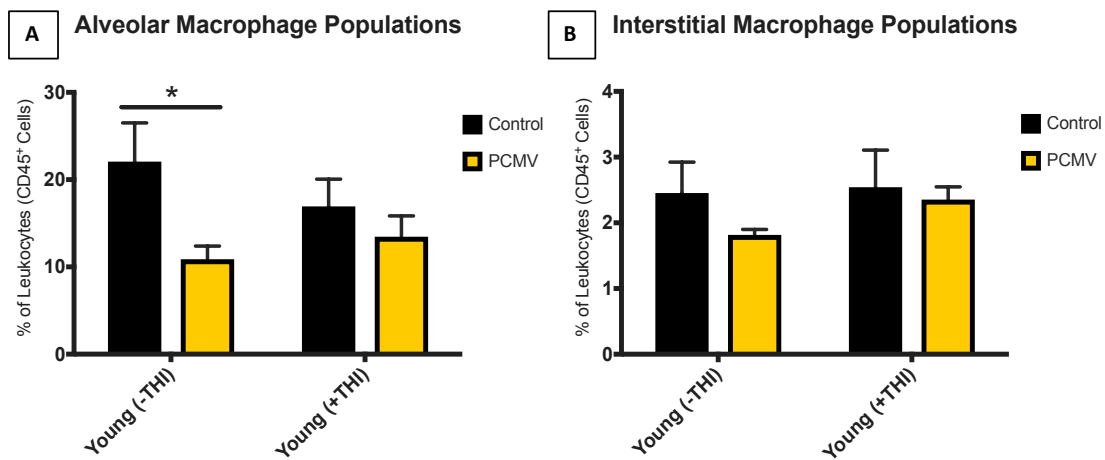


**Figure 44: Effects of Aging and High PCMV on Young Lung Macrophage Polarization in C57BL/6 Mice.** Quantifiable changes of young macrophage subsets were identified using the set of surface markers and gating strategy described in the methods. The populations of Alveolar (A) and Interstitial macrophages (B) are depicted as percentages of total CD45<sup>+</sup> Cells. Data are presented as mean +/- SEM, n ≥ 4 per experimental group. \* p<0.05, \*\* p<0.01, \*\*\* p<0.001, \*\*\*\* p<0.0001 as indicated.

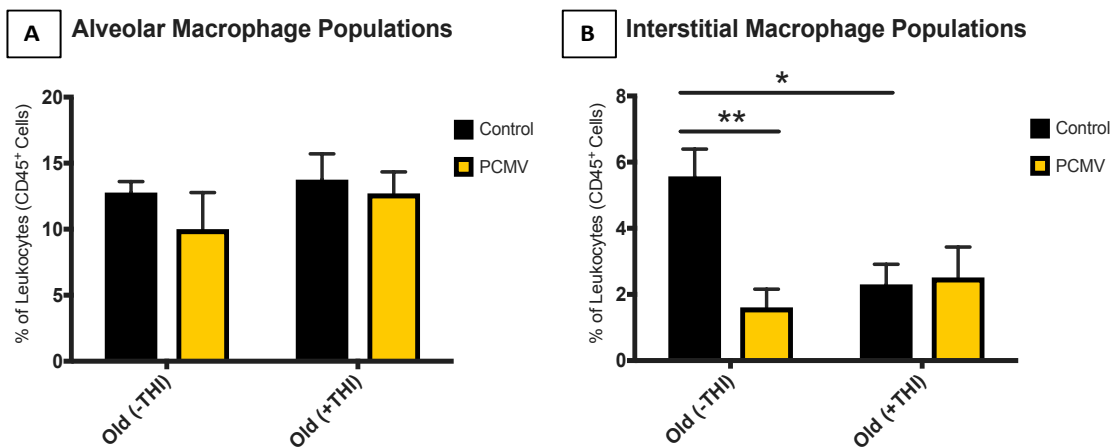


**Figure 45: Effects of Aging and High PCMV on Old Lung Macrophage Polarization in C57BL/6 Mice.** Quantifiable changes of old macrophage subsets were identified using the set of surface markers and gating strategy described in the methods. The populations of Alveolar (A) and Interstitial macrophages (B) are depicted as percentages of total CD45<sup>+</sup> Cells. Data are presented as mean +/- SEM, n ≥ 4 per experimental group. \* p<0.05, \*\* p<0.01, \*\*\* p<0.001, \*\*\*\* p<0.0001 as indicated.

THI treatment also influenced the lung macrophage populations of old mice. Interestingly, there was no change in alveolar macrophage populations of aged mice with or without THI (Figure 47A). Conversely, Old mice that received high PCMV resulted in a loss in total interstitial macrophage populations (Figure 47B); however, old mice that were administered THI prior to high PCMV led to no significant loss in total interstitial macrophages.

#### **THI Dosing Effects on Lung Macrophage Subpopulations Following High PCMV in Young Mice:**

THI treatment also had substantial effects on the subpopulations of alveolar and interstitial macrophages. Naïve interstitial macrophage populations were also amplified in young mice given THI prior to high PCMV compared to young control mice; however, there was no significant change to this cell population in young mice with THI that had high PCMV compared to young PCMV mice without THI. THI treatment also increased naïve alveolar macrophage populations compared to young mice that underwent high PCMV without THI. High PCMV increased M1 alveolar macrophages in young mice compared to young controls; however, this significant change was not detected in young mice that received THI prior to PCMV compared to young control mice (Figure 48A). Young mice stimulated with high PCMV also resulted in elevated CD80+/CD206+ alveolar macrophages compared to young control mice. There was a significant reduction in CD80+/CD206+ alveolar macrophages in young mice with THI prior to high PCMV compared to young PCMV mice without THI. THI treatment had no effect on M1, M2, or CD80+/CD206+ interstitial macrophage populations in young mice with or without PCMV. Interestingly, THI administration reduced M2 alveolar macrophage populations in young control mice compared to young control mice without THI; however, THI treatment did not alter M1 or CD80+/CD206+ alveolar macrophage populations in young control mice compared to young control mice without THI.

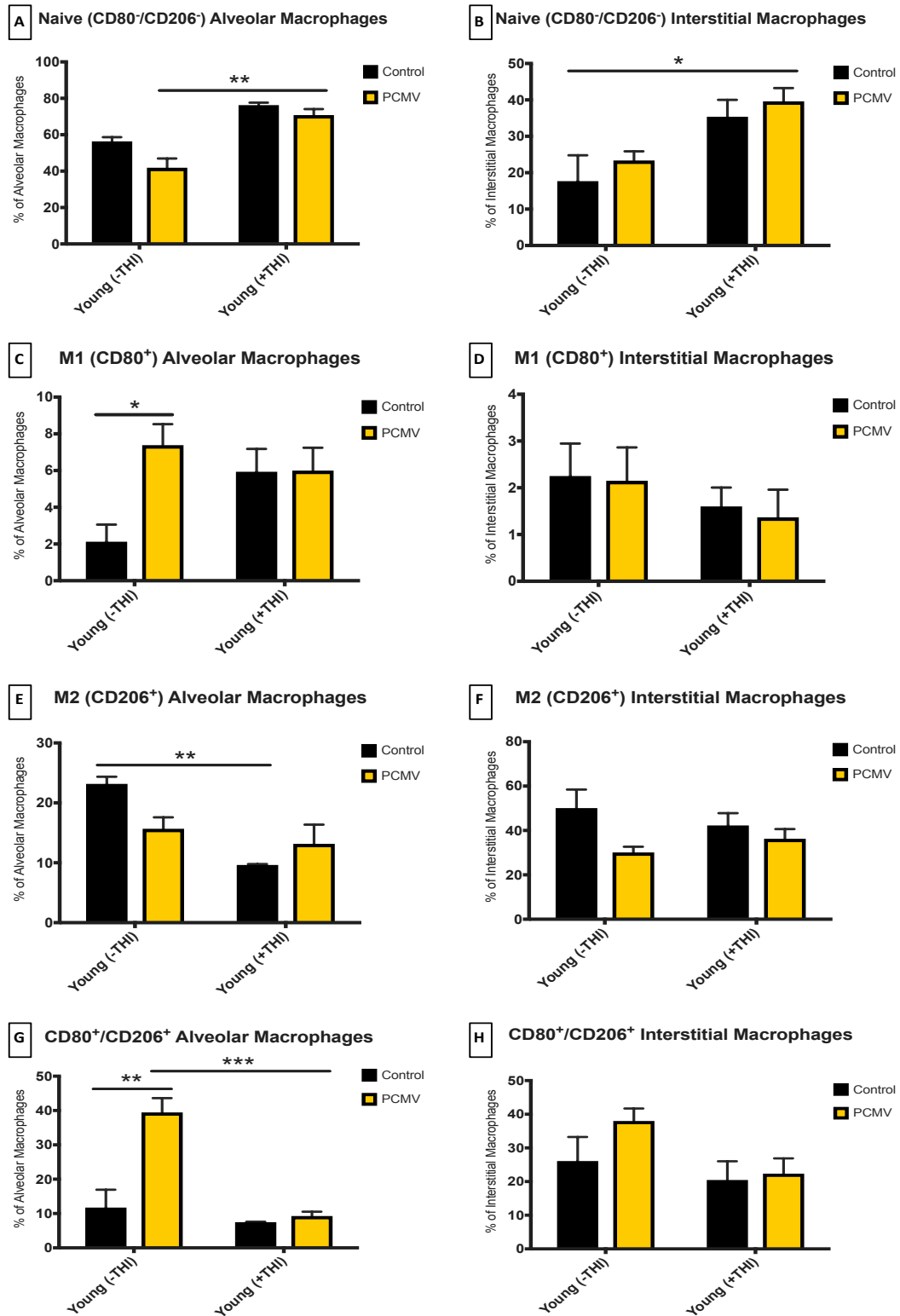


**Figure 46: Aging and High PCMV Influence Lung Macrophage Polarization in C57BL/6 Mice.** Quantifiable changes of macrophage subsets were identified using the set of surface markers and gating strategy described in the methods. The populations of CD80<sup>-</sup>/CD206<sup>-</sup> (A&B), CD80<sup>+</sup> (C&D), CD206<sup>+</sup> (E&F), and CD80<sup>+</sup>/CD206<sup>+</sup> (G&H) macrophages are depicted as percentages of total alveolar (A, C, E, G) and interstitial macrophage (B, D, F, H) populations. Data are presented as mean +/- SEM, n ≥ 4 per experimental group. \* p<0.05, \*\* p<0.01, \*\*\* p<0.001, \*\*\*\* p<0.0001 as indicated.

### **THI Treatment on Old Lung Macrophage Subpopulations Following Mechanical Injury:**

THI treatment also had a considerable impact on the subpopulations of old alveolar and interstitial macrophages. THI administration increased old naïve alveolar macrophage populations in PCMV mice compared to old control mice without PCMV or THI (Figure 49C); however, there was no significant change to this cell population in old mice with THI that had high PCMV compared to old PCMV mice without THI. PCMV with aged mice also caused a loss in naïve interstitial macrophages compared to old control mice; furthermore, THI treatment increased the naïve interstitial macrophage population when comparing old PCMV mice with THI to old PCMV mice without treatment. Interestingly, THI treatment produced an increase in naïve alveolar macrophage populations and a loss in total interstitial macrophage populations in old control mice compared to old control mice without THI. PCMV or THI had no significant effect on old M1 alveolar macrophages (Figure 49A); however, the administration of THI caused a substantial increase in old M2 alveolar macrophage populations compared to old mice that underwent high PCMV without THI. THI treatment also considerably reduced CD80+/CD206+ alveolar macrophages in aged mice stimulated with high PCMV compared to old PCMV mice without THI treatment. THI treatment had no influence on M1 or M2 interstitial macrophages in aged, PCMV mice compared to aged, PCMV mice without treatment; however, there was a reduction in CD80+/CD206+ interstitial macrophages in aged, PCMV mice that received THI treatment compared to aged, PCMV mice without THI. THI administration had no effect on both M1, or M2, alveolar and interstitial macrophages or CD80+/CD206+ alveolar macrophages in old control mice; however, THI treatment reduced CD80+/CD206+ interstitial macrophages in old control mice compared to old control mice without treatment.

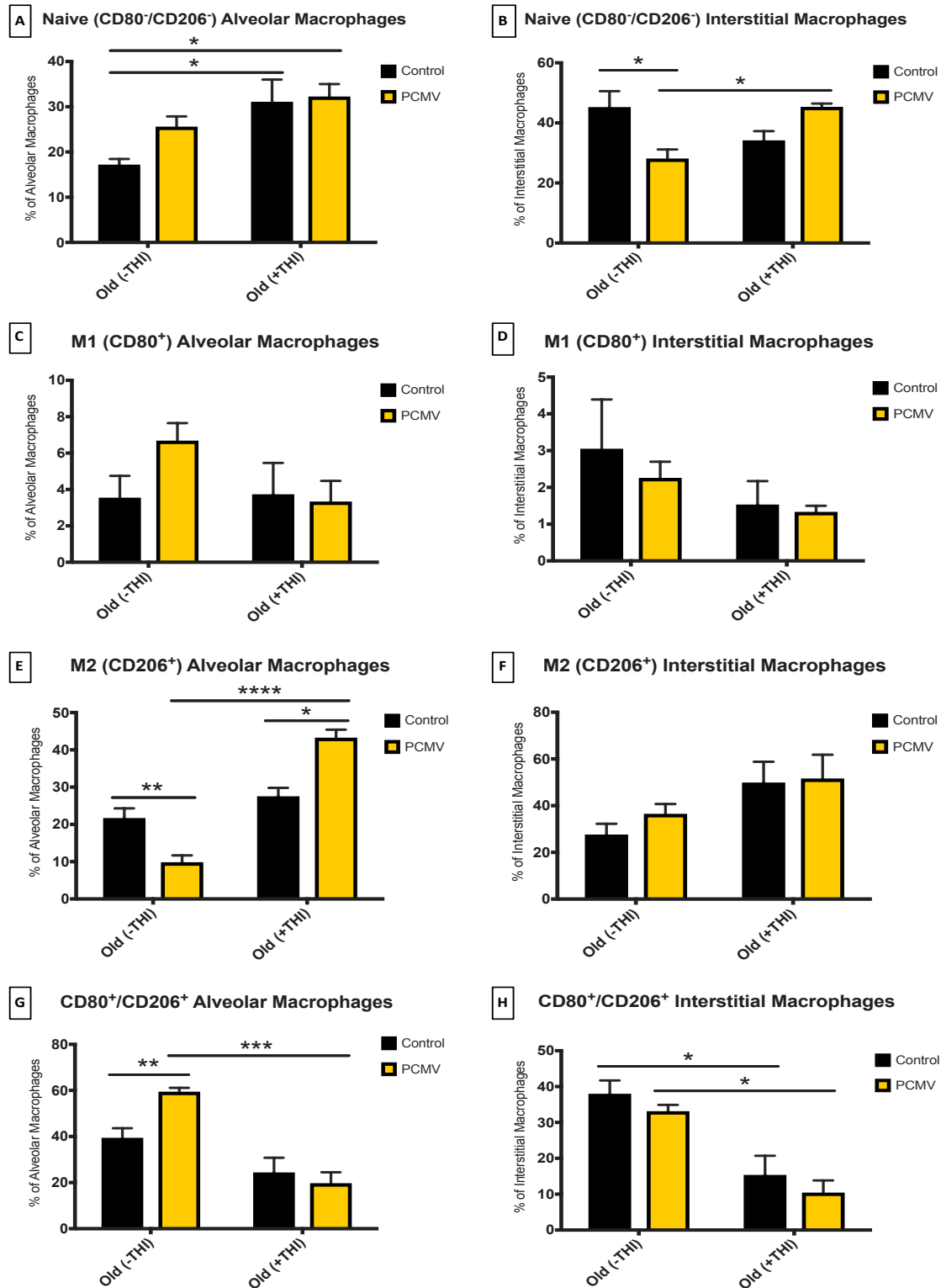


**Figure 47: Aging and High PCMV Influence Lung Macrophage Polarization in C57BL/6 Mice.** Quantifiable changes of macrophage subsets were identified using the set of surface markers and gating strategy described in the methods. The populations of CD80<sup>-</sup>/CD206<sup>-</sup> (A&B), CD80<sup>+</sup> (C&D), CD206<sup>+</sup> (E&F), and CD80<sup>+</sup>/CD206<sup>+</sup> (G&H) macrophages are depicted as percentages of total alveolar (A, C, E, G) and interstitial macrophage (B, D, F, H) populations. Data are presented as mean +/- SEM, n ≥ 4 per experimental group. \* p<0.05, \*\* p<0.01, \*\*\* p<0.001, \*\*\*\* p<0.0001 as indicated.

### **The Effects of THI on the Mechanical Properties of Young and Old Mice During High PCMV:**

We also assessed changes in tissue mechanics in young and old mice that received THI prior to mechanical ventilation and compared them to age-matched control groups that received THI or vehicle control (H2O). We initially examined the effect of THI on baseline mechanical properties of Young and Old mice. Although not shown, we found that THI treatment had no effect on the respiratory system resistance (R), the lung compliance (C), the newtonian resistance (Rn), and tissue damping mechanical properties at baseline of the Young and Old mice. Interestingly, THI treatment produced minor changes in inspiratory capacity, respiratory system elastance (E), and lung tissue elasticity (H) in young mice at baseline; however, THI therapy had no effect on the mechanical properties of old mice at baseline.

THI treatment also improved several tissue mechanical properties in young mice, as shown in Figure 51. The inspiratory capacity, the respiratory system compliance (C), and lung tissue elasticity (H) in young mice all showed improvements as early as 1 hour after high PCMV was initiated. It is important to note that there were less mechanical property deviations caused by high PCMV in young mice compared to old (shown in Figure 27). THI produced no change in airway resistance (Rn), respiratory system resistance (R), Lung tissue damping (G), respiratory system elastance, or quasi-static compliance (Cst) during induction of injury by high PCMV.

THI treatment also mitigated several lung and respiratory mechanical properties in old mice, as shown in Figure 52. The respiratory compliance (C), lung tissue damping (G), and quasi-static compliance (Cst) in old mice all revealed improvements after 2 hours of high PCMV. THI administration resulted in no significant difference in inspiratory capacity, respiratory system resistance (R), Lung tissue elasticity (H), or respiratory system elastance in old mice during induction of injury by high PCMV compared to old mice that were mechanically injured without THI treatment administered prior. However, it is important to note that there were significant deviations in inspiratory capacity, respiratory system compliance, respiratory system resistance, lung tissue damping, lung tissue elasticity, and respiratory system elastance caused by high PCMV without THI compared over the 2 hour period that was not observed in the old mice dosed with THI prior to mechanical injury.

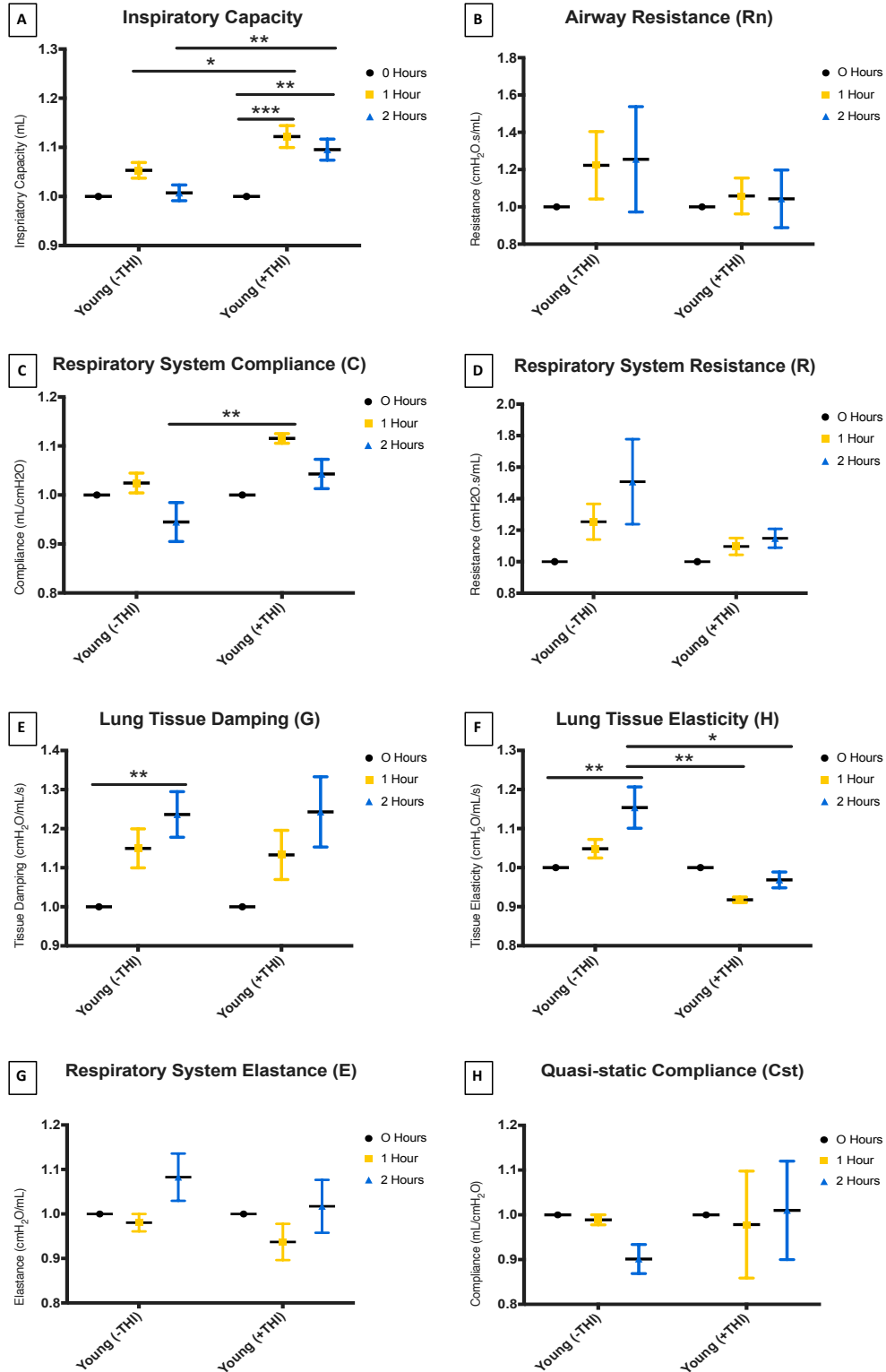


**Figure 48: THi treatment resulted in the attenuation of several tissue mechanical properties in young mice.** Tissue mechanics and lung function was determined with a SCIREQ FlexiVent rodent ventilator for mice. Figure depicts Changes were determined in inspiratory capacity (A), airway resistance (B), respiratory system compliance (C), respiratory system resistance (D), lung tissue damping (E), lung tissue elasticity (F), and quasi-static compliance (G). Data are presented as mean +/- SEM,  $n \geq 3$  per experimental group. \*  $p < 0.05$ , \*\*  $p < 0.01$ , \*\*\*  $p < 0.001$ , \*\*\*\*  $p < 0.0001$  as indicated.

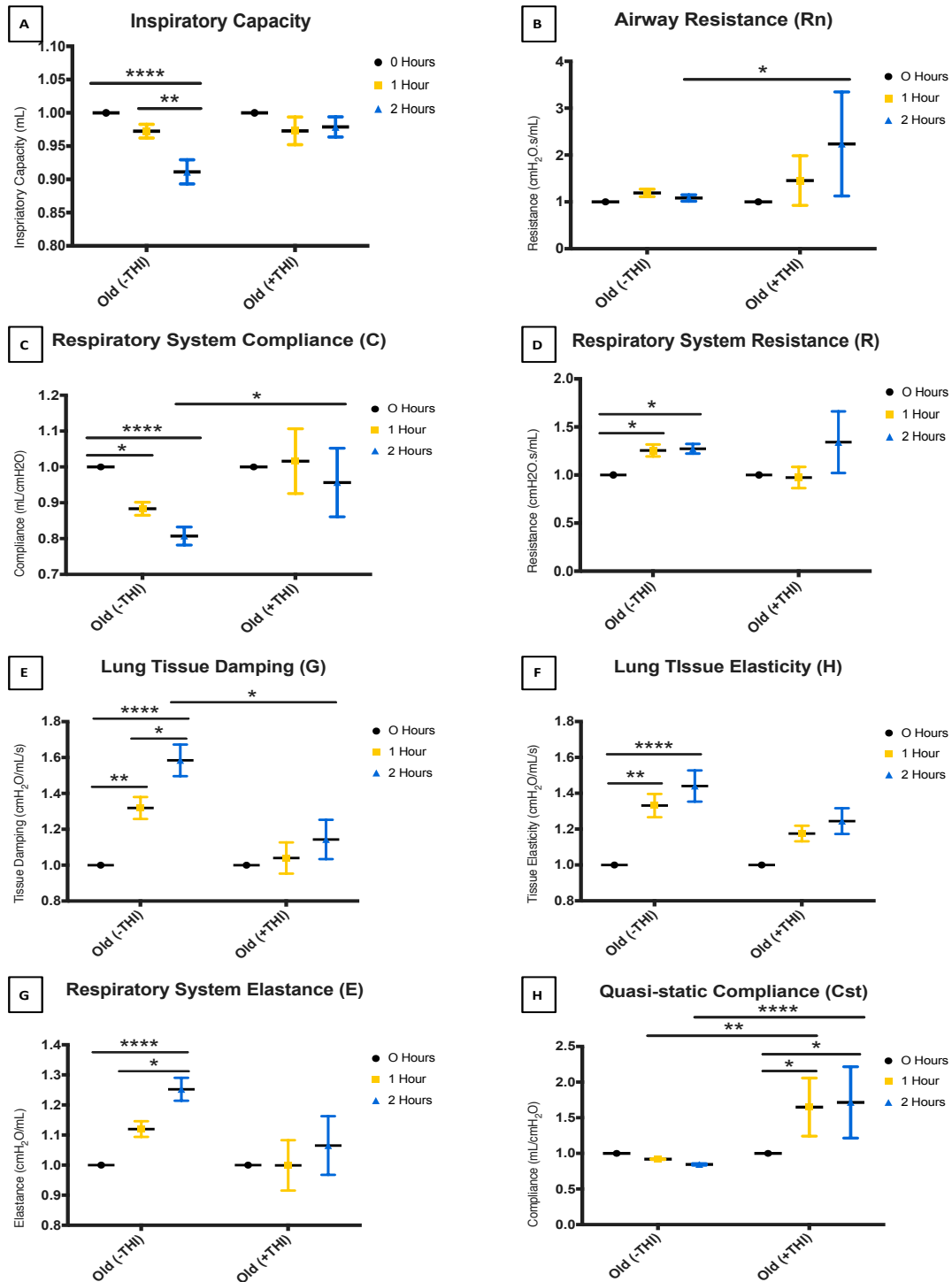


**Figure 49: TH1 treatment resulted in the attenuation of several tissue mechanical properties in old mice.** Tissue mechanics and lung function was determined with a SCIREQ FlexiVent rodent ventilator for mice. Figure depicts Changes were determined in inspiratory capacity (A), airway resistance (B), respiratory system compliance (C), respiratory system resistance (D), lung tissue damping (E), lung tissue elasticity (F), and quasi-static compliance (G). Data are presented as mean +/- SEM,  $n \geq 3$  per experimental group. \*  $p < 0.05$ , \*\*  $p < 0.01$ , \*\*\*  $p < 0.001$ , \*\*\*\*  $p < 0.0001$  as indicated.

#### **6.4 Discussion:**

Acute lung injuries, such as VILI, are damaging disorders that remain a major issue with high frequencies of annual hospitalizations, in-hospital mortality rates, and severe complications despite recent advances in understanding of the mechanisms and pathophysiology associated with the condition. Implementing “protective ventilator strategies” has only marginally improved negative outcomes, and the overall mortality rates for ventilated patients are still unacceptably high. Furthermore, few studies are performed on aged subjects, which is incongruent with the fact that elderly patients have a greater need for mechanical ventilation. These observations illustrate the major clinical need to develop treatments or therapies that prevent the cellular injury mechanisms and inflammation directly resulting from the pathological mechanical forces generated during mechanical ventilation. These age-related and injury-related impaired cellular responses represent potential molecular targets for therapeutic intervention for patients that are diagnosed with ALI or required mechanical ventilation.

In this study, we evaluated the role of S1PL that regulates intracellular S1P levels as an effective age-related therapeutic target of ALI/VILI. Sphingolipids, such as S1P and sphingolipid metabolizing enzymes, such as S1PL, have been shown to diversely impact various respiratory diseases<sup>80</sup>. S1P is involved in numerous cellular processes that include cell survival, growth and proliferation, apoptosis, endothelial and epithelial barrier function, immune regulation, and inflammation<sup>80,146,147</sup>. Our findings demonstrate that aging and/or mechanical injury produces elevated expression levels of S1PL in lung tissue. Aging and/or mechanical injury also resulted in substantial changes to several sphingoid bases present in lung tissue. The investigation revealed that S1P lung levels were considerably elevated in young mice lungs that underwent high PCMV; however, there was no substantial increase in S1P levels in old mouse lungs following high PCMV. This disparity also correlated with the injury outcomes associated with young and old mice following mechanical injury. Furthermore, our findings indicate that the administration of THI, a S1PL inhibitor that prevents the irreversible loss of S1P and enhances the accumulation of S1P in lung tissue, diminished several of the associated indications of acute lung injury. THI administration prior to mechanical injury reduced immune cell recruitment to alveolar regions, lung

protein accumulation, and deviations in lung and respiratory mechanical priorities in both young and old mice. Furthermore, THI treatment also altered macrophage polarization by increasing the number of naïve alveolar macrophages in young and old mice, increasing the number of naïve interstitial macrophages in old mice, reducing CD80+/CD206+ alveolar macrophages in young and old mice, reducing the CD80+/CD206+ interstitial macrophages in old mice, and increasing the number of M2 alveolar macrophages in old mice following induction of injury by high PCMV.

Lung conditions such as ALI/VILI are characterized by increased permeability and alveolar flooding, immune cell recruitment and activation, and an overall deterioration of the alveolar barrier integrity<sup>1,5</sup>. Overall, this research further indicates that regulating S1P and its related components provides a protective effect against the development and progression of ALI, which has been suggested in recent studies. For example, the administration of S1P diminished lung edema formation and promoted survival in an acute lung injury model produced by loss of Forkhead protein in endothelial cells<sup>80</sup>. Additionally, the knockdown of Forkhead protein leads to increased expression of S1P<sub>1</sub>, which was suggested to help maintain barrier integrity<sup>80</sup>. Sphk1 has also been shown to provide protection against radiation-induced lung injury, SphK1<sup>-/-</sup> mice were highly susceptible to the radiation damage; furthermore, S1P receptor agonists were administered and attenuated the radiation damage<sup>80</sup>. Additionally, SphK1<sup>-/-</sup> mice had greater vascular leakage and reduced recovery from LPS-induced ALI and these negative outcomes were assuaged by the administration of exogenous S1P<sup>80</sup>. In other LPS-induced murine ALI models, intravenous S1P administration also reduced lung vascular permeability and inflammation<sup>92</sup>. Collectively, studies generally suggest that the barrier enhancing effects of S1P occurs via ligation to S1P<sub>1</sub>. This activates downstream signaling cascades that includes Rac activation, cortactin translocation, myosin light chain phosphorylation, and focal adhesion and adherens junction protein rearrangement<sup>101</sup>. Conversely, several *in vitro* and *in vivo* studies demonstrated that elevated concentrations of S1P (>5-10uM) may produce barrier disruption. Furthermore, intravenous infusion of S1P at 0.5 mg/kg body weight produced pulmonary edema in mice<sup>93</sup>. Alternatively, to S1P<sub>1</sub> ligation, ligation of S1P to S1P<sub>3</sub> leads to cell migration and vascular barrier dysfunction<sup>101</sup>. Likewise, genetic knockdown of Sphk1 in mice

caused increased susceptibility and elevated negative outcomes in an LPS-induced ALI model<sup>94</sup>. S1PL expression also appears to be elevated in LPS-induced lung injury models, which reduces the S1P levels in the lung and increases inflammation and injury<sup>95</sup>. Collectively, these observations demonstrate the role and association of S1P signaling in various lung disorders and insinuate that the S1P metabolic pathway have vast therapeutic potential against ALI. Our findings suggest that blocking S1PL in order to elevate the intracellular levels of S1P in the lung by the administration of THI treatment was effective in reducing the increased permeability, immune cell recruitment, and deteriorations in tissue mechanical properties of the lung and respiratory system that's associated with mechanical lung injury.

Currently, there are numerous studies that focus on targeting various components of S1P signaling for several diseases, including some lung disorders. As studies have shown that S1PL expression is elevated in several ALI models, such as LPS-induced, that causes reduced S1P levels and increased inflammation, targeting S1PL has shown promise in attenuating many of the negative outcomes associated with ALI<sup>95</sup>. Targeting S1PL *in vitro* using siRNA in human lung microvascular endothelial cells that received LPS lead to reduced barrier disruption, IL-6 secretion, and LPS-induced p38 MAPK phosphorylation<sup>95</sup>. Zhao et al., further showed that inhibiting S1PL expression *in vivo* resulted in increased intracellular S1P levels and decreased LPS-induced inflammation. Mice that were treated with THI for 2 days retained raised S1P levels in the lung tissues and BALF fluids following intratracheal LPS instillation. Furthermore, THI treatment resulted in reduced neutrophil infiltration in the alveolar space and reduced IL-6 secretion as protection against LPS-induced lung injury<sup>95</sup>, further suggesting the therapeutic potential of targeting S1PL, specifically via THI intervention. Studies using direct, exogenous S1P administration revealed substantial limitations and often resulted in undesired side effects, such as bradycardia and airway hyper-responsiveness<sup>93</sup>. Modulation of intracellular S1P production is robustly controlled by its synthesis and degradation, and these S1P-related catabolism and metabolism components can also be manipulated to alter intracellular S1P levels<sup>95</sup>. S1P-mediated biosynthesis is catalyzed by SphKs and its degradation is mediated by S1PL and S1P phosphatases<sup>148–150</sup>. While several studies have investigated the protective effects of SphK regulation, the involvement and manipulation of

SphKs in lung injury remains controversial and appears to depend on the insult<sup>95</sup>. Many of these altered SphK studies in the context of ALI models resulted in enhanced pulmonary leak and injury, while other showed improvement<sup>94</sup>. These observations suggest the need to examine alternative methods for modulating intracellular S1P levels, such as inhibiting S1PL. In our investigation, oral treatment with THI mitigated several of the mechanical ventilator-induced indications of lung injury and inflammation, further suggesting a protective role for S1P and S1PL inhibition in ALI/VILI. Oral administration of THI over 3 days effectively alters S1P tissue levels and blocks S1PL enzymatic activity<sup>151</sup>. Furthermore, evidence suggests that 3 days of THI treatment to block S1PL activity and alter S1P tissue levels appears to be optimal compared to longer treatment durations. It was demonstrated that this treatment regimen results in elevated lung tissue S1P levels by Day 2 without altering plasma S1P levels. However; prolonged treatment, such as implementing S1PL knockout models, resulted in very high plasma and tissue S1P levels, which resulted in accumulation of ceramides and other sphingolipids in the liver<sup>152</sup>. Our investigation in regulating S1P lung levels by administering THI to block S1PL activity attenuated increases in alveolar barrier permeability and immune cell recruitment, changes in pulmonary structure and function, and macrophage polarization deviations caused by mechanical injury; furthermore, THI treatment also improved the injury and inflammatory indications of aged mice that were worsened compared to young mice following high PCMV-induced lung injury.

The research presented in this chapter shows that high PCMV for 2 hours induces substantial indications of lung injury that is exaggerated in old mice. Aged mice that received mechanical injury resulted in greater indications of pulmonary leak, immune cell influx, impairment to macrophage polarization, and diminished pulmonary mechanics and function compared to young mice. This further validates an age-related influence or susceptibility on the induction and progression of ALI/VILI. The study also revealed that high PCMV and aging alone caused vast changes in various sphingoid bases present in the lung, including S1P and several ceramide and sphingomyelin bases. Additionally, it provides novel evidence and endorsement for the clinical use of THI and S1PL inhibition as protective mechanisms in mechanical injury, especially for elderly individuals with increased susceptibility to lung injury and

inflammation. While there have been a few studies that have examined the role of S1P signaling in acute lung injury models, only a small fraction is focused on mechanically induced ALI. Suryadevara et al., indicated that volume-controlled mechanical ventilation (30 mL/kg,4hr) in mice resulted in elevated S1PL expression, reduced S1P levels in lung tissue, and increased inflammation, injury, and apoptosis<sup>36</sup>. They investigated deeper into the S1P mechanism and they demonstrated that deletion of SphK1 mitigated VILI in mice. Moreover, the authors revealed that alveolar epithelial MLE-12 cells exposed to 18% cyclic stretch caused increased S1PL expression and changes to levels of sphingoid bases compared to physiological stretch conditions<sup>36</sup>. Administration of 4-deoxyypyridozine, a S1PL inhibitor, prior to pathophysiological stretch also attenuated barrier dysfunction, cell apoptosis, and cytokine secretion<sup>36</sup>. In accordance, these findings further suggest that S1PL inhibition may have therapeutic potential and protection against VILI. While there are only a few investigating the protective roles of S1P and S1PL inhibition in VILI, there are no current studies investigating the influences of aging and mechanical injury on S1P and S1PL regulation.

The following are limitations of the scope of this study: It is important to note that this study does not assess or indicate which cell types in the lung are responsible for the increased S1PL expression or varying S1P levels caused by aging and/or mechanical lung injury; however, it is believed that ATII and immune cells, such as macrophages, exhibit substantial S1PL expression, which have been demonstrated in several *in vitro* ALI models<sup>101</sup>. It is particularly difficult to determine the sources of S1PL expression and S1P production *in vivo* with current techniques and due to the numerous types of cells present in the lung. This issue is further complicated by the several types of immune cells that infiltrate into the alveolar space during lung injury. Further studies should be conducted *in vitro* to determine specific ATII and macrophage contributions of S1P and S1PL expression in response to mechanical injury and aging. While also not addressed in this study, the S1P receptor signaling axis in the context of aging and mechanical injury should also be investigated in the future following the evidence provided by this research of the implication of S1P and S1PL inhibition as a protective role in ALI/VILI. Recent studies suggest that the Sphingosine-1-phosphate and the S1P receptors are extensively involved in the

development and progression of several diseases<sup>100</sup>. Evidence suggests that S1P binding to certain S1P receptors on macrophages produced specific functional responses. These macrophage responses have been implicated in particular diseases and conditions<sup>101</sup>. Yang et al., showed that bone marrow derived-macrophages expressed S1P<sub>1-3</sub>, but not S1P<sub>4/5</sub>. Furthermore, the authors found that S1P<sub>2/3</sub> mediated S1P-induced M1 macrophage polarization. Interestingly, S1P<sub>1</sub> had no effect on macrophage polarization. Additionally, the use of inhibitors prevented the upregulation of M1 gene expression mediated by S1P/S1PR<sub>2/3</sub><sup>100</sup>. Conversely, Muller et al., found that all 5 S1P receptors were expressed in bone marrow-derived macrophages<sup>102</sup>. They provided evidence that suggests that M1 and M2 polarized macrophages resulted in significant downregulation of S1P<sub>1</sub> and influenced the expression of S1P<sub>4</sub>. This study also indicated that S1P induced chemotaxis in M1 macrophages and altered cytokine secretion in M2 macrophages. Interestingly, S1P increased expression of iNOS only under M2-polarizing conditions, but it had no effect on phagocytosis of either M1 or M2 macrophages<sup>102</sup>. Evidence suggests that S1P<sub>3</sub> is implicated in LPS-induced ALI models and might be the most important S1P receptor on macrophages regulating inflammation<sup>101</sup>. Early studies in human alveolar macrophages indicated that S1P induced (NOX)2-dependent production of ROS to promote IL-1 $\beta$  and TNF- $\alpha$  production by murine peritoneal macrophages. Previously, Intracellular S1P produced by Sphk1 was also suggested as a cofactor involved in macrophage activation. IL-1 signaling, an activator in NF $\kappa$ B inflammation, also requires Sphk1-dependent S1P as an intracellular cofactor<sup>103</sup>. Sphk1 is also activated downstream of other inflammatory stimuli, such as LPS<sup>104-106</sup>. Stimulation of human THP-1 macrophages with LPS required Sphk1 activity to generate IL-6, IL-1 $\beta$ , TNF- $\alpha$ , and/or NO<sup>104</sup>. In RAW264.7 macrophages, S1P<sub>1</sub> and S1P<sub>2</sub> were involved in IL-6 production in a LPS-induced ALI model<sup>107</sup>. Furthermore, S1P<sub>1</sub> binding increased ARG1 activity and suppressed NO production, suggesting a shift from M1 to M2 polarization states in murine macrophages<sup>108</sup>. S1P<sub>5</sub> on macrophages is associated with impaired phagocytosis; however, it remains unclear if this S1P receptor impacts macrophage polarization<sup>101</sup>. Collectively, these observations suggest that S1P modulates macrophage activation and responses according to the local environment, the intracellular and extracellular concentrations of S1P, and the S1P receptors activated on specific<sup>101</sup>.

While our study revealed substantial changes to macrophage polarization states caused by aging and/or mechanical injury and that THI treatment reduces those deviations, it fails to address potential modulation by specific S1P receptor binding. Further *in vitro* studies should be conducted to determine how aging and mechanical injury impact S1P receptor binding and downstream effector functions that may correlate with the polarization changes seen in our study.

This investigation also has a few experimental limitations. Primarily, the panel of surface markers and flow cytometric analysis implemented investigated a limited number of associated macrophage polarization markers. While these are highly relevant and frequently published<sup>24,31,32,39,153</sup>, other related classical and alternative phenotypic markers for macrophages should be considered and assessed to further analyze more defined polarization states. Another limitation is the duration of high PCMV. While 2 hours of high PCMV was sufficient to induce ALI/VILI in both young and old mice, other durations should be evaluated to determine other temporal effects of PCMV on structural and cellular changes in the lung. Longer durations were initially tested; however, there was a high mortality for both young and old mice when ventilated up to 4 hours. Furthermore, this study mainly examines changes to macrophage populations; although these cells interact with many other cell lineages *in vivo*. Other lung cell populations, such as neutrophils and monocytes, should be further investigated to better understand the role of macrophage polarization in acute lung injury. Lastly, this study investigated murine macrophage polarization in the context of acute lung injury. Although murine macrophage cells were examined to simulate cellular responses in humans, many cellular responses and characterizations are conserved across species<sup>154</sup>. Animal models provide an exclusive approach to evaluate related mechanisms and potential new therapies by acting as proof of concepts in experimental studies. Further studies are necessary to determine differences that exist between murine and human macrophage populations, especially in the context of aging and ALI/VILI.

Overall, this research indicates that aging and/or mechanical injury result in vast changes in lung sphingoid bases that are implicated in the proposed protective S1P/S1PL signaling associated ALI. Aging and mechanical injury caused increased S1PL expression, while only young mice resulted in substantial

S1P levels following mechanical injury. Our findings further suggest that THI treatment effectively inhibits S1PL expression and increases the lung levels of S1P, which resulted in improved outcomes following mechanical injury and deviations caused by aging alone. Further investigation is critical to better understand the mechanistic effects and the roles of ATIIs and lung macrophages surrounding S1P signaling and S1PL inhibition in the context of aging and mechanical injury. The loss of S1P levels or elevated S1PL expression in the lungs of aged individuals appears to represent age-specific mechanisms leading to the elderly's increased susceptibility to lung injury. The molecular regulation of these signaling components represent promising, potential therapeutic targets for age-related ALI.

## **CHAPTER 7: CONCLUSIONS AND FUTURE DIRECTIONS**

Despite recent advances in our knowledge of the pathophysiology of ALI and VILI, “protective ventilator strategies” have had minimal impact, and no effective treatments nor therapies are available for this lung condition. The mortality rates remain high, especially for the elderly population<sup>19,95</sup>. The aim of this dissertation was to understand better how aging primes the lung to be more susceptible to ALI/VILI and identify cellular and structural response deviations that represent molecular, therapeutic targets for intervention. The outcomes of this investigation provide further evidence that aging exacerbates outcomes of mechanical injury, which resulted in a greater deterioration in lung function, pulmonary structural deviations, elevated lung inflammation at baseline, dysregulating inflammatory signaling following mechanical injury, and dysregulation in macrophage polarization. We also characterized indications of ER stress and S1P/S1PL in our experimental VILI models, which revealed significant age-induced and injury-induced implications in the progression of ALI/VILI. Furthermore, we evaluated the protective effects of ER stress reduction, via 4PBA, and S1PL inhibition, through THI, to determine the therapeutic potential of these age-related molecular targets.

As elderly patients comprise a substantial proportion of patients requiring mechanical ventilation in the clinic, we need to identify and elucidate the age-related factors that increase these patients' susceptibility to lung injury. These factors represent possible targets for more effective therapeutic intervention in the development and progression of lung injury, especially with the elderly population. Few studies are performed on aged subjects, which is incongruent with the fact that elderly patients have a greater need for mechanical ventilation. Our findings from these investigations identified and further validated considerable age-related associations and cellular responses that may offer vast therapeutic potential in ALI/VILI. Furthermore, we evaluated two related treatment opportunities, 4PBA and THI, that effectively reduced specific age-related factors, ER stress and S1P/S1PL activity, respectively, and several other negative outcomes associated with mechanical injury.

We first indicated the effects of aging on ATII and macrophage responses without mechanical injury, which is detailed fully in the third chapter of this dissertation. We demonstrated that aging alone increased the gene expression and secretion of several inflammatory mediators, suggesting a more intense inflammatory response at baseline, without mechanical injury. We then showed the influence of aging and mechanical injury on various pulmonary responses *in vivo*, which is described thoroughly in the fourth chapter of this thesis. Our findings revealed that the pulmonary structure, tissue mechanics and pulmonary function, and lung macrophages' polarization in mice is prominently altered with aging. Furthermore, aged lung macrophages and those that underwent high PCMV overexpressed both CD80 and CD206 associated polarization markers and the percentage of alveolar subset macrophage populations changed significantly due to age and/or high PCMV.

Following the assessments of aging and mechanical injury on ATII and macrophage signaling, as well as their effects on lung structure and function, we validated that ER stress is implicated in both mechanical injury and aging. We evaluated indications of ER stress in our age-related experimental VILI models, and our findings suggest that age increases susceptibility to stretch-induced ER stress and downstream inflammation in a primary ATII epithelial cell model. Administration of 4-PBA attenuated both the increased ER stress and proinflammatory responses from stretch and/or age and significantly reduced monocyte migration to ATII conditioned media. As the majority of patients that are diagnosed with VILI are the elderly, better understanding the age-dependent factors associated with the *mechanotransduction* between the alveolar epithelium and innate immune system is detrimental to developing treatments for these types of lung diseases.

Recent studies also indicated that S1P acts as a protective mechanism in LPS-induced ALI by producing endothelial cell barrier enhancement<sup>144</sup>, reducing lung edema and vascular leak<sup>95</sup>, and limiting lung injury indications and inflammation, while enhanced S1P lyase expression is believed to further reduce the S1P signaling and limit the protective potential of S1P<sup>35,80,95,144</sup>. Following the assessment of S1P/S1PL in our age-related experimental VILI models, we found that aging and/or mechanical injury result in vast changes in lung sphingoid bases that are implicated in the proposed protective S1P/S1PL

signaling associated ALI. Aging and mechanical injury caused increased S1PL expression, while only young mice resulted in substantial S1P levels following mechanical injury. Our findings further suggest that THI treatment effectively inhibits S1PL expression, which resulted in improved outcomes following mechanical injury and deviations caused by aging alone. Further investigation is critical to better understand the mechanistic effects and the roles of ATILs and lung macrophages surrounding S1P signaling and S1PL inhibition in the context of aging and mechanical injury. The loss of S1P levels or elevated S1PL expression in the lungs of aged individuals appears to represent age-specific mechanisms leading to the elderly's increased susceptibility to lung injury. The molecular regulation of these signaling components represent promising, potential therapeutic targets for age-related ALI. Our findings further indicate that S1P may act as a protective mechanism in ALI. This signaling appears to be reduced with aging and may represent potential age-related therapeutic intervention targets for patients with ALI. Interestingly, the deviations in the alveolar macrophage subpopulations and indications of injury reflect the similar changes in S1P signaling and S1P lyase expression due to aging and high PCMV. As macrophages are key cells in both injury/repair and inflammatory responses in the lung, the impairment to their polarization states caused by aging or injury may be a strong factor or determinant for the elderly's increased susceptibility to ALI (VILI) and worsened repair mechanisms. Our findings suggest that the age-related changes in S1P signaling and S1PL activity are associated with the macrophage polarization impairment and mechanical property changes that occur with aging. Furthermore, this signaling appears to be diminished with aging and may represent potential age-related therapeutic intervention targets for patients with ALI.

Many lung pathologies and age-associated diseases reflect high levels of inflammation in the tissue that results in high morbidity and mortality rates, which drives the desire to develop a therapy aimed to regulate the inflammatory processes that lead to these conditions. Improved understanding of how aging and physical forces from mechanical ventilators impact these epithelial *mechanotransduction* signaling mechanisms and macrophage polarization states may greatly assist in the generation of novel therapies that manipulate macrophage function or epithelial signaling to limit proinflammatory responses

or improve tissue remodeling during the repair stages of epithelial repair in the lung. Although our investigations focused on lung injury and inflammation provided insight that is lung-tissue specific, this knowledge can be applied across systems to examine comparisons of tissue-specific epithelial injury responses and macrophage polarization aspects that regulate inflammation.

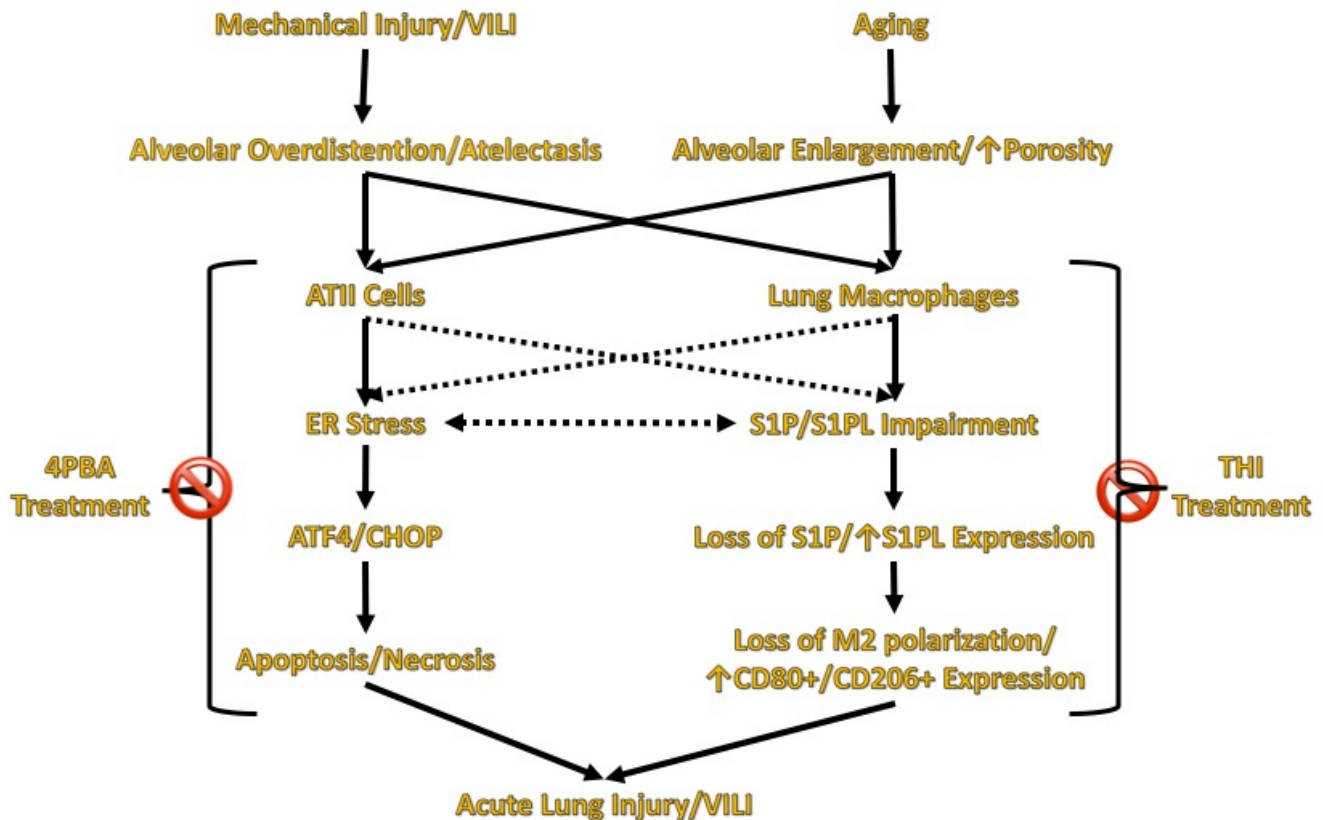
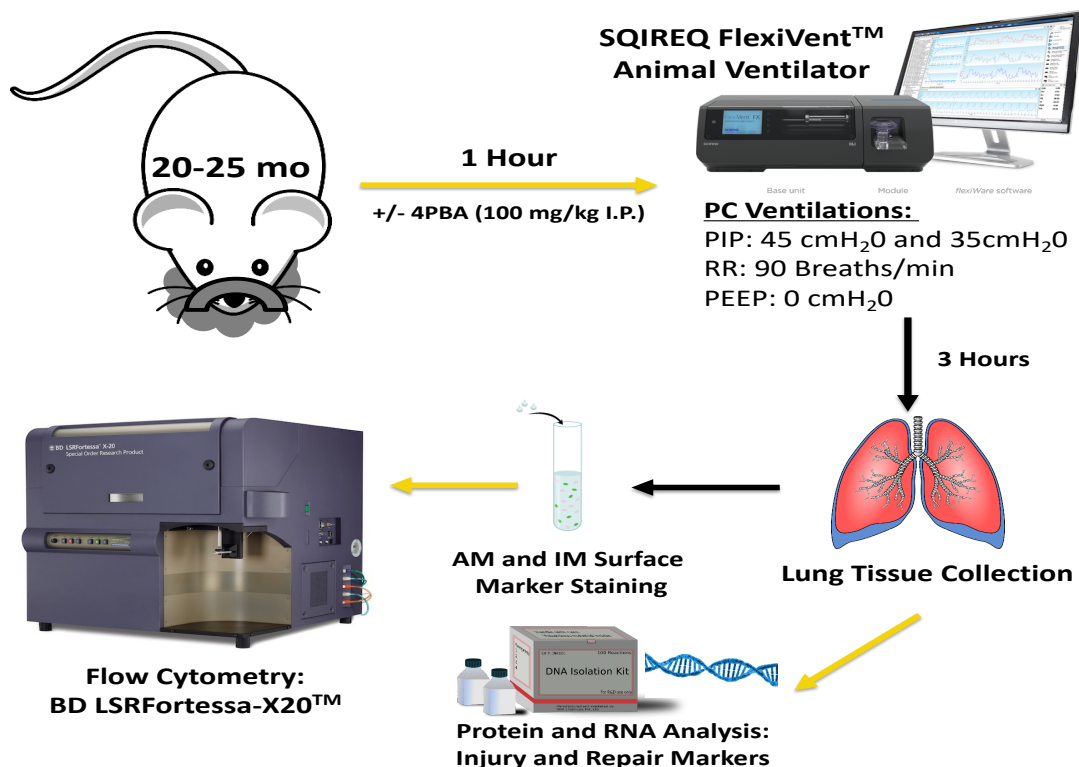


Figure 50: Summary Diagram of the Dissertation Findings and Inferences. The figure illustrates the effects of Mechanical Injury, Aging, 4PBA therapy, and THI treatment on the development and progression of ALI/VILI.

As depicted in Figure 52, our findings suggest that the implication of ER stress and the therapeutic intervention using 4PBA in the context of aging and ALI/VILI should be further investigated. Our research further indicated that mechanical injury induces ER stress, which is intensified in older individuals. Injurious cyclic cell-stretch using alveolar epithelial type II cells resulted in ER stress, inflammation, and other injury outcomes that were elevated in aged ATIIs. We also demonstrated that ER stress was associated, and possibly a determinant, of the biotrauma produced by mechanical injury, which included monocyte/macrophage recruitment. Furthermore, we demonstrated that 4PBA, an ER stress inhibitor, reduces indications of ER stress, inflammation, monocyte recruitment, and injury. These findings suggest

that 4PBA may be a viable, more effective treatment for the development and progression of ALI, especially for the elderly population that has greater susceptibility and responsiveness to lung injury. While this research evaluated ER stress and the therapeutic potential of 4PBA in an aging *in vitro* cell-stretch model, we were only able to evaluate this cell response in young mice stimulated with mechanical ventilation. The findings from both our *in vitro* and *in vivo* studies indicate that ER stress and 4PBA administration should be further assessed in aged mice receiving mechanical injury, as shown in Figure 53. As indications of ER stress were intensified in old ATE cells, both at baseline and following mechanical injury, compared to the young ATEs, this implication needs to be evaluated in aged mice. As the intensified injury and inflammatory responses produced by mechanical injury were associated with ER stress and attenuated with 4PBA treatment in the cell-stretch of old ATEs, we believe that ER stress in the aged mouse lungs also influences the inflammatory and injury responses produced from injurious mechanical ventilation. Our data suggests that 4PBA therapy has the potential to mitigate the age-dependent ER stress and inflammation that contributes to the elderly's susceptibility to ALI/VILI.



**Figure 51: The Schematic Overview of Methods to Further Examine ER Stress and 4PBA in the Aging VILI model. This aim will evaluate the factors of aging and mechanical injury on ER stress *in vivo*.**

The protective role of S1PL inhibition in the development and progression of ALI/VILI also warrants further investigation. While our research revealed that S1P/S1PL activity is associated with the injury and inflammation triggered by mechanical injury, aging influences S1P/S1PL levels and expression, and S1PL inhibition alters the phenotypes of lung macrophages, the study fails to determine the cell sources of S1P/S1PL activity in the lung. Furthermore, the effects of S1P/S1PL activity on macrophage polarization needs to be further elucidated. As mentioned before, recent studies suggest that S1P, along with the S1P signaling axis, can greatly influence macrophage differentiation and function under physiological and disease conditions<sup>101</sup>. Evidence suggests that S1P binding to certain S1P receptors on macrophages produced specific functional responses. These macrophage responses have been implicated in particular diseases and conditions<sup>101</sup>. The effects of aging and various S1P concentrations on macrophage phenotype and function should be further evaluated *in vitro* to understand better the findings from our research, as shown in Figure 54. This will help determine the underlying mechanisms that govern S1P-induced macrophage polarization and inflammatory responses with the implications of aging and mechanical injury. We believe these S1P-related mechanisms represent effective therapeutic targets for the prevention or attenuation of ALI, especially the elderly population.

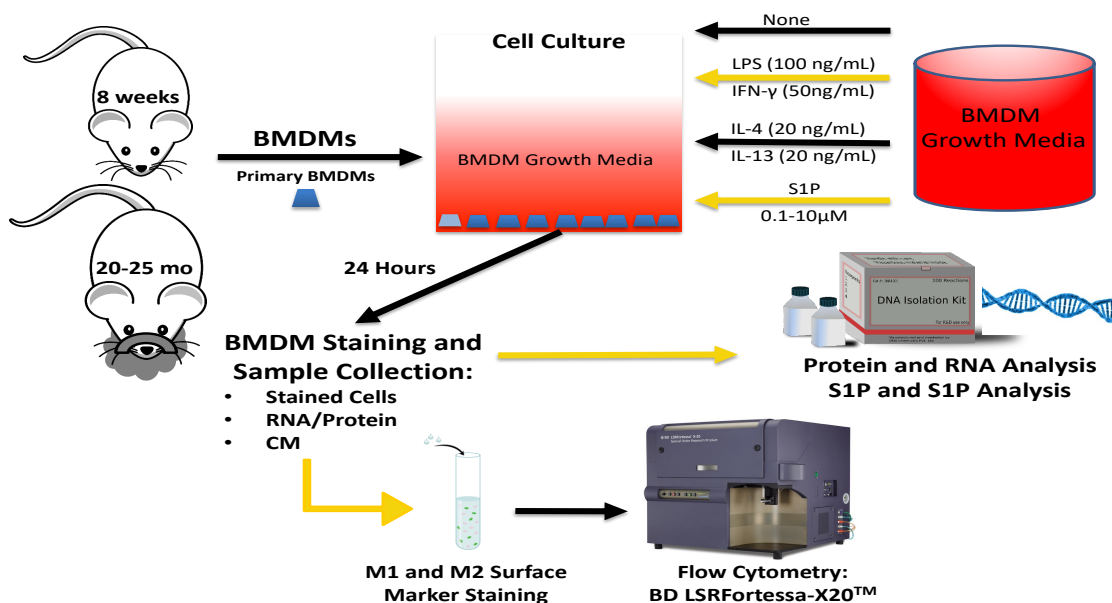


**Figure 52: The Schematic Overview of Methods to Further Examine S1P and Macrophage Polarization in VILI.**  
This aim will evaluate the factors of aging and various concentrations of S1P on macrophage phenotypes and function.

The effects of aging, mechanical injury, ER stress, and S1P/S1PL activity should also be evaluated in a “two-hit” VILI model with a recovery period established following mechanical injury, as shown in Figure 55. The “two-hit” VILI insult system usually consists of a secondary trigger of ALI, such as a bacterial infection, and better represents patients requiring mechanical ventilation with pre-existing lung conditions, which is far more common in VILI. The administration of LPS models a preexisting bacterial infection, which is common and more clinically relevant in patients with ARDS, a more severe form of ALI, that often necessitates mechanical ventilator. The fundamental mechanisms that drive the development and progression of ALI/VILI remain inadequately comprehended<sup>155</sup>. This is partially attributed to the cell culture systems utilized to study ALI/VILI, which are only partially able to model the complex pulmonary microenvironment and cell interactions that exist *in vivo*<sup>156</sup>. Furthermore, most experimental lung injury animal models only investigate a particular cause of ALI and fail to fully model the complex pathophysiology of clinical ALI, which is more often caused by several factors<sup>156</sup>. Therefore, “two-hit” VILI models are more translational and effective at capturing the complexity of ALI conditions, which could reveal greater understanding surrounding the mechanisms and compounded interactions that trigger ALI/VILI. A recovery period following mechanical injury should also be included to assess the effects of aging on repair and resolution mechanisms associated with ALI, such as their possible impairment or loss. Additionally, as mentioned before, clinical ALI patients often have sufficient injury or infections prior to mechanical ventilation; therefore, recovery should be investigated to better develop a therapy or treatment that can be administered after injury, which is more translational and likely to be effective in the clinical setting. These implications should be investigated following our evaluation of mechanical injury as a single factor in the induction and progression of ALI/VILI.

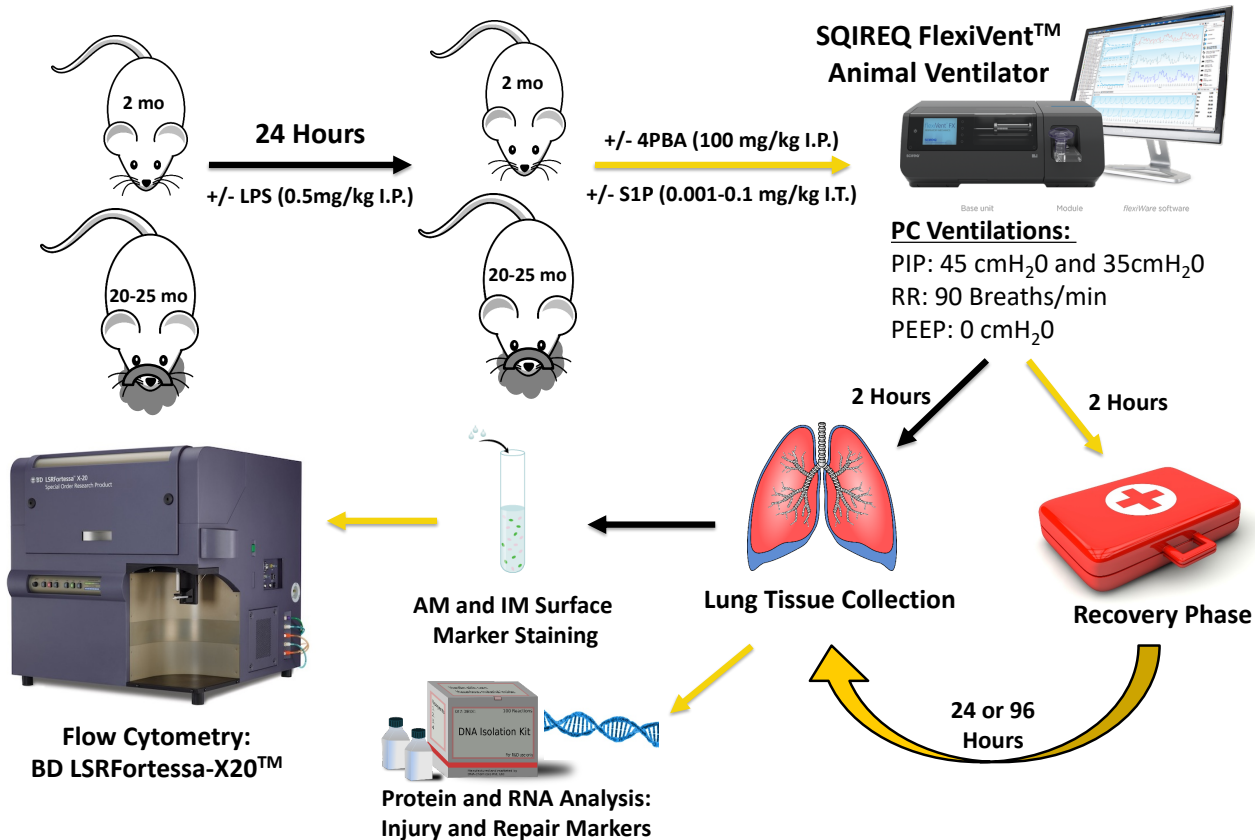


**Figure 53: The Schematic Overview of Methods for Future Directions Experiments.** This aim will evaluate the factors of aging and mechanical injury in a “two-hit” VILI model with Recovery.

Our findings suggest that age-specific cell signaling mechanisms by AII cells or macrophages represent viable therapeutic targets for patients requiring mechanical ventilation by preventing or regulating the exaggerated inflammatory response that often leads to sepsis and mortality. More recently, novel therapies attempt to target macrophage polarization, which could be an effective, innovative method to regulate the downstream inflammation and prevent subsequent alveolar barrier destruction. As the majority of patients that are diagnosed with VILI are the elderly, better understanding the age-dependent factors associated with the *mechanotransduction* between the alveolar epithelium and innate immune system is detrimental to developing treatments for these types of lung diseases.

## APPENDIX A

### MLI Analysis MATLAB Code:

```
%% Cells = imread('cells.tif');
[FileName,PathName]= uigetfile('*.tif','Select Image'); % Lauches user interface to
get file; saves file name and file path as a string in an array
  cells =imread(strcat(PathName,FileName)); % reads in previously loaded image file
and saves it as variable 'Cells'
Pixel_Length = (1*10^(-6)); % (1micrometer on histo Whiz images) Side length of a
single square pixel (in meters) based on pixel normalinzation
Pixel_Area = Pixel_Length^2; % Calculates area of a single pixel (meters^2)
level = graythresh(cells); % THIS IS IMPORTANT AND MAY REQUIRE ADJUSTMENT BASED ON
THE IMAGE
%GRAYTHRESH() FINDS THE MEAN THRESHOLD OF THE IMAGE
%SOMETIMES THIS NUMBER MAY NEED ADJUSTED BASED ON IMAGE QUALITY -- Ranges
%from 0-1. Best way to adjust is to run the code finding graythresh and
%raise or lower value from there

bw = im2bw(cells, level); % Converts image into binary form
wb = imcomplement(bw); % finds complement of image -- May or may not be
%necessary depending on image lighting. If software doesn't work properly,
%use bw instead of wb for the remainder of the code

se2 = strel('disk',2); %Creates structuring element to slightly sharpen
the image
closewb = imclose(wb, se2); %Closes off structures using above SE

se = strel('line',10,3); % Same
closewb2 = imclose(closewb,se); % Same

wb2 = bwareaopen(closewb2,150); %Fills tiny hold (under 150px threshold) that
aren't detected by original conversion

figure(1) % Shows converted image to demonstrate code is working
subplot(1,2,1)
imshow(wb)
subplot(1,2,2)
imshow(cells)

% subplot(1,2,1), subimage(cells)
% xlabel('Initial Image')
%
% subplot(1,2,2), subimage(wb2)
% xlabel('Binary Conversion')

%% Exclusion

% When running this section of code, be sure to carefully follow the steps:
% 1.) Run section
% 2.) Press '1' followed by enter if you would like to exclude area OR
```

```

% Press '0' followed by enter if you want to exit the exclusion process
% Only exclude spaces that are not airspaces (mainly vasculature)
% 3.) If excluding, click once in every space you would like to exclude
% Following clicking every desired space, double click within an
% excluded area to end the process. Then exit the image
% 4.) If you are done excluding press '0' followed by enter, if not
% press '1' followed by enter to exlude more area and repeat the above
% steps
% 5.) At this point, the image w/ excluded regions will appear for your
% verification. If it looks good, move on to the next section,
% otherwise, restart this section of code and try again

```

```

play = wb2;
question = 1;

```

```

while question == 1
    question = input('Press 1 to exclude area, press 0 to continue\n' );
    if question == 1
        play = imfill(play);
    end
end

```

```

xxx = play;
imshow(xxx)

```

```

%% MLI

```

```

%This section calculates MLI of the image (not the metric we use but still
%valuable for comparison)

```

```

for i = 1:5

    row_num = 130*i;
    lines(i,:) = xxx(row_num,:);

```

```

end

```

```

for i = 1:5

```

```

    intersect = find(lines(i,)==1)

    a = diff(intersect);
    b = find([a inf]>1);
    length_consec = diff([0 b])
    number_int(i) = length(length_consec)
    total_exclusion(i) = sum(length_consec)
    Lengths(i) = (940-sum(lines(i,:)))

```

```

end

```

```

L_m = (Lengths / number_int) % This is MLI

```

```

%% Individual Area

```

```

%This section calculates a variety of the region properties required for

```

```

%determination of the enlargement index.

ww = imcomplement(xxx);

stats = regionprops(ww , 'area');
Area_Pix = struct2array(stats);
Area_Actual = (Area_Pix * Pixel_Area);

stats2 = regionprops(ww, 'MajorAxisLength');
Major_Axis_Length_Pix = struct2array(stats2);
Major_Axis_Length_Actual = (Major_Axis_Length_Pix*Pixel_Length);

stats3 = regionprops(ww, 'MinorAxisLength');
Minor_Axis_Length_Pix = struct2array(stats3);
Minor_Axis_Length_Actual = (Minor_Axis_Length_Pix*Pixel_Length);

stats4 = regionprops(ww , 'perimeter');
Perimeter_Pixel = struct2array(stats4);
Perimeter_Actual = (Perimeter_Pixel*Pixel_Length);

Diameter_Average = 2*(sqrt(Area_Actual/pi));

Statistics = [Area_Actual; Diameter_Average; Major_Axis_Length_Actual;
Minor_Axis_Length_Actual];

Average = (Major_Axis_Length_Actual + Minor_Axis_Length_Actual)/2;

Comp = [Average ; Diameter_Average];

%% Using Area to approx diameter
%There are two methods to calculate enlargement index
%This section assumes every airspace is a circle and back-calculates
%diameter from the area (This is innaccurate as you'll see most of the
%airspaces are not circular

% D_0 = mean(Diameter_Average);
% Variance_Diameter = var(Diameter_Average);
% Skewness_Diameter = skewness(Diameter_Average);
%
% D_1 = ((D_0)*(1+(Variance_Diameter/(D_0)^2)));
%
% D_2 =
D_0*(1+((((Variance_Diameter)/(((D_0)^2)+Variance_Diameter))*(2+((sqrt(Variance_Dia
meter))*(Skewness_Diameter))/(D_0)))));
%

%% Using max and min axis
%This uses the major and minor axis to calculate the enlargement index

D_0 = mean(Average);
Variance_Diameter = var(Average);
Skewness_Diameter = skewness(Average);

D_1 = ((D_0)*(1+(Variance_Diameter/(D_0)^2)));

```

```

D_2 =
D_0*(1+(((Variance_Diameter)/((D_0)^2)+Variance_Diameter))*(2+((sqrt(Variance_Dia
meter))*(Skewness_Diameter))/(D_0)))));

D = [D_0 , D_1 , D_2]    % These are the 3 metrics calculated from the regionsprops
    % D_0 is simply the average of every major/minor average axis length
    % average(average(major+minor))
    % D_1 weights the index based on its variance in the average diameter
    % D_2 weights the index based on its variance and skewness in the average
diameter

%%
%This final section visually summarizes the analyzed images
final = (xxx - wb2);
figure

subplot(2,2,1), subimage(cells)
xlabel('Initial Image (Pixels)')

subplot(2,2,2), subimage(bw)
xlabel('Binary Conversion (Pixels)')

subplot(2,2,3), subimage(wb2)
xlabel('Pre-Exclusion (Pixels)')

subplot(2,2,4), subimage(xxx)
xlabel('Final Image(Pixels)')

% subplot(2,3,6)
% xlabel('Closed Binary(Pixels)')

title('100 Pixels is Approximately Equal to 100 micrometers')

%%
%USE THE FOLLOWING MICROSCOPE SETTINGS
%BE SURE TO UTILIZE THE BACKGROUND SUBTRACT FEATURE OF THE MICROSCOPY
%SOFTWARE (FOCUS SCOPE ON HISTOSECTION, REMOVE SLIDE, TAKE PICTURE OF
%BACKGROUND) REPLACE SLIDE AND CAPTURE IMAGE THEN SUBTRACT BACKGROUN

%USE THE SETTINGS BELOW
%Setting 3 10xhe with the 10 x lens
%QI CAM 12 bit 10x scale bar
%Non-destructive - set to 500 um
%Capture 5 randomly located images of every lung section average D_2 values
%for each sample

```

## REFERENCES

1. Carrasco Loza, R., Villamizar Rodríguez, G. & Medel Fernández, N. Ventilator-Induced Lung Injury (VILI) in Acute Respiratory Distress Syndrome (ARDS): Volutrauma and Molecular Effects. *Open Respir. Med. J.* **9**, 112–119 (2015).
2. Bernard, G. R. *et al.* The American-European Consensus Conference on ARDS. Definitions, mechanisms, relevant outcomes, and clinical trial coordination. *Am. J. Respir. Crit. Care Med.* **149**, 818–824 (1994).
3. Biehl, M., Kashiouris, M. G. & Gajic, O. Ventilator-induced lung injury: minimizing its impact in patients with or at risk for ARDS. *Respir. Care* **58**, 927–937 (2013).
4. The ARDS Definition Task Force\*. Acute respiratory distress syndrome: The Berlin definition. *JAMA* **307**, 2526–2533 (2012).
5. Chen, L., Xia, H.-F., Shang, Y. & Yao, S.-L. Molecular Mechanisms of Ventilator-Induced Lung Injury. *Chin. Med. J. (Engl.)* **131**, 1225–1231 (2018).
6. Carrasco Loza, R., Villamizar Rodríguez, G. & Medel Fernández, N. Ventilator-Induced Lung Injury (VILI) in Acute Respiratory Distress Syndrome (ARDS): Volutrauma and Molecular Effects. *Open Respir. Med. J.* **9**, 112–119 (2015).
7. Baudouin, S. Ventilator induced lung injury and infection in the critically ill. *Thorax* **56**, ii50–ii57 (2001).
8. de Prost, N., Ricard, J.-D., Saumon, G. & Dreyfuss, D. Ventilator-induced lung injury: historical perspectives and clinical implications. *Ann. Intensive Care* **1**, 1–15 (2011).
9. Halbertsma, F. J. J., Vaneker, M., Scheffer, G. J. & van der Hoeven, J. G. Cytokines and biotrauma in ventilator-induced lung injury: a critical review of the literature. *Neth. J. Med.* **63**, 382–392 (2005).
10. Herbert, J. A. *et al.* Conservative fluid management prevents age-associated ventilator induced mortality. *Exp. Gerontol.* **81**, 101–109 (2016).
11. Fan, E., Villar, J. & Slutsky, A. S. Novel approaches to minimize ventilator-induced lung injury. *BMC Med.* **11**, 85 (2013).

12. Hoegl, S. *et al.* Inhaled IL-10 reduces biotrauma and mortality in a model of ventilator-induced lung injury. *Respir. Med.* **103**, 463–470 (2009).
13. Guillot, L. *et al.* Alveolar epithelial cells: master regulators of lung homeostasis. *Int. J. Biochem. Cell Biol.* **45**, 2568–2573 (2013).
14. Vlahakis, N. E., Schroeder, M. A., Limper, A. H. & Hubmayr, R. D. Stretch induces cytokine release by alveolar epithelial cells in vitro. *Am. J. Physiol. - Lung Cell. Mol. Physiol.* **277**, L167–L173 (1999).
15. Rubins, J. B. Alveolar macrophages: wielding the double-edged sword of inflammation. *Am. J. Respir. Crit. Care Med.* **167**, 103–104 (2003).
16. Gardner, A., Borthwick, L. A. & Fisher, A. J. Lung epithelial wound healing in health and disease. *Expert Rev. Respir. Med.* **4**, 647–660 (2010).
17. Lieberman, D. *et al.* Elderly patients undergoing mechanical ventilation in and out of intensive care units: a comparative, prospective study of 579 ventilations. *Crit. Care* **14**, R48 (2010).
18. MEINDERS, A. J., VAN DER HOEVEN, J. G. & MEINDERS, A. E. The Outcome of Prolonged Mechanical Ventilation in Elderly Patients: Are the Efforts Worthwhile? *Age Ageing* **25**, 353–356 (1996).
19. Nin, N. *et al.* Aging increases the susceptibility to injurious mechanical ventilation. *Intensive Care Med.* **34**, 923–931 (2008).
20. Setzer, F. *et al.* Susceptibility to ventilator induced lung injury is increased in senescent rats. *Crit. Care* **17**, R99 (2013).
21. Bonomo, L., Larici, A. R., Maggi, F., Schiavon, F. & Berletti, R. Aging and the respiratory system. *Radiol. Clin. North Am.* **46**, 685–702, v–vi (2008).
22. Britto, R. R., Zampa, C. C., de Oliveira, T. A., Prado, L. F. & Parreira, V. F. Effects of the Aging Process on Respiratory Function. *Gerontology* **55**, 505–510 (2009).
23. Brandenberger, C. & Mühlfeld, C. Mechanisms of lung aging. *Cell Tissue Res.* **367**, 469–480 (2017).

24. Gibon, E. *et al.* Aging Affects Bone Marrow Macrophage Polarization: Relevance to Bone Healing. *Regen. Eng. Transl. Med.* **2**, 98–104 (2016).
25. Franceschi, C. & Campisi, J. Chronic Inflammation (Inflammaging) and Its Potential Contribution to Age-Associated Diseases. *J. Gerontol. A. Biol. Sci. Med. Sci.* **69**, S4–S9 (2014).
26. Hussell, T. & Bell, T. J. Alveolar macrophages: plasticity in a tissue-specific context. *Nat. Rev. Immunol.* **14**, 81–93 (2014).
27. Childs, L. M., Paskow, M., Jr, S. M. M., Hesse, M. & Strogatz, S. From Inflammation to Wound Healing: Using a Simple Model to Understand the Functional Versatility of Murine Macrophages. *Bull. Math. Biol.* **73**, 2575–2604 (2011).
28. Spieth, P. M. *et al.* Mechanotransduction in the lungs. *Minerva Anesthesiol.* **80**, 933–941 (2014).
29. Frank, J. A., Wray, C. M., McAuley, D. F., Schwendener, R. & Matthay, M. A. Alveolar macrophages contribute to alveolar barrier dysfunction in ventilator-induced lung injury. *Am. J. Physiol.-Lung Cell. Mol. Physiol.* **291**, L1191–L1198 (2006).
30. Wong, C. K. *et al.* Aging Impairs Alveolar Macrophage Phagocytosis and Increases Influenza-Induced Mortality in Mice. *J. Immunol. Baltim. Md 1950* (2017) doi:10.4049/jimmunol.1700397.
31. Misharin, A. V., Morales-Nebreda, L., Mutlu, G. M., Budinger, G. R. S. & Perlman, H. Flow Cytometric Analysis of Macrophages and Dendritic Cell Subsets in the Mouse Lung. *Am. J. Respir. Cell Mol. Biol.* **49**, 503–510 (2013).
32. D. Smith, T., J. Tse, M., L. Read, E. & F. Liu, W. Regulation of macrophage polarization and plasticity by complex activation signals. *Integr. Biol.* **8**, 946–955 (2016).
33. Mahbub, S., Deburghraeve, C. R. & Kovacs, E. J. Advanced Age Impairs Macrophage Polarization. *J. Interferon Cytokine Res.* **32**, 18–26 (2012).
34. Brown, M. K. & Naidoo, N. The endoplasmic reticulum stress response in aging and age-related diseases. *Front. Physiol.* **3**, 263 (2012).

35. Natarajan, V. *et al.* Sphingosine-1-Phosphate, FTY720, and Sphingosine-1-Phosphate Receptors in the Pathobiology of Acute Lung Injury. *Am. J. Respir. Cell Mol. Biol.* **49**, 6–17 (2013).
36. Suryadevara, V. *et al.* Sphingolipids in Ventilator Induced Lung Injury: Role of Sphingosine-1-Phosphate Lyase. *Int. J. Mol. Sci.* **19**, 114 (2018).
37. Ebenezer, D. L., Panfeng Fu & Natarajan, V. Targeting Sphingosine-1-Phosphate Signaling in Lung Diseases. *Pharmacol. Ther.* **168**, 143–157 (2016).
38. Franceschi, C., Garagnani, P., Vitale, G., Capri, M. & Salvioli, S. Inflammaging and ‘Garb-aging’. *Trends Endocrinol. Metab.* **28**, 199–212 (2017).
39. Wang, N., Liang, H. & Zen, K. Molecular Mechanisms That Influence the Macrophage M1–M2 Polarization Balance. *Front. Immunol.* **5**, (2014).
40. Mahbub, S., Deburghraeve, C. R. & Kovacs, E. J. Advanced age impairs macrophage polarization. *J. Interferon Cytokine Res. Off. J. Int. Soc. Interferon Cytokine Res.* **32**, 18–26 (2012).
41. Barrett, J. P., Costello, D. A., O’Sullivan, J., Cowley, T. R. & Lynch, M. A. Bone marrow-derived macrophages from aged rats are more responsive to inflammatory stimuli. *J. Neuroinflammation* **12**, 67 (2015).
42. Gibon, E. *et al.* Aging Affects Bone Marrow Macrophage Polarization: Relevance to Bone Healing. *Regen. Eng. Transl. Med.* **2**, 98–104 (2016).
43. Copley, S. J. *et al.* Effect of aging on lung structure in vivo: assessment with densitometric and fractal analysis of high-resolution computed tomography data. *J. Thorac. Imaging* **27**, 366–371 (2012).
44. Skloot, G. S. The Effects of Aging on Lung Structure and Function. *Clin. Geriatr. Med.* **33**, 447–457 (2017).
45. Curley, G. F., Laffey, J. G., Zhang, H. & Slutsky, A. S. Biotrauma and Ventilator-Induced Lung Injury. *Chest* **150**, 1109–1117 (2016).
46. Knudsen, L. & Ochs, M. The micromechanics of lung alveoli: structure and function of surfactant and tissue components. *Histochem. Cell Biol.* **150**, 661–676 (2018).

47. Cong, X., Hubmayr, R. D., Li, C. & Zhao, X. Plasma membrane wounding and repair in pulmonary diseases. *Am. J. Physiol. - Lung Cell. Mol. Physiol.* **312**, L371–L391 (2017).
48. Beitler, J. R. *et al.* Volume delivered during recruitment maneuver predicts lung stress in acute respiratory distress syndrome. *Crit. Care Med.* **44**, 91–99 (2016).
49. Gattinoni, L. *et al.* Physical and biological triggers of ventilator-induced lung injury and its prevention. *Eur. Respir. J.* **22**, 15s–25s (2003).
50. Henderson, W. R., Chen, L., Amato, M. B. P. & Brochard, L. J. Fifty Years of Research in ARDS. Respiratory Mechanics in Acute Respiratory Distress Syndrome. *Am. J. Respir. Crit. Care Med.* **196**, 822–833 (2017).
51. González-López, A. & Albaiceta, G. M. Repair after acute lung injury: molecular mechanisms and therapeutic opportunities. *Crit. Care* **16**, 209 (2012).
52. Marciniak, S. J. & Ron, D. Endoplasmic Reticulum Stress Signaling in Disease. *Physiol. Rev.* **86**, 1133–1149 (2006).
53. Naidoo, N. ER and aging—Protein folding and the ER stress response. *Ageing Res. Rev.* **8**, 150–159 (2009).
54. Brown, M. K. & Naidoo, N. The endoplasmic reticulum stress response in aging and age-related diseases. *Front. Physiol.* **3**, (2012).
55. Macario, A. J. L. & de Macario, E. C. Sick Chaperones, Cellular Stress, and Disease. *N. Engl. J. Med.* **353**, 1489–1501 (2005).
56. Paz Gavilán, M. *et al.* Cellular environment facilitates protein accumulation in aged rat hippocampus. *Neurobiol. Aging* **27**, 973–982 (2006).
57. Hussain, S. G. & Ramaiah, K. V. A. Reduced eIF2 $\alpha$  phosphorylation and increased proapoptotic proteins in aging. *Biochem. Biophys. Res. Commun.* **355**, 365–370 (2007).
58. Rajawat, Y. S. & Bossis, I. Autophagy in aging and in neurodegenerative disorders. *Hormones* **7**, 46–61 (2008).

59. Chen, X. *et al.* Heme Oxygenase-1 Reduces Sepsis-Induced Endoplasmic Reticulum Stress and Acute Lung Injury. *Mediators Inflamm.* **2018**, (2018).
60. Marciniak, S. J. Endoplasmic reticulum stress in lung disease. *Eur. Respir. Rev.* **26**, (2017).
61. Burman, A., Tanjore, H. & Blackwell, T. S. Endoplasmic reticulum stress in pulmonary fibrosis. *Matrix Biol. J. Int. Soc. Matrix Biol.* **68–69**, 355–365 (2018).
62. Zeng, M. *et al.* 4-PBA inhibits LPS-induced inflammation through regulating ER stress and autophagy in acute lung injury models. *Toxicol. Lett.* **271**, 26–37 (2017).
63. Dolinay, D. T., Himes, D. B. E., Shumyatcher, M. M., Lawrence, M. G. G. & Margulies, P. S. S. Integrated Stress Response Mediates Epithelial Injury In Mechanical Ventilation. *Am. J. Respir. Cell Mol. Biol.* (2017) doi:10.1165/rcmb.2016-0404OC.
64. Yang, F. *et al.* ER-stress regulates macrophage polarization through pancreatic EIF-2alpha kinase. *Cell. Immunol.* (2018) doi:10.1016/j.cellimm.2018.12.008.
65. Imarisio, C. *et al.* Oxidative and ER stress-dependent ASK1 activation in steatotic hepatocytes and Kupffer cells sensitizes mice fatty liver to ischemia/reperfusion injury. *Free Radic. Biol. Med.* **112**, 141–148 (2017).
66. Rao, J. *et al.* ATF6 Mediates a Pro-Inflammatory Synergy Between ER Stress and TLR Activation in the Pathogenesis of Liver Ischemia-Reperfusion Injury. *Am. J. Transplant.* **14**, 1552–1561 (2014).
67. Macrophage Cytokine And UPR Responses To ER Stress Is Dependent On M1/M2 Polarization | A23. CHRONIC OBSTRUCTIVE PULMONARY DISEASE: PATHOGENESIS. *Am. Thorac. Soc. Int. Conf. Meet. Abstr. Am. Thorac. Soc. Int. Conf. Meet. Abstr.*
68. Yao, Y. *et al.* Chop Deficiency Protects Mice Against Bleomycin-induced Pulmonary Fibrosis by Attenuating M2 Macrophage Production. *Mol. Ther.* **24**, 915–925 (2016).
69. Oh, J. *et al.* Endoplasmic Reticulum Stress Controls M2 Macrophage Differentiation and Foam Cell Formation. *J. Biol. Chem.* **287**, 11629–11641 (2012).

70. Wang, Y. *et al.* Role of C/EBP homologous protein and endoplasmic reticulum stress in asthma exacerbation by regulating the IL-4/signal transducer and activator of transcription 6/transcription factor EC/IL-4 receptor  $\alpha$  positive feedback loop in M2 macrophages. *J. Allergy Clin. Immunol.* **140**, 1550-1561.e8 (2017).
71. Kim, H. J. *et al.* Inhibition of endoplasmic reticulum stress alleviates lipopolysaccharide-induced lung inflammation through modulation of NF- $\kappa$ B/HIF-1 $\alpha$  signaling pathway. *Sci. Rep.* **3**, (2013).
72. Yam, G. H.-F., Gaplovska-Kysela, K., Zuber, C. & Roth, J. Sodium 4-Phenylbutyrate Acts as a Chemical Chaperone on Misfolded Myocilin to Rescue Cells from Endoplasmic Reticulum Stress and Apoptosis. *Invest. Ophthalmol. Vis. Sci.* **48**, 1683–1690 (2007).
73. Frank, J. A. & Matthay, M. A. Science review: Mechanisms of ventilator-induced injury. *Crit. Care* **7**, 233–241 (2003).
74. Waters, C. M., Ridge, K. M., Sunio, G., Venetsanou, K. & Sznajder, J. I. Mechanical stretching of alveolar epithelial cells increases Na<sup>+</sup>-K<sup>+</sup>-ATPase activity. *J. Appl. Physiol.* **87**, 715–721 (1999).
75. Nakos, G. *et al.* Phospholipases A2 and platelet-activating-factor acetylhydrolase in patients with acute respiratory distress syndrome\*. *Read Online Crit. Care Med. Soc. Crit. Care Med.* **33**, 772–779 (2005).
76. Liu, M., Gu, C. & Wang, Y. Upregulation of the tight junction protein occludin: effects on ventilation-induced lung injury and mechanisms of action. *BMC Pulm. Med.* **14**, 94 (2014).
77. Uhlig, U. *et al.* Ventilation-induced activation of the mitogen-activated protein kinase pathway. *Eur. Respir. J.* **20**, 946–956 (2002).
78. Lam, A. P. & Dean, D. A. Cyclic stretch-induced nuclear localization of transcription factors results in increased nuclear targeting of plasmids in alveolar epithelial cells. *J. Gene Med.* **10**, 668–678 (2008).
79. Maceyka, M., Harikumar, K. B., Milstien, S. & Spiegel, S. SPHINGOSINE-1-PHOSPHATE SIGNALING AND ITS ROLE IN DISEASE. *Trends Cell Biol.* **22**, 50–60 (2012).
80. Mohammed, S. & Harikumar, K. B. Sphingosine 1-Phosphate: A Novel Target for Lung Disorders. *Front. Immunol.* **8**, (2017).

81. Chi, H. Sphingosine 1-phosphate and immune regulation: trafficking and beyond. *Trends Pharmacol. Sci.* **32**, 16–24 (2011).
82. Spiegel, S. & Milstien, S. The outs and the ins of sphingosine-1-phosphate in immunity. *Nat. Rev. Immunol.* **11**, 403–415 (2011).
83. Garcia, J. G. N. *et al.* Sphingosine 1-phosphate promotes endothelial cell barrier integrity by Edg-dependent cytoskeletal rearrangement. *J. Clin. Invest.* **108**, 689–701 (2001).
84. Mehta, D., Konstantoulaki, M., Ahmmed, G. U. & Malik, A. B. Sphingosine 1-Phosphate-induced Mobilization of Intracellular Ca<sup>2+</sup> Mediates Rac Activation and Adherens Junction Assembly in Endothelial Cells. *J. Biol. Chem.* **280**, 17320–17328 (2005).
85. Lee, M.-J. *et al.* Vascular Endothelial Cell Adherens Junction Assembly and Morphogenesis Induced by Sphingosine-1-Phosphate. *Cell* **99**, 301–312 (1999).
86. Lavieu, G. *et al.* Regulation of Autophagy by Sphingosine Kinase 1 and Its Role in Cell Survival during Nutrient Starvation. *J. Biol. Chem.* **281**, 8518–8527 (2006).
87. Huang, L. S. & Natarajan, V. SPHINGOLIPIDS IN PULMONARY FIBROSIS. *Adv. Biol. Regul.* **57**, 55–63 (2015).
88. Chalfant, C. E. & Spiegel, S. Sphingosine 1-phosphate and ceramide 1-phosphate: expanding roles in cell signaling. *J. Cell Sci.* **118**, 4605–4612 (2005).
89. Saba Julie D. & Hla Timothy. Point-Counterpoint of Sphingosine 1-Phosphate Metabolism. *Circ. Res.* **94**, 724–734 (2004).
90. Brinkmann, V. & Baumruker, T. Pulmonary and vascular pharmacology of sphingosine 1-phosphate. *Curr. Opin. Pharmacol.* **6**, 244–250 (2006).
91. Proia, R. L. & Hla, T. Emerging biology of sphingosine-1-phosphate: its role in pathogenesis and therapy. *J. Clin. Invest.* **125**, 1379–1387 (2015).
92. McVerry, B. J. & Garcia, J. G. N. Endothelial cell barrier regulation by sphingosine 1-phosphate. *J. Cell. Biochem.* **92**, 1075–1085 (2004).

93. Sammani, S. *et al.* Differential Effects of Sphingosine 1–Phosphate Receptors on Airway and Vascular Barrier Function in the Murine Lung. *Am. J. Respir. Cell Mol. Biol.* **43**, 394–402 (2010).
94. Wadgaonkar, R. *et al.* Differential regulation of sphingosine kinases 1 and 2 in lung injury. *Am. J. Physiol. - Lung Cell. Mol. Physiol.* **296**, L603–L613 (2009).
95. Zhao, Y. *et al.* Protection of LPS-induced murine acute lung injury by sphingosine-1-phosphate lyase suppression. *Am. J. Respir. Cell Mol. Biol.* **45**, 426–435 (2011).
96. Trayssac, M., Hannun, Y. A. & Obeid, L. M. Role of sphingolipids in senescence: implication in aging and age-related diseases. *J. Clin. Invest.* **128**, 2702–2712 (2018).
97. Papsdorf, K. & Brunet, A. Linking Lipid Metabolism to Chromatin Regulation in Aging. *Trends Cell Biol.* **29**, 97–116 (2019).
98. Czubowicz, K., Jęśko, H., Wencel, P., Lukiw, W. J. & Strosznajder, R. P. The Role of Ceramide and Sphingosine-1-Phosphate in Alzheimer’s Disease and Other Neurodegenerative Disorders. *Mol. Neurobiol.* **56**, 5436–5455 (2019).
99. Ghidoni, R., Caretti, A. & Signorelli, P. Role of Sphingolipids in the Pathobiology of Lung Inflammation. *Mediators Inflamm.* **2015**, (2015).
100. Yang, J. *et al.* Sphingosine 1-Phosphate (S1P)/S1P Receptor2/3 Axis Promotes Inflammatory M1 Polarization of Bone Marrow-Derived Monocyte/Macrophage via G(α)i/o/PI3K/JNK Pathway. *Cell. Physiol. Biochem. Int. J. Exp. Cell. Physiol. Biochem. Pharmacol.* **49**, 1677–1693 (2018).
101. Weigert, A., Olesch, C. & Brüne, B. Sphingosine-1-Phosphate and Macrophage Biology—How the Sphinx Tames the Big Eater. *Front. Immunol.* **10**, (2019).
102. Müller, J., von Bernstorff, W., Heidecke, C.-D. & Schulze, T. Differential S1P Receptor Profiles on M1- and M2-Polarized Macrophages Affect Macrophage Cytokine Production and Migration. *BioMed Res. Int.* **2017**, 1–10 (2017).

103. Harikumar, K. B. *et al.* K63-linked polyubiquitination of transcription factor IRF1 is essential for IL-1-induced production of chemokines CXCL10 and CCL5. *Nat. Immunol.* **15**, 231–238 (2014).
104. Pchejetski, D. *et al.* The involvement of sphingosine kinase 1 in LPS-induced Toll-like receptor 4-mediated accumulation of HIF-1 $\alpha$  protein, activation of ASK1 and production of the pro-inflammatory cytokine IL-6. *Immunol. Cell Biol.* **89**, 268–274 (2011).
105. Nayak, D. *et al.* Sphingosine kinase 1 regulates the expression of proinflammatory cytokines and nitric oxide in activated microglia. *Neuroscience* **166**, 132–144 (2010).
106. Hammad, S. M. *et al.* Dual and distinct roles for sphingosine kinase 1 and sphingosine 1 phosphate in the response to inflammatory stimuli in RAW macrophages. *Prostaglandins Other Lipid Mediat.* **85**, 107–114 (2008).
107. Jin, J. *et al.* LPS and palmitate synergistically stimulate sphingosine kinase 1 and increase sphingosine 1 phosphate in RAW264.7 macrophages. *J. Leukoc. Biol.* **104**, 843–853 (2018).
108. Hughes Jeniter E. *et al.* Sphingosine-1-Phosphate Induces an Antiinflammatory Phenotype in Macrophages. *Circ. Res.* **102**, 950–958 (2008).
109. Pyne, N. J. & Pyne, S. Sphingosine 1-phosphate and cancer. *Nat. Rev. Cancer* **10**, 489–503 (2010).
110. Kunkel, G. T., Maceyka, M., Milstien, S. & Spiegel, S. Targeting the sphingosine-1-phosphate axis in cancer, inflammation and beyond. *Nat. Rev. Drug Discov.* **12**, 688–702 (2013).
111. Sabbadini, R. A. Sphingosine-1-phosphate antibodies as potential agents in the treatment of cancer and age-related macular degeneration. *Br. J. Pharmacol.* **162**, 1225–1238 (2011).
112. Cabrera-Benitez, N. E. *et al.* Mechanical Ventilation–associated Lung Fibrosis in Acute Respiratory Distress Syndrome A Significant Contributor to Poor Outcome. *Anesthesiology* **121**, 189–198 (2014).
113. Chambers, R. C. & Mercer, P. F. Mechanisms of Alveolar Epithelial Injury, Repair, and Fibrosis. *Ann. Am. Thorac. Soc.* **12**, S16–S20 (2015).

114. Carney, D. E. *et al.* The Mechanism of Lung Volume Change during Mechanical Ventilation. *Am. J. Respir. Crit. Care Med.* **160**, 1697–1702 (1999).
115. Corti, M., Brody, A. R. & Harrison, J. H. Isolation and primary culture of murine alveolar type II cells. *Am. J. Respir. Cell Mol. Biol.* **14**, 309–315 (1996).
116. Yuan, R., Peters, L. L. & Paigen, B. Mice as a Mammalian Model for Research on the Genetics of Aging. *ILAR J. Natl. Res. Counc. Inst. Lab. Anim. Resour.* **52**, 4–15 (2011).
117. Trouplin, V. *et al.* Bone Marrow-derived Macrophage Production. *J. Vis. Exp. JoVE* (2013)  
doi:10.3791/50966.
118. Murray, M. Y. *et al.* Macrophage Migration and Invasion Is Regulated by MMP10 Expression. *PLOS ONE* **8**, e63555 (2013).
119. Yu, Y.-R. A. *et al.* Flow Cytometric Analysis of Myeloid Cells in Human Blood, Bronchoalveolar Lavage, and Lung Tissues. *Am. J. Respir. Cell Mol. Biol.* **54**, 13–24 (2016).
120. Kolaczowska, E. & Kubes, P. Neutrophil recruitment and function in health and inflammation. *Nat. Rev. Immunol.* **13**, 159–175 (2013).
121. Esteban, A. *et al.* Outcome of older patients receiving mechanical ventilation. *Intensive Care Med.* **30**, 639–646 (2004).
122. Aoshiba, K. & Nagai, A. Chronic lung inflammation in aging mice. *FEBS Lett.* **581**, 3512–3516 (2007).
123. Yona, S. *et al.* Fate mapping reveals origins and dynamics of monocytes and tissue macrophages under homeostasis. *Immunity* **38**, 79–91 (2013).
124. Landsman, L. & Jung, S. Lung Macrophages Serve as Obligatory Intermediate between Blood Monocytes and Alveolar Macrophages. *J. Immunol.* **179**, 3488–3494 (2007).
125. Beck-Schimmer, B. *et al.* Alveolar macrophages regulate neutrophil recruitment in endotoxin-induced lung injury. *Respir. Res.* **6**, 61 (2005).

126. Maus, U. A. *et al.* Monocytes Are Potent Facilitators of Alveolar Neutrophil Emigration During Lung Inflammation: Role of the CCL2-CCR2 Axis. *J. Immunol.* **170**, 3273–3278 (2003).
127. Waters, C. M., Roan, E. & Navajas, D. Mechanobiology in Lung Epithelial Cells: Measurements, Perturbations, and Responses. *Compr. Physiol.* **2**, 1–29 (2012).
128. Taniguchi, L. U., Caldini, E. G., Velasco, I. T. & Negri, E. M. Cytoskeleton and mechanotransduction in the pathophysiology of ventilator-induced lung injury. *J. Bras. Pneumol.* **36**, 363–371 (2010).
129. Link, P. A. *et al.* Electrospayed extracellular matrix nanoparticles induce a pro-regenerative cell response. *J. Tissue Eng. Regen. Med.* (2018) doi:10.1002/term.2768.
130. Mukai, S. *et al.* Novel Treatment of Chronic Graft-Versus-Host Disease in Mice Using the ER Stress Reducer 4-Phenylbutyric Acid. *Sci. Rep.* **7**, 41939 (2017).
131. Xiao, C., Giacca, A. & Lewis, G. F. Sodium Phenylbutyrate, a Drug With Known Capacity to Reduce Endoplasmic Reticulum Stress, Partially Alleviates Lipid-Induced Insulin Resistance and  $\beta$ -Cell Dysfunction in Humans. *Diabetes* **60**, 918 (2011).
132. Kolb, P. S. *et al.* The therapeutic effects of 4-phenylbutyric acid in maintaining proteostasis. *Int. J. Biochem. Cell Biol.* **61**, 45–52 (2015).
133. Valentine, M. S. *et al.* Inflammation and Monocyte Recruitment Due to Aging and Mechanical Stretch in Alveolar Epithelium are Inhibited by the Molecular Chaperone 4-Phenylbutyrate. *Cell. Mol. Bioeng.* **11**, 495–508 (2018).
134. Bless, N. M. *et al.* Role of CC Chemokines (Macrophage Inflammatory Protein-1 $\beta$ , Monocyte Chemoattractant Protein-1, RANTES) in Acute Lung Injury in Rats. *J. Immunol.* **164**, 2650–2659 (2000).
135. Shallo, H., Plackett, T. P., Heinrich, S. A. & Kovacs, E. J. Monocyte chemoattractant protein-1 (MCP-1) and macrophage infiltration into the skin after burn injury in aged mice. *Burns* **29**, 641–647 (2003).
136. Shi, C. & Pamer, E. G. Monocyte recruitment during infection and inflammation. *Nat. Rev. Immunol.* **11**, 762.

137. Cohen, T. S., Cavanaugh, K. J. & Margulies, S. S. Frequency and peak stretch magnitude affect alveolar epithelial permeability. *Eur. Respir. J.* **32**, 854–861 (2008).
138. Davidovich, N. *et al.* Cyclic Stretch–Induced Oxidative Stress Increases Pulmonary Alveolar Epithelial Permeability. *Am. J. Respir. Cell Mol. Biol.* **49**, 156–164 (2013).
139. Heise, R. L., Stober, V., Cheluvvaraju, C., Hollingsworth, J. W. & Garantziotis, S. Mechanical Stretch Induces Epithelial-Mesenchymal Transition in Alveolar Epithelia via Hyaluronan Activation of Innate Immunity. *J. Biol. Chem.* **286**, 17435–17444 (2011).
140. Hayashi, G., Labelle-Dumais, C. & Gould, D. B. Use of sodium 4-phenylbutyrate to define therapeutic parameters for reducing intracerebral hemorrhage and myopathy in Col4a1 mutant mice. *Dis. Model. Mech.* **11**, (2018).
141. Luo, T., Chen, B. & Wang, X. 4-PBA prevents pressure overload-induced myocardial hypertrophy and interstitial fibrosis by attenuating endoplasmic reticulum stress. *Chem. Biol. Interact.* **242**, 99–106 (2015).
142. Mizukami, T. *et al.* Sodium 4-phenylbutyrate protects against spinal cord ischemia by inhibition of endoplasmic reticulum stress. *J. Vasc. Surg.* **52**, 1580–1586 (2010).
143. Yang, J. *et al.* Sphingosine 1-Phosphate (S1P)/S1P Receptor2/3 Axis Promotes Inflammatory M1 Polarization of Bone Marrow-Derived Monocyte/Macrophage via G( $\alpha$ )i/o/PI3K/ JNK Pathway. **17** (2018).
144. Peng, X. *et al.* Protective Effects of Sphingosine 1-Phosphate in Murine Endotoxin-induced Inflammatory Lung Injury. *Am. J. Respir. Crit. Care Med.* **169**, 1245–1251 (2004).
145. Milara, J. *et al.* Sphingosine-1-phosphate is increased in patients with idiopathic pulmonary fibrosis and mediates epithelial to mesenchymal transition. *Thorax* **67**, 147–156 (2012).
146. Strub, G. M., Maceyka, M., Hait, N. C., Milstien, S. & Spiegel, S. Extracellular and Intracellular Actions of Sphingosine-1-Phosphate. in *Sphingolipids as Signaling and Regulatory Molecules* (eds. Chalfant, C. & Poeta, M. D.) vol. 688 141–155 (Springer New York, 2010).

147. Vogt, D. & Stark, H. Therapeutic Strategies and Pharmacological Tools Influencing S1P Signaling and Metabolism: TOOLS ON S1P SIGNALING AND METABOLISM. *Med. Res. Rev.* **37**, 3–51 (2017).
148. Pyne, S. & Pyne, N. Sphingosine 1-phosphate signalling via the endothelial differentiation gene family of G-protein-coupled receptors. *Pharmacol. Ther.* **88**, 115–131 (2000).
149. Hla, T. *et al.* Sphingosine-1-Phosphate Signaling via the EDG-1 Family of G-Protein-Coupled Receptors. *Ann. N. Y. Acad. Sci.* **905**, 16–24 (2000).
150. Rosen, H. & Goetzl, E. J. Sphingosine 1-phosphate and its receptors: an autocrine and paracrine network. *Nat. Rev. Immunol.* **5**, 560–570 (2005).
151. Schwab, S. R. *et al.* Lymphocyte Sequestration Through S1P Lyase Inhibition and Disruption of S1P Gradients. *Science* **309**, 1735–1739 (2005).
152. Bektas, M. *et al.* Sphingosine 1-Phosphate Lyase Deficiency Disrupts Lipid Homeostasis in Liver. *J. Biol. Chem.* **285**, 10880–10889 (2010).
153. Raggi, F. *et al.* Regulation of Human Macrophage M1–M2 Polarization Balance by Hypoxia and the Triggering Receptor Expressed on Myeloid Cells-1. *Front. Immunol.* **8**, (2017).
154. Ying, W., Cheruku, P. S., Bazer, F. W., Safe, S. H. & Zhou, B. Investigation of Macrophage Polarization Using Bone Marrow Derived Macrophages. e50323 (2013) doi:10.3791/50323.
155. Vadász, I. & Brochard, L. Update in Acute Lung Injury and Mechanical Ventilation 2011. *Am. J. Respir. Crit. Care Med.* **186**, 17–23 (2012).
156. Hoegl, S. *et al.* Capturing the multifactorial nature of ARDS – “Two-hit” approach to model murine acute lung injury. *Physiol. Rep.* **6**, (2018).
157. Morales-Nebreda, L., Misharin, A., Perlman, H., Budinger, G. R. S. The heterogeneity of lung macrophages in the susceptibility to disease *European Respiratory Review.* **24** (137) 505-509, (2015)
158. Herold S, Mayer K, Lohmeyer J. Acute lung injury: how macrophages orchestrate resolution of inflammation and tissue repair. *Front Immunol.* **2**:65. (2011).

159. Stahl EC, Haschak MJ, Popovic B, Brown BN. Macrophages in the Aging Liver and Age-Related Liver Disease. *Front Immunol.* 2018;9:2795. (2018).
160. Garg AD, Kaczmarek A, Krysko O, Vandenabeele P, Krysko DV, Agostinis P. ER stress-induced inflammation: does it aid or impede disease progression?. *Trends Mol Med.* 18(10):589-598. (2012).
161. Tanjore H, Lawson WE, Blackwell TS. Endoplasmic reticulum stress as a pro-fibrotic stimulus. *Biochim Biophys Acta.* 1832(7):940-947. (2013).
162. González-Fernández B, Sánchez DI, González-Gallego J, Tuñón MJ. Sphingosine 1-Phosphate Signaling as a Target in Hepatic Fibrosis Therapy. *Front Pharmacol.* 8:579. (2017).

# MICHAEL S. VALENTINE

Doctoral Candidate/Graduate Research Assistant, Department of Biomedical Engineering  
Pulmonary Mechanobiology and Tissue Engineering Lab – Virginia Commonwealth University  
1655 Skilift Lane Richmond VA 23225 · (757) 692-5897  
[mvalentine@vcu.edu](mailto:mvalentine@vcu.edu) · [linkedin.com/in/mvalentine](https://www.linkedin.com/in/mvalentine)

---

I am a highly motivated biomedical engineer and research scientist with 8+ years of biomedical research experience and expertise in aging, regenerative medicine, immunology/immunoengineering, biomechanics/mechanobiology, and the pulmonary system.

## EDUCATION

### Doctor of Philosophy in Biomedical Engineering

Virginia Commonwealth University: Richmond, VA  
Pulmonary Mechanobiology and Tissue Engineering Lab  
Advisor/PI: Dr. Rebecca Heise, Ph.D.

Doctoral Committee: Dr. John Ryan, Dr. Angela Reynolds, Dr. Christopher Lemmon, Dr. Rene Olivares-Navarete  
Proposed Dissertation Title: *"The Impact of Aging and Mechanical Forces on Alveolar Epithelial and Macrophage Responses in Acute Lung Injury and Inflammatory Diseases"*

EXPECTED:  
5/2020

### Bachelor of Science in Biology

University of Virginia: Charlottesville, VA

2013

## RESEARCH AND PROFESSIONAL EXPERIENCE

### GRADUATE RESEARCH ASSISTANT – VCU BME Department

Virginia Commonwealth University: Richmond, VA  
Pulmonary Mechanobiology and Tissue Engineering Lab

- ◆ Developed and characterized a novel aging animal model of acute lung injury for biomarker and therapeutic testing that is more clinically translatable/relevant.
- ◆ Investigated age-related acute lung injury mechanisms and therapies in cellular and animal models utilizing Flexcell's Tension System and SCIREQ's FlexiVent Animal Ventilator.
- ◆ Studied influence of aging and mechanical forces on various pulmonary and immune cell and lung tissue responses in both healthy and diseased states.
- ◆ Investigated novel therapeutic interventions in experimental models of Ventilator-induced lung injury (VILI), Chronic Obstructive Pulmonary Disease (COPD), and Infantile/Acute Respiratory Distress Syndrome (IRDS/ARDS).
- ◆ Established an original surfactant depletion rat model to explore innovative surfactant replacement technologies and therapies, such as the development of aerosolized Enhanced Excipient Growth (EEG) Survanta-based dry powder formulations to improve pulmonary mechanics for IRDS and ARDS applications.
- ◆ Identified and characterized underlying mechanisms in age-related experimental models of acute lung injury and VILI: Endoplasmic Reticulum Stress, Sphingosine-1-phosphate signaling, inflammasome, and macrophage polarization.
- ◆ Assessed macrophage reprogramming using electrosprayed extracellular nanoparticles for tissue repair applications.
- ◆ Coordinated experiments and projects with several physicians, research scientists, graduate students, undergraduate students, and high school students. Initiated several collaborations with other biomedical research labs.
- ◆ Trained and supervised 12 undergraduate students and 3 high school students in complementary research projects.

2015-  
PRESENT

### LAB MANAGER – VCU BME Department

Virginia Commonwealth University: Richmond, VA  
Pulmonary Mechanobiology and Tissue Engineering Lab

- ◆ Trained and mentored incoming laboratory personnel, supervised lab safety and conduct, provided lab administrative support, and developed standard operating procedures.
- ◆ Managed and maintained laboratory equipment, documentation, software, and scheduling.
- ◆ Conducted supply ordering and reduced laboratory operating expenses by acquiring new sources of products or services for the laboratory. Interacted with biotechnology companies and vendors to facilitate laboratory purchases and development.

2014-2015

<p><b>LAB TECHNICIAN/SPECIALIST– VCU BME Department</b>  <b>Virginia Commonwealth University: Richmond, VA</b>  <b>Pulmonary Mechanobiology and Tissue Engineering Lab</b></p> <ul style="list-style-type: none"> <li>◆ Investigated effects of aging and mechanical forces on various lung cells, immune cells, and whole pulmonary tissue responses in several <i>in vitro</i> and <i>in vivo</i> projects.</li> <li>◆ Evaluated the therapeutic benefits of stem cells and decellularized lung extracellular matrix to regenerate lung tissue in a rat emphysema model and mouse acute lung injury models.</li> <li>◆ Operated and managed specialized lab equipment: Flexcell’s Tension System, SCIREQ’s Animal Ventilator, ELISA/western blot resources, cell culture hoods, and animal surgical resources.</li> </ul>	2013-2015
<p><b>UNDERGRADUATE RESEARCH ASSISTANT – UVA Anesthesiology Dept.</b>  <b>University of Virginia: Charlottesville, VA</b>  <b>Todorovics Labs – Anesthesiology and Pharmacology Research</b></p> <ul style="list-style-type: none"> <li>◆ Investigated pharmacological and toxicological effects and underlying mechanisms of various anesthetic drugs on the central nervous system <i>in vitro</i> and <i>in vivo</i>.</li> <li>◆ Assisted lab personnel with cell and animal studies: tissue collection, sample processing, animal behavioral assessments, reagent production, and equipment management.</li> </ul>	2011-2013
<b>TEACHING AND MENTORING EXPERIENCE</b>	
<p><b>Mechanobiology Research Experience - VCU BME Department</b>  <b>Virginia Commonwealth University: Richmond, VA</b></p> <ul style="list-style-type: none"> <li>◆ Mentored 2 undergraduate students under this program funded by the NSF regarding techniques and conceptual knowledge related to mechanobiology of disease and general biomedical engineering research.</li> <li>◆ Trained students several interdisciplinary skills related to cell mechanics, mechanobiology, pulmonary drug delivery, pulmonary biomechanics, and general regenerative medicine.</li> <li>◆ Instructed students on how to develop collaborations with biomedical research labs and basic scientific methods, statistics skills, and research ethics.</li> </ul>	2018-2019
<p><b>Medical Sciences Internship Program - VCU BME Department</b>  <b>Virginia Commonwealth University: Richmond, VA</b></p> <ul style="list-style-type: none"> <li>◆ Advised 2 high school students under this program by the VCU School of Medicine that focused on exposing students to medical research lab environments and developing of biomedical engineering research projects.</li> <li>◆ Assisted students in conducting biomedical research: developing hypotheses, performing experiments, processing samples, and analyzing results.</li> </ul>	2017-2019
<p><b>Deans Undergraduate Research Initiative – VCU BME Department</b>  <b>Virginia Commonwealth University: Richmond, VA</b></p> <ul style="list-style-type: none"> <li>◆ Selected (2x) as a graduate student mentor for 2 separate undergraduate students over one-year fellowships.</li> <li>◆ Designed independent research project proposals for students that were reviewed and approved.</li> <li>◆ Trained students with technical and conceptual knowledge, utilizing both <i>in vitro</i> and <i>in vivo</i> models to better understand how aging and mechanical forces impact lung injury and repair.</li> <li>◆ Reinforced mentoring, managing, leadership, and communication expertise, while reinforcing lab skills and knowledge.</li> <li>◆ Received \$500 DURF Travel Grant (2x) to attend and present project at a scientific conference.</li> </ul>	2015-2019
<p><b>Pulmonary Mechanobiology Lab Student Mentor - VCU BME Department</b>  <b>Virginia Commonwealth University: Richmond, VA</b></p> <ul style="list-style-type: none"> <li>◆ Trained and supervised 12 undergraduate students, 3 high school students, and an international student visiting from Columbia in complementary research projects over graduate career.</li> <li>◆ Developed students’ technical and conceptual knowledge focused on biomedical research in mechanobiology of disease and reinforced personal expertise in this field of research.</li> <li>◆ Instructed students how to utilize cell-stretch and animal models, as well as techniques such as cell culture, primary cell isolations, animal handling and surgery, tissue collection, Flow Cytometry/FACS, qPCR, , ELISAs, western blotting, immunofluorescence and IHC staining, microscopy, immunoassays, and other research skills to study pulmonary mechanobiology of disease.</li> </ul>	2013-2019
<p><b>Deans Early Research Initiative – VCU BME Department</b>  <b>Virginia Commonwealth University: Richmond, VA</b></p> <ul style="list-style-type: none"> <li>◆ Selected as a graduate student mentor to work with a high school student over a year long program.</li> <li>◆ Designed independent research project proposal for student that was reviewed and assessed.</li> <li>◆ Enhanced student’s development of critical skills in biomedical engineering research and research proposal writing.</li> </ul>	2016-2017

- ◆ Mentored students on how to implement cellular and animal models to investigate influence of aging and mechanical forces on pulmonary cell and tissue responses.
- ◆ Strengthened mentoring, managing, leadership, and communication proficiency.
- ◆ Received \$500 DERI Travel Grant to attend and present project at a scientific conference.

### **Teaching Assistant – VCU BME Department**

2015-2017

*Virginia Commonwealth University: Richmond, VA*

- ◆ Assisted EGRB102: Intro to Biomedical Engineering for 4 semesters under 3 different professors.
- ◆ Conducted seminars, grading, tutoring, student evaluations, and demonstrations during lecture and lab sessions.
- ◆ Managed and designed lab sessions/activities for students independently.
- ◆ Contributed to design of lecture and lab curriculum/examinations.
- ◆ Further developed communication, public speaking, and teaching expertise.

### **Peer Teaching Program – UVA Biology Department**

2012-2013

*University of Virginia: Charlottesville, VA*

- ◆ Served as a learning assistant for BIOL2100: Introduction to Biology: Cell Biology and Genetics Laboratory with Dr. David Kittleson for 2 semesters.
- ◆ Contributed to students' learning experience and further developed communication and teaching skills by leading lab sessions and assisting professor, graduate students, and undergraduate students with assignments and activities.
- ◆ Fostered excitement and enthusiasm and promoted further understanding of the material for students and acted as a liaison between the students and professor.
- ◆ Expanded knowledge and understanding regarding DNA analysis, such as extraction, cloning, transformation, restriction mapping, sequencing, and bioinformatics, and enzyme analysis.

## **LEADERSHIP**

### **Community Engagement and Outreach Leader**

2017-2019

*Virginia Commonwealth University: Richmond, VA*

- ◆ Lead and managed several VCU community outreach program sessions : Early Engineers, Teacher Professional Development Workshops, STEAM Day Camp, and local Innovation Day events.
- ◆ Conducted and assisted activities and demonstrations for community outreach events and programs initiated by VCU College of Engineering for students, educators, and administrators in grades K-12.
- ◆ Designed and optimized lung modeling STEAM activity for students and teachers in early education.
- ◆ Presented "Research and Careers in Regenerative Medicine and Biomedical Engineering" at local high schools and college events to encourage students to pursue BME degrees and research experience in the field.

### **Recruitment Chair – VCU Biomedical Graduate Student Council**

2017-2019

*Virginia Commonwealth University: Richmond, VA*

- ◆ Co-founder of the graduate student organization: Assisted in establishing the VCU charter and forming student council to support the Biomedical Engineering graduate student body at VCU.
- ◆ Elected Recruitment Chair and Council Member and established the following initiatives:
  - ◆ *VCU BME Prospective Graduate Student Visits*
  - ◆ *Recruitment Efforts at Biomedical Engineering Society and other Annual Conferences*
  - ◆ *BME Graduate Student Ambassador Program*
  - ◆ *Webinar Informational Sessions: Pursuing a Graduate Degree in BME at VCU*
- ◆ Facilitate all recruiting efforts for prospective graduate students in the Biomedical Engineering program at VCU.
- ◆ Responsible for planning, organizing, and implementing events and services that help promote interest and applications for the VCU Biomedical Engineering graduate program.
- ◆ Served as a representative for the graduate student body in the BME program and liaison between the BME administration and student body.

### **Treasurer – VCU Biomedical Graduate Student Council**

2017-2018

*Virginia Commonwealth University: Richmond, VA*

- ◆ Elected Treasurer of student council organization.
- ◆ Established annual budgets to support organization's imitative programs and events.
- ◆ Coordinated with VCU BME financial department and VCU BME graduate dean to secure funding.
  - Procured \$20,000 in funding by VCU BME Department and VCU Graduate School.
  - Determined funding allocation to internal committees and sponsored events.
- ◆ Generated budget reports that assessed the financial efficiency and efficacy of sponsored initiatives and events.

## RELATED SKILLS

### Laboratory/Research Skills

- Regenerative Medicine
- Immunoengineering
- Aging Research
- Cell Culture
- Flow Cytometry/FACS
- Animal Handling
- Histology
- Animal Surgery
- qPCR
- Immunoassays
- Tissue Collection
- Immunofluorescence/IHC
- Pulmonary Drug Development and Delivery
- Biomechanical Modeling and Testing
- Biomaterial Development
- Nanoparticle Development and Testing
- Mechanobiology
- Tissue Engineering
- Experimental Design
- Lab Safety
- Animal Models
- Cell-Stretch Models
- Cytology
- Stem Cells
- Microscopy
- Mechanical Ventilation
- Sample Processing
- ELISAs
- Western Blotting
- Data Analysis
- Precision Cut Lung Slicing (PCLS)
- Transepithelial electrical resistance (TEER) Testing

### Computer/Interpersonal Skills

- GraphPad Prism
- Microsoft Office
- LabView
- Quartz
- Statistics
- Image Processing
- Image Analysis
- R Programming
- Communication
- Problem Solving
- Leadership
- Collaboration
- Consulting
- Creative Thinking
- Image J/FIJI
- MATLAB
- Adobe Acrobat
- Grant Writing
- Teaching
- Mentoring
- Public Speaking
- Teamwork
- Project Management
- Networking
- Conflict Management
- Interviewing

## AWARDS AND HONORS

VCU Graduate School Travel Grant Award (5x)	2015-2019
VCU Engineering Graduate School Travel Grant Award (5x)	2015-2019
VCU Board of Visitors Student Representative	2018
World Congress of Biomechanics Travel Bursary Award	2018
Virginia Academy of Science Best Student Presentation Award	2018

## PROFESSIONAL SOCIETY MEMBERSHIPS

Sigma Xi, Scientific Research Honor Society	2018-PRESENT
Virginia Academy of Science (VAS)	2016-PRESENT
Virginia Biotechnology Association (VA Bio)	2016-PRESENT
American Physiological Society (APS)	2016-PRESENT
Biomedical Engineering Society (BMES)	2015-PRESENT

## PEER-REVIEWED PUBLICATIONS

1. Robert A. Pouliot, Patrick Link, Nabil Mikhael, Matthew Schneck, **Michael S. Valentine**, Franck J. Kamga Gninzeko, Joseph A. Herbert, Masahiro Sakagami, Rebecca L. Heise. **Development and characterization of a naturally derived lung extracellular matrix hydrogel**. Journal of Biomedical Materials Research Part A. doi:10.1002/jbm.a.35726. 2016.
2. Joseph A. Herbert, **Michael S. Valentine**, Nivi Saravanan, Matthew B. Schneck, Ramana Pidaparti, Alpha A. Fowler III, Angela M. Reynolds, Rebecca L. Heise, **Conservative fluid management prevents age-associated ventilator induced mortality**. Experimental Gerontology, Volume 81, August 2016, Pages 101-109, ISSN 0531-5565, <http://dx.doi.org/10.1016/j.exger.2016.05.005>.
3. **Michael S. Valentine**, Patrick Link, Joseph Herbert, Matthew Schneck, Keerthana Shankar, Jewel Nkwocha, Angela M. Reynolds, Rebecca L. Heise. **Inflammation and Monocyte Recruitment due to Aging and Mechanical Stretch in Alveolar Epithelium are Inhibited by the Molecular Chaperone 4-phenylbutyrate**. Cellular and Molecular Bioengineering, June 2018. <https://doi.org/10.1007/s12195-018-0537-8>
4. Patrick A. Link, Alexandria M. Ritchie, Gabrielle M. Cotman, **Michael S. Valentine**, Bret S. Dereski, Rebecca L. Heise. **Electrosprayed ECM Nanoparticles Induce a Pro-regenerative Cell Response**. Journal of Tissue Engineering and Regenerative Medicine, October 2018. DOI:10.1002/term.2768

## MANUSCRIPTS IN REVIEW/PREPARATION

1. Kamga Gninzeko FJ, **Valentine MS**, Tho CK, Chindal SR, Boc S, Dhapare S, Momin MM, Hassan A, Hindle M, Farkas D, Longest PW, Heise RL: Excipient Enhanced Growth (EEG) Aerosol Surfactant Replacement Therapy In An In Vivo Rat Lung Injury Model. J Aerosol Med Pulm Drug Deliv. Jan 2020 (*In review*).
2. S. B. Minucci, R. L. Heise, **M. S. Valentine**, F. J. Kamga Gninzeko, A. M. Reynolds. Understanding the Role of Macrophages in Lung Inflammation Through Mathematical Modeling. Journal of Theoretical Biology. April 2020 (*In review*)
3. **Michael S. Valentine**, Franck J. Kamga Gninzeko, Cynthia Tho, Cynthia Weigel, Sarah Spiegel, Rebecca L. Heise. **Macrophage Polarization and Sphingosine-1-Phosphate (S1P) Signaling in the Lung are Impaired by Aging and High Pressure-Controlled Mechanical Ventilation**. Aging and Disease. (*In preparation*)

## CONFERENCE PRESENTATIONS

1. Herbert J, **Valentine M**, Patel P, Pidaparti R, Reynolds A, Heise R. The Effect of Age on the Severity of Ventilator Induced Lung Injury in an Aging Mouse Model. **Poster presentation**, American Thoracic Society, 2014; San Diego, CA.
2. Schneck MB, **Valentine M**, Herbert JA, Pidaparti R, Reynolds A, and Heise RL. 2015. Quantification of Airspace Enlargement due to Ventilator Induced Lung Injury in an Aging Lung Model. **Poster Presentation**, Biomedical Engineering Society, 2015 Annual Meeting, Tampa, FL.
3. Gninzeko FK, **Valentine M**, Herbert J, Schneck M, Heise R. Cellular Endoplasmic Reticulum Stress and Cytokine Response in Age-Associated Experimental Ventilator Induced Lung Injury. **Poster Presentation**, Biomedical Engineering Society, 2016 Annual Meeting, Minneapolis, MN.
4. Herbert J, **Valentine M**, Patel P, Pidaparti R, Reynolds A, Heise R. Age Related Changes in Pulmonary Mechanics and Inflammatory Response to Experimental Ventilator Induced Lung Injury. **Oral Presentation**, Biomedical Engineering Society, 2014; San Antonio, TX
5. Herbert J, **Valentine M**, Patel P, Nkwocha J, Fowler A, Pidaparti R, Reynolds A, Heise R. Aging and Mechanical Stretch Increase Inflammatory Gene Expression and ER Stress in In Vitro and In Vivo Models of Lung Injury. **Oral Presentation**, Biomedical Engineering Society, 2015; Tampa, FL.
6. **Valentine M**, Herbert J, Gninzeko FK, Schneck M, Reynolds A, Heise R. Alveolar Type II Epithelial Cells Exhibit Age-dependent Differential Response to Mechanical Stretch and Monocyte Recruitment. **Oral Presentation**, VCU ACHOO Series, September 21, 2016; Richmond, VA.

7. **Valentine M**, Herbert J, Gninzeko FK, Schneck M, Reynolds A, Heise R. Alveolar Type II Epithelial Cells Exhibit Age-dependent Differential Response to Mechanical Stretch and Monocyte Recruitment. **Oral Presentation**, Biomedical Engineering Society, 2016; Minneapolis, MN.
8. Gninzeko FK, **Valentine M**, Herbert J, Link P, Reynolds A, Heise R. Age as a Factor of Endoplasmic Reticulum Stress in Ventilator Induced Lung Injury. **Poster Presentation**, Virginia Academy of Science Annual Meeting, 2017; Richmond, VA.
9. **Valentine M**. Research and Careers in Regenerative Medicine and Biomedical Engineering. **Oral Presentation**, Colonial Heights STEM Night, 2017; Colonial Heights, VA.
10. **Valentine M**, Gninzeko FK, Herbert J, Link P, Parekh M, Shankar K, Reynolds A, Heise R. Advanced Age Alters Cytokine Secretion and Macrophage Polarization in a Pressure-Controlled Ventilator-Induced Lung Injury Mouse Model. **Poster Presentation**, Graduate Research Symposium, 2018; Richmond, VA.
11. **Valentine M**, Gninzeko FK, Herbert J, Link P, Parekh M, Shankar K, Heise R. Aging and Mechanical Stretch Influence Alveolar Epithelial Injury Responses and Monocyte Recruitment. **Oral Presentation**, Virginia Academy of Science Annual Meeting, 2018; Farmville, VA.
12. Ritchie A, Link P, **Valentine M**, Cotman G, Heise R. Nanoparticles formed from porcine lung extracellular matrix guide pro-regenerative macrophage phenotype *in vitro* and *in vivo*. **Oral Presentation**, Virginia Academy of Science Annual Meeting, 2018; Farmville, VA.
13. **Valentine M**, Gninzeko FK, Herbert J, Link P, Parekh M, Shankar K, Reynolds A, Heise R. The Impact of Aging and Mechanical Stretch on Monocyte Recruitment and Macrophage Polarization in Experimental Ventilator-Induced Lung Injury. **Oral Presentation**, World Congress of Biomechanics, 2018; Dublin, Ireland.
14. **Valentine M**, Link P, Gninzeko FK, Parekh M, Ritchie A, Cotman G, Reynolds A, Heise R. Macrophage Polarization and Reprogramming Using ECM Nanoparticles in Experimental Lung Injury. **Poster Presentation**, Biomedical Engineering Society, 2018; Atlanta, GA.
15. Gninzeko FK, **Valentine M**, Chindal S, Boc S, Dhapare S, Hindle M, Farkas D, Longest PW, Heise R. Aerosolized Surfactant Replacement Therapy In An In Vivo Rodent Lung Injury Model. **Oral Presentation**, Summer Biomechanics, Bioengineering, and Biotransport Conference, 2019; Seven Springs, PA.
16. **Valentine M**, Gninzeko FK, Chindal S, Parekh M, Reynolds A, Heise R. High Pressure-Controlled Mechanical Ventilation Induces Age-Specific Alterations in Lung Tissue Mechanics and Macrophage Polarization. **Poster Presentation**, Graduate Research Symposium, 2019; Richmond, VA.
17. **Valentine M**, Gninzeko FK, Chindal S, Parekh M, Weigel C, Reynolds A, Spiegel S, Heise R. Mechanical and Cellular Changes Induced by Aging and High Pressure-Controlled Mechanical Ventilation. **Oral Presentation**, Virginia Academy of Science Annual Meeting, 2019; Farmville, VA.
18. **Valentine M**, Gninzeko FK, Chindal S, Parekh M, Weigel C, Spiegel S, Heise R. Macrophage Polarization and Sphingosine-1-Phosphate (S1P) Signaling in the Lung are Impaired by Aging and High Pressure-Controlled Mechanical Ventilation. **Poster Presentation**, Gordon Research Conference, 2019; Lewiston, ME.
19. **Valentine M**, Gninzeko FK, Chindal S, Parekh M, Weigel C, Spiegel S, Heise R. Age-Specific Alterations in Lung Mechanics and Macrophage Polarization Induced by High Pressure-Controlled Mechanical Ventilation Are Impaired via Diminished Sphingosine-1-Phosphate. **Oral Presentation**, Biomedical Engineering Society, 2019; Philadelphia, PA.